Delay estimation and predictor-based control of time-delay systems with a class of various delays

Yang Deng

CENTRALE NANTES

THÈSE DE DOCTORAT DE

L'ÉCOLE CENTRALE DE NANTES

ÉCOLE DOCTORALE N° 601
Mathématiques et Sciences et Technologies de l'Information et de la Communication
Spécialité : *Automatique, Productique et Robotique*

Par

Yang DENG

Delay estimation and predictor-based control of time-delay systems with a class of various delays

Thèse présentée et soutenue à Nantes, le 8 juillet, 2020
Unité de recherche : UMR 6004, Laboratoire des Sciences du Numérique de Nantes (LS2N)

Rapporteurs avant soutenance :

Alexandre SEURET	Directeur de Recherche CNRS, LAAS-CNRS, Toulouse
Pierdomenico PEPE	Professeur associé, Université de L'Aquila, Italie

Composition du Jury :

Président :	Jean-Pierre RICHARD	Professeur des universités, Centrale Lille, Villeneuve d'Ascq
Examinateurs :	Alexandre SEURET	Directeur de Recherche CNRS, LAAS-CNRS, Toulouse
	Pierdomenico PEPE	Professeur associé, Université de L'Aquila, Italie
Directeur de thèse :	Franck PLESTAN	Professeur des universités, École Centrale de Nantes, Nantes
Co-dir de thèse :	Emmanuel MOULAY	Chargé de Recherche HDR CNRS, XLIM, Poitiers
Co-encadrant :	Vincent LÉCHAPPÉ	Maître de conférence, INSA de Lyon, Villeurbanne

Remerciements

J'adresse également toute ma reconnaissance aux personnes mentionées ci-dessous qui me soutient pour finir la thèse.

Tout d'abord, je tiens à adresser mes sincères remerciements à mon directeur de thèse Prof. Franck Plestan, et mes deux co-encadrants Dr. Emmanuel Moulay et Dr. Vincent Léchappé. J'ai beaucoup profité de nos discussions chaque semaine, et j'ai été beaucoup encouragé par eux. Ils jouent des rôles différents dans ma thèse: Franck génère les progrès et l'orientation globale de la thèse, Emmanuel m'aide beaucoup sur la partie théorique de la thèse (*e.g.* les modélisations et les preuves), Vincent communique avec moi plus fréquemment, et il travaille avec moi dans tous les détails. Sans l'aide de l'un d'eux, ma thèse n'aurait pas la qualité actuelle. Je tiens à vous témoigner ma gratitude pour la confiance et l'inspiration que vous m'avez données.

Ensuite, je voudrais exprimer ma gratitude à mon affiliation (École Centrale de Nantes) et à l'organisation CSC (China Scholarship Council) qui me donnent cette opportunité de faire ma thèse en France. Dans le même temps, je suis également témoin de l'approfondissement de la coopération entre la France et la Chine dans le domaine de l'éducation et la recherche, et j'espère sincèrement que l'amitié entre les deux pays s'approfondira.

Il y a deux éxperimentations dans la thèse, je voudrais remercier ceux qui m'ont aidé dans des éxperimentations. Pour les expérimentations d'estimation du retard, M. Sébastien Rouquet m'a quand même aidé à faire les éxperimentations même si son papier n'était pas encore fini, cela m'a touché beaucoup. Je remercie également mes collègues en Chine et en Australie (Prof. Qing-Long Han, Prof. Dajun Du, et M. Changda Zhang), ils m'ont donné l'opportunité d'aller à l'Université de Shanghai pour des éxperimentations et m'ont aidé pendant et après le séjour en Chine.

Je voudrais remercier les membres du jury (Prof. Jean-Pierre Richard, Prof. Alexandre Seuret et Prof. Pierdomenico Pepe) pour ma thèse, vos commentaires m'ont aidé à améliorer mon travail.

Enfin, je remercie ma famille pour ses encouragements et son soutien lorsque je rencontre des difficultés de recherche, ils sont ma grande motivation pour progresser la thèse.

Table of Contents

List of Figures

List of Tables

List of Acronyms

TDS Time-delay System 17
NCS Networked Control System 13
RCS Remote Control System 13
TDE Time-delay Estimation 35
NIPVSS Networked Inverted Pendulum Visual Servo System 18
LTI Linear Time-Invariant 39
RFDE Retarded Functional Differential Equation 153
SM Sliding Mode 94
STW Super-Twisting 94
ASTW Adaptive Super-Twisting 94
PDE Partial Differential Equation 20
LMI Linear Matrix Inequality 20
FSA Finite Spectrum Assignment 22
ROS Robot Operating System 98
LQR Linear–Quadratic Regulator 142
GUAS Golbally Uniformly Asymptotically Stable 62
GUES Globally Uniformly Exponentially Stable 60

CONTEXTE ET ORGANISATION DE LA THÈSE

Motivation

L'objectif de cette thèse est de développer des lois de commande pour les systèmes à retard avec retards longs inconnus ou incertains. L'idée principale est d'estimer les retards et de stabiliser le système avec une méthode de commande prédictive. Le retard est un phénomène largement présent dans le monde physique, comme par exemple dans:

— systèmes hydrauliques (Fridman 2014a, Chapitre 1.1.1);
— systèmes biochimiques (Schell and Ross 1986);
— systèmes pneumatiques (F. Yang et al. 2017).

La deuxième source de retard est la transmission des données. Les systèmes commandés à distance (remote control systems, Remote Control System (RCS)) et les systèmes commandés en réseau (networked control systems, Networked Control System (NCS)) sont aujourd'hui de plus en plus utilisés. Dans ces syst'emes, les capteurs, les contrôleurs, et les actionneurs ne sont plus connectés physiquement et des retards apparaissent à cause des canaux de transmission sans fil.
La troisième source de retard est le temps de calcul des systèmes complexes. Par exemple, le véhicule autonome (Furgale et al. 2013) utilise les techniques de reconstruction 3D pour générer des cartes et éviter les obstacles, mais la complexité de calcul de ces algorithmes est grande et nécessite beaucoup de temps de calcul. Par conséquent, ce type de retard est généralement plus long que les deux autres types des retards (de l'ordre de plusieurs dizaines de millisecondes).
De nombreux systèmes de commande contiennent plusieurs types de retards différents. Les travaux de (Zhan, Du, and Fei 2017; Du, C. Zhang, et al. 2019) détaillés ci-dessous illustrent les différents types de retards:

Asservissement visuel d'un pendule inverse commandé en réseau

Sur la platforme de (Zhan, Du, and Fei 2017; Du, Wangpei Li, et al. 2016), les mouvements du pendule inverse et du chariot sont mesurés par une caméra industrielle *Aca640-120gm*, les états du système sont estimés par l'algorithme de traitement d'image basé sur *Microsoft Visual Studio 2010* et *OpenCV 2.4.11*. Les informations sont transférées au contrôleur en réseau et sont utilisées pour calculer la loi de commande. Finalement, le signal de commande est envoyé à la carte de commande de mouvement *GT-400-SV-PCI* en réseau. Enfin, la commande est appliquée à un driver *MSDA023A1A* qui actionne le chariot pour stabiliser le pendule.

Les retards suivants apparaissent donc sur la platforme de (Zhan, Du, and Fei 2017; Du, C. Zhang, et al. 2019):

1. **Retards physiques:** le temps d'exposition de la caméra industrielle et le temps d'actionnement du driver du moteur (presque négligeable);
2. **Retards de transmission:** les retards introduits par le réseau entre le capteur, le contrôleur et l'actionneur (quelques millisecondes);
3. **Retards de calcul:** le temps de calcul de l'algorithme de traitement d'image (environ 20 ms) et le temps de calcul du contrôleur (presque négligeable).

Les discussions ci-dessus expliquent que le retard est un phénomène commun dans les systèmes réels. De plus, le retard peut affecter les performances du système, il est une source d'instabilité qui doit être compensée (Fridman 2014a, p.vii). En outre, si les retards sont longs, les techniques conventionnelles ne peuvent plus stabiliser les systèmes à retard. Par conséquent, le premier objectif de la thèse est formulé ainsi:

Premier objectif de la thèse: Développer des lois de commande qui stabilise les systèmes avec retards longs (retards constants ou variants dans le temps).

La commande prédictive est une solution qui compense les retards arbitrairement longs, mais les valeurs des retards et des paramètres du système doivent être connues à priori. Dans les systèmes réels, les retards sont souvent incertains ou inconnus ce qui rend la stratégie de commande plus difficile. Pour résoudre ces problèmes, le deuxième objectif de la thèse est proposé ci-dessous:

Deuxième objectif de la thèse: Développer les techniques d'estimation du retard qui peuvent estimer les retards constants ou variants.

En conclusion, après avoir considéré les deux objectifs mentionnés précédemment, l'objectif général de la thèse est:

Objectif général de la thése: Construire les lois de commande pour les systèmes avec retards longs, inconnus ou incertains en utilisant des techniques d'estimation du retard et la commande prédictive.

Selon les différents types des systèmes et de retards, les trois cas suivant seront analysés dans la thèse:

— Systèmes continus avec retards inconnus et constants;
— Systèmes commandés à distance avec retards inconnus et variants;
— Systèmes commandés en réseau avec retards variants et incertains.

Organisation de la thèse

Dans les Chapitres 1-3, les lois de commande des trois types de systèmes sont analysées, l'organisation de chaque chapitre est détaillée ci-dessous:

— Chapitre 1 propose un nouvel algorithme d'estimation du retard pour des systèmes avec retards constants et inconnus. L'algorithme utilise l'historique du signal de commande pour estimer les retards, il est toujours croissant et inférieur au retard constant inconnu (la condition initiale est plus petite que le retard). Lorsque l'erreur est suffisamment petite, la stabilité en boucle fermée est assurée. Dans les sous-sections 1.2.2-1.2.4, trois estimateurs de retard basés sur cette idée sont introduits pour stabiliser le système avec un seul retard sur l'entrée. Un observateur de Luenberger est utilisé dans sous-section 1.2.5 pour la commande des systèmes avec retards sur l'entrée et la sortie et pour lesquels tout l'état n'est pas mesuré. Enfin, des simulations illustrent les performances des méthodes proposées et il est montré que les estimateurs de retard proposés sont robustes par rapport aux incertitudes du modèle.
— Dans le Chapitre 2, l'estimation de retard et la commande prédictive pour les systèmes commandés à distance sont développées. Les retards variants sont estimés de manière pratique: une boucle de communication spécifique est utilisée pour estimer le retard, et le système est stabilisé par une commande prédictive. L'algorithme d'estimation de retard est basé sur les méthodes de mode glissants d'ordres 1 et 2, et la convergence en temps fini est assurée. Il a été montré que les retards variants sont correctement estimés expérimentalement sur un réseau WiFi et que la méthode est robuste par rapport aux bruits et aux cyber-attaques notamment. Enfin, les preuves démontrent que la combinaison de la commande prédictive et l'estimation du retard pratique peuvent stabiliser le système. Les contraintes sur la variation du retard de sortie sont assez faibles et la stabilité est préservée si le retard d'entrée varie suffisamment lentement.
— L'objectif du Chapitre 3 est la commande prédictive basée sur la méthode discrète pour les systèmes commandés en réseau. Dans ce type de système, le retard capteur-contrôleur peut être directement mesuré à l'aide de la synchronisation d'horloge, et le retard contrôleur-actionneur est considéré incertain. En effet, grâce à la modélisation discrète, la méthode proposée peut compenser les retards longs et variants, et compenser les ré-ordonnancements de paquets dans le canal capteur-contrôleur. Un autre avantage de cette méthode est la

possibilité d'avoir une période d'échantillonnage plus longue. Finalement, cette méthode est validée sur une maquette asservissement visuel de pendule inverse commandée en réseau (Zhan, Du, and Fei 2017; Du, C. Zhang, et al. 2019). Les performances sont meilleures que les méthodes de commande non-prédictives.

Certains des résultats de la thèse ont été publiés ou acceptés dans des conférences ou des revues.

Revues internationales

[1] Y. Deng, V. Léchappé, S. Rouquet, E. Moulay, and F. Plestan, *Super-twisting algorithm based time-varying delay estimation with external signal*, publié en ligne dans IEEE Transactions on Industrial Electronics. doi: `10.1109/TIE.2019.2960739`.

[2] Y. Deng, V. Léchappé, E. Moulay, and F. Plestan, *State feedback control and delay estimation for LTI system with unknown input-delay*, publié en ligne dans International Journal of Control. doi:`10.1080/00207179.2019.1707288`.

[3] Y. Deng, V. Léchappé, E. Moulay, and F. Plestan, *Predictor-based control of LTI remote systems with estimated time-varying delays*, dans IEEE Control Systems Letters, vol 5, issue 1, pages 289-294, Jan 2021.

Conférences internationales

[1] Y. Deng, V. Léchappé, E. Moulay, and F. Plestan, *Prediction-based control with delay estimation of LTI systems with input-output delays*, communiqué dans 2019 American Control Conference (ACC), Philadelphie, USA, pages 3702-3707.

[2] Y. Deng, V. Léchappé, S. Rouquet, E. Moulay, and F. Plestan, *A practical online time-varying delay estimation of remote control system based on adaptive super-twisting algorithm*, accepté dans 2020 IEEE Conference on Control Technology and Applications (CCTA), Montréal, Canada.

General Introduction

Contents

Motivation

This thesis is devoted to the predictor-based control and delay estimation of time-delay systems (Time-delay System (TDS)). Time-delay is a widely-found physical phenomenon in many real systems, including but not limited to:

— hydraulic systems (Fridman 2014a, Chapter 1.1.1);
— bio-chemical systems (Schell and Ross 1986);
— pneumatic systems (F. Yang et al. 2017).

In recent decades, with the development of telecommunication and network, remote control systems (S.-H. Yang 2011) (RCS) and networked control systems (X.-M. Zhang, Han, and Yu 2015) (NCS) have attracted the attention of the control community. In such systems, the components (sensors, controllers, and actuators) are no longer directly connected to each other, they communicate through wireless communication. As a result of data transmissions, communication protocols, and network

congestions, RCS and NCS are subject to the communication latencies called “transmission delay” or “network-induced delays”.

Computation time is another source of time-delay, since more and more control systems deal with complex objectives (*e.g.* self-driving car (Furgale et al. 2013), networked visual servo robot (H. Wu et al. 2012), networked visual servo inverted pendulum (Du, C. Zhang, et al. 2019)). In such systems, the controller designs include complex computations (*e.g.* 3D reconstruction and online map generation in (Furgale et al. 2013), image-processing algorithm in (H. Wu et al. 2012; Du, C. Zhang, et al. 2019)), and the computation times of such algorithms are more than 10 milliseconds. In such systems, one must consider the effects of the computation time since they are even longer than the network-induced delays (Alasmary and Zhuang 2012, Fig. 9(b)).

Consider the networked inverted pendulum visual servo system (Networked Inverted Pendulum

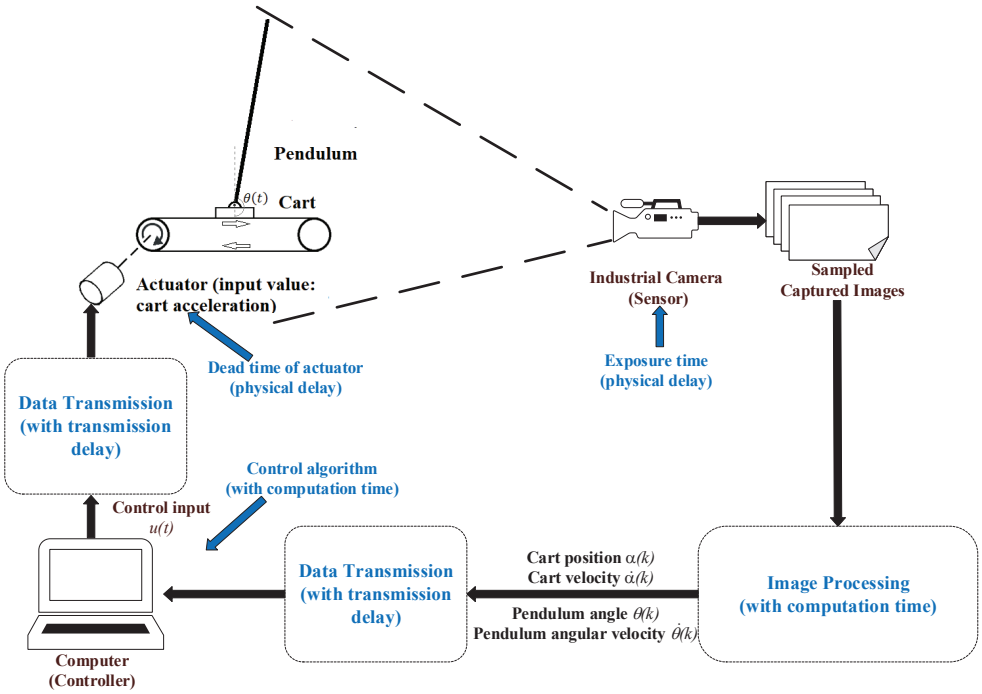

Figure 1 – Control framework of the NIPVSS (Du, C. Zhang, et al. 2019).

Visual Servo System (NIPVSS)) given in (Du, C. Zhang, et al. 2019) as an example (see Figure 1), the movement of the inverted pendulum is captured by an *Aca640-120gm* monochrome industrial camera, then the state information $x(t)$ is obtained by the image processing algorithm (based on *Microsoft Visual Studio 2010* and *OpenCV 2.4.11*) on each frame. The computer receives the resolved state information via a communication network and runs the control algorithm, then it sends the control signal to a *GT-400-SV-PCI* movement control card via network. Finally, a *MSDA023A1A* servo driver receives the control signal and drives the cart to move on the rail. The NIPVSS is subject to the following time-delays: c The NIPVSS is subject to the combination of the 3 different

types of time-delays (physical delay, transmission delay, computation time) mentioned before, and some time-delays (time-delays 2, 3, 5) are non-ignorable and time-varying. Thus, these delays are taken into account by the authors of (Du, C. Zhang, et al. 2019) in the modeling and controller design (see (Du, C. Zhang, et al. 2019, Fig. 2)).

On the one hand, the above discussions on the NIPVSS (Du, C. Zhang, et al. 2019) explain that time-delay is a widespread phenomenon in various control systems that should be considered. On the other hand, time-delay is a source of instability (Fridman 2014a, p. vii) that must be compensated. If one does not consider the time-delay in the controller design, the control performance will be degraded (slower response, worse disturbance attenuation). Moreover, if the time-delay is long, the conventional control techniques (*i.e.* memoryless control techniques) cannot be guarantee closed-loop stability. Thus, the first objective of the thesis is clarified as follows:

The first objective of this thesis is to propose control solutions that can compensate long time-delays of control systems.

Predictor-based controller (Karafyllis and Miroslav Krstic 2017) is one of the well-known controllers that deals with long time-delays. If the system model and the delay value are known, one can perfectly compensate the time-delay by predicting the future state of the system. However, the time-delays of many real control systems are unknown or uncertain, that makes the controller design more difficult. According to the previous discussion, the second objective of this thesis is raised:

The second objective of this thesis is to develop delay estimation approaches that assist the predictor-based controller in stabilizing the system.

Thus, the main objective of the thesis is summarized as:

The objective of this thesis is to build control law for systems with long, unknown or uncertain time-delay by using predictor-based controller and delay estimation.

The objective of this thesis is challenging since the control strategies for different systems with different time-delays are quite different. Thus, the following three objectives are investigated in this thesis:

— predictor-based control of systems with unknown constant delays;
— predictor-based control of remote control systems with unknown time-varying delays;
— predictor-based control of networked control systems with time-varying delays.

State feedback of systems with small delay

In this section, one presents the fact that the convential control strategies (*e.g.* state feedback) can stabilize the systems with sufficiently small delay by using the results given in (Fridman 2014a, Section 5.2.1). Consider the input-delay system

$$\dot{x}(t) = Ax(t) + Bu(t - \tau(t)), \quad t \geq 0 \tag{1}$$

with $x(t) \in \mathbb{R}^n$, $u(t) \in \mathbb{R}^m$, the time-varying delay $\tau(t)$ satisfies $\tau(t) \in [0, h]$ and $|\dot{\tau}(t)| \leq d < 1$. The state feedback control $u(t) = Kx(t)$ leads to the closed-loop system

$$\dot{x}(t) = Ax(t) + BKx(t - \tau(t)), \quad t \geq 0. \tag{2}$$

As stated in (Fridman 2014a, Section 5.2.1), in order to make the closed-loop system (1) uniformly asymptotically stable, one must search for appropriate matrices P, Q, R, and S such that the following linear matrix inequality (Linear Matrix Inequality (LMI)) is feasible:

$$\begin{bmatrix} A^TP + PA + S + Q - R & 0 & PBK + R & hA^TR \\ * & -S - R & R & 0 \\ * & * & -(1-d)Q - 2R & hK^TB^TR \\ * & * & * & -R \end{bmatrix} < 0. \tag{3}$$

Remind that the sufficient stability condition (3) is a "delay-dependent" condition to the uniform asymptotic stability since the delay bound h appears in the LMI (3) and it can affect the feasibility of (3). Indeed, it is impossible to find feasible solution P, Q, R, S, K for (3) if the bound (on the time-varying delay $\tau(t)$) h exceeds a certain value. In this case, one cannot find any stable state feedback control solution via (3).
Thus, the discussions explain that the conventional control techniques are effective to the systems with small enough delays, and the control law must be improved if the system is subject to long time-delays.

Predictor-based control of systems with long time-delay

As stated in the previous section, the conventional control methods cannot effectively stabilize the systems with arbitrarily-long time-delay. Predictor-based controller (Karafyllis and Miroslav Krstic 2017) is a well-known solution to such problems, an overview of this method is given in the sequel (according to different types of systems and time-delays):

— **Continuous-time system, constant delay**: Smith predictor (Smith 1959), Finite Spectrum Assignment (Manitius and Olbrot 1979), model reduction (Artstein 1982), predictor-based controller with backstepping transformation (Bekiaris-Liberis and Miroslav Krstic 2013);

— **Continuous-time system, time-varying delay**: predictor-based controller with Partial Differential Equation (PDE) transformation (Bekiaris-Liberis and Miroslav Krstic 2013, Chapter 6), dynamic observation-predictor-based control (Léchappé, Moulay, and Plestan 2016; Weston, Malisoff, and Frédéric Mazenc 2017);

— **Networked control system, constant delay**: sampled predictor-based control (Seliv-

anov and Fridman 2016b), discrete predictor-based controller (Lozano et al. 2004; Léchappé, Moulay, Plestan, and Han 2019);

— **Networked control system, time-varying delay**: discrete predictor-based controller (Hu and Zhu 2003; Cloosterman et al. 2009).

The cited references will be introduced in details in the sequel.

Predictor-based control of continuous-time systems with constant delays

In this part, the conventional predictor-based control techniques of systems with constant delay are introduced. In the 1950's, Smith predictor (Smith 1959) is firstly introduced to compensate the dead time (input-delay) of control systems with the use of an inner loop that works as a "predictor". Consider a delay-free system $H_0(s)$ which is subject to a constant dead time h, then the open-loop transfer function of the TDS reads as

$$H(s) = H_0(s)e^{-hs} = \frac{N(s)e^{-hs}}{D(s)} \tag{4}$$

where $N(s)$ and $D(s)$ are characteristic polynomials of the delay-free plant $H_0(s)$.

The control diagram of the Smith predictor presented in Figure 2, one firstly computes the transfer

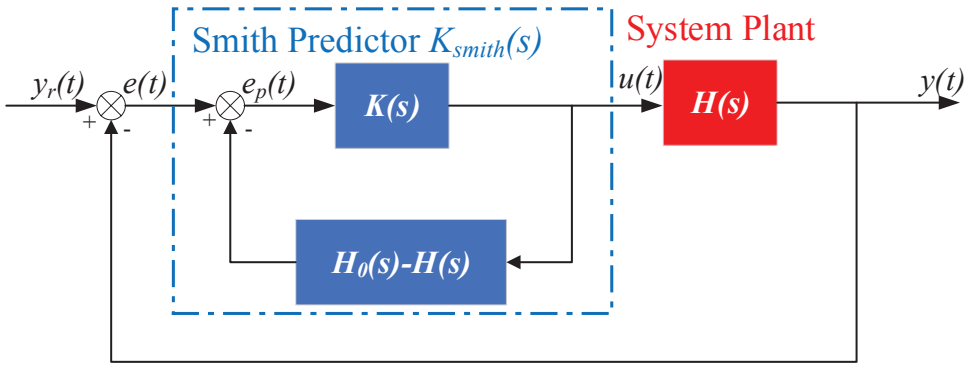

Figure 2 – Control diagram of the Smith predictor (Smith 1959).

function of the inner-loop system with

$$\frac{U(s)}{E(s)} = K_{Smith}(s) = \frac{K(s)}{1 + K(s)[H_0(s) - H(s)]} = \frac{K(s)D(s)}{D(s) + K(s)N(s)(1 - e^{-hs})}. \tag{5}$$

According to (5), the closed-loop transfer function is given as follows:

$$\frac{Y(s)}{Y_r(s)} = \frac{K_{Smith}(s)H(s)}{1 + K_{Smith}(s)H(s)} = \frac{K(s)N(s)}{D(s) + K(s)N(s)}e^{-hs}. \tag{6}$$

As shown in (6), the delay term e^{-hs} cannot affect the closed-loop stability, and $K(s)$ can be computed as if the open-loop system is delay-free. The Smith predictor is the first control solution dealing with arbitrarily long time-delay, but it cannot deal with unstable plant. Several works (Watanabe and Ito 1981; Furukawa and Shimemura 1983) have solved this problem, and these results are called "modified Smith predictor".

A few decades later, the Smith predictor is extended to the state-space representation with Finite Spectrum Assignment (Finite Spectrum Assignment (FSA)) (Manitius and Olbrot 1979) and model reduction (Artstein 1982), the time-domain control law is derived to stabilize unstable open-loop systems. The control strategies of the two methods are similar, they predict the future state of the system and transform the closed-loop system into a delay-free form, the predictive control law is then obtained by using the prediction and the delay-free system. The FSA technique is firstly introduced, consider the input-delay system

$$\dot{x}(t) = Ax(t) + Bu(t-h), \quad t \geq 0 \tag{7}$$

where $x(t) \in \mathbb{R}^n$, $u(t) \in \mathbb{R}^m$, $A \in \mathbb{R}^{n\times n}$, $B \in \mathbb{R}^{n\times m}$, and $h > 0$ is a known input-delay. Different from the state feedback control given in the previous section, one chooses $u(t) = Kx(t+h)$ as the control, then the closed-loop dynamics becomes to the following delay-free system:

$$\dot{x}(t) = Ax(t) + BKx(t+h-h) = (A+BK)x(t) \tag{8}$$

for all $t \geq h$, and K can be calculated with pole placement techniques. By integrating (7) from t to $t+h$ with initial condition $x(t)$, the prediction $x(t+h)$ reads as

$$x(t+h) = e^{Ah}x(t) + \int_{t-h}^{t} e^{A(t-s)}Bu(s)\mathrm{d}s. \tag{9}$$

Consider (8)-(9), the closed-loop system satisfies that

$$\dot{x}(t) = \begin{cases} e^{At}x(0) + \int_0^t e^{A(t-s)}Bu_0(s)\mathrm{d}s, 0 < t < h \\ (A+BK)x(t), \quad t \geq h \end{cases} \tag{10}$$

where $u_0(s) = u(s-h), \quad 0 \leq s \leq h$ denotes the initial condition of the system (7). It is observed that the closed-loop system (10) becomes to delay-free after a finite-time transient, and the input-delay is perfectly compensated after this transient.

After introducing the main idea of FSA, the model reduction method (Artstein 1982) is introduced. At this time, the auxiliary variable

$$z(t) = x(t) + \int_{t-h}^{t} e^{A(t-s-h)}Bu(s)\mathrm{d}s \tag{11}$$

is used to replace the explicit prediction (9). Differentiating (11) along the trajectories of (7) leads to the following delay-free system

$$\dot{z}(t) = Az(t) + e^{-Ah}Bu(t). \tag{12}$$

Indeed, (11) transforms the original system into the delay-free system (12), then one can build a state feedback control law based on the reduced model (12), and finally the original system (7) is also stabilized. Comparing (9) and (11), it is easy to find that

$$x(t+h) = e^{Ah}z(t) \tag{13}$$

which explains the similarity of the FSA and model reduction: they are just two different solutions based on the same concept.

The last part of this subsection is to introduce another representation of the predictor-based control of (7) with backstepping transformation (Bekiaris-Liberis and Miroslav Krstic 2013, Chapter 2.1.2). The control solution is shown in Figure 3, the main idea is to transform the infinite-dimensional

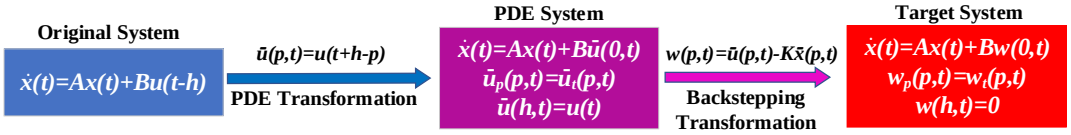

Figure 3 – Mathematical transformations of the predictor-based controller given in (Bekiaris-Liberis and Miroslav Krstic 2013, Chapter 2.1.2).

term $u_t(\theta)$, $\theta \in [-h, 0]$ into a partial differential equation (PDE) form by using the following transformation:

$$\bar{u}(p,t) = u(t-h+p), \quad p \in [0,h]. \tag{14}$$

With the help of the PDE transformation (14), the future state of the system reads as

$$\bar{x}(p,t) = x(t+p) = e^{Ap}x(t) + \int_0^p e^{A(p-y)}B\bar{u}(y,t)\mathrm{d}y, \qquad p \in [0,h]. \tag{15}$$

Thus, the predictor-based control law is computed with

$$u(t) = \bar{u}(h,t) = K\bar{x}(h,t) \tag{16}$$

where K makes $A+BK$ Hurwitz.

Remind that last system of Figure 3 is the target system of the backstepping transformation, and the term $Bw(0,t)$ is a "disturbance term" of the nominal target system $\dot{x}(t) = (A+BK)x(t)$ that vanishes in finite time. Finally, the exponential stability of the backstepping target system ensures

the exponential stability of the original system. Consider the control laws (16) and (9), it is evident that they are equivalent. Indeed, as stated in (Bekiaris-Liberis and Miroslav Krstic 2013, Chapter 2.1.3), the backstepping transformation allows for the construction of a Lyapunov functional for the target system, which is simpler than the FSA technique .

Example: Conventional state feedback and predictor-based control

Consider the system

$$\dot{x}(t) = \underbrace{\begin{bmatrix} 0 & 1 \\ 0.1 & 0.1 \end{bmatrix}}_{A} x(t) + \underbrace{\begin{bmatrix} 0 \\ 1 \end{bmatrix}}_{B} u(t-h) \tag{17}$$

with $h = 0.5$, it is controlled by the conventional state feedback $u(t) = Kx(t)$ and the predictor-based controller

$$u(t) = K\left[e^{Ah}x(t) + \int_{t-h}^{t} e^{A(t-s)}Bu(s)\mathrm{d}s\right]. \tag{18}$$

In order to fairly compare the two controller, the matrix K is set to $K = \begin{bmatrix} -2.1 & -3.1 \end{bmatrix}$ for both of them (the eigenvalues of $A + BK$ are set to -1 and -2).
Figure 4 claims that the conventional state feedback control fails to stabilize the system, since the time-delay is longer than the allowable value of this controller. However, the predictor-based control is effective, which implies that the predictor-based control deals with longer time-delays than the conventional state feedback control.

Remark 1. *As stated in (Van Assche et al. 1999), some numerical problems can arise from the calculation of the integral term of* (9) *since it is an infinite-dimensional term, inappropriate implementation can lead to unstable closed-loop system. To overcome this problem, some techniques are available:*

- *a safety implementation technique given in (Mondié and Michiels 2003) is proposed to overcome the instability, the control law is modified with the help of a low-pass filter;*
- *in (Zhou 2014b; Zhou, Q. Liu, and Frédéric Mazenc 2017), an artificial finite-dimensional system that predicts the future state is used to replace the infinite-dimensional predictor;*
- *the work of (Bresch-Pietri, Chauvin, and Petit 2012, p.1548) indicated that a trapezoidal discretization method and a periodic reset can be used to overcome the numerical issues.*

In this subsection, four predictor-based control solutions of systems with arbitrarily long constant delay are introduced, although they are computed in different ways, they stand on the same concept:

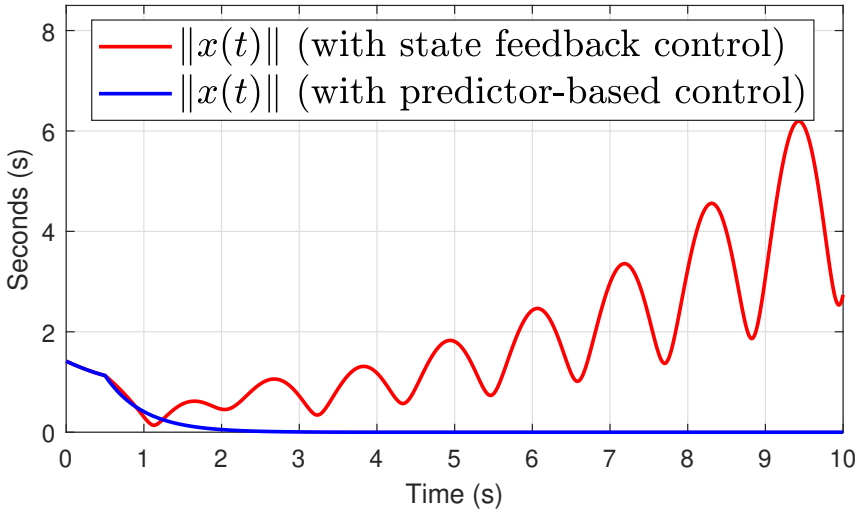

Figure 4 – State evolution of system (17) with state feedback control and predictor-based control.

transforming the original time-delay system to a delay-free form via predictive techniques, then designing the controller based on the delay-free system. The following table gives an overview of these predictive approaches:

Methods	System type	Open-loop system type
Smith predictor (Smith 1959)	Transfer function	Stable
FSA (Manitius and Olbrot 1979)	State space	Stable, unstable
Model reduction (Artstein 1982)	State space	Stable, unstable
Backstepping (Bekiaris-Liberis and Miroslav Krstic 2013)	State space, PDE	Stable, unstable

Table 1 – Overview of the predictor-based control techniques.

Predictor-based control of continuous-time systems with time-varying delays

Various of real control systems are subject to time-varying delays (*e.g.* remote servo motor control (Lai and Hsu 2010), visual servo control (Chakraborty et al. 2017), NIPVSS (Du, C. Zhang, et al. 2019)) due to transmission delays and computation times, then the predictor-based control of such system has application prospects. In this subsection, two types of predictor-based controllers are introduced, the first one (Bekiaris-Liberis and Miroslav Krstic 2013, Chapter 6) is based on the backstepping method, and the second one (Weston, Malisoff, and Frédéric Mazenc 2017; Léchappé, Moulay, and Plestan 2016) uses observation dynamics to calculate the prediction.
One firstly introduce the predictor-based control with backstepping transformation (Bekiaris-Liberis

and Miroslav Krstic 2013, Chapter 6), and one considers the system

$$\dot{x}(t) = Ax(t) + Bu(t - h(t)), \quad t \geq 0 \tag{19}$$

with $x(t) \in \mathbb{R}^n$, $u(t) \in \mathbb{R}^m$, $A \in \mathbb{R}^{n\times n}$, $B \in \mathbb{R}^{n\times m}$, and $h(t) > 0$.

Since the time-delay is no longer constant, the control scheme of this case (see Figure 5) is more

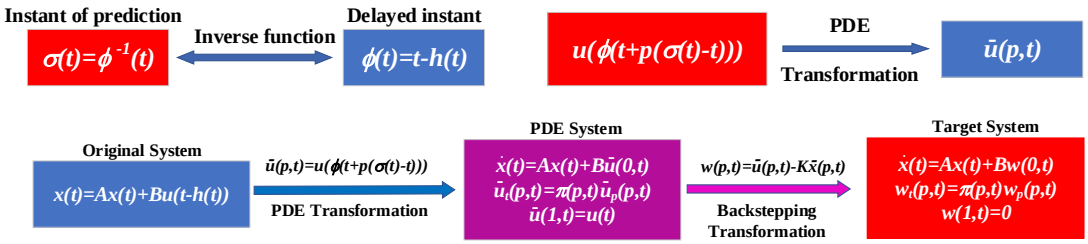

Figure 5 – Mathematical transformations of the predictor-based controller given in (Bekiaris-Liberis and Miroslav Krstic 2013, Chapter 6).

complicated than the one of Figure 3, and the functions $\phi(t) = t - h(t)$, $\sigma(t)$ are necessary to the following PDE transformation:

$$\bar{u}(p,t) = u\left(\phi(t + p(\phi^{-1}(t) - t))\right). \tag{20}$$

After a careful calculation, system (19) is transformed into the PDE system given in Figure 5 with:

$$\pi(p,t) = \frac{1 + p\left(\frac{d\left(\phi^{-1}(t)\right)}{dt} - 1\right)}{\phi^{-1}(t) - t}. \tag{21}$$

Next, the future state of the system reads as

$$\bar{x}(p,t) = e^{Ap(\sigma(t)-t)}x(t) + (\sigma(t) - t)\int_0^p e^{A(p-y)(\sigma(t)-t)}B\bar{u}(y,t)\mathrm{d}y \tag{22}$$

and the control law satisfies

$$u(t) = \bar{u}(1,t) = K\bar{x}(1,t) \tag{23}$$

with $A + BK$ Hurwitz. Thus, by virtue of the backstepping transformation

$$w(p,t) = \bar{u}(p,t) - K\bar{x}(p,t), \tag{24}$$

the target system is obtained, as shown in Figure 5.

Finally, the exponential stabilities of the target system and the original system are guaranteed by the Lyapunov-Krasovskii analysis, the details of the proof are given in (Bekiaris-Liberis and Miroslav

Krstic 2013, p.122-127). Remind that the predictor (15) for constant delay is a particular case of the predictor (22). The fact $h(t) = h$ implies $\sigma(t) = t + h$, then one has $\pi(p, t) = 1/h$, and consequently the PDE and target systems displayed in Figure 5 are reduced to the simplified versions presented in Figure 3.

The drawback of the conventional predictor (22) is twofold:

— in real applications, the numerical computation of the infinite-dimensional term (*i.e.* the integral term) may lead to unstable closed-loop system (Van Assche et al. 1999);

— the inverse function $\sigma(t)$ cannot be easily computed in real control systems with explicit form, it can only be estimated by an adaptation law (Witrant et al. 2007), which may degrade the performance of the control system.

To handle the issues mentioned above, the dynamic observation-predictor-based control (Weston, Malisoff, and Frédéric Mazenc 2017; Léchappé, Moulay, and Plestan 2016) is proposed. With this technique, the infinite-dimensional term and the inverse function $\sigma(t)$ are no longer required, and an observer-like dynamic is used to approximately estimate the prediction (15). The main results of (Léchappé, Moulay, and Plestan 2016) are used to introduce the main idea of the dynamic observation-prediction. Consider the system with time-varying input-delay and partial state knowledge:

$$\begin{cases} \dot{x}(t) = Ax(t) + Bu(t - h(t)) \\ y(t) = Cx(t) \end{cases} \tag{25}$$

with $x(t) \in \mathbb{R}^2$, $u(t) \in \mathbb{R}^m$, $y(t) \in \mathbb{R}^p$, $A \in \mathbb{R}^{n\times n}$, $B \in \mathbb{R}^{n\times m}$, $C \in \mathbb{R}^{p\times n}$, and $h(t) > 0$. Firstly, suppose that delay-free system can be stabilized by a globally Lipschitz controller $u : \mathbb{R}^n \mapsto \mathbb{R}^m$. In a similar way, one supposes that there exists a globally Lipschitz function $g : \mathbb{R}^p \mapsto \mathbb{R}^n$ such that the Luenberger observer

$$\dot{\hat{x}}(t) = A\hat{x}(t) + Bu(t - h(t)) + g(C\hat{x}(t) - y(t)) \tag{26}$$

exponentially converges to $x(t)$. After stating the necessary assumptions, the observation-predictor-based controller

$$\begin{cases} \dot{z}(t) = Az(t) + Bu(t) + g\left[Cz(t - h(t)) - y(t)\right] \\ u(t) = u(z(t)) \end{cases} \tag{27}$$

stabilizes the system (25) if the time-varying delay $h(t)$ satisfies

$$h(t) \leq h^*, \quad |\dot{h}(t)| \leq \delta^* \tag{28}$$

with sufficiently small positive constants h^*, δ^* (*i.e.* the time-varying delay $h(t)$ and its derivative are sufficiently small). Indeed, the "dynamic observation" $z(t)$ is an approximation of the future state $x(\sigma(t))$, and the observation is established without using $\sigma(t)$ explicitly, this is the reason why

this technique is called "observation-prediction". However, according to (28), this method only deals with small and slow-varying delays. Thus, the following sub-predictors are proposed:

$$\begin{cases} \dot{z}_1(t) & = Az_1(t) + Bu(t-(r-1)\bar{h}(t)) + g_1\left[Cz_1(t-\bar{h}(t)) - Cx(t)\right] \\ \dot{z}_2(t) & = Az_2(t) + Bu(t-(r-2)\bar{h}(t)) + g_2\left[Cz_2(t-\bar{h}(t)) - Cz_1(t)\right] \\ & \vdots \\ \dot{z}_i(t) & = Az_i(t) + Bu(t-(r-i)\bar{h}(t)) + g_i\left[Cz_i(t-\bar{h}(t)) - Cz_{i-1}(t)\right] \\ & \vdots \\ \dot{z}_r(t) & = Az_r(t) + Bu(t) + g_r\left[Cz_r(t-\bar{h}(t)) - Cz_{r-1}(t)\right] \end{cases} \tag{29}$$

with a sufficiently large integer r. Then the system (25) can be stabilized with control law $u(z_r(t))$. The main concept of the sub-predictors (29) is that, although $h(t)$ and $\dot{h}(t)$ can be large, there always exists a sufficiently large r, such that $\bar{h}(t) = h(t)/r$ and $\dot{\bar{h}}(t) = \dot{h}(t)/r$ are sufficiently small for the controller design. Thus, each dynamic given in (29) can successfully converge the true state predictions, and then the constraints (28) is relaxed.

To well explain how this technique works, Figure 6 is provided. Assume that the time-varying

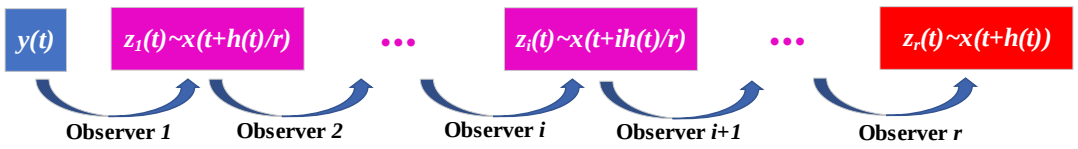

Figure 6 – Estimation chain of the observer-based sub-predictors (29).

delay $h(t)$ and its derivative $\dot{h}(t)$ are large, then one use r sub-predictors to stabilize the system. One inserts the system output $y(t) = Cx(t)$ into the first predictor of (29) in order to make $z_1(t)$ converges to $x(t+\bar{h}(t)) = x(t+h(t)/r)$, and $z_1(t)$ is applied in the second predictor to estimate the future state $x(t+2\bar{h}(t))$. Recursively, the rth observer converges to the expected future state $x(t+h(t))$, and it is used to stabilize the system (25). With the observation chain displayed in Figure (6), larger bounds on the delay value and delay derivative is endured for the control law design.

Example: Comparison between 1-sub predictor and 2-sub predictor

Consider the system (17) with partial state knowledge $y(t) = Cx(t) = \begin{bmatrix} 1 & 0 \end{bmatrix} x(t)$, and time-varying delay $h(t) = 0.9 + 0.5 \sin 0.8\cdot$. It is controlled by the observation-predictor-based controller (27) and the sub-predictors technique (29). The functions $g(\cdot)$ and $u(\cdot)$ are set to $u(z) = \begin{bmatrix} -2.1 & -3.1 \end{bmatrix} \cdot z$ and $g(e) = \begin{bmatrix} -1.6 & -0.76 \end{bmatrix}^T \cdot e$, respectively.
See Figure 7, the controller (27) is a special case of the other one (29) with $r = 1$. It shows that the system is stabilized only with the case $r = 2$ which highlights the use of the sub-predictors, this technique can increase the allowable bounds on the delay value and the delay derivative.

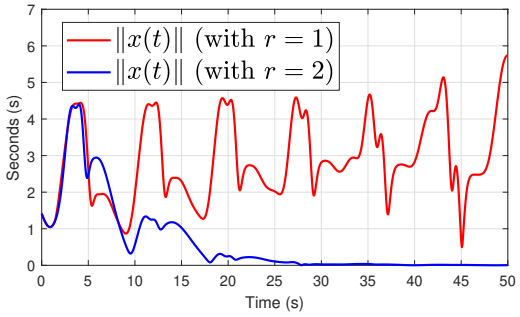

(a) State evolution of the two observation-based controllers for system (17).

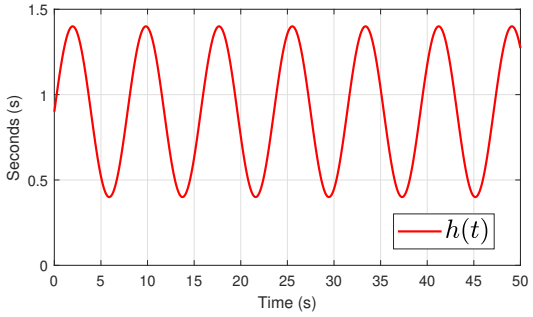

(b) Time-varying delay $h(t) = 0.9 + 0.5 \sin 0.8\cdot$ versus time.

Figure 7 – Comparison of the observation-predictor-based controller (27) and the sub-predictors technique (29).

The above discussed methods given in (Bekiaris-Liberis and Miroslav Krstic 2013; Léchappé, Moulay, and Plestan 2016; Weston, Malisoff, and Frédéric Mazenc 2017) require the value of the time-varying delay $h(t)$, so they may not be easily applied on real control systems. In the sequel, another control solution named "interval prediction" (Polyakov et al. 2013) is introduced, and only the bounds on the time-varying delay $h(t)$(upper bound $\bar{h}$, lower bound $\underline{h}$) are used to compute the approximated prediction. Firstly, the componentwise bounds of signal $B'u(t)$ on interval $[0, \bar{h} - \underline{h}]$ are defined as follows

$$\begin{aligned} \underline{B'u}(t) &= \min_{\theta \in [0, \bar{h} - \underline{h}]} B'u(t - \theta), \\ \overline{B'u}(t) &= \max_{\theta \in [0, \bar{h} - \underline{h}]} B'u(t - \theta) \end{aligned} \tag{30}$$

with componentwise functions $\max(\cdot)$ and $\min(\cdot)$. The core idea of this method is to use two different approximated predictions to build the control law

$$u(t) = \frac{1}{2} K(\bar{z}(t) + \underline{z}(t)) \tag{31}$$

with approximated predictions $\bar{z}(t)$, $\underline{z}(t)$ defined as

$$\begin{aligned}\bar{z}(t) &= e^{\tilde{A}\bar{h}}\bar{x}(t) + \int_{-\underline{h}}^{0} e^{-A\theta}\underline{\tilde{B}u}(t+\theta)\mathrm{d}\theta,\\ \underline{z}(t) &= e^{\tilde{A}\underline{h}}\underline{x}(t) + \int_{-\underline{h}}^{0} e^{-A\theta}\overline{\tilde{B}u}(t+\theta)\mathrm{d}\theta.\end{aligned} \tag{32}$$

The terms $\bar{x}(t)$ and $\underline{x}(t)$ of (31) are generated by the following approximated observations:

$$\begin{aligned}\dot{\underline{x}}(t) &= \tilde{A}\underline{x}(t) + \underline{\tilde{B}u}(t-\underline{h}) + \tilde{L}\left[\tilde{C}\underline{x}(t) - Cx(t)\right],\\ \dot{\bar{x}}(t) &= \tilde{A}\bar{x}(t) + \overline{\tilde{B}u}(t-\underline{h}) + \tilde{L}\left[\tilde{C}\bar{x}(t) - Cx(t)\right]\end{aligned} \tag{33}$$

with appropriate transformation matrix S, and

$$\tilde{A} = S^{-1}AS, \quad \tilde{B} = S^{-1}B, \quad \tilde{L} = S^{-1}L, \quad \tilde{C} = SC. \tag{34}$$

With the interval predictor-based control (31) -(33), the system can be stabilized for well-tuned gains K, L (*i.e.* they are generated by the stability LMIs) without the precise knowledge of the time-varying delay $h(t)$. By comparing with the conventional predictor-based control (Bekiaris-Liberis and Miroslav Krstic 2013; Witrant et al. 2007) and the observation predictor-feedback (Léchappé, Moulay, and Plestan 2016; Weston, Malisoff, and Frédéric Mazenc 2017), this method requires less information about the time-varying delay $h(t)$, but this method is more complex and conservative than the other methods.

Predictor-based control of networked control systems with network-induced delays

In the previous subsections, the existing works on the predictor-based control of continuous-time systems are investigated. However, vast time-delays in real control systems are introduced by wireless communications and networks. Therefore, networked control system has become to a hot topic in the control community for the last decades. In this subsection, the predictor-based control of networked control systems is introduced, the first method (Selivanov and Fridman 2016b) is the sampled-data version of the continuous predictor-based controller, whereas the second method (Léchappé, Moulay, Plestan, and Han 2019) transforms the NCS to a discrete-time system.
The predictor-based controller in (Selivanov and Fridman 2016b) is still designed in a continuous-time way. Indeed, it is almost the sampled-data version of the continuous-time one given in (9). The closed-loop stability of this method is based on the time-delay approach (K. Liu, Selivanov, and Fridman 2019), and this method is still effective to the variable sampling. However, the stability condition of this method depends on the size of the maximum allowable transmission interval (MATI), which is the upper bound on the variable sampling period. If the sampling period of the

control algorithm exceeds the MATI, then the stability is no longer ensured.
Another control solution is the discrete predictor-based controller (Léchappé, Moulay, Plestan, and Han 2019), in which the original NCS is transformed into an extended discrete-time representation. Since the extended system is delay-free, then the control law design can be easily built for this system, the continuous-time plant is stabilized as well. As stated in (Léchappé, Moulay, Plestan, and Han 2019, Secrion 7.1), the discrete predictor-based controller can stabilize NCS with arbitrarily long sampling period and arbitrarily long constant delays. This discrete-time representation is also involved in (Hu and Zhu 2003; Cloosterman et al. 2009) to handle the control problem of NCS with long time-varying delays. However, all of the above cited discrete-time approaches cannot work with variable sampling, some additional conditions must be checked in order to ensure the stability under aperiodic sampling (Hetel et al. 2017).
In conclusion, two types of predictor-based controller can stabilize NCS with long network-induced delays, the advantages of them are:

— **Sampled predictor-based control (Selivanov and Fridman 2016b):** handling variable sampling;
— **Discrete predictor-based control (Léchappé, Rouquet, et al. 2016; Hu and Zhu 2003; Cloosterman et al. 2009):** enduring longer sampling period and time-varying delays.

Predictor-based control of systems with uncertain delays

The previous section provides the summary of the predictor-based control technique of different systems (continuous-time system and networked control system) with different delays (constant delay and time-varying delay). However, in all of the above cited references, the value of the time-delay is assumed to be perfectly known. In this section, the predictor-based control of systems with uncertain delays is investigated, it is shown that the predictor-based controller is robust with respect to slight delay uncertainties.
In (Bresch-Pietri, Chauvin, and Petit 2012; Léchappé, Moulay, and Plestan 2018a), the predictor-based control schemes of continuous-time systems with uncertain delays are designed. In (Bresch-Pietri, Chauvin, and Petit 2012), the backstepping method (Bekiaris-Liberis and Miroslav Krstic 2013) based stability analysis is given to present that the predictor-based controller can stabilize systems with model uncertainties, external disturbances, and uncertain constant input-delay. The authors of (Léchappé, Moulay, and Plestan 2018a) demonstrate that the predictor-based controller deals with the combination of uncertain time-varying input and output delays.
For instance, the work of (Léchappé, Moulay, and Plestan 2018a) is briefly introduced in the sequel.

Consider the system with input-output time-varying delays given in the sequel:

$$\begin{cases} \dot{x}(t) = Ax(t) + Bu(t - h_i(t)) \\ y(t) = Cx(t - h_o(t)) \end{cases} \tag{35}$$

with $x(t)\ in\mathbb{R}^n$, $u(t) \in \mathbb{R}^m$, $y(t) \in \mathbb{R}^p$, $A \in \mathbb{R}^{n\times n}$, $B \in \mathbb{R}^{n\times m}$, $C \in\ \times$, and $h_i(t), h_o(t) > 0$. Suppose that the input and output delays have bounded derivatives such that

$$|\dot{h}_i(t)| \leq \delta_i, \quad |\dot{h}_o(t)| \leq \delta_o \tag{36}$$

for all $t \geq 0$. The round-trip delay of system (35) is defined as

$$h(t) = h_o(t) + h_i(t - h_o(t)) \tag{37}$$

due to the transport phenomenon. Remind that the precise values of $h_i(t)$, $h_o(t)$, and $h(t)$ are not known, only the nominal value $\hat{h}(t)$ of $h(t)$ satisfying

$$|h(t) - \hat{h}(t)| \triangleq D(t) \leq D, \quad |\dot{\hat{h}}(t)| \leq \hat{\delta} \tag{38}$$

with positive constants D and $\hat{\delta}$, is available for the controller design. The output-feedback control law

$$\begin{aligned} \dot{\hat{x}}(t) &= A\hat{x}(t) + Bu(t - \hat{h}(t)) + L\left[C\hat{x}(t) - y(t)\right] \\ u(t) &= K\left[e^{A\hat{h}(t)}\hat{x}(t) + \int_{t-\hat{h}(t)}^{t} e^{A(t-\theta)}Bu(\theta)\mathrm{d}\theta\right] \end{aligned} \tag{39}$$

where K, L make $A+BK$, $A+LC$ Hurwitz, stabilizes the system (35) if D, $\hat{\delta}$, and δ_o are sufficiently small. Namely, there exists predefined constants $D^*, \hat{\delta}^*, \delta_o^* > 0$, if

$$D \leq D^*, \quad \hat{\delta} \leq \hat{\delta}^*, \quad \delta_o \leq \delta_o^* \tag{40}$$

holds, then the system (35) controlled by (39) is globally uniformly asymptotically stable.
The works of (Léchappé, Moulay, and Plestan 2018a) state that the predictor-based controller can stabilize the system (35) even if the delay value is not perfectly known, this property is also called "robustness with respect to delay mismatch" (Bresch-Pietri, Chauvin, and Petit 2012; Bresch-Pietri and Petit 2014).

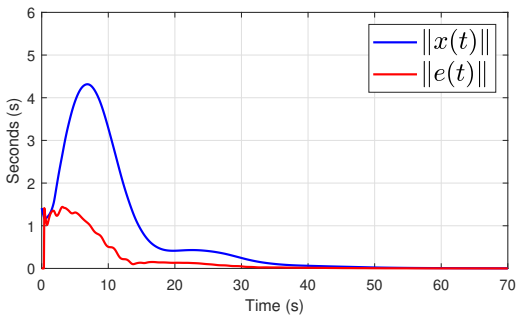

(a) Evolution of the state and observation error versus time of (35) controlled by (39).

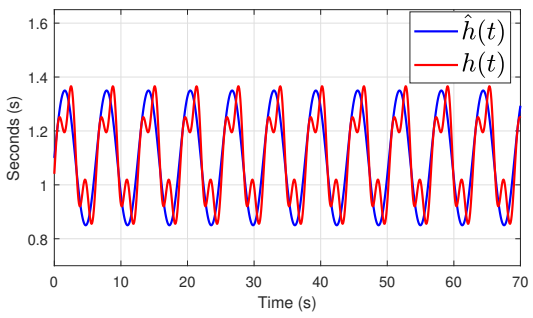

(b) Real round-trip delay $h(t)$ and the nominal delay $\hat{h}(t)$ used in (39).

Figure 8 – Simulation results of system (35) controlled by the output-feedback predictor-based controller (39).

Example: predictor-based control with uncertain time-varying delays

Consider the system (35) with

$$A = \begin{bmatrix} 0 & 1 \\ 0.1 & 0.1 \end{bmatrix}, \qquad B = \begin{bmatrix} 0 \\ 1 \end{bmatrix}, \qquad C = \begin{bmatrix} 1 & 0 \end{bmatrix}, \tag{41}$$

and

$$h_i(t) = 0.8 + 0.2 \sin t, \qquad h_o(t) = 0.3 + 0.1 \sin(3 \cdot t). \tag{42}$$

One assumes that the round-trip delay induced from (42) is uncertain, and the nominal value $\hat{h}(t) = 1.1 + 0.25 \sin t$ is used to compute the output-feedback control law (39) with $K = \begin{bmatrix} -2.1 & -3.1 \end{bmatrix}$ and $L = \begin{bmatrix} -1.6 & -0.76 \end{bmatrix}^T$.
Figure 8 shows that the system (35) can be stabilized by the output-feedback predictor-based controller (39) if the difference between the real round-trip delay $h(t)$ and the nominal delay $\hat{h}(t)$ is sufficiently small. Thus, the robustness of the predictor-based controller with respect to delay mismatch is validated by this example.

Next, one moves on to the discrete predictor-based control of systems with uncertain delays. The analysis given in (Lozano et al. 2004, Section 5) explains that the discrete predictor-based controller is also robust with respect to slight model uncertainties and delay uncertainties as the continuous-time one (Bresch-Pietri, Chauvin, and Petit 2012). Moreover, the theoretical results of (Lozano et al. 2004) are illustrated on the yaw control of a mini-quadrotor. In (Zhan, Du, and Fei 2017), the stochastic discrete predictor-based controller is designed for the visual servo control system (NIPVSS, see Figure 1). The stochastic stability is achieved even if the time-delay introduced by

the image-processing algorithm is random. Besides the above two method, the methods of (Hu and Zhu 2003; Cloosterman et al. 2009) are also able to deal with NCS with uncertain delays.

Predictor-based control of systems with unknown constant time-delays

The discussions given in the previous section explain that the predictor-based technique can stabilize systems with uncertain time-delays. In this section, one considers a more challenging problem: predictor-based control of systems with unknown time-delays. Indeed, the stabilization of systems with unknown time-varying delay is still challenging to the control community, and the unknown time-delays in NCS can be identified by virtue of the clock synchronization (Martı et al. 2008) (IEEE 1588 protocol) and time-stamp technique (Lai and Hsu 2010). Thus, some significant control strategies for continuous-time systems with unknown constant delays are introduced in this section.

Existing approaches on the predictor-based control of systems with unknown constant time-delays

The authors of (Miroslav Krstic and Bresch-Pietri 2009; Bresch-Pietri and Miroslav Krstic 2010) have extended the backstepping method (Bekiaris-Liberis and Miroslav Krstic 2013) to the adaptive backstepping (Kokotovic, Krstic, and Kanellakopoulos 1992; Freeman and Kokotović 1993) version. By virtue of the backstepping transformation, the unknown time-delay becomes to an unknown parameter of the PDE system. Then the adaptive method is applied to recursively estimate the unknown time-delay and stabilize the target system, and the stability of the original system is guaranteed by an analysis based on the alternative version of the Barbalat's Lemma (Tao 1997).
In (Herrera and Ibeas 2012), a multi-model based delay estimation algorithm is combined with a modified Smith predictor to regulate the step response of stable and unstable systems. The controller sends the control signal not only to the delayed plant but also to a multi-model system that is comprised of the delay-free plant model and distinct time-delays. A switch algorithm compares the system output and the virtual outputs of the multi-model system and estimates the time-delay online. Finally, the modified Smith predictor stabilizes the system with the help of the delay estimator.
The truncated predictor-based control technique (Zhou 2014c) is used in (Cacace, Conte, and Germani 2017; Wei and Lin 2019) to deal with systems with unknown input-delay, it can be considered as a simplified version of the predictor-based controller (9) since it only uses the finite-dimensional term of the state prediction to calculate the control law, and the infinite-dimensional term is said to be "truncated". The work of (Wei and Lin 2019) is based on the low-gain feedback, a decreasing feedback gain is used to make the response time slower and slower, and the closed-loop stability is guaranteed when the response time is larger than the unknown delay. In (Cacace, Conte, and

Germani 2017), the combination of a piecewise-constant delay estimator and a truncated predictor-based controller is used to ensure the exponential stability of the closed-loop system. However, the works of (Cacace, Conte, and Germani 2017; Wei and Lin 2019) have constraints on the open-loop system due to the limitations of the truncated predictor-based controller.

Discussions on the existing approaches

Consider the existing methods presented in the previous subsection, the majority of them (Miroslav Krstic and Bresch-Pietri 2009; Bresch-Pietri and Miroslav Krstic 2010; Herrera and Ibeas 2012; Cacace, Conte, and Germani 2017) adopt the following strategies to stabilize the systems with unknown input-delays:

— estimate the unknown input delay with different methods (*e.g.* Lyapunov analysis (Miroslav Krstic and Bresch-Pietri 2009; Bresch-Pietri and Miroslav Krstic 2010), switching logic (Herrera and Ibeas 2012), anti-gradient approach (Cacace, Conte, and Germani 2017));

— compute the approximated predictor-based control law with the help of the online delay estimator.

Among the existing methods introduced in the previous subsection, only the work of (Wei and Lin 2019) did not use the delay estimation technique, the reason is due to the fact that it only deals with the systems with poles equal to zero.

After the investigation of the existing methods, time-delay estimation (Time-delay Estimation (TDE)) plays an important role in the control of systems with unknown time-delays, and this technique needs further analysis and discussions.

Time-delay estimation techniques for constant and time-varying delays

This section presents an overview of the existing TDE approaches for different types of time-delays (*i.e.* constant delays, time-varying delays), in order to assist the predictor-based controller in stabilizing such time-delay systems. The first part of this section presents some conventional TDE methods (*i.e.* estimating the time-delay with input information and system dynamics), whereas the second part introduces the practical TDE techniques of RCS and NCS (*i.e.* TDE methods with specific communication loops and protocols).

Conventional time-delay estimation techniques

In this subsection, the existing conventional TDE techniques are summarized, and the majority of them are based on delay-identifiability theory (Orlov et al. 2002; Drakunov et al. 2006) that must be introduced at the beginning of the subsection.

Definition 1. *Consider the system*

$$\dot{x}(t) = Ax(t) + Bu(t - h(t)) \tag{43}$$

with $x(t) \in \mathbb{R}^n$, $u(t) \in \mathbb{R}^m$, $A \in \mathbb{R}^{n\times n}$, $B \in \mathbb{R}^{n\times m}$, *and* $h(t) > 0$. *System* (43) *is said to be delay identifiable under arbitrary initial conditions if there exists an input signal* $u(t)$ *such that the equality* $x(t) \equiv \hat{x}(t)$ *implies* $h(t) \equiv \hat{h}(t)$.

The delay identifiability is the ability of the system to resolve the delay value from the state trajectory. If two different delays $h_1(t)$, $h_2(t)$ lead to the same system trajectory, then it is impossible to identify the true delay value from the system trajectory. Indeed, the delay identifiability depends not only on the system parameters, but also on the choice of the input signal $u(t)$. If the input signal is constant, then the system is not identifiable since $u(t - h(t)) \equiv const$ leads to the same trajectory for arbitrary $h(t)$. In general, $u(t)$ should be chosen as a sufficiently rich input (*i.e.* sufficiently "discontinuous" or "time-varying") to guarantee the delay identifiability.
TDE methods are firstly studied by the researchers from the acoustic and signal processing communities to develop sonar techniques (Knapp and Glifford Carter 1976; GC Carter 1981; Etter and Stearns 1981). The autocorrelation analysis is proposed in (Knapp and Glifford Carter 1976) to estimate the time-delay. In (GC Carter 1981; Etter and Stearns 1981), the time-delays are respectively estimated by using the least-square and mean-square minimization of a cost function $J(h-\hat{h})$. More signal processing based methods are presented in the survey thesis (Björklund 2003). However, these methods are offline, it cannot handle online TDE problems oriented for controller design.
A vast literature is available on the control oriented TDE methods, they are classified in details as follows:

— Cost function based methods (Diop et al. 2001; Léchappé, Rouquet, et al. 2016): similar with the signal processing based method (GC Carter 1981), these methods intend to estimate the time-delay by minimizing the cost function $J(h - \hat{h})$ online. The work of (Diop et al. 2001) deals with constant delay estimation problems with the use of a Lyapunov function based delay estimator. In (Léchappé, Rouquet, et al. 2016), the gradient-descent algorithm is applied to minimize the cost function and estimate the slow-varying delay.
— Adaptive TDE algorithms (Ren et al. 2005; X. Wu et al. 2013): these methods consider the time-delay as an unknown parameter of the system, then it can be estimated with adaptive algorithm. The method proposed by (X. Wu et al. 2013) can also estimate time-varying delays, but the performance is not good if the time-delay is fast-varying.
— Convolution-based algebraic methods (Belkoura 2005; Belkoura and J.-p. Richard 2006; Belkoura, J.-P. Richard, and Fliess 2009): these methods use the convolution-based algebraic methods to estimate the unknown parameters and unknown constant delay of linear systems. As claimed in (Belkoura and J.-p. Richard 2006), these methods can provide a faster

convergence speed than (Ren et al. 2005) by adopting a distributional formulation. But these methods are not yet extended to the time-varying delay estimation problem.

— Sliding mode base methods (Drakunov et al. 2006; Zheng, Polyakov, and Levant 2018): sliding mode algorithm is involved in these methods, they deal with time-varying delay of linear systems (Drakunov et al. 2006) and constant delay of nonlinear systems (Zheng, Polyakov, and Levant 2018), respectively. However, both of them cannot ensure global convergence, the initial condition of the delay estimator has to be sufficiently close to the exact value.

— Neural network-based method (Tan 2004): this method estimates the slow-varying delays of nonlinear systems with the help of neural network, but the estimation accuracy is not very high and the computation cost will be heavy if the neural network is not well trained.

In order to compare the performances of the existing conventional TDE methods introduced in this subsection, Table 2 given in the sequel is used the summarize and classify such methods.

See Table 2, only a few existing methods can handle time-varying delay estimation problem, and

Method	Online/ Offline	Delay type	Convergence type
(Knapp and Glifford Carter 1976)	Offline	Constant delay	Global convergence
(GC Carter 1981)	Offline	Constant delay	Global convergence
(Etter and Stearns 1981)	Offline	Constant delay	Global convergence
(Diop et al. 2001)	Online	Constant delay	Global convergence
(Belkoura 2005)	Online	Constant delay	Global convergence
(Belkoura and J.-p. Richard 2006)	Online	Constant delay	Global convergence
(Belkoura, J.-P. Richard, and Fliess 2009)	Online	Constant delay	Global convergence
(Ren et al. 2005)	Online	Constant delay	Global convergence
(Zheng, Polyakov, and Levant 2018)	Online	Constant delay	Local convergence
(Drakunov et al. 2006)	Online	Fast-varying delay	Local convergence
(X. Wu et al. 2013)	Online	slow-varying delay	Global convergence
(Tan 2004)	Online	slow-varying delay	Global convergence
(Léchappé, Rouquet, et al. 2016)	Online	slow-varying delay	Global convergence

Table 2 – Main properties of the existing TDE techniques.

they cannot perfectly estimate fast-varying delays. As claimed in (X. Wu et al. 2013, Remark 5) and (Léchappé, Rouquet, et al. 2016, Theorem 1), the estimation errors of these methods increase as the time-delay varies faster. The work of (Tan 2004) can neither deal with fast-varying delays since it supposed that the change in the time-delay is much slower than the sampling rate, in order to ensure that the time-delay can be considered as a constant during one sample period (Tan 2004, p.64). The fast-varying delay estimation problem is tackled in (Drakunov et al. 2006), but this method has two drawbacks:

— this method cannot ensure the global convergence of the delay estimation;

— high order derivatives of the state $x(t)$ and the input signal $u(t)$ are used in this method, so

it is not robust with respect to noises.

Thus, the existing control-oriented TDE techniques cannot perfectly estimate fast-varying delays, this research topic is still challenging for the control community.

Practical online time-delay estimation method of remote control systems and networked control systems

Consider the conventional TDE techniques presented in Table 2, it is observed that the TDE methods mentioned above cannot estimate fast-varying delays with global convergences. However, since the fast-varying delay is more frequently found in the remote control systems (S.-H. Yang 2011) and networked control systems (X.-M. Zhang, Han, and Yu 2015) (*e.g.* communication latencies, network-induced delays), then one can provide some practical TDE technique for such systems.

The work of (Lai and Hsu 2010) provides a practical TDE solution for remote control systems

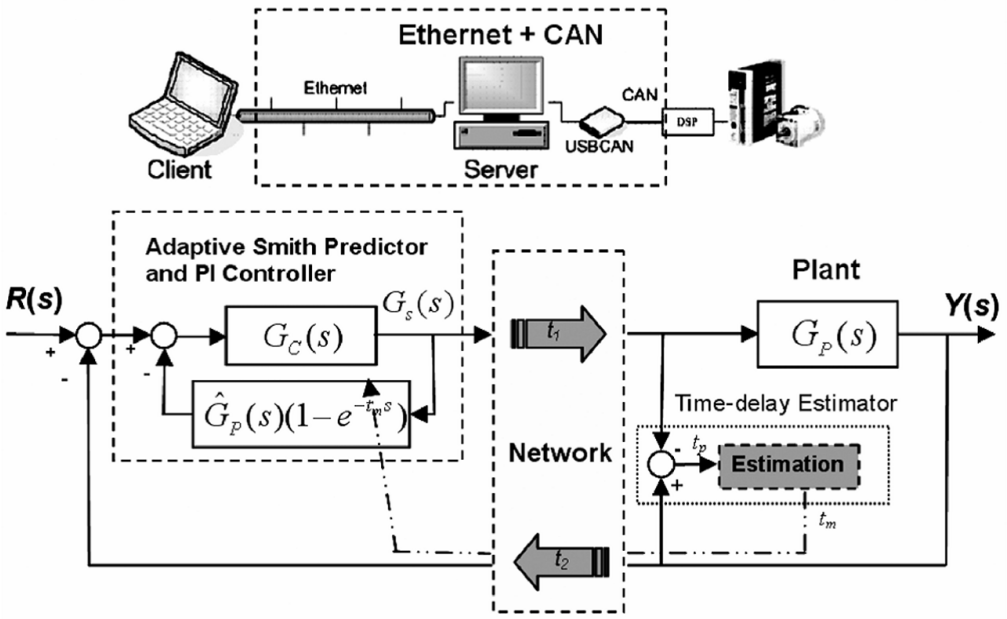

Figure 9 – Practical delay measurement approach (Lai and Hsu 2010) of remote control system.

(see Figure 9). The controller sends the system clock to the plant, a digital signal processor (DSP) implemented on the plant receives the system clock and sends it back to the controller. Finally, the round-trip delay of the remote control system is estimated by taking the difference between the current system clock and the delayed system clock sent back from the DSP. This method can estimate fast-varying delay with global convergence in a practical way, and the delay identifiability is no longer required since the time-delay is estimated by the system clock.

This method can also be used in the networked control systems, one can firstly synchronize the components (*i.e.* sensor, controller, actuator) via IEEE 1588 protocol (Martı et al. 2008), then use

this method to estimate the network-induced delays.

Organizations and contributions of this thesis

This thesis is composed of three parts:

— The first part presents a novel type of time-delay estimation algorithm of linear time-invariant (Linear Time-Invariant (LTI)) systems with unknown input and output delays, the closed-loop stability under the combination of this new delay estimation approach and the predictor-based controller is also studied.

— The second part is dedicated to the delay estimation and predictor-based control of remote control systems with time-varying input and output delays. The practical delay measurement method (Lai and Hsu 2010) is modified by a more robust one, and this new delay measurement approach is validated on a real WiFi network. Finally, some analysis and simulation results ensure that this method can be combined with the predictor-based controller in order to stabilize the system.

— The last part focuses on the discrete predictor-based control of a class of networked control systems with time-varying delays. It is shown that this new control strategy deals with time-varying delays and message rejections. This method is implemented on the networked inverted pendulum visual servo system (Du, C. Zhang, et al. 2019) with fairly good control performances.

The detailed organization of this thesis is given in the sequel.

In Chapter 1, a new type of monotonic delay estimation algorithm is proposed to estimate the constant delay of LTI systems (subsection 1.2.1), then it is plugged into a predictor-based controller in order to stabilize the system. The first version of this delay estimation technique (subsection 1.2.2) has been published in the proceedings of *2019 American Control Conference*. The first version is then modified by a "normalized" version (subsection 1.2.3), and the number of tuning parameters in the stability condition is reduced. With this modified method, the global uniform asymptotic stability is ensured by a Lyapunov-Razumikhin analysis. The second approach is extended to the third version of the method (subsection 1.2.4), which guarantees the global uniform exponential stability of the closed-loop system. The third version of this method is accepted for publication in an upcoming issue of and online published in *International Journal of Control*. At the end of the chapter (section 1.3), some discussions and simulation results are provided to demonstrate the robustness and the efficacy of these methods.

Chapter 2 deals with the control of remote control systems with time-varying input and output delays. In this chapter, a similar framework of the practical delay measurement approach (Lai and Hsu 2010) is considered, and a class of sliding mode based practical TDE methods are proposed. In section 2.2, the theoretical convergence results with conventional sliding mode, super-twisting

method are firstly presented, these results are accepted for publication in an upcoming issue of and online published in *IEEE Transactions on Industrial Electronics*. This method is thereafter extended to the adaptive super-twisting algorithm based TDE method, this work is submitted to *2020 IEEE Conference on Control Technology and Applications (CCTA)*. Some simulation results are provided to illustrate that the sliding mode based techniques are robuster than the sliding mode based techniques are robuster than (Lai and Hsu 2010) with respect of channel inherent noises (Shannon 1984) and deception attacks (Ding et al. 2017). Next, the TDE methods mentioned above are implemented on a real WiFi network composed of two computers in subsection 2.2.6, and the performances of them are discussed and compared with each other. In section 2.3, the sliding mode based practical TDE techniques are combined with the predictor-based controller, the closed-loop stability is achieved by discussions and simulation results, this work is submitted to *IEEE Control Systems Letters with CDC (59th IEEE Conference on Decision and Control) option*.
In Chapter 3, the discrete predictor-based control of a class of networked control systems are considered. The problem formulations addressed in subsection 3.1.1 explain the main motivations of this Chapter, and this Chapter is dedicated to the controller design of networked control systems with sensor-to-controller time-varying delays and controller-to-actuator uncertain constant delays, and the proposed control technique can be used for visual servo control systems (Zhan, Du, and Fei 2017) and networked visual servo control systems (H. Wu et al. 2012; Du, C. Zhang, et al. 2019). The main theoretical results of this Chapter are given in section 3.2, it is shown that the discrete predictor-based controller combined with a state predictor can tackle sensor-to-controller time-varying delays and message rejections at the same time. Some simulation results are given to illustrate that the discrete predictor-based controller can stabilize the same system given in (Selivanov and Fridman 2016b, Section 5) with larger allowable sampling periods. In the end (section 3.3), the proposed control techniques are implemented on the networked inverted pendulum visual servo system (NIPVSS) (Du, C. Zhang, et al. 2019), the performances and robustness are validated by the experimental results.
Some of the results presented in this thesis have been published or accepted in the following journals and conferences.

Journal papers

[1] Y. Deng, V. Léchappé, S. Rouquet, E. Moulay, and F. Plestan, *Super-twisting algorithm based time-varying delay estimation with external signal*, online published in IEEE Transactions on Industrial Electronics. doi: 10.1109/TIE.2019.2960739.

[2] Y. Deng, V. Léchappé, E. Moulay, and F. Plestan, *State feedback control and delay estimation*

for LTI system with unknown input-delay, online published in International Journal of Control. doi: 10.1080/00207179.2019.1707288.

[3] Y. Deng, V. Léchappé, E. Moulay, and F. Plestan, *Predictor-based control of LTI remote systems with estimated time-varying delays*, in IEEE Control Systems Letters, vol 5, issue 1, pages 289-295, Jan 2021.

Conference papers

[1] Y. Deng, V. Léchappé, E. Moulay, and F. Plestan, *Prediction-based control with delay estimation of LTI systems with input-output delays*, 2019 American Control Conference (ACC), Philadelphia, USA, pages 3702-3707.

[2] Y. Deng, V. Léchappé, S. Rouquet, E. Moulay, and F. Plestan, *A practical online time-varying delay estimation of remote control system based on adaptive super-twisting algorithm*, accepted in 2020 IEEE Conference on Control Technology and Applications (CCTA), Montréal, Canada.

List of notations

Throughout this thesis, the following mathematical notations are used.

Notations	Meanings
$\mathbb{N}$	The set of non-negative integers
$\mathbb{N}_+$	The set of strictly positive integers
$\mathbb{R}^n$	The set of real vectors with dimension n
$\mathbb{R}^{n\times m}$	The set of real matrices with n rows and m columns
P^T	Transpose of the matrix P
$I_{n\times n}$	Identity matrix with n columns and n rows
I	Identity matrix with appropriate dimensions
0	Scalar 0 or zero matrix with appropriate dimensions
$P > 0$, $P < 0$	The matrix P is positive definite and negative definite, respectively
$\bar{\lambda}(P)$, $\underline{\lambda}(P)$	Maximum and minimum eigenvalues of matrix P, respectively
$\|x\|$	Absolute value of scalar x
$\|x\|$	Euclidean norm of vector x
$\|P\|$	Spectral norm (2-norm) of matrix P
$\mathbf{C}^n$	The set of functions with n-times continuously differentiable derivatives
$x_t : [-h, 0] \mapsto \mathbb{R}^n$	$x_t(\theta) = x(t+\theta)$ with $\theta \in [-h, 0]$
$\dot{f}(g(t))$	Time-derivative of function $f(\cdot)$ at instant $g(t)$
$\frac{d}{dt}f(g(t))$	Time derivative of the function composition $t \mapsto f(g(t))$ at instant t

Table 3 – List of notations of this thesis.

Chapter 1

Predictor-based control and delay estimation of LTI system with unknown constant delays

Contents

The main results of this Chapter are accepted in the following international journal and conference papers:

[1] Y. Deng, V. Léchappé, E. Moulay, and F. Plestan, *State feedback control and delay estimation for LTI system with unknown input-delay*, online published in International Journal of Control. doi: 10.1080/00207179.2019.1707288.

[2] Y. Deng, V. Léchappé, E. Moulay, and F. Plestan, *Prediction-based control with delay estimation*

of LTI systems with input-output delays, 2019 America Control Conference (ACC), pages 3702-3707.

1.1 Introduction

This chapter is dedicated to the predictor-control of LTI systems with unknown constant delays, the first system to study is the input-delay system

$$\dot{x}(t) = Ax(t) + Bu(t-h), \qquad t \geq 0 \tag{1.1}$$

with $A \in \mathbb{R}^{n\times n}$, $B \in \mathbb{R}^{n\times m}$, unknown constant input delay $h > 0$, and initial conditions

$$\begin{aligned} &x(0) = x_0, \\ &u(\theta) = \phi_u(\theta) \in \mathbf{C}([-2\bar{h}, 0), \mathbb{R}^m). \end{aligned} \tag{1.2}$$

In (1.2), the initial condition of $u(t)$ is defined on $[-2\bar{h}, 0)$ instead of $[-\bar{h}, 0)$ because the delay estimator given in the sequel needs the knowledge of $u(t)$ on $[-2\bar{h}, -\bar{h})$.
The second system to analyze is the input-output delay systems

$$\begin{cases} \dot{x}(t) = Ax(t) + Bu(t-h_i), & t \geq 0 \\ y(t) = Cx(t-h_o) \end{cases} \tag{1.3}$$

with unknown h_i, and h_o. The initial condition of system (1.3) in

$$\begin{aligned} &x(\theta) = \phi_x(\theta) \in \mathbf{C}([-h_o, 0), \mathbb{R}^n), \\ &u(\theta) = \phi_u(\theta) \in \mathbf{C}([-2\bar{h}, 0), \mathbb{R}^m). \end{aligned} \tag{1.4}$$

and in this case the parameter $\bar{h}$ is the upper bound on the round-trip delay $h_i + h_o$. This section begins with a presentation about the existing methods dealing with the same problem, and then the control problems are formulated. The modeling of the system and some necessary assumptions are given as well.

1.1.1 Overviews and limitations of the related works

In this subsection, the existing methods mentioned in General Introduction are discussed in details.

Adaptive backstepping method

Consider the system (1.1), and one assumes that the input-delay $h > 0$ is unknown and upper bounded by a positive constant $\bar{h}$. This method is based on the backstepping transformation

$$\bar{u}(p,t) = u(t - h(p-1)), \quad p \in [0,1], \tag{1.5}$$

and the control law reads as

$$u(t) = K\left[e^{A\hat{h}(t)}x(t) + \hat{h}(t)\int_0^1 e^{A\hat{h}(t)(1-y)}B\bar{u}(y,t)\mathrm{d}y\right] \tag{1.6}$$

where K is the feedback matrix that makes $A+BK$ Hurwitz, and $\hat{h}(t)$ is a delay estimator used to build approximated predictor-based control law. The delay estimator $\hat{h}(t)$ is governed by the update law

$$\dot{\hat{h}}(t) = \gamma \mathrm{Proj}_{[0,\bar{h}]}\{\tau(t)\} \tag{1.7}$$

with sufficiently large $\gamma > 0$, and the standard projector operator

$$\mathrm{Proj}_{[0,\bar{h}]}\{\tau\} = \tau \begin{cases} 0, & \hat{h}(t) = 0 \text{ and } \tau < 0 \\ 0, & \hat{h}(t) = \bar{h} \text{ and } \tau > 0 \\ 1, & \text{otherwise} \end{cases}. \tag{1.8}$$

The dynamic of $\tau(t)$ satisfies that

$$\tau(t) = -\frac{\int_0^1 (1+p)w(p,t)Ke^{A\hat{h}(t)}\mathrm{d}p\,[Ax(t) + B\bar{u}(0,t)]}{1 + x^T(t)Px(t) + b\int_0^1 (1+p)w^2(p,t)\mathrm{d}p} \tag{1.9}$$

with

$$w(p,t) = \bar{u}(p,t) - \hat{h}(t)\int_0^p Ke^{A\hat{h}(t)(p-y)}B\bar{u}(y,t)\mathrm{d}y - Ke^{A\hat{h}(t)p}x(t). \tag{1.10}$$

The symmetric positive definite matrix P is the solution to the following Lyapunov equation

$$(A+BK)^T P - P(A+BK) = -Q \tag{1.11}$$

for arbitrarily chosen symmetric positive definite matrix Q, and then the parameter b in (1.9) is chosen such that

$$b \geq \frac{4\|PB\|^2\bar{h}}{\underline{\lambda}(Q)}. \tag{1.12}$$

By using the control law derived from (1.5)-(1.12), the original system (1.1) with unknown input-delay is globally uniformly asymptotically stable, and the delay estimator $\hat{h}(t)$ converges in a small region around the nominal delay h.

The adaptive backstepping method (Miroslav Krstic and Bresch-Pietri 2009; Bresch-Pietri and Miroslav Krstic 2010) transforms the original system (1.1) to a PDE system with zero boundary condition. Then a Lyapunov-Krasovskii functional is designed for the closed-loop PDE system. By using this method, the global asymptotic stability of the ODE system is ensured.

Multi-model based technique

Different from the theoretical solution given in (Bekiaris-Liberis and Miroslav Krstic 2013), a more practical method is given in (Herrera and Ibeas 2012). This method is an output regulation based on the transfer function.

The main idea of this method is presented in Figure 1.1, when the control input $u(t)$ is injected

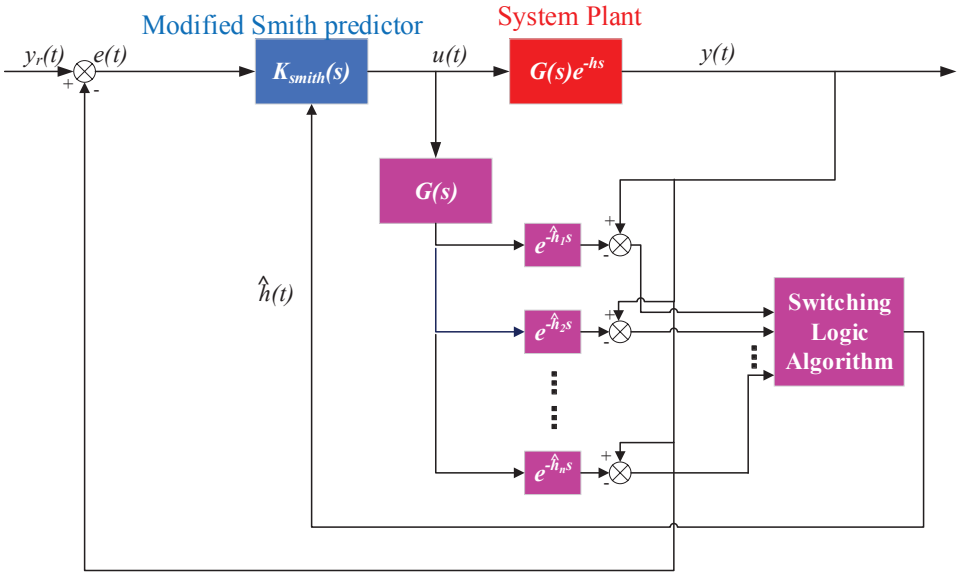

Figure 1.1 – Delay estimation and control diagram of the multi-model based technique (Herrera and Ibeas 2012).

into the time-delay system $G(s)e^{-hs}$, it is also applied to several virtual systems with distinct time-delays $\hat{h}_1, \hat{h}_2, \cdots, \hat{h}_n$. The outputs of the virtual systems are compared with the system output, and the unknown time-delay is estimated by a switching logic algorithm. Finally, the control law is calculated with the delay estimation and a modified Smith predictor.

Truncated predictor-based control methods

In this subsection, the truncated predictor-based controllers (Wei and Lin 2019; Cacace, Conte, and Germani 2017) are introduced in details.

In (Wei and Lin 2019), the system (1.1) with unknown input-delay $h > 0$ is taken into account. The

following time-varying feedback control law

$$u(t) = -B^T P\left(\gamma(t)\right) x(t), \quad t \geq 0 \tag{1.13}$$

where $P(\gamma(t))$ is the solution of the following time-varying algebraic Riccati equation

$$A^T P(\gamma(t)) + P(\gamma(t))A - P(\gamma(t))BB^T P(\gamma(t)) = -\gamma(t)P(\gamma(t)), \quad \gamma(t) > 0 \tag{1.14}$$

is used to stabilize the time-delay system (1.1). The time-varying parameter $\gamma(t)$ given in (1.13) and (1.14) is chosen as $\gamma(t) = \frac{m}{\hat{\tau}(t)}$ with the following properties:

— $m > 0$ is a sufficiently small constant;

— $\hat{\tau}(t)$ satisfies that $\hat{\tau}(t) > 0$, $\lim\limits_{t\to+\infty} \hat{\tau}(t) = \bar{\tau}$, and $\lim\limits_{t\to+\infty} \dot{\hat{\tau}}(t) = 0$.

With this method, the time-varying feedback gain $-B^T P(\gamma(t))$ is decreasing in order to make the closed-loop dynamics slower than the unknown delay value, this is the reason why this technique is named "low gain feedback". However, this method cannot deal with unstable system plant, all of the open-loop poles are supposed to be zero.

Different from the low gain feedback method, (Cacace, Conte, and Germani 2017) combines the truncated predictor-based controller

$$u(t) = Ke^{(A+BK)\hat{h}(t)}x(t), \quad t \geq 0 \tag{1.15}$$

with a piecewise constant delay estimation technique. The anti-gradient based approach is used to make the delay estimation evolving along the opposite direction of the gradient of an error system. On the contrary of (Wei and Lin 2019), this method is effective to unstable open-loop systems, but it cannot compensate arbitrarily long time-delay since the integral term is neglected, and the maximal allowable delay value $\bar{h}_{max}$ depends on the matrices A, B, and K.

The main benefit of the truncated predictor-based control methods (Wei and Lin 2019; Cacace, Conte, and Germani 2017) is the abandon of the integral term, which makes the control law easy to implement, and the numerical issues claimed in (Van Assche et al. 1999) are also avoided.

Limitations of the existing methods

Consider the existing methods mentioned above, they have the following limitations:

— Although the adaptive backstepping method (Miroslav Krstic and Bresch-Pietri 2009; Bresch-Pietri and Miroslav Krstic 2010) is one of the best theoretical solutions to the problem, it is difficult to be implemented on the real control system, both the controller (1.6) and the delay estimator (1.7)-(1.9) contain infinite dimensional terms, and the delay estimator must be transformed to an explicit form in real applications.

— The multi-model method is easy to implement, but the computation cost is high if the time-

delay is large (large time-delay requires large numbers of virtual systems).

— The truncated predictor-based control techniques (Cacace, Conte, and Germani 2017; Wei and Lin 2019) is also easy to implement, but they have constraints on the system parameters, and they are weak in the control of unstable systems with arbitrarily long unknown time-delay.

The main objective of this chapter is to build control laws for input-delay system (1.1) and input-output delay system (1.3) with a trade-off between the theories and the applications.

1.1.2 Preliminaries and problem formulations

Problem formulation of input-delay system

Consider the input-delay system (1.1) where $x(t) \in \mathbb{R}^n$, $u(t) \in \mathbb{R}^m$, $A \in \mathbb{R}^{n\times n}$, and $B \in \mathbb{R}^{n\times m}$. The input-delay h is supposed to be constant and unknown. Moreover, one assumes that h is bounded in $[\underline{h}, \bar{h}]$, the bounds $\underline{h}$ and $\bar{h}$ are known. In order to build control law for system (1.1), the following assumption are clarified.

Assumption 1. *The pair (A, B) is stabilizable.*

Assumption 1 ensures the existence of a feedback matrix $K \in \mathbb{R}^{m\times n}$ such that $A + BK$ is Hurwitz. It yields that for all positive constant c_u, there exists a positive definite matrix $P \in \mathbb{R}^{n\times n}$ such that the following algebraic equation (Slotine, Weiping Li, et al. 1991)[equation (3.19)] holds

$$(A + BK)^T P + P(A + BK) = -c_u I_n. \tag{1.16}$$

Based on the feedback matrix K given after Assumption 1, one defines the controller as

$$u(t) = Kz(t), \quad t \geq 0 \tag{1.17}$$

where $z(t)$ is the approximated predictor relies on the knowledge of the delay estimation $\hat{h}(t)$ (the definition of $\hat{h}(t)$ will be given in the next section)

$$z(t) = e^{A\hat{h}(t)}x(t) + \int_{t-\hat{h}(t)}^{t} e^{A(t-s)}Bu(s)\mathrm{d}s, \quad t \geq 0. \tag{1.18}$$

The initial condition of $z(t)$ is defined as

$$z(\theta) = \phi_z(\theta) \in \mathbf{C}([-2\bar{h}, 0), \mathbb{R}^n). \tag{1.19}$$

Similarly, the initial condition of $z(t)$ is defined on $[-2\bar{h}, 0)$ in order to ensure that the delay estimator is computable.

Remark 2. *To simplify the calculations, one chooses the initial condition of $z(t)$ such that*

$$\|\phi_u(\theta)\| \leq \|K\|\|\phi_z(\theta)\|, \quad \theta \in [-2\bar{h}, 0). \tag{1.20}$$

Moreover, one requires that $u(t)$ and $z(t)$ are continuous at $t = 0$ gives that

$$\begin{aligned} \lim_{\theta \to 0^-} \phi_u(\theta) &= u(0), \\ \lim_{\theta \to 0^-} \phi_z(\theta) &= z(0). \end{aligned} \tag{1.21}$$

Equations (1.21) *ensures the continuity of the controller $u(t)$ and the predictor $z(t)$ for all $t \geq -2\bar{h}$.*

Assumption 2. *The delayed input value $u(t-h)$ is available for measurements.*

The proposed technique uses the knowledge of $u(t-h)$ to estimate the unknown input-delay. The delayed input value $u(t-h)$ can be stored and sent to the controller in practice. The same assumption is given in (Léchappé, Rouquet, et al. 2016; Diop et al. 2001) in order to solve the delay estimation problem. For the stabilization problems, the adaptive backstepping approaches (Miroslav Krstic and Bresch-Pietri 2009, pp.4500), (Bekiaris-Liberis and Miroslav Krstic 2010, pp.278) also claim that the infinite-dimensional state (1.5) with the unknown input-delay h, is available for measurement for all $p \in [0, 1]$. Thus, Assumption 2 is a standard assumption for this problem. Moreover, Assumption 2 can be verified in a class of remote control systems (RCS) (S.-H. Yang 2011, Chapter 3.4). Consider a RCS with full-state measurement:

$$\begin{cases} \dot{x}(t) = Ax(t) + Bu(t - h_i) \\ y(t) = x(t - h_o) \end{cases} \tag{1.22}$$

where h_i and h_o are the unknown constant input and output delays arisen from the remote data transmission. Firstly, one assumes that the plant sends the measured state $x(t)$ and the delayed input $u(t-h_i)$ back to the controller in the same communication channel (the data transmission of the delayed control signal is shown by the dashed arrows in Figure 1.2), then the controller receives $y(t)$ and $u(t-h_i-h_o)$ at the same time. In other words, at the controller side, the delayed signal $u(t-h_i-h_o)$ is available for measurements. Secondly, since h_o is constant, the dynamics of $y(t)$ reads as

$$\dot{y}(t) = \dot{x}(t - h_o) = Ax(t - h_o) + Bu(t - h_i - h_o). \tag{1.23}$$

Remind that, if one defines $h = h_i + h_o$, system (1.23) is equivalent to an input-delay system

$$\dot{y}(t) = Ay(t) + Bu(t - h) \tag{1.24}$$

where $u(t-h)$ is available for measurements. This example shows that the input and output delays of

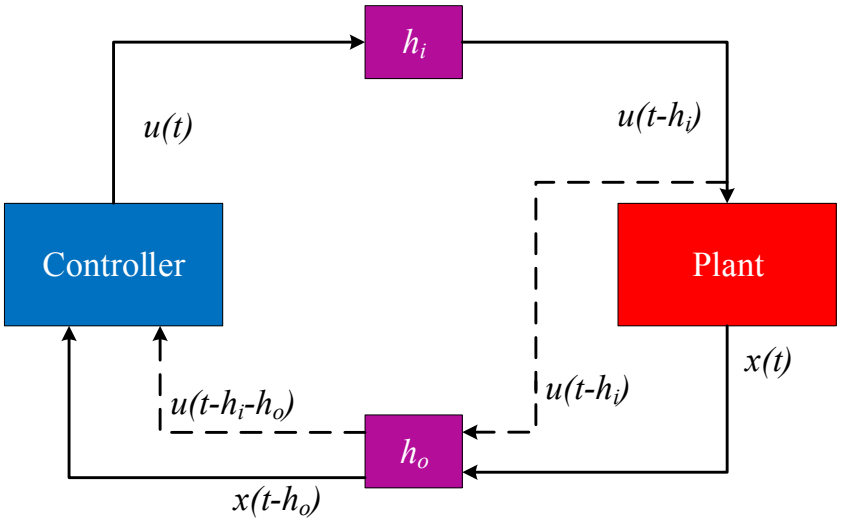

Figure 1.2 – Control framework of RCS (1.22) with full state measurement.

the remote control system (1.22) can be lumped together, and this system can be equally considered as an input-delay system (1.24) in which Assumption 2 is satisfied.
The control objective is to seek for an appropriate delay estimator $\hat{h}(t)$ such that the approximated predictor-based controller (1.17)-(1.18) can stabilize the system (1.1) with unknown constant input delay.

Problem formulation of input-output delay system

The problem formulation of the input-output delay system (1.3) is almost the same as the one of input-delay system, only some small changes are made.
First, assumptions 1-2 are modified in order to adjust system (1.3). Assumption 1 is extended to the following form:

Assumption 3. *The pairs (A, B) and (A, C) are stabilizable and observable, respectively.*

Assumption 3 implies that, given a matrix $C \in \mathbb{R}^{p\times n}$, for all positive constants c_l, there exists a matrix $L \in \mathbb{R}^{n\times p}$ and a symmetric positive definite matrix $Q \in \mathbb{R}^{n\times n}$ which is the solution to the following Lyapunov equation

$$(A - LC)^T Q + Q(A - LC) = -c_l I_n. \tag{1.25}$$

Define round-trip delay $h_{rt} = h_i + h_o$, Assumption 2 is then extended to:

Assumption 4. *The delayed input value $u(t - h_{rt})$ is available for measurements.*

Assumption 4 can be easily verified by using the technique displayed in Figure 1.2.
Second, thanks to Assumption 4, it is possible to use the delayed input signal $u(t-h_{rt})$ to establish the following luenberger observer

$$\dot{\hat{x}}(t) = A\hat{x} + Bu(t-h_{rt}) + L\left[y(t) - C\hat{x}(t)\right]. \tag{1.26}$$

And the predictor (1.18) is modified to

$$z(t) = e^{A\hat{h}(t)}\hat{x}(t) + \int_{t-\hat{h}(t)}^{t} e^{A(t-s)}Bu(s)\mathrm{d}s, \quad t \geq 0 \tag{1.27}$$

since the full state $x(t)$ is no longer available.
The control objective is to use an appropriate delay estimator $\hat{h}(t)$ to estimate the round-trip delay h_{rt}, and then use the approximated output-feedback predictor-based controller (1.26)-(1.27) to stabilize the system (1.3) with unknown constant input-output delays.

1.2 Predictor-based control of LTI systems with unknown constant delays

At the beginning of this section, a monotonic delay estimation algorithm which is the key to the controller design is introduced. The closed-loop stability under the predictor-based controller and the proposed delay estimation techniques is analyzed. Some simulations and discussions are given to illustrate the performances and robustness of such control techniques.

1.2.1 Properties of the monotonic delay estimator

In this subsection, a new monotonic delay estimator is introduced, and then some detailed discussions about this new delay estimator are given subsequently.
The main idea of the monotonic delay estimator is to use the delayed input signal $u(t-h)$ to estimate the unknown time-delay, as the references (Diop et al. 2001; Drakunov et al. 2006; Miroslav Krstic and Bresch-Pietri 2009; Léchappé, Rouquet, et al. 2016). Remind that this signal is available for the controller due to assumptions 2 and 4, and the technique described in Figure 1.2. The prototype of the delay estimator is given as follows:

$$\dot{\hat{h}}(t) = \|u(t-h) - u(t-\hat{h}(t))\| \tag{1.28}$$

with initial condition $\hat{h}(0) \leq h$. This delay estimator is monotonic since the right-hand side of (1.28) is non-negative.

Lemma 1. *Consider the delay estimation dynamic* (1.28)*, the delay estimator* $\hat{h}(t)$ *with initial condition* $\hat{h}(0) \leq h$ *satisfies that*

$$\hat{h}(t) \leq h, \quad t \geq 0 \tag{1.29}$$

and then one has

$$0 \leq h - \hat{h}(t) \leq h - \hat{h}(0). \tag{1.30}$$

Proof. The first part of the proof is to derive (1.29) by contradiction. Assume that there exists an instant $t_0 > 0$ such that $\hat{h}(t_0) > h$, then there must exist another instant $t_1 \in [0, t_0)$ such that

$$\hat{h}(t_1) = h, \quad \dot{\hat{h}}(t_1) > 0 \tag{1.31}$$

thanks to the fact $\hat{h}(0) \leq h$, the continuity of $\hat{h}(t)$, the monotonicity of $\hat{h}(t)$ and the intermediate value theorem (Beals 2004, Theorem 8.9). However, $\dot{\hat{h}}(t_1) > 0$ cannot be true while $\hat{h}(t_1) = h$ holds. As a consequence of $\hat{h}(t_1) = h$, one has

$$\dot{\hat{h}}(t_1) = \|u(t_1 - h) - u(t_1 - \hat{h}(t_1))\| = \|u(t_1 - h) - u(t_1 - h)\| = 0. \tag{1.32}$$

There is a contradiction between (1.31) and (1.32), then inequality (1.29) is proven. Thus, delay estimator (1.28) is increasing and upper bounded by h such that

$$\hat{h}(0) \leq \hat{h}(t) \leq h, \quad t \geq 0 \tag{1.33}$$

which further derives (1.30). □

Lemma 1 explains that the delay estimator $\hat{h}(t)$ given in (1.28) is always getting closer and closer to the exact delay value h, and it dynamic will be stopped when:

— $\hat{h}(t) = h$ is ensured at a finite time t_0, then it leads to perfect delay estimation for all $t \geq t_0$;

— $\hat{h}(t)$ is close enough to the exact delay value, then the system can be stabilized with this "inaccurate" delay estimation due to the robustness with respect to the delay mismatch (Bresch-Pietri and Petit 2014; Léchappé, Moulay, and Plestan 2018a). As a result, the control signal $u(t)$ is no longer "sufficiently rich" in the sense of the delay indentifiability theory (Orlov et al. 2002; Drakunov et al. 2006), and one cannot perfectly estimate the time-delay (see the example displayed in Figure 1.3).

Indeed, consider the two cases mentioned above, although the time-delay cannot always be accurately estimated, the closed-loop stability can be ensured. Thus, this kind of delay estimation technique is a control oriented closed-loop TDE technique.

However, (1.28) cannot be directly used in the control system since the stability analysis is complicated. In the rest of this chapter, (1.28) is extended to the following three versions:

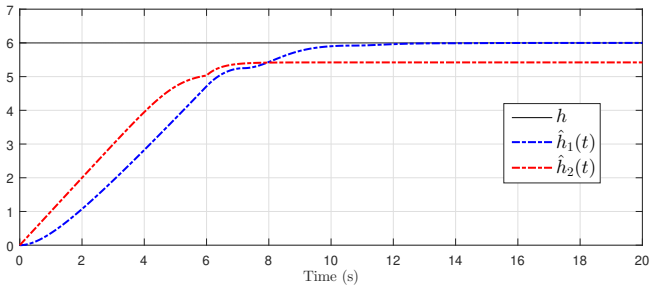

(a) Unknown time-delay $h = 6$s, delay estimator $\hat{h}_1(t)$ (with $u_1(t) = \sin(t)$), and delay estimator $\hat{h}_2(t)$ (with $u_2(t) = e^{-2t}$) versus time.

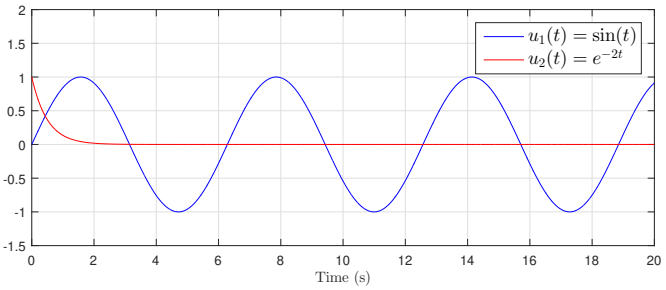

(b) Control signals $u_1(t) = \sin(t)$, and $u_2(t) = e^{-2t}$ versus time.

Figure 1.3 – Delay estimations $\hat{h}_1(t)$, $\hat{h}_2(t)$ versus time via (1.28) with "sufficiently rich" control signal $u_1(t) = \sin(t)$ and "insufficiently rich" control signal $u_2(t) = e^{-2t}$.

Saturated monotonic delay estimator:

$$\dot{\hat{h}}(t) = \min\left\{\|u(t-h) - u(t-\hat{h}(t))\|, \bar{\delta}\right\}, \quad t \geq 0. \tag{1.34}$$

Normalized monotonic delay estimator:

$$\dot{\hat{h}}(t) = \frac{\|u(t-h) - u(t-\hat{h}(t))\|}{\|z(t)\| + \epsilon}, \quad t \geq 0. \tag{1.35}$$

Modified normalized monotonic delay estimator:

$$\dot{\hat{h}}(t) = \frac{\|u(t-h) - u(t-\hat{h}(t))\|}{\max_{s\in[t-2\bar{h},t]} \|z(s)\| + \epsilon}, \quad t \geq 0 \tag{1.36}$$

1.2.2 Predictor-based control and saturated monotonic delay estimation of input-delay systems

In this subsection, the saturated version of the monotonic delay estimator (1.34) with $0 < \bar{\delta} < 1$, is combined with the approximated predictor-based controller (1.17)-(1.18) to stabilize the input-delay system (1.1). The theoretical results are divided into 3 parts:

— The trajectories of $z(t)$ and $\dot{z}(t)$ are bounded on interval $t \in [0, \bar{h})$.
— The Lyapunov-Krasovskii analysis of the reduction model $z(t)$ for all $t \geq \bar{h}$.
— The exponential stability of $z(t)$ and the exponential convergence of $x(t)$ for all $t \geq 0$.

Lemma 2. *Consider the input-delay system* (1.1) *with initial conditions* (1.2)-(1.19) *satisfying conditions* (1.20)-(1.21)*, controlled by the approximated predictor-based controller* (1.17)-(1.18) *and the saturated monotonic delay estimator* (1.34)*. The trajectories of* $z(t)$ *satisfy that*

$$\max_{s\in[0,\bar{h}]} \|z(s)\| \leq ke^{b\bar{h}}, \quad \max_{s\in[0,\bar{h}]} \|\dot{z}(s)\| \leq bke^{b\bar{h}} \tag{1.37}$$

with

$$\begin{aligned} k &= \max_{s\in[-\bar{h},0]} \|z(s)\|, \\ b &= \|A + BK\| + \bar{\delta}\|A\| + e^{\|A\|\bar{h}}\|B\|\|K\|(2 + \bar{\delta} + \bar{\delta}\|A\|\bar{h}). \end{aligned} \tag{1.38}$$

Proof. Taking the time-derivative of (1.18) along the trajectories of (1.1) and (1.17) leads to

$$\begin{aligned} \dot{z}(t) =& (A + BK)z(t) + e^{A\hat{h}(t)}B[u(t-h) - u(t-\hat{h}(t))] + \dot{\hat{h}}(t)Az(t) \\ & - \dot{\hat{h}}(t)A\int_{t-\hat{h}(t)}^{t} e^{A(t-s)}Bu(s)\mathrm{d}s + \dot{\hat{h}}(t)e^{A\hat{h}(t)}Bu(t-\hat{h}(t)), \quad t \geq 0. \end{aligned} \tag{1.39}$$

Consider a scalar function $N(t)$ defined as follows

$$N(t) = \begin{cases} z^T(t)z(t) = \|z(t)\|^2, & t \geq 0 \\ \phi_z^T(\theta)\phi_z(\theta) = \|\phi_z(\theta)\|^2, & -2\bar{h} \leq \theta < 0 \end{cases}. \tag{1.40}$$

Remind that one has (1.20), then $N(t)$ is continuous for all $t \geq -2\bar{h}$. Differentiating $N(t)$ along the trajectories of (1.39) leads to

$$\begin{aligned} \dot{N}(t) =& 2z^T(t)(A+BK)z(t) + 2z^T(t)e^{A\hat{h}(t)}B[u(t-h) - u(t-\hat{h}(t))] + 2\dot{\hat{h}}(t)z^T(t)Az(t) \\ & - 2\dot{\hat{h}}(t)z^T(t)A\int_{t-\hat{h}(t)}^{t} e^{A(t-s)}Bu(s)\mathrm{d}s + 2\dot{\hat{h}}(t)z^T(t)e^{A\hat{h}(t)}Bu(t-\hat{h}(t)), \quad t \geq 0. \end{aligned} \tag{1.41}$$

Taking the norm of the right-hand side of (1.41) and using the fact $|\dot{\hat{h}}(t)| \leq \bar{\delta}$, it follows that

$$\begin{aligned} \dot{N}(t) \leq & 2\|A+BK\|\|z(t)\|^2 + 4e^{\|A\|\bar{h}}\|B\|\|K\|\|z(t)\| \max_{s\in[t-\bar{h},t]}\|z(s)\| + 2\bar{\delta}\|A\|\|z(t)\|^2 \\ & + 2\bar{\delta}\|A\|e^{\|A\|\bar{h}}\|B\|\|K\|\bar{h}\|z(t)\| \max_{s\in[t-\bar{h},t]}\|z(s)\| + 2\bar{\delta}e^{\|A\|\bar{h}}\|B\|\|K\|\|z(t)\| \max_{s\in[t-\bar{h},t]}\|z(s)\|, \quad t \geq 0. \end{aligned} \tag{1.42}$$

Due to the fact that $\|z(t)\| \leq \max_{s\in[t-\bar{h},t]}\|z(s)\|$, (1.42) is upper bounded as

$$\dot{N}(t) \leq 2b\left(\max_{s\in[t-\bar{h},t]}\|z(s)\|\right)^2 = 2b\max_{s\in[t-\bar{h},t]}N(s), \quad t \geq 0 \tag{1.43}$$

where b is defined in (1.38). The analysis given in (Bresch-Pietri, Frédéric Mazenc, and Petit 2018, Appendix B, pp.232-233) proves that the trajectory of $N(t)$ satisfies the following inequality:

$$N(t) \leq \max_{s\in[-\bar{h},0]}N(s)e^{2bt}, \quad t \geq 0. \tag{1.44}$$

Since $\max_{s\in[-\bar{h},0]}N(s) = k^2$, one proves that [1]

$$\|z(t)\| \leq ke^{bt}, \quad t \geq 0 \tag{1.45}$$

where k and b are defined in (1.38). Given that $\|z(\theta)\| \leq k$ for all $\theta \in [-\bar{h}, 0]$, then one has

$$\max_{s\in[t-\bar{h},t]}\|z(s)\| \leq ke^{bt}, \quad t \geq 0. \tag{1.46}$$

Next, one takes the norm of (1.39) and one repeats the calculations given in (1.42) and (1.43), it

1. A similar result is also given in (Selivanov and Fridman 2016b, Appendix A, (A.5)-(A.6)) with the use of the Gronwall-Bellman Lemma.

follows that

$$\|\dot{z}(t)\| \leq b \max_{s\in[t-\bar{h},t]} \|z(s)\|, \quad t \geq 0. \tag{1.47}$$

Combining (1.46) and (1.47) leads to

$$\|\dot{z}(t)\| \leq bke^{bt}, \quad t \geq 0. \tag{1.48}$$

Inequalities (1.45) and (1.48) result in (1.37), and this ends the proof. □

Lemma 2 claims that the trajectory of $z(t)$ is bounded by (1.37) during the transient $t \in [0, \bar{h})$, and it is also observed that the closed-loop system (1.39) does not have finite escape time thanks to the linearity and the saturation bound $\bar{\delta}$.
After analyzing the system trajectories on the transient $t \in [0, \bar{h})$, one focuses on the Lyapunov-Krasovskii analysis of the model reduction $z(t)$ for all $t \geq \bar{h}$.

Lemma 3. *Consider the Lyapunov-Krasovskii functional*

$$V(z, u_t, \dot{u}_t, t) = V_1(z) + \alpha V_2(u_t, t) + \beta V_3(\dot{u}_t, t) \tag{1.49}$$

with positive constants α, β and

$$\begin{aligned} V_1(z) &= z(t)^T P z(t), \\ V_2(u_t, t) &= \int_{t-\hat{h}(t)}^{t} (2\bar{h} + s - t)\|u(s)\|^2 \mathrm{d}s, \\ V_3(\dot{u}_t, t) &= \int_{t-h}^{t} (h + s - t)\|\dot{u}(s)\|^2 \mathrm{d}s. \end{aligned} \tag{1.50}$$

If the parameters $D \triangleq h - \hat{h}(\bar{h})$ and $\bar{\delta}$ are sufficiently small, then there exists $\eta > 0$ such that

$$V(t) \leq V(\bar{h})e^{-2\eta(t-\bar{h})}, \quad t \geq \bar{h}. \tag{1.51}$$

Proof. At the beginning of the proof, the following inequality is reminded

$$0 \leq h - \hat{h}(t) \leq h - \hat{h}(\bar{h}) = D, \quad \forall t \geq \bar{h} \tag{1.52}$$

with the help of Lemma 1. For all $t \geq \bar{h}$, differentiating $V_1(z)$ along the trajectory of (1.39) and using Lyapunov equation (1.16) leads to:

$$\begin{aligned} \dot{V}_1(z(t)) = &-c_u\|z(t)\|^2 + 2\dot{\hat{h}}(t)z^T(t)PAz(t) + 2z^T(t)Pe^{A\hat{h}(t)}B[u(t-h) - u(t-\hat{h}(t))] \\ &- 2\dot{\hat{h}}(t)z^T(t)PA\int_{t-\hat{h}(t)}^{t} e^{A(t-s)}Bu(s)\mathrm{d}s + 2\dot{\hat{h}}(t)z^T(t)Pe^{A\hat{h}(t)}Bu(t-\hat{h}(t)), \quad t \geq \bar{h}. \end{aligned} \tag{1.53}$$

Taking the norm of (1.53), applying the triangle inequality for integrals (Rudin 2006, Theorem 1.33) and the fact that $|\dot{\hat{h}}(t)| \leq \bar{\delta}$, one gets

$$\begin{aligned}\dot{V}_1(z(t)) \leq & -c_u\|z(t)\|^2 + 2\bar{\delta}\|PA\|\|z(t)\|^2 + 2\bar{\delta}e^{\|A\|\bar{h}}\|B\|\|P\|\|z(t)\|\|u(t-\hat{h}(t))\| \\ & + 2\bar{\delta}\|PA\|e^{\|A\|\bar{h}}\|B\|\|z(t)\|\|v(t)\| + 2e^{\|A\|\bar{h}}\|B\|\|P\|\|z(t)\|\|w(t)\|\end{aligned} \tag{1.54}$$

where $\|v(t)\| = \int_{t-\hat{h}(t)}^{t} \|u(s)\|\mathrm{d}s$ and $\|w(t)\| = \int_{t-h}^{t-\hat{h}(t)} \|\dot{u}(s)\|\mathrm{d}s$. Define $c_1 = 2\|PA\|$, $c_2 = 2e^{\|A\|\bar{h}}\|B\|\|P\|$, $c_3 = 2\|PA\|e^{\|A\|\bar{h}}\|B\|$, then (1.54) is equivalent to

$$\dot{V}_1(z) \leq -(c_u - \bar{\delta}c_1)\|z(t)\|^2 + \bar{\delta}c_2\|z(t)\|\|u(t-\hat{h}(t))\| + \bar{\delta}c_3\|z(t)\|\|v(t)\| + c_2\|z(t)\|\|w(t)\|. \tag{1.55}$$

Then, by completing the squares, (1.55) implies that

$$\begin{aligned}\dot{V}_1(z) \leq & -(c_u - \bar{\delta}c_1)\|z(t)\|^2 + \frac{\bar{\delta}c_2}{2}(\|z(t)\|^2 + \|u(t-\hat{h}(t))\|^2) \\ & + \frac{\bar{\delta}c_3}{2}(\|z(t)\|^2 + \|v(t)\|^2) + \left(\frac{Dc_2^2}{\beta}\|z(t)\|^2 + \frac{\beta}{4D}\|w(t)\|^2\right).\end{aligned} \tag{1.56}$$

For all $t \geq \bar{h}$, differentiating $V_2(u_t, t)$ gives that

$$\dot{V}_2(u_t,t) \leq 2\bar{h}\|K\|^2\|z(t)\|^2 - (1-\dot{\hat{h}}(t))(2\bar{h}-\hat{h}(t))\|u(t-\hat{h}(t))\|^2 - \int_{t-\hat{h}(t)}^{t} \|u(s)\|^2\mathrm{d}s. \tag{1.57}$$

Remind that $1-\dot{\hat{h}}(t) \geq 1-\bar{\delta} \geq 0$ and $2\bar{h}-\hat{h}(t) \geq \bar{h} \geq 0$, one has

$$(1-\dot{\hat{h}}(t))(2\bar{h}-\hat{h}(t)) \geq (1-\bar{\delta})\bar{h} \geq 0. \tag{1.58}$$

Combining (1.57) and (1.58) leads to

$$\dot{V}_2(u_t,t) \leq 2\bar{h}\|K\|^2\|z(t)\|^2 - (1-\bar{\delta})\bar{h}\|u(t-\hat{h}(t))\|^2 - \int_{t-\hat{h}(t)}^{t} \|u(s)\|^2\mathrm{d}s. \tag{1.59}$$

Using the Jensen's inequality (Gu, J. Chen, and Kharitonov 2003, Proposition B.8) and the fact that $0 \leq \hat{h}(t) \leq \bar{h}$, the integral term of (1.59) is upper bounded as follows

$$-\int_{t-\hat{h}(t)}^{t} \|u(s)\|^2\mathrm{d}s \leq -\frac{1}{\hat{h}(t)}\left[\int_{t-\hat{h}(t)}^{t} \|u(s)\|\mathrm{d}s\right]^2 \leq -\frac{1}{\bar{h}}\left[\int_{t-\hat{h}(t)}^{t} \|u(s)\|\mathrm{d}s\right]^2. \tag{1.60}$$

Using (1.60), inequality (1.59) is developed to

$$\dot{V}_2(u_t,t) \leq 2\bar{h}\|K\|^2\|z(t)\|^2 - (1-\bar{\delta})\bar{h}\|u(t-\hat{h}(t))\|^2 - \frac{1}{2\bar{h}}\|v(t)\|^2 - \frac{1}{2}\int_{t-\hat{h}(t)}^{t} \|u(s)\|^2\mathrm{d}s. \tag{1.61}$$

For all $t \geq \bar{h}$, differentiating $V_3(\dot{u}_t, t)$ leads to

$$\dot{V}_3(\dot{u}_t, t) \leq \bar{h}\|K\|^2\|\dot{z}(t)\|^2 - \int_{t-h}^{t} \|\dot{u}(s)\|^2 \mathrm{d}s. \tag{1.62}$$

Remind that one has (1.52), then one also has $-\frac{1}{h-\hat{h}(t)} \leq -\frac{1}{D} \leq 0$. So inequality (1.62) becomes to

$$\begin{aligned} \dot{V}_3(\dot{u}_t, t) &\leq \bar{h}\|K\|^2\|\dot{z}(t)\|^2 - \frac{1}{2}\int_{t-h}^{t-\hat{h}(t)} \|\dot{u}(s)\|^2 \mathrm{d}s - \frac{1}{2}\int_{t-h}^{t} \|\dot{u}(s)\|^2 \mathrm{d}s \\ &\leq \bar{h}\|K\|^2\|\dot{z}(t)\|^2 - \frac{1}{2D}\|w(t)\|^2 - \frac{1}{2}\int_{t-h}^{t} \|\dot{u}(s)\|^2 \mathrm{d}s. \end{aligned} \tag{1.63}$$

For $t \geq \bar{h}$, taking the norm of (1.39) and taking account of the fact that $|\dot{\hat{h}}(t)| \leq \bar{\delta}$, one has

$$\begin{aligned} \|\dot{z}(t)\| \leq & \|A + BK\|\|z(t)\| + \bar{\delta}\|A\|\|z(t)\| + e^{\|A\|\bar{h}}\|B\|\|w(t)\| \\ & + \bar{\delta}\|A\|e^{\|A\|\bar{h}}\|B\|\|v(t)\| + \bar{\delta}e^{\|A\|\bar{h}}\|B\|\|u(t-\hat{h}(t))\|. \end{aligned} \tag{1.64}$$

Squaring (1.64) and using the power means inequality given in (Bullen 2013, pp.203, Theorem 1) yields that

$$\|\dot{z}(t)\|^2 \leq (c_4 + c_5\bar{\delta}^2)\|z(t)\|^2 + c_6\|w(t)\|^2 + c_7\bar{\delta}^2\|v(t)\|^2 + c_6\bar{\delta}^2\|u(t-\hat{h}(t))\|^2 \tag{1.65}$$

where $c_4 = 5\|A + BK\|^2$, $c_5 = 5\|A\|^2$, $c_6 = 5e^{2\|A\|\bar{h}}\|B\|^2$ and $c_7 = 5\|A\|^2e^{2\|A\|\bar{h}}\|B\|^2$. Thus, (1.63) is upper bounded by

$$\begin{aligned} \dot{V}_3(\dot{u}_t, t) \leq & \bar{h}\|K\|^2\left[(c_4 + c_5\bar{\delta}^2)\|z(t)\|^2 + c_6\|w(t)\|^2 + c_7\bar{\delta}^2\|v(t)\|^2 + c_6\bar{\delta}^2\|u(t-\hat{h}(t))\|^2\right] \\ & - \frac{1}{2D}\|w(t)\|^2 - \frac{1}{2}\int_{t-h}^{t} \|\dot{u}(s)\|^2 \mathrm{d}s. \end{aligned} \tag{1.66}$$

Futhermore, the Lyapunov-Krasovskii functional (1.49) is upper bounded by

$$V(z, u_t, \dot{u}_t, t) \leq \bar{\lambda}(P)\|z(t)\|^2 + 2\alpha\bar{h}\int_{t-\hat{h}(t)}^{t} \|u(s)\|^2 \mathrm{d}s + \beta\bar{h}\int_{t-h}^{t} \|\dot{u}(s)\|^2 \mathrm{d}s. \tag{1.67}$$

For $t \geq \bar{h}$, taking account of (1.56), (1.61), (1.66) and (1.67) gives that

$$\begin{aligned}\dot{V} + 2\eta V \leq & -\Big[c_u - \bar{\delta}c_1 - \bar{\delta}(c_2+c_3)/2 - Dc_2^2/\beta - 2\alpha\bar{h}\|K\|^2 - \beta\bar{h}\|K\|^2(c_4 + c_5\bar{\delta}^2) - 2\eta\bar{\lambda}(P)\Big]\|z(t)\|^2 \\ & - \Big[\alpha\bar{h} - \alpha\bar{h}\bar{\delta} - \bar{\delta}c_2/2 - \beta\bar{h}\|K\|^2 c_6\bar{\delta}^2\Big]\|u(t-\hat{h}(t))\|^2 - \Big[\alpha/2 - 4\alpha\bar{h}\eta\Big]\int_{t-\hat{h}(t)}^{t}\|u(s)\|^2\mathrm{d}s \\ & - \Big[\beta/(2D) - \beta/(4D) - \beta\bar{h}\|K\|^2 c_6\Big]\|w(t)\|^2 - \Big[\alpha/(2\bar{h}) - \bar{\delta}c_3/2 - \beta\bar{h}\|K\|^2 c_7\bar{\delta}^2\Big]\|v(t)\|^2 \\ & - \Big[\beta/2 - 2\beta\bar{h}\eta\Big]\int_{t-h}^{t}\|\dot{u}(s)\|^2\mathrm{d}s.\end{aligned} \tag{1.68}$$

Thus, one obtains the stability conditions as follows

$$\begin{cases} c_u - \bar{\delta}c_1 - \bar{\delta}(c_2+c_3)/2 - Dc_2^2/\beta - 2\alpha\bar{h}\|K\|^2 - \beta\bar{h}\|K\|^2(c_4 + c_5\bar{\delta}^2) - 2\eta\bar{\lambda}(P) \geq 0, & (1.69)\\ \alpha\bar{h} - \alpha\bar{h}\bar{\delta} - \bar{\delta}c_2/2 - \beta\bar{h}\|K\|^2 c_6\bar{\delta}^2 \geq 0, & (1.70)\\ \alpha/(2\bar{h}) - \bar{\delta}c_3/2 - \beta\bar{h}\|K\|^2 c_7\bar{\delta}^2 \geq 0, & (1.71)\\ \beta/(2D) - \beta/(4D) - \beta\bar{h}\|K\|^2 c_6 \geq 0, & (1.72)\\ \alpha/2 - 4\alpha\bar{h}\eta \geq 0, & (1.73)\\ \beta/2 - 2\beta\bar{h}\eta \geq 0. & (1.74)\end{cases}$$

Firstly, one chooses α, β and η sufficiently small in order to verify (1.73), (1.74) and the following inequality

$$c_u/2 - 2\alpha\bar{h}\|K\|^2 - \beta\bar{h}\|K\|^2 c_4 - 2\eta\bar{\lambda}(P) \geq 0. \tag{1.75}$$

Secondly, it is possible to find sufficiently small $\bar{\delta}$ and D satisfying (1.70), (1.71), (1.72) and the following inequality:

$$c_u/2 - \bar{\delta}c_1 - \bar{\delta}(c_2+c_3)/2 - Dc_2^2/\beta - \beta\bar{h}\|K\|^2 c_5\bar{\delta}^2 \geq 0. \tag{1.76}$$

Thus, there exist $\bar{\delta}^* > 0$ and $D^* > 0$ such that for all $\bar{\delta} \leq \bar{\delta}^*$ and $D \leq D^*$, the stability conditions (1.69)-(1.74) are all guaranteed. The Lyapunov-Krasovskii theorem (Fridman 2014a, Theorem 3.1) ensures that $z(t)$ is uniformly asymptotically stable for all $t \geq \bar{h}$. Moreover, one has

$$V(z, u_t, \dot{u}_t, t) \geq w(\|z(t)\|) \tag{1.77}$$

with $w(s) = \underline{\lambda}(P)s^2$. Since one has $\lim_{s\to+\infty} w(s) = +\infty$, it implies that the closed-loop z-system is globally uniformly asymptotically stable for all $t \geq \bar{h}$ such that

$$\dot{V}(z, u_t, \dot{u}_t, t) \leq -2\eta V(z, u_t, \dot{u}_t, t), \quad t \geq \bar{h} \tag{1.78}$$

Finally, (1.51) is proven by using (1.78). □

Lemma 3 shows that stability of $z(t)$ is ensured if the delay estimation $\hat{h}(t)$ is sufficiently accurate and sufficiently slow-varying (*i.e.* $\bar{\delta}$ is sufficiently small) for all $t \geq \bar{h}$. Combine the results of Lemmas 2-3, the exponential stabilities of $z(t)$ and the exponential convergences of $x(t)$ for all $t \geq 0$ are derived.

Lemma 4. *If Lemma 3 holds, then the closed-loop system of $z(t)$ is globally uniformly exponentially stable (Globally Uniformly Exponentially Stable (GUES)), and the true state $x(t)$ exponentially converges to zero. Namely, there exist positive constants M_1, M_2 such that*

$$\|z(t)\| \leq M_1 \max_{s\in[-\bar{h},0]} \|z(s)\|e^{-\eta t}, \quad t \geq 0 \tag{1.79}$$

and

$$\|x(t)\| \leq M_2 \max_{s\in[-\bar{h},0]} \|z(s)\|e^{-\eta t}, \quad t \geq 0 \tag{1.80}$$

with η given in Lemma 3.

Proof. To obtain the stability of $z(t)$ for all $t \geq 0$, the boundedness of $V(\bar{h})$ is necessary, one firstly bounds the term $V(\bar{h})$ by using (1.49)-(1.50) as follows

$$\begin{aligned} V(\bar{h}) &\leq \bar{\lambda}(P)\|z(\bar{h})\|^2 + 2\alpha\bar{h}\|K\|^2 \int_0^{\bar{h}} \|z(s)\|^2 \mathrm{d}s + \beta\bar{h}\|K\|^2 \int_0^{\bar{h}} \|\dot{z}(s)\|^2 \mathrm{d}s \\ &\leq \bar{\lambda}(P)\|z(\bar{h})\|^2 + 2\alpha\bar{h}^2\|K\|^2 \max_{s\in[0,\bar{h}]} \|z(s)\|^2 + \beta\bar{h}^2\|K\|^2 \max_{s\in[0,\bar{h}]} \|\dot{z}(s)\|^2. \end{aligned} \tag{1.81}$$

Taking account of (1.81), (1.37) and (1.45), the upper bound of $V(\bar{h})$ satisfies that

$$V(\bar{h}) \leq \left[\bar{\lambda}(P)e^{2b\bar{h}} + 2\alpha\bar{h}^2\|K\|^2 e^{2b\bar{h}} + \beta\bar{h}^2\|K\|^2 b^2 e^{2b\bar{h}}\right] k^2. \tag{1.82}$$

Define $M_0^2 = \bar{\lambda}(P)e^{2b\bar{h}} + 2\alpha\bar{h}^2\|K\|^2 e^{2b\bar{h}} + \beta\bar{h}^2\|K\|^2 b^2 e^{2b\bar{h}}$, inequalities (1.77), (1.82) and (1.51) yield that

$$\|z(t)\| \leq \frac{M_0 e^{\eta\bar{h}}}{\sqrt{\underline{\lambda}(P)}} k e^{-\eta t}, \quad t \geq \bar{h}. \tag{1.83}$$

Moreover, during the transient on $0 \leq t \leq \bar{h}$, $e^{\eta(\bar{h}-t)}$ is larger than 1. From (1.46), $z(t)$ is upper bounded as follows

$$\|z(t)\| \leq ke^{b\bar{h}} \leq ke^{b\bar{h}}e^{\eta(\bar{h}-t)} \leq ke^{(b+\eta)\bar{h}}e^{-\eta t}, \quad 0 \leq t \leq \bar{h}. \tag{1.84}$$

Define

$$M_1 = \frac{M_0 e^{\eta\bar{h}}}{\sqrt{\underline{\lambda}(P)}} \tag{1.85}$$

which is larger than $e^{(b+\eta)\bar{h}}$ since

$$M_1 \geq \frac{\sqrt{\bar{\lambda}(P)e^{2b\bar{h}}}}{\sqrt{\underline{\lambda}(P)}}e^{\eta\bar{h}} \geq e^{(b+\eta)\bar{h}} \geq 1. \tag{1.86}$$

Therefore, (1.83) and (1.84) result in the exponential stability (1.79). The next part of the proof is to demonstrate (1.80). Rearranging (1.18), one gets

$$x(t) = e^{-A\hat{h}(t)}z(t) - \int_{t-\hat{h}(t)}^{t} e^{A[t-\hat{h}(t)-s]}Bu(s)\mathrm{d}s, \quad t \geq 0. \tag{1.87}$$

Taking the norm of (1.87) and using (1.20), the upper bound of $\|x(t)\|$ reads as follows

$$\|x(t)\| \leq e^{\|A\|\bar{h}}\|z(t)\| + e^{\|A\|\bar{h}}\|B\|\|K\|\bar{h}\max_{s\in[t-\bar{h},t]}\|z(s)\|, \quad t \geq 0. \tag{1.88}$$

Consider (1.79) and (1.86), then $\max_{s\in[t-\bar{h},t]}\|z(s)\|$ satisfies

$$\max_{s\in[t-\bar{h},t]}\|z(s)\| \leq \begin{cases} M_1 k, & 0 \leq t \leq \bar{h} \\ M_1 k e^{-\eta(t-\bar{h})}, & t \geq \bar{h} \end{cases}. \tag{1.89}$$

Note that $e^{\eta(\bar{h}-t)} \geq 1$ for all $0 \leq t \leq \bar{h}$, then (1.89) provides that

$$\max_{s\in[t-\bar{h},t]}\|z(s)\| \leq M_1 e^{\eta\bar{h}} k e^{-\eta t}, \quad t \geq 0. \tag{1.90}$$

Substituting (1.79) and (1.90) into (1.88), the upper bound of $x(t)$ is developed to

$$\begin{aligned} \|x(t)\| &\leq e^{\|A\|\bar{h}}M_1 k e^{-\eta t} + e^{\|A\|\bar{h}}\|B\|\|K\|\bar{h}M_1 e^{\eta\bar{h}} k e^{-\eta t} \\ &\leq \left[e^{\|A\|\bar{h}} + e^{\|A\|\bar{h}}\|B\|\|K\|e^{\eta\bar{h}}\bar{h}\right] M_1 k e^{-\eta t}, \quad t \geq 0. \end{aligned} \tag{1.91}$$

Thus, the exponential convergence (1.80) is proven with $M_2 = \left[e^{\|A\|\bar{h}} + e^{\|A\|\bar{h}}\|B\|\|K\|e^{\eta\bar{h}}\bar{h}\right] M_1$. □

Sum up the theoretical results presented by Lemmas 2-4, the stability analysis of the system (1.1) under the control laws (1.17)-(1.18)-(1.34) is presented subsequently.

Theorem 1. *Consider the input-delay system* (1.1) *with initial conditions* (1.2)-(1.19) *satisfying conditions* (1.20)-(1.21)*, controlled by the approximated predictor-based controller* (1.17)-(1.18) *and the saturated monotonic delay estimator* (1.34)*. If the positive parameters* $\bar{D} \triangleq h - \hat{h}(0)$ *and* $\bar{\delta}$ *are sufficiently small, then there exist positive constants* M_1*,* M_2 *and* η *such that* $z(t)$ *is GUES with decay rate* η *(as shown in* (1.79)*). Moreover, the state* $x(t)$ *globally converges to zero with decay rate* η *(as shown in* (1.80)*).*

Theorem 1 presents the first control solution based on the monotonic delay estimation (1.28), the saturation bound $\bar{\delta}$ is used to ensure that $\hat{h}$ is always slow-varying. However, this saturation parameter should be tuned sufficiently small, which degrades the performances of the controller since it makes the system trajectory pass through a divergent transient.

1.2.3 Predictor-based control and normalized monotonic delay estimation of input-delay systems

In order to improve the control performances and handle the problem of the (1.34) mentioned in the end of subsection 1.2.2, the normalized monotonic delay estimator (1.35), with sufficiently small constant ϵ, is proposed. The denominator of (1.35) works as a "normalization factor", and it replaces the parameter $\bar{\delta}$ of (1.34). Moreover, the only use of the parameter ϵ is to avoid the singularity, it cannot affect the stability of the control system. In the sequel, the Lyapunov-Razumikhin analysis of the closed-loop stability is presented.

Theorem 2. *Consider the input-delay system* (1.1) *with initial conditions* (1.2)-(1.19) *satisfying conditions* (1.20)-(1.21)*, controlled by the approximated predictor-based controller* (1.17)-(1.18) *and the normalized monotonic delay estimator* (1.35)*. If the positive parameters* $\bar{D} \triangleq h - \hat{h}(0)$ *is sufficiently small, then* $z(t)$ *is globally uniformly asymptotically stable (Golbally Uniformly Asymptotically Stable (GUAS)), and the state* $x(t)$ *globally converges to zero.*

Proof. The proof is divided into two parts, the first part claims that the system trajectory never escape in finite time as the results of Lemma 2, the second part derives the global uniform asymptotic stability of $z(t)$ and the global convergence of $x(t)$ via Lyapunov-Razumikhin theorem (Fridman 2014a, Theorem 3.2).

Part 1. In this part, one proves that the trajectory of $z(t)$ is bounded by an exponential function, which is very similar to the results of Lemma 2.

Consider the normalized delay estimation algorithm (1.35), the triangle inequality, and the fact (1.20), it is upper bounded as follows

$$\dot{\hat{h}}(t) \leq 2\|K\| \frac{\max_{s\in[t-\bar{h},t]} \|z(s)\|}{\|z(t)\| + \epsilon}, \quad \forall t \geq 0. \tag{1.92}$$

Repeating the proof of Lemma 2 till (1.41), and replacing all of the parameters $\bar{\delta}$ given in (1.42)

with (1.92) leads to

$$\begin{aligned}\dot{N}(t) \leq\ & 2\|A+BK\|\|z(t)\|^2 + 4\|K\|\frac{\max_{s\in[t-\bar{h},t]}\|z(s)\|}{\|z(t)\|+\epsilon}\|A\|\|z(t)\|^2 \\ & + 4\|K\|\frac{\max_{s\in[t-\bar{h},t]}\|z(s)\|}{\|z(t)\|+\epsilon}\|A\|e^{\|A\|\bar{h}}\|B\|\|K\|\bar{h}\|z(t)\|\max_{s\in[t-\bar{h},t]}\|z(s)\| \\ & + 4\|K\|\frac{\max_{s\in[t-\bar{h},t]}\|z(s)\|}{\|z(t)\|+\epsilon}e^{\|A\|\bar{h}}\|B\|\|K\|\|z(t)\|\max_{s\in[t-\bar{h},t]}\|z(s)\| \\ & + 4e^{\|A\|\bar{h}}\|B\|\|K\|\|z(t)\|\max_{s\in[t-\bar{h},t]}\|z(s)\|, \quad t\geq 0.\end{aligned} \tag{1.93}$$

Since one has $\frac{\|z(t)\|}{\|z(t)\|+\epsilon} < 1$ and $\|z(t)\| \leq \max_{s\in[t-\bar{h},t]}\|z(s)\|$, then (1.93) implies (1.43) where b is re-defined as

$$b = \|A+BK\| + 2\|K\|\|A\| + 2e^{\|A\|\bar{h}}\|B\|\|K\|(1+\|K\|+\|K\|\|A\|\bar{h}). \tag{1.94}$$

By using the same way as Lemma 2, the trajectories of $z(t)$ is bounded such that

$$\|z(t)\| \leq \max_{s\in[-\bar{h},0]}\|z(s)\|e^{bt}, \quad t\geq 0. \tag{1.95}$$

Therefore, it is demonstrated that $z(t)$ can never escape in finite time due to (1.95).

Part 2. In this part, one moves on to the stability analysis via Lyapunov-Razumikhin theorem (Fridman 2014a, Theorem 3.2). Consider the Lyapunov function

$$V(z(t)) = z(t)^T P z(t), \tag{1.96}$$

and the Razumikhin condition

$$V(z(t-s)) \leq \kappa V(z(t)), \quad s\in[0,2\bar{h}] \tag{1.97}$$

with $\kappa > 1$. Inequality (1.97) implies that

$$\|z(t-s)\| \leq c_1\|z(t)\| \quad \text{for} \quad s\in[0,2\bar{h}] \tag{1.98}$$

with $c_1 = \sqrt{\kappa\bar{\lambda}(P)/\underline{\lambda}(P)}$. Therefore, if the Razumikhin condition (1.98) holds, then (1.92) can be further bounded as:

$$\dot{\hat{h}}(t) \leq 2\|K\|\frac{\max_{s\in[t-\bar{h},t]}\|z(s)\|}{\|z(t)\|+\epsilon} \leq 2\|K\|c_1, \quad \forall t\geq 0. \tag{1.99}$$

By using the result of (1.92) and the Razumukhin condition (1.98), it is possible to bound $\|\dot{z}(t-s_1)\|$

with $s_1 \in [\hat{h}(t), h]$, one first calculates the value of $\dot{z}(t-s_1)$ by using (1.39):

$$\begin{aligned}\dot{z}(t-s_1) =&(A+BK)z(t-s_1) + e^{A\hat{h}(t-s_1)}B[u(t-s_1-h) - u(t-s_1-\hat{h}(t-s_1))]\\ &+ \dot{\hat{h}}(t-s_1)Az(t-s_1) + \dot{\hat{h}}(t-s_1)e^{A\hat{h}(t-s_1)}Bu(t-s_1-\hat{h}(t-s_1))\\ &- \dot{\hat{h}}(t-s_1)A\int_{t-s_1-\hat{h}(t-s_1)}^{t-s_1} e^{A(t-s_1-s)}Bu(s)\mathrm{d}s, \quad t \geq 2\bar{h}.\end{aligned} \tag{1.100}$$

Secondly, taking the norm of (1.100), and using (1.98), (1.99) leads to

$$\begin{aligned}\|\dot{z}(t-s_1)\| \leq&\|A+BK\|c_1\|z(t)\| + 2e^{\|A\|\bar{h}}\|BK\|c_1\|z(t)\| + 2\|K\|\|A\|c_1^2\|z(t)\|\\ &+ 2\|K\|e^{\|A\|\bar{h}}\|BK\|c_1^2\|z(t)\| + 2\|K\|\|A\|e^{\|A\|\bar{h}}\|BK\|\bar{h}c_1^2\|z(t)\|\\ &\leq c_2\|z(t)\|, \quad t \geq 2\bar{h}\end{aligned} \tag{1.101}$$

with

$$c_2 = \|A+BK\|c_1 + 2\|K\|\|A\|c_1^2 + 2e^{\|A\|\bar{h}}\|BK\|\left(c_1 + \|K\|c_1^2 + \|K\|\|A\|\bar{h}c_1^2\right). \tag{1.102}$$

Inequality (1.101) is next used to bound the term $\|u(t-h) - u(t-\hat{h}(t))\|$, by using the mean value theorem for vector-valued functions (Rudin et al. 1964, Theorem 5.19), there exists $s_1 \in [\hat{h}(t), h]$ such that

$$\|u(t-h) - u(t-\hat{h}(t))\| \leq (h-\hat{h}(t))\|K\|\|\dot{z}(t-s_1)\| \leq (h-\hat{h}(t))\|K\|c_2\|z(t)\|. \tag{1.103}$$

After obtaining (1.98), (1.99) and (1.103), one moves on to the Lyapunov analysis. Differentiating the Lyapunov function (1.96) along the trajectories of (1.39) yields

$$\begin{aligned}\dot{V}(z(t)) =& - c_u\|z(t)\|^2 + 2\dot{\hat{h}}(t)z(t)^TPe^{A\hat{h}(t)}Bu(t-\hat{h}(t)) + 2z(t)^TPe^{A\hat{h}(t)}[Bu(t-h) - Bu(t-\hat{h}(t))]\\ &+ 2\dot{\hat{h}}(t)z(t)^TPAz(t) - 2\dot{\hat{h}}(t)z(t)^TPA\int_{t-\hat{h}(t)}^{t} e^{A(t-s)}Bu(s)ds\end{aligned} \tag{1.104}$$

Take norm of the right-hand side of (1.104), consider the delay estimator (1.35), and apply the Razumikhin condition (1.98) it follows that

$$\begin{aligned}\dot{V}(z(t)) \leq& - c_u\|z(t)\|^2 + 2\|u(t-h) - u(t-\hat{h}(t))\|\|P\|e^{\|A\|\bar{h}}\|B\|\|z(t)\|\\ &+ 2\|u(t-h) - u(t-\hat{h}(t))\|\frac{\|z(t)\|}{z(t)+\epsilon}\|PA\|\|z(t)\|\\ &+ 2\|u(t-h) - u(t-\hat{h}(t))\|\frac{\|z(t)\|}{z(t)+\epsilon}\|PA\|e^{\|A\|\bar{h}}\|BK\|\bar{h}c_1\|z(t)\|\\ &+ 2\|u(t-h) - u(t-\hat{h}(t))\|\frac{\|z(t)\|}{z(t)+\epsilon}\|P\|e^{\|A\|\bar{h}}\|BK\|c_1\|z(t)\|.\end{aligned} \tag{1.105}$$

Substituting (1.103) into (1.105) leads to

$$\dot{V}(z(t)) \leq -c_u\|z(t)\|^2 + (h - \hat{h}(t))(c_3 + c_4 + c_5 + c_6)\|z(t)\|^2 \tag{1.106}$$

with $c_3 = 2\|P\|e^{\|A\|\bar{h}}\|B\|\|K\|c_2$, $c_4 = 2\|PA\|\|K\|c_2$, $c_5 = 2\|PA\|e^{\|A\|\bar{h}}\|BK\|\|K\|\bar{h}c_1c_2$, and $c_6 = 2\|P\|e^{\|A\|\bar{h}}\|BK\|\|K\|c_1c_2$. Thus, if the parameter $\bar{D} = h - \hat{h}(0)$ satisfies

$$\bar{D} \leq \frac{\zeta c_u}{(c_3 + c_4 + c_5 + c_6)}, \quad \zeta \in (0, 1) \tag{1.107}$$

then the closed-loop system (1.39) is globally uniformly asymptotically stable (GUAS) for all $t \geq 2\bar{h}$ according to the Lyapunov-Razumikhin theorem (Fridman 2014a, Theorem 3.2). Recall the first part of this proof, one has

$$\|z(t)\| \leq \max_{s\in[t-\bar{h},t]} \|z(s)\|e^{2b\bar{h}}, \quad \forall t \in [0, 2\bar{h}] \tag{1.108}$$

then one has the following global convergence

$$\lim_{t\to+\infty} \|z(t)\| = 0. \tag{1.109}$$

Finally, consider the boundedness given in (1.88) and the global convergence (1.109), it leads to

$$\lim_{t\to+\infty} \|x(t)\| = 0 \tag{1.110}$$

that ends the proof. □

Theorem 2 improves the results of Theorem 1, the differences between them are summarized as follows:

— With Theorem 2, the parameter $\bar{\delta}$ is no longer required. Under the Razumikhin condition (1.97), $\dot{\hat{h}}(t)$ becomes sufficiently small when $h - \hat{h}(t)$ is sufficiently small by virtue of the "normalized factor".

— The normalized monotonic delay estimator (1.35) makes the convergence $\lim_{t\to+\infty} \hat{h}(t)$ easier to achieve, this property will be discussed later in details.

— The stability analysis of Theorem 2 is based on the Lyapunov-Razumikhin theorem (Fridman 2014a, Theorem 3.2), which can only ensure the asymptotic stability of the closed-loop system.

1.2.4 Predictor-based control and modified normalized monotonic delay estimation of input-delay system

Although the normalized monotonic delay estimator (1.35) exhibits better delay estimation and closed-loop performances than the saturated delay estimator (1.34), but it con only ensure the global

uniform asymptotic stability, as claimed in Theorem 2. In order to derive the exponential stability of this kind of delay estimator, some changes must be made to (1.35), as done in (1.36) (with sufficiently small positive constant ϵ). With the modified version (1.36), sufficiently small $h - \hat{h}(t)$ directly derives sufficiently small $\dot{\hat{h}}(t)$, no matter if the Razumikhin condition (1.97) holds or not.

Theorem 3. *Consider the input-delay system* (1.1) *with initial conditions* (1.2)-(1.19) *satisfying conditions* (1.20)-(1.21)*, controlled by the approximated predictor-based controller* (1.17)-(1.18) *and the modified normalized monotonic delay estimator* (1.36)*. If the positive parameters* $\bar{D} \triangleq h - \hat{h}(0)$ *is sufficiently small, then there exist positive constants* M_1'*,* M_2' *and* η *such that* $z(t)$ *is GUES with decay rate* η'

$$\|z(t)\| \leq M_1' \max_{s\in[-\bar{h},0]} \|z(s)\| e^{-\eta t}, \quad t \geq 0, \tag{1.111}$$

and the state $x(t)$ *globally converges to zero with decay rate* η *such that*

$$\|x(t)\| \leq M_2' \max_{s\in[-\bar{h},0]} \|z(s)\| e^{-\eta t}, \quad t \geq 0. \tag{1.112}$$

Proof. The proof of Theorem 3 follows the three steps given in Lemmas 2-4.

Part 1. This part is dedicated to the boundedness analysis of the trajectories of $z(t)$ on interval $t \in [0, \bar{h})$. Consider the modified delay estimator (1.36), the triangle inequality, and the fact (1.20), it leads to the following uniform boundedness

$$\dot{\hat{h}}(t) \leq 2\|K\| \frac{\max_{s\in[t-\bar{h},t]} \|z(s)\|}{\max_{s\in[t-2\bar{h},t]} \|z(s)\| + \epsilon} \leq 2\|K\|. \tag{1.113}$$

The rest of this part is the same as the proof of Lemma 2, except that the parameter b is re-defined as (1.94). Thus, the boundedness (1.37) still holds with the new parameter b.

Part 2. In this part, the Lyapunov-Krasovskii analysis of the closed-loop system under control solutions (1.17)-(1.18)-(1.36) for all $t \geq \bar{h}$. At the first time, one demonstrates the fact that sufficiently small $h - \hat{h}(t)$ directly derives sufficiently small $\dot{\hat{h}}(t)$. Indeed, for all $r \in [\hat{h}(t), h]$, one has

$$\begin{aligned}
\dot{z}(t-r) =& (A+BK)z(t-r) + e^{A\hat{h}(t-r)}B[u(t-r-h) - u(t-r-\hat{h}(t-r))] \\
&+ \dot{\hat{h}}(t-r)Az(t-r) + \dot{\hat{h}}(t-r)e^{A\hat{h}(t-r)}Bu(t-r-\hat{h}(t-r)) \\
&- \dot{\hat{h}}(t-r)A\int_{t-r-\hat{h}(t-r)}^{t-r} e^{A(t-r-s)}Bu(s)\mathrm{d}s, \quad t \geq \bar{h}.
\end{aligned} \tag{1.114}$$

Taking the norm of (1.114), and using (1.113) leads to

$$\|\dot{z}(t-r)\| \leq b \max_{s\in[t-2\bar{h},t]} \|z(s)\|, \quad t \geq \bar{h} \tag{1.115}$$

for all $r \in [\hat{h}(t), h]$, where the parameter b is defined in (1.94). By using the same way as (1.103),

and considering the fact (1.115), the boundedness of $\|u(t-h)-u(t-\hat{h}(t))\|$ is obtained as follows

$$\|u(t-h)-u(t-\hat{h}(t))\| \leq (h-\hat{h}(t))\|K\|\|\dot{z}(t-r)\| \leq (h-\hat{h}(t))\|K\|b \max_{s\in[t-2\bar{h},t]} \|z(s)\| \tag{1.116}$$

with a constant $r \in [\hat{h}(t), h]$. Therefore, the dynamic of $\hat{h}(t)$ is bounded with

$$\dot{\hat{h}}(t) = \frac{\|u(t-h)-u(t-\hat{h}(t))\|}{\max_{s\in[t-2\bar{h},t]} \|z(s)\|+\epsilon} \leq (h-\hat{h}(t))\|K\|b\frac{\max_{s\in[t-2\bar{h},t]} \|z(s)\|}{\max_{s\in[t-2\bar{h},t]} \|z(s)\|+\epsilon} \leq (h-\hat{h}(t))\|K\|b \tag{1.117}$$

for all $t \geq \bar{h}$. Thus, it is clear that

$$|\dot{\hat{h}}(t)| \leq \hat{\delta} \triangleq D\|K\|b \tag{1.118}$$

for all $t \geq \bar{h}$ with D defined in Lemma 3.

The rest of this part is the repetition of the proof of Lemma 3 by considering the same Lyapunov-Krasovskii functional (1.49)-(1.50), and the stability conditions are the same as (1.69)-(1.74), expect that the saturation parameter $\bar{\delta}$ is replaced by $\hat{\delta}$. Consequently, as stated in Lemma 3, there exist sufficiently small constants $\hat{\delta}^*, D^* > 0$, such that the stability conditions (1.69)-(1.74) can be guaranteed by for all $\hat{\delta} \leq \hat{\delta}^*$ and $D \leq D^*$. Moreover, recall the definition (1.118), it is shown that if one tunes D sufficiently small such that

$$D \leq \min\left\{D^*, \frac{\hat{\delta}^*}{\|K\|b}\right\}, \tag{1.119}$$

then the stability stability conditions (1.69)-(1.74) are all satisfied and the inequality (1.51) is guaranteed.

Part 3. This part derives the exponential stability (1.111) and the exponential convergence (1.112). The proof of this part is exactly the same as the proof of Lemma 4, one only need the change the parameters M_1, M_2 to M_1', M_1', which are computed with the re-defined parameter (1.94). □

Theorem 3 extends the normalized monotonic delay estimator given in Theorem 2 to an uniformly bounded version. By virtue of this modification, the Lyapunov-Krasovskii theorem (Fridman 2014a, Theorem 3.1) is successfully applied, and the global uniform exponential stability is ensured. However, the benefit of (1.36) by comparing with (1.35) is only in theory, the delay estimation speed and the response time are slower since the "normalized factor" (*i.e.* the denominator) of (1.36) is always larger the one of (1.35).

1.2.5 Predictor-based control and saturated monotonic delay estimation of input-output delay system

In this subsection, the input-output system (1.3) is considered, and the main results of Theorem 1 are extended to the output-feedback version. Consider the system (1.3), and one supposes that the round-trip delay of the system is bounded such that

$$0 \leq h_{rt} \leq \bar{h}. \tag{1.120}$$

Next, consider the delayed state $x(t-h_o)$, since the output delay h_o is constant, its dynamic reads as

$$\dot{x}(t-h_o) = Ax(t-h_o) + Bu(t-h_o-h_i) = Ax(t-h_o) + Bu(t-h_{rt}). \tag{1.121}$$

Indeed, the Luenberger observer (1.26) cannot estimate the real-time state $x(t)$, but the delayed state $x(t-h_o)$, since its first two terms constitute the copy of system (1.121) and $y(t) = Cx(t-h_o)$. Thus, if one defines the estimation error as

$$e(t) = x(t-h_o) - \hat{x}(t), \tag{1.122}$$

then the estimation error dynamic reads as

$$\dot{e}(t) = (A-LC)e(t). \tag{1.123}$$

Combine (1.27) and (1.122) yields that

$$x(t) = e(t+h_o) + e^{-A\hat{h}(t+h_o)}z(t+h_o) - \int_{t+h_o-\hat{h}(t+h_o)}^{t+h_o} e^{A(t+h_o-s)}Bu(s)\mathrm{d}s, \quad t \geq 0. \tag{1.124}$$

After explaining the preparation works, the main results are given in the sequel.

Theorem 4. *Consider the input-output system* (1.3) *with initial conditions* (1.2)-(1.19) *satisfying conditions* (1.20)-(1.21)*, controlled by the output-feedback approximated predictor-based controller* (1.17)-(1.27)-(1.26) *and the saturated monotonic delay estimator*

$$\dot{\hat{h}}(t) = \min\left\{\|u(t-h_{rt}) - u(t-\hat{h}(t))\|, \bar{\delta}\right\}, \quad t \geq 0. \tag{1.125}$$

If the positive parameters $\bar{D} \triangleq h - \hat{h}(0)$ *and* $\bar{\delta}$ *are sufficiently small, then there exist positive constants* M_3 *and* η_1 *such that coupled state* (z, e) *is GUES such that*

$$\|z(t)\|^2 + \|e(t)\|^2 \leq M_3\left(\max_{s\in[-\bar{h},0]}\|z(s)\|^2 + \|e(0)\|^2\right)e^{-2\eta_1 t}. \tag{1.126}$$

Moreover, there also exist positive constant M_4 such that the system state $x(t)$ exponentially converges to zero such that

$$\|x(t)\| \leq M_4 \left(\max_{s\in[-\bar{h},0]} \|z(s)\|^2 + \|e(0)\|^2 \right)^{0.5} e^{-\eta_1 t}. \tag{1.127}$$

Proof. The proof of Theorem 4 is also based on the 3-step proof given by Lemmas 2-4, and it is also divided into 3 parts, as done for Theorem 3.

Part 1. Since the predictor (1.27) is based on the state observer $\hat{x}(t)$, then the dynamic of $z(t)$ (1.39) is modified to

$$\begin{aligned} \dot{z}(t) =&(A+BK)z(t) + e^{A\hat{h}(t)}B[u(t-h) - u(t-\hat{h}(t))] + \dot{\hat{h}}(t)Az(t) + e^{A\hat{h}(t)}LCe(t) \\ &- \dot{\hat{h}}(t)A\int_{t-\hat{h}(t)}^{t} e^{A(t-s)}Bu(s)\mathrm{d}s + \dot{\hat{h}}(t)e^{A\hat{h}(t)}Bu(t-\hat{h}(t)), \quad t \geq 0. \end{aligned} \tag{1.128}$$

Then, the scalar function $N(t)$ (1.40) is re-defined as

$$N(t) = \begin{cases} z^T(t)z(t) + e^T(t)e(t) = \|z(t)\|^2 + \|e(t)\|^2, & t \geq 0 \\ \phi_z^T(\theta)\phi_z(\theta) + e^T(0)e(0) = \|\phi_z(\theta)\|^2 + \|e(0)\|^2, & -2\bar{h} \leq \theta < 0 \end{cases}. \tag{1.129}$$

Differentiating $N(t)$ along the trajectories of (1.128) and (1.123) leads to

$$\begin{aligned} \dot{N}(t) =&2z^T(t)(A+BK)z(t) + 2z^T(t)e^{A\hat{h}(t)}B[u(t-h) - u(t-\hat{h}(t))] + 2\dot{\hat{h}}(t)z^T(t)Az(t) \\ &- 2\dot{\hat{h}}(t)z^T(t)A\int_{t-\hat{h}(t)}^{t} e^{A(t-s)}Bu(s)\mathrm{d}s + 2\dot{\hat{h}}(t)z^T(t)e^{A\hat{h}(t)}Bu(t-\hat{h}(t)) \\ &+ 2z^T(t)e^{A\hat{h}(t)}LCe(t) + 2e^T(t)(A-LC)e(t), \quad t \geq 0. \end{aligned} \tag{1.130}$$

Next, taking the norm of (1.130), using the facts

$$2e^{\|A\|\bar{h}}\|LC\|\|z(t)\|\|e(t)\| \leq e^{\|A\|\bar{h}}\|LC\| \left(2\|z(t)\|^2 + \frac{1}{2}\|e(t)\|^2 \right) \tag{1.131}$$

and $|\dot{\hat{h}}(t)| \leq \bar{\delta}$. Then, repeating the calculations between (1.42)-(1.43) gives

$$\dot{N}(t) \leq 2b_1 \left(\max_{s\in[t-\bar{h},t]} \|z(s)\| \right)^2 + 2b_2\|e(t)\|^2 \leq 2\bar{b} \max_{s\in[t-\bar{h},t]} N(s) \tag{1.132}$$

with

$$\begin{aligned} b_1 &= \|A+BK\| + \bar{\delta}\|A\| + e^{\|A\|\bar{h}}\|LC\| + e^{\|A\|\bar{h}}\|BK\|(2+\bar{\delta}+\bar{\delta}\|A\|\bar{h}), \\ b_2 &= \|A-LC\| + \frac{1}{4}e^{\|A\|\bar{h}}\|LC\|, \qquad\qquad \bar{b} = \max\{b_1, b_2\}. \end{aligned} \tag{1.133}$$

The rest of the proof of this part is the same as Lemma 2, one derives the following boundedness:

$$\|z(t)\|^2 + \|e(t)\|^2 \leq k^2 e^{2\bar{b}t}, \quad \|\dot{z}(t)\| \leq b_1 k e^{\bar{b}t}, \quad t \geq 0. \tag{1.134}$$

with $k^2 = \max_{s\in[-\bar{h},0]} \|z(s)\|^2 + \|e(0)\|^2$.

Part 2. This part is similar to the proof of Lemma 3, and the following Lyapunov-Krasovskii functional is considered:

$$V(z, e, u_t, \dot{u}_t, t) = V_1(z) + \alpha V_2(u_t, t) + \beta V_3(\dot{u}_t, t) + \gamma V_4(e) \tag{1.135}$$

where $V_1(z)$, $V_2(u_t, t)$, $V_3(\dot{u}_t, t)$ are given in (1.50), and the additional term $V_4(e)$ reads as

$$V_4(e) = e^T(t) Q e(t). \tag{1.136}$$

Consider the Lyapunov equation (1.25), the derivative of $V_4(e)$ along the trajectories of (1.123) yields

$$\dot{V}_4(e) \leq -c_l \|e(t)\|^2. \tag{1.137}$$

With the use of the Luenberger observer (1.26), the derivatives of $V_1(z)$ and $V_3(\dot{u}_t, t)$ are changed. First, a cross term $2z^T(t) P e^{A\hat{h}(t)} LCe(t)$ is added into the right-hand side of (1.53), and its norm is bounded as

$$\| - 2z^T(t) P e^{A\hat{h}(t)} LCe(t)\| \leq \frac{c_8^2}{2\gamma c_l} \|z(t)\|^2 + \frac{\gamma c_l}{2} \|e(t)\|^2 \tag{1.138}$$

with $c_8 = 2e^{\|A\|\bar{h}} \|P\| \|LC\|$. Next, (1.64) and (1.66) are also modified due to the cross term, the derivative $\dot{V}_3(\dot{u}_t, t)$ now reads as

$$\begin{aligned} \dot{V}_3(\dot{u}_t, t) \leq & \bar{h}\|K\|^2 \left[(c_4' + c_5' \bar{\delta}^2) \|z(t)\|^2 + c_6' \|w(t)\|^2 + c_7' \bar{\delta}^2 \|v(t)\|^2 + c_6' \bar{\delta}^2 \|u(t - \hat{h}(t))\|^2 + c_9 \|e(t)\|^2 \right] \\ & - \frac{1}{2D} \|w(t)\|^2 - \frac{1}{2} \int_{t-h}^{t} \|\dot{u}(s)\|^2 \mathrm{d}s, \end{aligned} \tag{1.139}$$

with $c_4' = 6\|A + BK\|^2$, $c_5' = 6\|A\|^2$, $c_6' = 6e^{2\|A\|\bar{h}} \|B\|^2$, $c_7' = 6\|A\|^2 e^{2\|A\|\bar{h}} \|B\|^2$, and $c_9 = 6e^{2\|A\|\bar{h}} \|LC\|^2$.

Therefore, by tuning the functional $\dot{V}(z, e, u_t, \dot{u}_t, t) + \eta_1 V(z, e, u_t, \dot{u}_t, t)$ negative definite, the follow-

ing stability conditions should be satisfied:

$$\begin{cases} c_u - \bar{\delta}c_1 - \bar{\delta}(c_2+c_3)/2 - Dc_2^2/\beta - 2\alpha\bar{h}\|K\|^2 \\ \qquad -\beta\bar{h}\|K\|^2(c_4' + c_5'\bar{\delta}^2) - \dfrac{c_8^2}{2\gamma c_l} - 2\eta_1\bar{\lambda}(P) \geq 0, & (1.140) \\ \alpha\bar{h} - \alpha\bar{h}\bar{\delta} - \bar{\delta}c_2/2 - \beta\bar{h}\|K\|^2 c_6'\bar{\delta}^2 \geq 0, & (1.141) \\ \alpha/(2\bar{h}) - \bar{\delta}c_3/2 - \beta\bar{h}\|K\|^2 c_7'\bar{\delta}^2 \geq 0, & (1.142) \\ \beta/(2D) - \beta/(4D) - \beta\bar{h}\|K\|^2 c_6' \geq 0, & (1.143) \\ \alpha/2 - 4\alpha\bar{h}\eta_1 \geq 0, & (1.144) \\ \beta/2 - 2\beta\bar{h}\eta_1 \geq 0, & (1.145) \\ \gamma c_l - \dfrac{\gamma}{2}c_l - \beta\bar{h}\|K\|^2 c_9 - 2\eta_1\gamma\bar{\lambda}(Q) \geq 0. & (1.146) \end{cases}$$

In order to satisfy the stability conditions (1.140)-(1.146), the following parameter tuning are made. Firstly, tuning α, β, and η_1 sufficiently small in order to ensure (1.144), (1.145), and the following inequalities

$$\begin{gathered} c_u/3 - 2\alpha\bar{h}\|K\|^2 - \beta\bar{h}\|K\|^2 c_4' - 2\eta_1\bar{\lambda}(P) \geq 0, \\ \gamma c_l/4 - 2\eta_1\gamma\bar{\lambda}(Q) \geq 0. \end{gathered} \tag{1.147}$$

Secondly, setting D and $\bar{\delta}$ sufficiently small to satisfy (1.141)-(1.143), and the inequality given in the sequel

$$c_u/3 - \bar{\delta}c_1 - \bar{\delta}(c_2+c_3)/2 - Dc_2^2/\beta - \beta\bar{h}\|K\|^2 - c_5'\bar{\delta}^2 \geq 0. \tag{1.148}$$

Finally, choosing γ sufficiently large in order to verify

$$\frac{c_u}{3} - \frac{c_8^2}{2\gamma c_l} \geq 0, \quad \frac{\gamma}{4}c_l - \beta\bar{h}\|K\|^2 c_9 \geq 0, \tag{1.149}$$

then all of the stability conditions (1.140)-(1.146) are satisfied. Thus, the exponential stability

$$V(t) \leq V(\bar{h})e^{-2\eta_1(t-\bar{h})}, \quad t \geq \bar{h} \tag{1.150}$$

holds for all $t \geq \bar{h}$.

Part 3. The last part derives the global uniform exponential stability (1.126) and the global exponential convergence (1.127).

By using the same technique as (1.82)-(1.86), then considering (1.134) and the fact

$$\underline{\lambda}(P)\|z(t)\|^2 + \gamma\underline{\lambda}(Q)\|e(t)\|^2 \leq V(z, e, u_t, \dot{u}_t, t), \tag{1.151}$$

the exponential stability (1.126) is ensured with

$$M_0' = \left[\bar{\lambda}(P) + \gamma\bar{\lambda}(Q) + 2\alpha\bar{h}^2\|K\|^2 + \beta\bar{h}^2\|K\|^2 b_1^2\right] e^{2\bar{b}\bar{h}} \tag{1.152}$$

and

$$M_3 = \frac{M_0'}{\lambda_{min}} e^{2\eta_1\bar{h}}, \quad \lambda_{min} = \min\left\{\underline{\lambda}(P), \gamma\underline{\lambda}(Q)\right\}. \tag{1.153}$$

With the exponential stability (1.126), it is apparent to obtain

$$\begin{aligned} \|z(t+h_o)\| &\leq \sqrt{M_3}\left(\max_{s\in[-\bar{h},0]}\|z(s)\|^2 + \|e(0)\|^2\right)^{0.5} e^{-\eta_1(t+h_o)}, \quad t \geq 0, \\ \|e(t+h_o)\| &\leq \sqrt{M_3}\left(\max_{s\in[-\bar{h},0]}\|z(s)\|^2 + \|e(0)\|^2\right)^{0.5} e^{-\eta_1(t+h_o)}, \quad t \geq 0, \end{aligned} \tag{1.154}$$

and

$$\max_{[t+h_o-\bar{h},t+h_o]}\|z(s)\| \leq \sqrt{M_3}\left(\max_{s\in[-\bar{h},0]}\|z(s)\|^2 + \|e(0)\|^2\right)^{0.5} e^{\eta_1\bar{h}} e^{-\eta_1(t+h_o)}, \quad t \geq 0. \tag{1.155}$$

Finally, taking the norm of (1.124), and considering (1.154)-(1.155), the exponential convergence (1.127) is proven with

$$M_4 = \left[1 + e^{\|A\|\bar{h}} + e^{(\|A\|+\eta_1)\bar{h}}\|BK\|\bar{h}\right]\sqrt{M_3}e^{-\eta_1 h_o}. \tag{1.156}$$

□

Theorem 4 extends the results of Theorem 1 to the output feedback case, the exponential stability of the coupled system (z, e) is studied and the global exponential convergence of the system state is still ensured, as the full-state feedback version.

1.3 Discussions and simulation results

In this section, the performances and properties of Theorems 1-4 are discussed in details, then some simulations are given to compare their performances, and the discussions are also illustrated.

1.3.1 Discussions about the monotonic delay estimators

In this part, the performances of Theorems 1-4 are discussed in the following two aspects:

— The constraint on the initial condition of the delay estimator $\hat{h}(0)$.

— The robustness with respect to the model uncertainties.

Hereafter, the main results of Theorems 1-4 are compared with each other.

Constraint on the initial condition $\hat{h}(0)$

Remind that the theoretical results of Theorems 1-4 have constraints on the initial condition of the delay estimator. Namely, the parameter $\bar{D} = h - \hat{h}(0)$ is required to be sufficiently small for Theorems 1-4. However, the difference between h and $\hat{h}(0)$ can be much larger in applications. The reason is twofold:

— The Lyapunov analysis (Fridman 2014a, Theorems 3.1-3.2) is conservative.
— Theorems (1)-(4) are sufficient conditions to the closed-loop stability, and the constraint on $\hat{h}(0)$ is only claimed to ensure that $\hat{h}(t)$ is sufficiently close to h for all $t \geq \bar{h}$.

To well explain the second point of the above discussions, one takes the saturated delay estimator (1.34) and the proofs given in subsection 1.2.2 as an example. Consider the case when $\hat{h}(0)$ is not close to h, but $\hat{h}(t)$ is sufficiently close h for all $t \geq \bar{h}$, then the parameter D defined in Lemma 3 is sufficiently small. Consequently, Lemmas 2-4 are all satisfied and they derive the closed-loop stability (1.79) and the global convergence (1.80).
Another analytic discussion is given to explain this fact, if the difference between h and $\hat{h}(t)$ is large, then the system is divergent due to the delay mismatch, but the trajectories can never escape in finite time (with the help of the proof of Lemma 2, and Theorems 2-4). During this transient, the control signal $u(t)$ is also divergent, and it is "sufficiently rich" in the sense of the delay identifiability theory (Orlov et al. 2002). As a result, the delay estimator $\hat{h}(t)$ keeps converging to the real delay h, and the difference between them becomes smaller and smaller. The evolution of $\hat{h}(t)$ can only be terminated when the delay estimation error $h - \hat{h}(t)$ is sufficiently small, and then the closed-loop stability is achieved.

Robustness with respect to the model uncertainties

The key to the stability results of Theorems 1-4 is the monotonic delay estimator (1.28), then it is important to analyze the robustness of this method. Indeed, the delay estimator (1.28) is totally based on the control signal, since the delayed signal $u(t-h)$ is available for measurement (due to Assumptions 2 and 4), and the term $u(t - \hat{h}(t))$ is stored by the controller. Due to this fact, the model uncertainties cannot affect the delay estimation (1.3), since no system information is required by the estimation algorithm.

Comparison between Theorems 1-3

The first part analyzes Theorem 1 and the saturated delay estimator (1.34). In this work, one use the parameter $\bar{\delta}$ to force the delay estimation dynamic contain in $[0, \bar{\delta}]$, in order to satisfy the stability conditions (1.69)-(1.74). However, this parameter slows down the convergence speed of the delay estimator, and the response time of the closed-loop system. This issue is overcome by the normalized

delay estimator (1.35), and only one parameter $\bar{D}$ is required to be tuned in order to obtain the stability results of Theorem 2. Moreover, the "normalized factor" can accelerate the speed of the delay estimation algorithm when the control signal is not "sufficiently rich", because $\|z(t)\| + \epsilon$ is much smaller than 1 in this case. Although the modified delay estimator (1.36) leads to the exponential stability of Theorem 3, its convergence speed is slower than (1.35) since $\max_{s\in[t-2\bar{h},t]} \|z(s)\| + \epsilon$ is always larger than $\|z(t)\| + \epsilon$.
The above discussions are summarized by Table 1.1.

	Nb. of tuning parameters	stability	TDE accuracy
Saturated delay estimator (1.34)	2	GUES	the third accurate
Normalized delay estimator (1.35)	1	GUAS	the most accurate
Modified delay estimator (1.36)	1	GUES	the second accurate

Table 1.1 – Comparison of the three delay estimators of Theorems 1-3.

All of the above mentioned properties will be illustrated by the simulation results given in the sequel.

1.3.2 Simulation results

In this subsection, some simulation results are given to illustrate the performances and the properties (constraint on the initial condition $\hat{h}(0)$, robustness with respect to model uncertainties, and convergence speed) of the main theoretical results given in subsections 1.2.2-1.2.5.
Throughout this section, the integral terms of (1.18) **and** (1.27) **are numerically calculated by the method proposed in (Bresch-Pietri, Chauvin, and Petit 2012),** *i.e.* **they are computed by the trapezoid discretization method with periodic reset.**

Input-delay system (Zhou 2014a)
Consider the input-delay system (1.157) inspired by the linearized liquid propellant rocket motors (Zhou 2014a, Example 2), where the delay value $h = 2$s is unknown.

$$\dot{x}(t) = \begin{bmatrix} -1 & 0 & 1 & 0 \\ 0 & 0 & 0 & -1 \\ -1 & 0 & -1 & 1 \\ 0 & 1 & -1 & 0 \end{bmatrix} x(t) + \begin{bmatrix} 0 \\ 1 \\ 0 \\ 0 \end{bmatrix} u(t-h), \quad t \geq 0. \tag{1.157}$$

Suppose that the unknown input-delay h given in (1.157) is upper bounded by $\bar{h} = 4$s, and the initial conditions of the system read as $x(0) = \begin{bmatrix} 0.5 & 0.6 & -0.6 & 0.5 \end{bmatrix}^T$, and $u(\theta) = -3.1452$ for all $\theta \in [-2\bar{h}, 0)$. The feedback matrix $K = \begin{bmatrix} 6 & -8 & 13 & -12 \end{bmatrix}$ leads to the eigenvalues $\{-1; -1; -3; -5\}$

for $A+BK$. The initial condition of $z(t)$ is set to $z(\theta) = \begin{bmatrix} 0.2962 & 0.0502 & -0.6335 & -0.3096 \end{bmatrix}^T$ for all $\theta \in [-2\bar{h}, 0)$ that guarantees (1.20). The parameters $\bar{\delta}$ and ϵ are set to 0.3 and 0.05, respectively. In the simulations, the three delay estimators (1.34), (1.35), (1.36) are tested with three initial conditions $\hat{h}(0) = 0$s, $\hat{h}(0) = 1$s, and $\hat{h}(0) = 1.5$s, in order to test if the constraint on the initial condition $\hat{h}(0)$ is restrictive.

The simulation results are presented in Figure 1.4, and the control performances are discussed in the following aspects:

— **The constraint on the initial condition $\hat{h}(0)$:** in Figures 1.4a, 1.4c, and 1.4e, the system state $x(t)$ converges to zero under the control laws proposed in Theorems 1-3, even if some initial conditions $\hat{h}(0)$ are far from the unknown input-delay value. The simulation results illustrate the explanations given in the previous subsection such that the stability condition on $\hat{h}(0)$ is much less restrictive in practice than theory.

— **Accuracy of different delay estimators:** consider the simulation results displayed in Figures 1.4b, 1.4d, and 1.4f, the convergence speed of the saturated delay estimator (1.34) with $\bar{\delta}$ is slower than ones of (1.35) and (1.36). See Figure 1.4f, the delay estimator (1.34) cannot ensure the convergence $\lim_{t\to+\infty} \hat{h}(t) = h$ in this case since the convergence speed of the system is faster than the delay estimator, that makes the control signal $u(t)$ "insufficient rich" and the delay identifiability of the system is lost. However, in this figure, (1.35) and (1.36) still accurately estimate the unknown time-delay thanks to the "normalized factors". Next, the performances of (1.35) and (1.36) are compared, Figure 1.4b and the zoomed sub-figures in Figures 1.4d, 1.4f show that the normalized delay estimator (1.35) converges slightly faster to the unknown input-delay than its modified version (1.36), that illustrates the comparisons given in Table 1.1.

Thus, the simulation results displayed in Figure 1.4 highlight the practical use of the theoretical results of Theorems 1-3, and the comparisons provided by Table 1.1 are also illustrated and emphasized.

Input-output delay system (Selivanov and Fridman 2016a)

After illustrating the results of Theorems 1-3, one moves on to the validation of the output feedback technique given by Theorem 4. Consider the linearized inverted pendulum with partial state knowledge (only the cart position and the pendulum angle are available) given in (Selivanov and

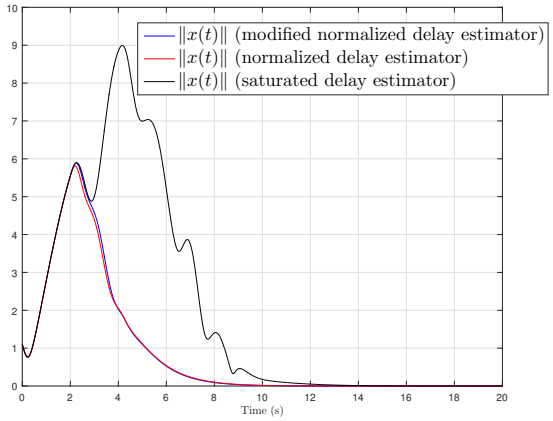

(a) State of the system (1.157) under control solutions of Theorems 1-3 with initial condition $\hat{h}(0) = 0$s.

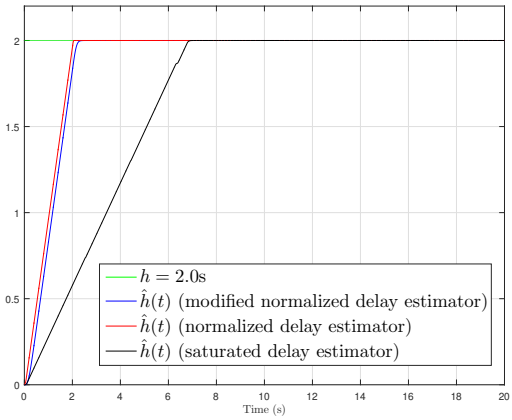

(b) Delay estimation of the system (1.157) under control solutions of Theorems 1-3 with initial condition $\hat{h}(0) = 0$s.

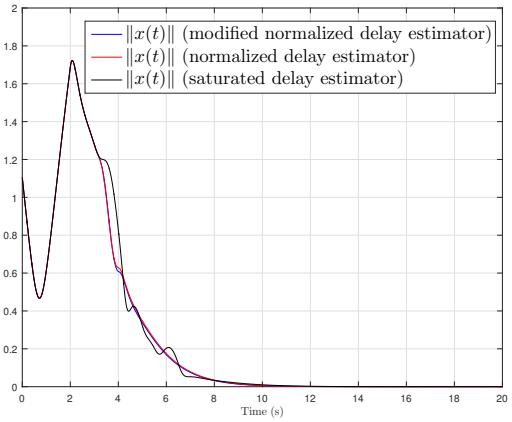

(c) State of the system (1.157) under control solutions of Theorems 1-3 with initial condition $\hat{h}(0) = 1$s.

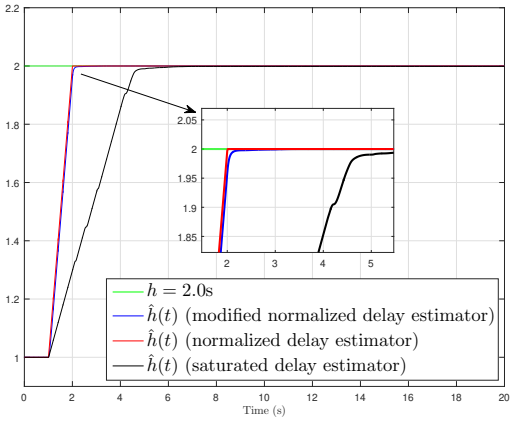

(d) Delay estimation of the system (1.157) under control solutions of Theorems 1-3 with initial condition $\hat{h}(0) = 1$s.

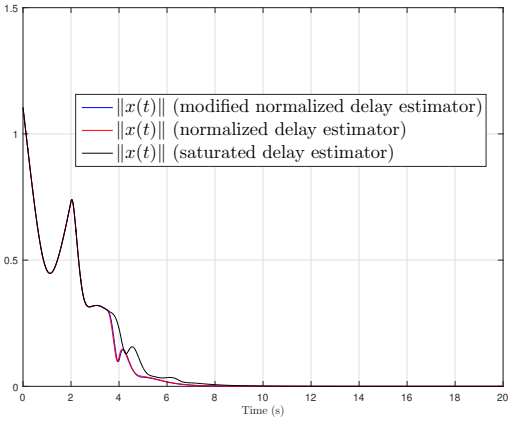

(e) State of the system (1.157) under control solutions of Theorems 1-3 with initial condition $\hat{h}(0) = 1.5$s.

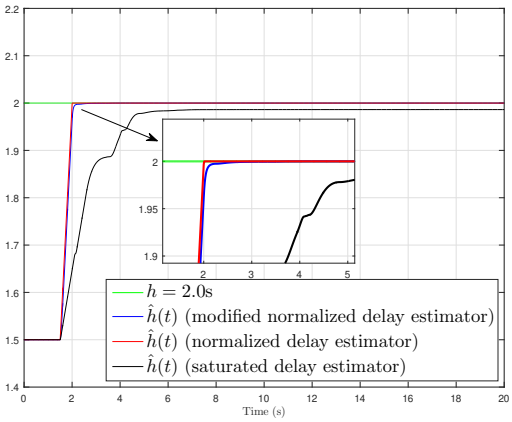

(f) Delay estimation of the system (1.157) under control solutions of Theorems 1-3 with initial condition $\hat{h}(0) = 1.5$s.

Figure 1.4 – State evolution and delay estimation of the input-delay system (1.157) under control solutions of Theorems 1-3 with initial conditions.

Fridman 2016a, Section 5)

$$\begin{cases} \dot{x}(t) = \begin{bmatrix} 0 & 1 & 0 & 0 \\ 0 & 0 & -mg/M & 0 \\ 0 & 0 & 0 & 1 \\ 0 & 0 & g/l & 0 \end{bmatrix} x(t) + \begin{bmatrix} 0 \\ 1/M \\ 0 \\ -1/(Ml) \end{bmatrix} u(t-h_i), \\ y(t) = \begin{bmatrix} 1 & 0 & 0 & 0 \\ 0 & 0 & 1 & 0 \end{bmatrix} x(t-h_o). \end{cases} \tag{1.158}$$

where $m = 1\text{kg}$, $M = 10\text{kg}$, $l = 3\text{m}$, $g = 10\text{m/s}^2$, and the unknown constant delays $h_i = 0.5\text{s}$, $h_o = 0.3\text{s}$, is controlled by the output feedback controller given in Theorem 4. Assume that the known bound on the round-trip delay $h_{rt} = 0.8\text{s}$ is $\bar{h} = 1.5\text{s}$. The initial conditions are set to $x(0) = \begin{bmatrix} 0.98 & 0 & 0.2 & 0 \end{bmatrix}^T$, $\hat{x}(0) = \begin{bmatrix} 1 & 0 & 0.1 & 0 \end{bmatrix}^T$, $z(\theta) = \begin{bmatrix} 0.9916 & -0.0437 & 0.1279 & 0.1455 \end{bmatrix}^T$, and $u(\theta) = 42.658$ for all $\theta \in [-2\bar{h}, 0)$. The feedback gains K and L read as

$$K = \begin{bmatrix} 5.76 & 21.04 & 368.98 & 207.12 \end{bmatrix}, \quad L = \begin{bmatrix} 13.1074 & -2.1276 \\ 35.8132 & -10.9329 \\ -2.1426 & 8.8926 \\ -10.0367 & 19.5199 \end{bmatrix}. \tag{1.159}$$

In the simulation, the delay estimator (1.125) given in Theorem 4 is tested with different initial conditions (*i.e.* $\hat{h}(0) = 0.0\text{s}$, $\hat{h}(0) = 0.4\text{s}$, and $\hat{h}(0) = 0.7\text{s}$), the simulation results are presented in the sequel.

In Figure 1.5a, the system state $x(t)$ and the observation error $e(t)$ converges to zero no matter the initial condition $\hat{h}(0)$ is close to h_{rt} or not, and the simulation results of Figure 1.5a illustrate that the delay estimator (1.125) is able to estimate the unknown round-trip delay.

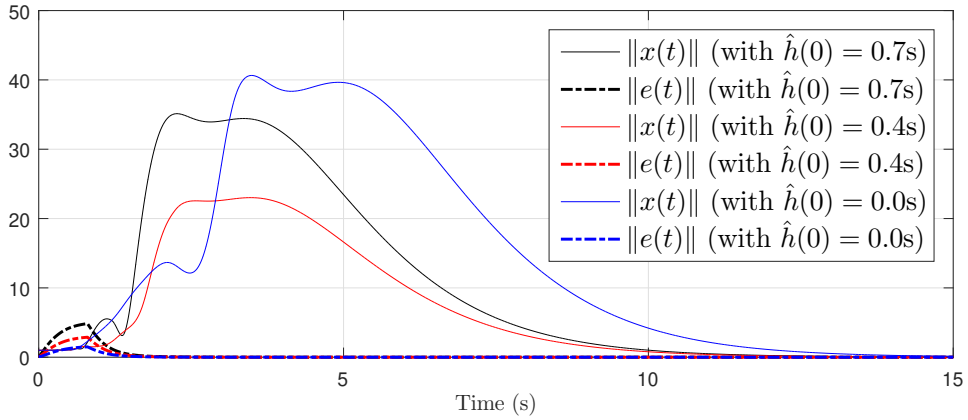

(a) System state $x(t)$ and observation error $e(t)$ of the system (1.158) under control solution of Theorem 4 with initial conditions $\hat{h}(0) = 0.0$s, $\hat{h}(0) = 0.4$s, and $\hat{h}(0) = 0.7$s.

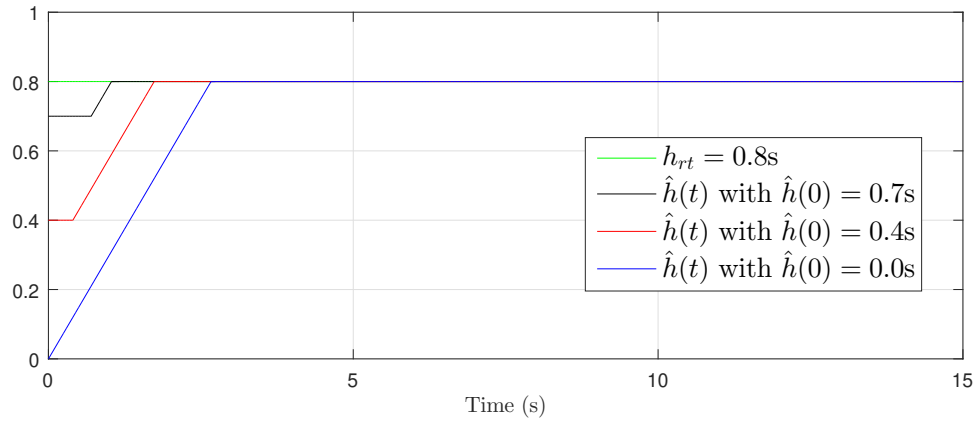

(b) Delay estimation of the system (1.158) under control solution of Theorem 4 with initial conditions $\hat{h}(0) = 0.0$s, $\hat{h}(0) = 0.4$s, and $\hat{h}(0) = 0.7$s.

Figure 1.5 – Evolutions of the state, the observation error, and the delay estimation of the system (1.158) under control solution of Theorem 4 with initial conditions $\hat{h}(0) = 0.0$s, $\hat{h}(0) = 0.4$s, and $\hat{h}(0) = 0.7$s.

Next, consider the same system (1.158) with unknown model uncertainties ΔA, ΔB, and ΔC:

$$\begin{cases} \dot{x}(t) = \left(\begin{bmatrix} 0 & 1 & 0 & 0 \\ 0 & 0 & -mg/M & 0 \\ 0 & 0 & 0 & 1 \\ 0 & 0 & g/l & 0 \end{bmatrix} + \underbrace{\begin{bmatrix} 0 & 0 & 0 & 0 \\ -0.05 & 0 & 0.02 & 0 \\ 0 & 0 & 0 & 0 \\ 0 & 0 & 0.02 & -0.05 \end{bmatrix}}_{\Delta A} \right) x(t) \\ \qquad\qquad + \left(\begin{bmatrix} 0 \\ 1/M \\ 0 \\ -1/(Ml) \end{bmatrix} + \underbrace{\begin{bmatrix} 0 \\ -0.005 \\ 0 \\ 0 \end{bmatrix}}_{\Delta B} \right) u(t - h_i), \\ y(t) = \left(\begin{bmatrix} 1 & 0 & 0 & 0 \\ 0 & 0 & 1 & 0 \end{bmatrix} + \underbrace{\begin{bmatrix} 0 & 0.01 & 0 & 0 \\ 0 & 0 & 0.01 & -0.01 \end{bmatrix}}_{\Delta C} \right) x(t - h_o). \end{cases} \tag{1.160}$$

All of the other parameters are the same as the ones of (1.158), the state observation and control law are computed by using the knowledge of the nominal system (1.158), and the initial condition of the delay estimator (1.125) is set to $\hat{h}(0) = 0.4$s.

The simulation results are presented in Figure 1.6. First, the simulation results displayed in Figure 1.6b illustrate the discussions given in the previous subsection, such that the monotonic delay estimator (1.28) is robust with respect to the model uncertainties. Second, Figure 1.6a show that the uncertain system (1.160) is stabilized, as the nominal system (1.158). However, the model uncertainties degrades the system performances, and there exist oscillations on the curves of $\|x(t)\|$ and $\|e(t)\|$.

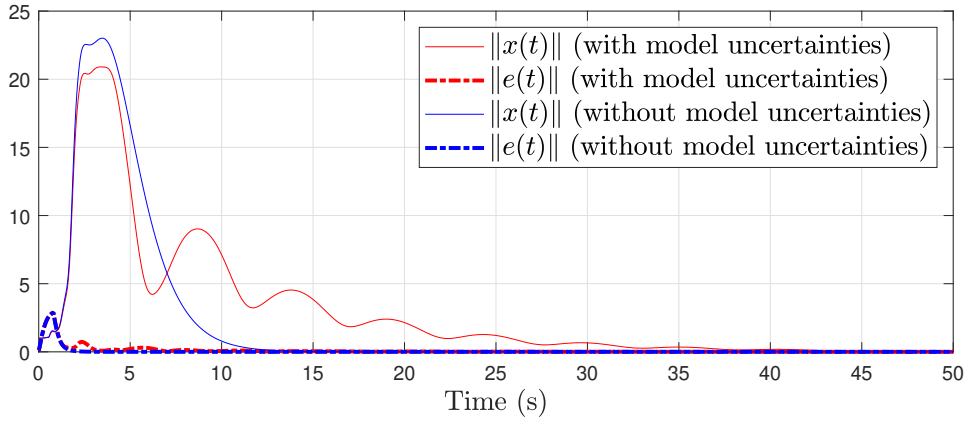

(a) System state $x(t)$ and observation error $e(t)$ of the nominal system (1.158) and the uncertain system (1.160) under control solution of Theorem 4 with initial condition $\hat{h}(0) = 0.4$s.

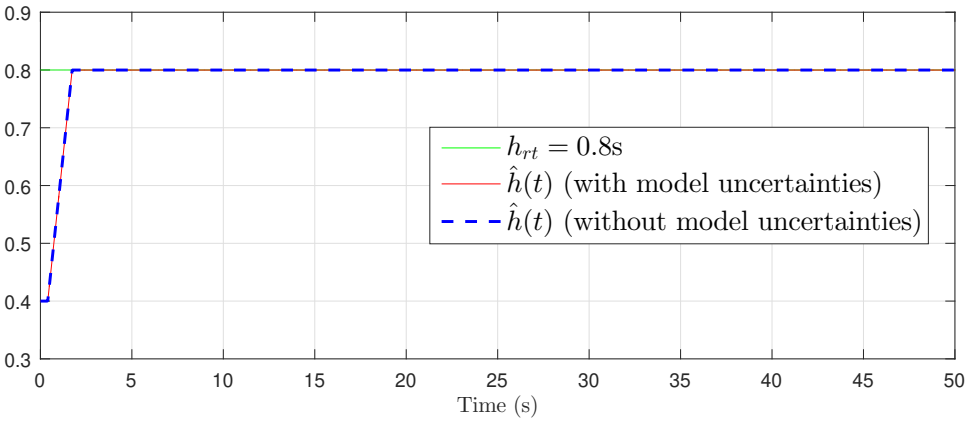

(b) Delay estimation of the nominal system (1.158) and the uncertain system (1.160) under control solution of Theorem 4 with initial condition $\hat{h}(0) = 0.4$s.

Figure 1.6 – Evolutions of the state, the observation error, and the delay estimation of the nominal system (1.158) and the uncertain system (1.160) under control solution of Theorem 4 with initial condition $\hat{h}(0) = 0.4$s.

Chapter 2

Stabilization of Remote control systems with time-varying delays

Contents

The main results of this Chapter are accepted in, and submitted to the following international journals and conference:

[1] Y. Deng, V. Léchappé, S. Rouquet, E. Moulay, and F. Plestan, *Super-twisting algorithm based time-varying delay estimation with external signal*, online published in IEEE Transactions on Industrial Electronics. doi: 10.1109/TIE.2019.2960739.

[2] Y. Deng, V. Léchappé, S. Rouquet, E. Moulay, and F. Plestan, *A practical online time-varying delay estimation of remote control system based on adaptive super-twisting algorithm*, accepted in

2020 IEEE Conference on Control Technology and Applications (CCTA).

[3] Y. Deng, V. Léchappé, E. Moulay, and F. Plestan, *Predictor-based control of LTI remote systems with estimated time-varying delays*, in IEEE Control Systems Letters, vol 5, issue 1, pages 289-294, Jan 2021.

2.1 Preliminaries and problem formulation

This section is dedicated to the stabilization of remote control systems with unknown time-varying input and output delays. Indeed, the time-varying delays, especially fast-varying delays, make the controller design challenging:

— On the one hand, the fast-varying delays affect the existence of predictor feedback law. For instance, (Bekiaris-Liberis and Miroslav Krstic 2013, Chapter 6) considers the control of systems with a single input-delay $h_i(t)$, and the works of (Sanz, Garcia, and Miroslav Krstic 2019) studies the output feedback of systems with a single output delay $h_o(t)$, both of them can only deal with slowing-varying delays because they stand on the assumption such that the functions $\phi_i(t) = t - h_i(t)$, $\phi_o(t) = t - h_o(t)$ are invertible, respectively.

— On the other hand, if the time-varying delays are unknown, one must estimate it at the first time. However, the majority of the existing TDE methods cannot estimate fast-varying delays, as shown in Table 2.

In applications, the delay estimation and control law design of remote control systems can be separated, as done in (Lai and Hsu 2010). Since the input and output delays of such systems are arisen from the data transmission, then one can use the system clock and specific communication protocols to directly measure the round-trip delay, and then an appropriate controller is designed. The work of (Lai and Hsu 2010) presents a practical solution to the stabilization of remote control with time-varying delays.

Inspired by the work of (Lai and Hsu 2010), this chapter considers the practical stabilization of the following remote control systems with full-state measurement:

$$\begin{cases} \dot{x}(t) = Ax(t) + Bu(t - h_i(t)), & t \geq 0 \\ y(t) = x(t - h_o(t)) \end{cases} \tag{2.1}$$

where $x(t) \in \mathbb{R}^n$, $u(t) \in \mathbb{R}^m$, $A \in \mathrm{R}^{n\times n}$, $B \in \mathbb{R}^{n\times m}$, and $h_i(t), h_o(t) > 0$ are time-varying delays. Next, assume that the round-trip delay of system (2.1) is upper bounded by a known value $\bar{h}$, then

the initial condition of the system reads as

$$\begin{aligned} x(\theta) &= \phi_x(\theta) \in \mathbf{C}([-\bar{h}, 0), \mathbb{R}^n) \\ u(\theta) &= \phi_u(\theta) \in \mathbf{C}([-\bar{h}, 0), \mathbb{R}^m). \end{aligned} \tag{2.2}$$

The main contributions of this chapter are clarified in the sequel:

— The delay measurement approach (Lai and Hsu 2010) is extended to dynamic delay estimators, and the sliding mode methods are involved to ensure the finite time convergence of the delay estimation. It is shown that the dynamic delay estimation algorithms are more robust than (Lai and Hsu 2010) with respect to noises and cyber attacks.

— The sliding mode based delay estimation approaches are implemented on a test bench, which is composed of two computers and the communication between them via WiFi network.

— The round-trip delay estimated by the sliding mode based methods is plugged into a predictor-based controller to stabilize the system (2.1), the closed-loop stability is ensured if $h_i(t)$ varies sufficiently slowly. Moreover, the closed-loop stability is preserved even if the derivative of $h_o(t)$ is large.

2.1.1 Framework of the practical delay estimation technique

Consider the remote control system (2.1) with time-varying delays $h_i(t)$, $h_o(t)$ introduced by the data transmission between the sensor, the controller, and the plant.

The framework of the practical delay estimation techniques are displayed in Figure 2.1. The delay

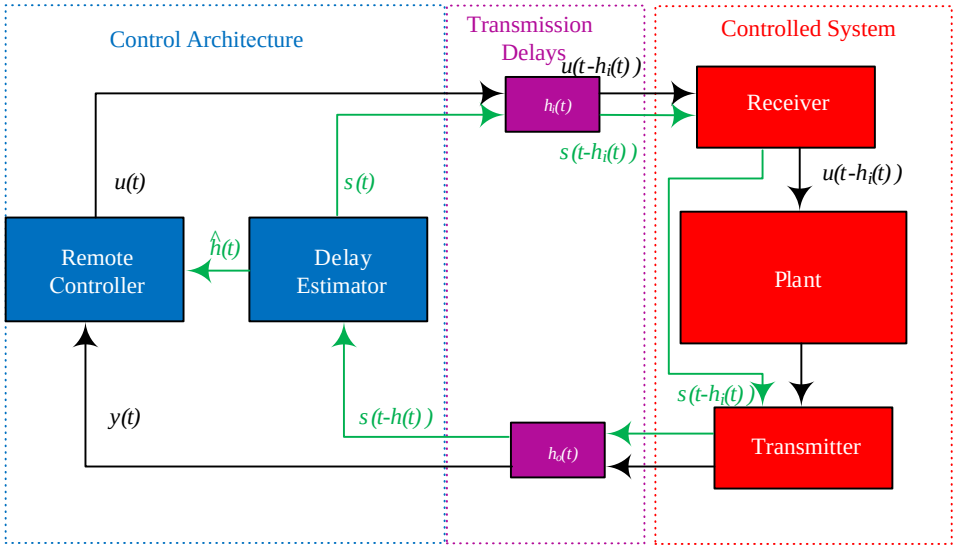

Figure 2.1 – Framework of the practical delay estimation techniques.

estimator sends an external signal $s(t)$ (green arrows) to the plant's receiver through the same channel as the one used for the control signal $u(t)$ (black arrows). After that, the delayed control input $u(t - h_i(t))$ is injected to the plant and the signal $s(t - h_i(t))$ is transferred to the plant's transmitter. Next, the transmitter sends the state measurement $x(t)$ and the delayed signal $s(t - h_i(t))$ back to the controller side. Finally, the controller side receives $y(t)$ and $s(t-h(t))$ at the same time, where

$$h(t) = h_o(t) + h_i(t - h_o(t)) \tag{2.3}$$

is called the "round-trip delay" of system (2.1). The first objective of this chapter is to design of an online update law $\dot{\hat{h}}(t)$ that ensures the global finite-time convergence of $\hat{h}(t)$ to $h(t)$ by using $s(t)$ and $s(t - h(t))$. After the first objective is achieved, the second objective of this chapter is to stabilize the remote control system (2.1) with the delay estimation and a predictor-based controller.

Remark 3. *The external signal $s(t)$ is totally defined by the user and is independent of the control system, it can be regarded as a special communication loop (the green loop of Figure 2.1) whose only use is to provide the online estimation of the round-trip delay* (2.3)*. Indeed, the delay measurement technique (Lai and Hsu 2010) is a special case of the same framework, since it uses the system clock to measure the round-trip delay, so it is possible to say that (Lai and Hsu 2010) chooses an external signal $s(t) = t$ to estimate the time-delay.*

The benefit of the framework presented in Figure 2.1 is twofold:

— The unknown time-varying round-trip delay can be accurately estimated with fairly simple methods, and low computation cost, only some scalar computations are required by (Lai and Hsu 2010) and the methods to be proposed in this chapter.

— This framework relaxes the requirements on the control system, neither linearity nor delay identifiability is required, since the round-trip delay is estimated only by the inner loop (green loop) of Figure 2.1.

2.1.2 Framework of the remote control system

This part introduces the control scheme of the remote control system (2.1). Similar to the problem formulation given in subsection 1.1.2, the pair (A, B) is supposed to be stabilizable, and the Lyapunov equation

$$(A + BK)^T P + P(A + BK) = -c_u I_n \tag{2.4}$$

is still required with a positive parameter c_u and a symmetric positive definite matrix $P \in \mathbb{R}^{n\times n}$. According to Figure 2.1, the delayed state measurement $x(t - h_o(t))$ and the delay estimation $\hat{h}(t)$ are available for the controller at instant t, based on the information, the following predictor-based

controller is adopted

$$u(t) = Kz(t) = K\left[e^{A\hat{h}(t)}x(t-h_o(t)) + \int_{t-h(t)}^{t} e^{A(t-s)}Bu(s)\mathrm{d}s\right], \quad t \geq 0 \tag{2.5}$$

with K given in (2.4). In order to simplify the stability analysis, the initial condition of $z(t)$ is defined as

$$z(\theta) = \phi_z(\theta) \in \mathbf{C}([-\bar{h}, 0), \mathbb{R}^n), \tag{2.6}$$

and the following inequalities are fulfilled

$$\begin{aligned} \|\phi_u(\theta)\| &\leq \|K\|\|\phi_z(\theta)\|, \quad \theta \in [-\bar{h}, 0), \\ \|\dot{\phi}_u(\theta)\| &\leq \|K\|\|\dot{\phi}_z(\theta)\|, \quad \theta \in [-\bar{h}, 0). \end{aligned} \tag{2.7}$$

As done in Remark 2, one also supposes that the predictor $z(t)$ and the control input $u(t)$ are continuous at instant $t = 0$, such that

$$\begin{aligned} \lim_{\theta \to 0^-} \phi_u(\theta) &= u(0), \\ \lim_{\theta \to 0^-} \phi_z(\theta) &= z(0). \end{aligned} \tag{2.8}$$

2.1.3 Assumptions and definitions

After introducing the frameworks of the delay estimation loop and the control loop of system (2.1), some necessary definitions of the sliding mode method and some assumptions on the signal $s(t)$ and the round-trip delay $h(t)$ are given in this subsection.

Assumption 5. *The external signal $s(t) \in \mathbf{C}^2$ satisfies that*

$$\underline{\epsilon} \leq |\dot{s}(t)| \leq \bar{\epsilon}, \quad t \geq -\bar{h}, \tag{2.9}$$

and

$$|\ddot{s}(t)| \leq \epsilon', \quad t \geq -\bar{h}. \tag{2.10}$$

The positive constants $\underline{\epsilon}, \bar{\epsilon}$, and ϵ' are assumed to be known.

Assumption 5 implies that the external signal $s(t)$ is strictly monotonic, it can be easily ensured since the signal $s(t)$ is generated by the user (*e.g.* if one sets $s(t) = kt$, then one has $\underline{\epsilon} = \bar{\epsilon} = k$ and $\epsilon' = 0$).

Remark 4. *In (Zheng, Polyakov, and Levant 2018) and (Drakunov et al. 2006), the delay-identifiability of the time-delay system is required. Indeed, Assumption 5 shows that $s(t)$ is globally identifiable in the sense of the delay identifiability theory (Zheng, Polyakov, and Levant 2018, p.268, Definition 2).*

However, as stated in Remark 3, this signal $s(t)$ is generated by the user and it is independent of the control system. In other words, with the proposed approach, the round-trip delay is estimated by using a specific delay-identifiable signal, but not the system information. Thus, the delay identifiability of the control system can be relaxed by using the framework of Figure 2.1.

Assumption 6. *The input and output delays have bounded derivatives*

$$|\dot{h}_i(t)| \leq \delta_i, \quad |\dot{h}_o(t)| \leq \delta_o \tag{2.11}$$

with positive constants δ_i and δ_o. As a result of (2.3) *and* (2.11)*, there also exists $\delta > 0$ such that the derivative of the round-trip delay $h(t)$ satisfies*

$$|\dot{h}(t)| \leq \delta. \tag{2.12}$$

Moreover, suppose that the second derivative of $h(t)$ is also bounded with

$$|\ddot{h}(t)| \leq \delta'. \tag{2.13}$$

Assumption 6 can be verified in application, for instance, consider the round-trip delay $h(t)$ and its upper bound $\bar{h}$, it is possible to find the bounds

$$\delta \leq \frac{\bar{h}}{T_s}, \tag{2.14}$$

and

$$\delta' \leq \frac{\frac{\bar{h}}{T_s} - (-\frac{\bar{h}}{T_s})}{T_s} = \frac{2\bar{h}}{T_s^2}, \tag{2.15}$$

with T_s the sampling period of the practical delay estimation method on a real test-bench. Consider the case when $h(t)$ varies from $\bar{h}$ to 0 in one sampling period, then its derivative is bounded as (2.14), and (2.15) can be ensured in the same way. In other words, the statements given in (Fiengo et al. 2019, Section 4) and (Horalek, Svoboda, and Holik 2016) explain that the time-delays in wireless communication systems are often bounded and slow-varying, large transmission delays usually cased by network-induced imperfections (X.-M. Zhang, Han, and Yu 2015). Thus, Assumption 6 is not restrictive in theories, nor in applications.

Next, some definitions which are corresponding to the sliding mode method, are introduced in the sequel. To design a sliding mode controller/ estimator, the sign-function (Shtessel, Edwards, et al. 2014, eqs. (1.13)-(1.14)) is necessary, it satisfies

$$\text{sign}(x) = \begin{cases} 1, & \text{if} \quad x > 0 \\ -1, & \text{if} \quad x < 0 \end{cases} \tag{2.16}$$

and $\text{sign}(0) \in [-1, 1]$.

Definition 2. ***2-ideal sliding mode and 2-real sliding mode (Levant 2003, p.926)*** *Given the sliding variable $\sigma(s,t)$, the "2-ideal sliding mode" of the variable s is defined as*

$$\mathcal{S} = \{s : |\sigma(s,t)| \equiv |\dot{\sigma}(s,t)| \equiv 0\}, \quad t \geq t_F \tag{2.17}$$

whereas the "2-real sliding mode" reads as

$$\mathcal{S}^* = \{s : |\sigma(s,t)| \leq \eta_1, \quad |\dot{\sigma}(s,t)| \leq \eta_2\}, \quad t \geq t_F \tag{2.18}$$

with $\eta_1, \eta_2, t_F > 0$.

2.2 Sliding mode based practical delay estimation techniques with external signal

In this section, three delay estimators are proposed to estimate the round-trip delay $h(t)$ given in (2.3). The first two of them establish the 2-ideal sliding mode, and the third method provides the finite time convergence to the 2-real sliding mode.

2.2.1 Conventional sliding mode (SM) based delay estimation

In this subsection, the conventional sliding mode method is involved in the practical delay estimation techniques, in order to provide a finite time convergence of the delay estimator.

Theorem 5. *Consider that the external signal $s(t)$ satisfies Assumptions 5, and the time-varying delay $h(t)$ satisfies Assumption 6. Define the delay estimator dynamics*

$$\dot{\hat{h}}(t) = 1 - \frac{1}{\dot{s}(t - \hat{h}(t))} w(t) \tag{2.19}$$

with $w(t)$ defined as

$$w(t) = -L \cdot sign(\sigma(t)), \tag{2.20}$$

and

$$\sigma(t) = s(t - \hat{h}(t)) - s(t - h(t)). \tag{2.21}$$

If the gain L is sufficiently large, such that $L > \bar{\epsilon}(1+\delta)$ holds, then there exist $t_F > 0$ that guarantees the following finite time convergences

$$\sigma(t) \equiv 0, \quad \hat{h}(t) \equiv h(t), \quad \forall t \geq t_F. \tag{2.22}$$

Proof. The proof is divided into two parts. Part 1 shows that the finite-time convergence of $\sigma(t)$ to zero induces the finite-time convergence of $\hat{h}(t)$ to $h(t)$. Step 2 provides the finite-time convergence of the error term $\sigma(t)$ to zero.

Part 1.

In this part, the relation between the convergences of $\sigma(t)$ and $\hat{h}(t)$ is analyzed. As stated after Assumption 5, the external signal $s(t)$ is strictly monotonic for all $t \geq -\bar{h}$. Therefore, $s(t)$ is bijective for all $t \geq -\bar{h}$ by using the results given in (Muresan 2009, p.165, Corollary 4.9). Assume that $\sigma(t)$ converges to zero in a finite-time T, it implies that

$$s(t - \hat{h}(t)) = s(t - h(t)), \quad \text{for all} \quad t \geq T. \tag{2.23}$$

Since $s(t)$ is bijective, (2.23) is equivalent to

$$t - \hat{h}(t) = t - h(t), \quad \text{for all} \quad t \geq T \tag{2.24}$$

which implies that

$$\hat{h}(t) = h(t), \quad \text{for all} \quad t \geq T. \tag{2.25}$$

Part 2.

The aim of the second part is to demonstrate the finite convergence of $\sigma(t)$ to zero. Recall the chain rule given in (Apostol 1974, Theorem 5.5), the relation between the right-hand time-derivative of the function $s(\cdot)$ at instant $t - h(t)$ (writes as $\dot{s}(t - h(t))$), and the right-hand time-derivative of the function composition $t \mapsto s(t - h(t))$ (writes as $\frac{d}{dt}s(t - h(t))$) reads as

$$\frac{d}{dt}s(t - h(t)) = \dot{s}(t - h(t))(1 - \dot{h}(t)). \tag{2.26}$$

Thus, the right-hand time-derivative of the error term $\sigma(t)$ (2.21) satisfies that

$$\begin{aligned} \dot{\sigma}(t) &= \dot{s}(t - \hat{h}(t))(1 - \dot{\hat{h}}(t)) - \frac{d}{dt}s(t - h(t)) \\ &= \dot{s}(t - \hat{h}(t)) - \frac{d}{dt}s(t - h(t)) - \dot{s}(t - \hat{h}(t))\dot{\hat{h}}(t). \end{aligned} \tag{2.27}$$

By virtue of Assumption 5, one has $\dot{s}(t - \hat{h}(t)) \neq 0$ for all $t \geq 0$, then it is possible to substitute the first dynamic of (2.19) into (2.27) without the risk of singularity. Consider (2.27), (2.19), and (2.20), it follows that

$$\dot{\sigma}(t) = -\frac{d}{dt}s(t - h(t)) - L \cdot \text{sign}(\sigma(t)). \tag{2.28}$$

With the help of assumptions 5-6, the term $-\frac{d}{dt}s(t-h(t))$ is bounded by

$$\left|-\frac{d}{dt}s(t-h(t))\right| = |\dot{s}(t-h(t))||(1-\dot{h}(t))| \leq \bar{\epsilon}(1+\delta). \tag{2.29}$$

Set $L = \bar{\epsilon}(1+\delta)+L_1/\sqrt{2}$ with $L_1 > 0$, then consider (2.29) and the Lyapunov function $V(t) = \frac{1}{2}\sigma(t)^2$, it leads to

$$\dot{V}(t) \leq -L_1\sqrt{V(t)}. \tag{2.30}$$

The analysis of (Shtessel, Edwards, et al. 2014, eqs. (1.8)-(1.0)) explains that the Lyapunov function $V(t)$ reaches zero in a finite time $t_F = 2\sqrt{V(0)}/L_1$ that ends the proof. □

2.2.2 Super-twisting algorithm (STW) based delay estimation

Theorem 5 provides a conventional sliding mode based practical online time-delay estimation algorithm with the framework of Figure 2.1, the unknown round-trip delay is estimated in finite time. However, the main drawback of this method is the imperfection in the sign-function implementation, it can result in a high frequency oscillation named chattering (Shtessel, Edwards, et al. 2014, p.8) which is undesirable in applications (Slotine, Weiping Li, et al. 1991, p.283). In order to overcome this practical issue, the second-order sliding mode (super-twisting algorithm) is adopted, the theoretical results are presented subsequently.

Theorem 6. *Consider that the external signal $s(t)$ satisfies Assumptions 5, and the time-varying delay $h(t)$ satisfies Assumption 6. The delay estimator is with the form* (2.19)*, and the term $w(t)$ is replaced by the super-twisting algorithm:*

$$w(t) = -\lambda|\sigma(t)|^{1/2}sign(\sigma(t)) + w_1(t), \tag{2.31}$$

with the error term (2.21)*, and the term $w_1(t)$ is given by the following dynamic*

$$\dot{w}_1(t) = -\alpha \cdot sign(\sigma(t)). \tag{2.32}$$

If the parameters λ, α are large enough such that

$$\begin{aligned} \alpha &\geq C = \bar{\epsilon}\delta' + \epsilon'(1+\delta)^2, \\ \lambda^2 &\geq 4C\frac{\alpha+C}{\alpha-C}, \end{aligned} \tag{2.33}$$

then the 2-ideal sliding mode (2.17) *is established with a finite settle time $t_F > 0$. Finally, the delay estimator $\hat{h}(t)$ converges to the unknown round-trip delay $h(t)$ for all $t \geq t_F$.*

Proof. The majority of the proof is the same with Theorem 5, one only needs to prove that the error term $\sigma(t)$ vanishes in finite time by using the super twisting algorithm (2.19)-(2.31)-(2.33).

Substituting the super-twisting term (2.31) into the dynamic of $\sigma(t)$ yields that

$$\dot{\sigma}(t) = a(t) + w(t) \tag{2.34}$$

where $a(t) = -\frac{d}{dt}s(t - h(t))$. Moreover, (2.34) equals to the following representation

$$\ddot{\sigma}(t) = \dot{a}(t) + \dot{w}(t) \tag{2.35}$$

that satisfies the form given by (Perruquetti and Barbot 2002, equation (3.30)). By using the chain rule (2.26), the derivative of $a(t)$ is computed as:

$$\dot{a}(t) = \dot{s}(t - h(t))\ddot{h}(t) - \ddot{s}(t - h(t))(1 - \dot{h}(t))^2. \tag{2.36}$$

Assumptions 5-6 imply that the dynamic of (2.36) is upper bounded by the parameter C given in (2.33). Consider the second-order system (2.35) that is linearly dependent on the correction term $w(t)$ and consider the super-twisting updating law constructed by (2.31)-(2.32), if the convergence conditions (2.33) are ensured, then the 2-ideal sliding mode (2.17) is established according to the simplified super-twisting algorithm and its convergence condition (Perruquetti and Barbot 2002, Chapter 3.6.4, equation (3.42)). As long as the error term $\sigma(t)$ reaches the 2-ideal sliding mode (2.17), the finite time convergence of the delay estimator is also ensured that ends the proof. □

In Theorem 6, the conventional sliding mode method (2.20) is replaced by the super-twisting algorithm (2.31)-(2.32). The main benefit of Theorem 6 by comparing with Theorem 5 is twofold:

— The chattering phenomenon is reduced since the term $|\sigma|^{1/2}\text{sign}(\sigma)$ is continuous and the discontinuous term (2.32) lies in the integral (Shtessel, Edwards, et al. 2014, p.35). If the two methods are implemented discrete-time system with sampling period T_s, it is well known that the accuracy of the super-twisting algorithm (2.31)-(2.32) (that is a second-order sliding mode approach) is proportional to T_s^2 whereas the accuracy of the first-order sliding mode (2.20) is proportional to T_s.

— The conventional sliding mode method (2.20) has only one tuning parameter L, then it cannot converge fastly and reduce the chattering at the same time. As claimed in (Plestan et al. 2010, p.1907), if one increases the gain L, then it results in larger chattering that makes the delay estimation worse. However, if one decreases the gain L in order to reduce the chattering, the analysis in (Shtessel, Edwards, et al. 2014, equations (1.10), (1.17)) shows that the sliding variable converges to zero more slowly. However, the super-twisting method (2.31)-(2.32) can achieve these two objectives at meantime since it is a high-order sliding mode algorithm, and it has two tuning parameters.

2.2.3 Adaptive super-twisting algorithm (ASTW) based delay estimation

Although Theorem 6 provides a better performance than Theorem 5, it also has a drawback: its estimation performance totally depends on the choice of the parameters α and λ (namely, the bounds δ and δ'). If the parameters are too small, then the delay estimator fails to converge, and if the parameters are too large, they can also result in undesirable chattering in applications. Indeed, the bounds δ and δ' may not be perfectly known beforehand, in order to deal with this problem, the adaptive super-twisting algorithm is proposed.

Theorem 7. *Consider that the external signal $s(t)$ satisfies Assumptions 5, and the time-varying delay $h(t)$ satisfies Assumption 6. The delay estimator is with the form* (2.19)*, and the dynamic of $w(t)$ reads as*

$$w(t) = -\lambda(t)|\sigma(t)|^{1/2} sign(\sigma(t)) + w_1(t), \tag{2.37}$$

where $\sigma(t)$ is given in (2.21)*, and the dynamic of $w_1(t)$ satisfies that*

$$\dot{w}_1(t) = -\frac{\alpha(t)}{2} \cdot sign(\sigma(t)). \tag{2.38}$$

The adaptive parameters $\lambda(t)$ and $\alpha(t)$ have the following updating laws

$$\begin{aligned} \dot{\lambda}(t) &= \begin{cases} \omega_1 \sqrt{\frac{\gamma_1}{2}} sign(|\sigma(t)| - \mu), & \text{if } \lambda(t) > \lambda_m \\ \eta, & \text{if } \lambda(t) \leq \lambda_m \end{cases} \\ \alpha(t) &= 2\zeta\lambda(t) \end{aligned} \tag{2.39}$$

where $\zeta > 0$, $\omega_1 > 0$, $1 > \gamma_1 > 0$, $\eta > 0$ are arbitrarily chosen, and $\lambda_m > 0$ is sufficient small. If $\lambda(0) > \lambda_m$, then there exist $\eta_1 > \mu$, $\eta_2 > 0$, and $t_F > 0$ such that the 2-real sliding mode (2.18) *is established for all $t \geq t_F$. Finally, the delay estimation error $e(t) = h(t) - \hat{h}(t)$ satisfies that*

$$|e(t)| \leq \frac{\eta_1}{\underline{\epsilon}}, \quad t \geq t_F. \tag{2.40}$$

Proof. The proof is also composed of two parts, the first part demonstrates that the error term $\sigma(t)$ enters and then stays in the boundary layers of the 2-real sliding mode in finite time, and the second part derives the delay estimation error bound (2.40).

Part 1.

The beginning of this part is totally the same as the proof of Theorem 6, until (2.34). Indeed, (2.34) can be equally written as

$$\dot{\sigma}(t) = a(t) + bw(t) \tag{2.41}$$

where $a(t)$ keeps its definition in Theorem 6, and $b = 1$. In (2.41), since $a(t)$ has bounded derivative (according to (2.36) and assumptions 5-6) and b is constant, then the dynamic (2.41) satisfies all

of the 5 assumptions given in (Shtessel, Taleb, and Plestan 2012, p.760, A1-A5). Finally, according to (Shtessel, Taleb, and Plestan 2012, Theorem 1), the super-twisting algorithm (2.37)-(2.38) with adaptive parameters (2.39) establishes the 2-real sliding mode (2.18) in finite time $t_F > 0$.

Part 2.

Next, one derives the estimation error (2.40) from the 2-real sliding mode (2.18). Apply the mean value theorem (Apostol 1974, Theorem 5.11) to (2.21), there exists $h_1 \in [\min\{(h(t)), \hat{h}(t)\}, \max\{(h(t)), \hat{h}(t)\}]$ such that

$$\begin{aligned} |\sigma(t)| &= |\dot{s}(t-h_1)||t-\hat{h}(t)-(t-h(t))| \\ &= |\dot{s}(t-h_1)||e(t)|. \end{aligned} \tag{2.42}$$

Thus, with the use of Assumption 5, the estimation error satisfies that

$$|e(t)| = \frac{|\sigma(t)|}{|\dot{s}(t-h_1)|} \leq \frac{|\sigma(t)|}{\underline{\epsilon}}. \tag{2.43}$$

Finally, the main convergence result (2.40) can be obtained by combining (2.43) and (2.18). □

Theorem 7 presents an adaptive super-twisting algorithm based time-delay estimation technique, it has the following properties:

— the parameter tuning (2.33) is no longer required, it is replaced by the adaptive gains (2.39);

— the delay estimation $\hat{h}(t)$ cannot reach the ideal finite-time convergence (2.17), it can only establish the 2-real sliding mode (2.18). However, one can improve the estimation accuracy by tuning the parameter μ in (2.39) smaller.

2.2.4 Discussions about the three delay estimators

In this subsection, the theoretical results of Theorems 5-7 are discussed and compared.

First, Theorem 5 is based on the conventional sliding mode method, it is simple and easy to implement since it has only one tuning gain L, but the drawback is the high-amplitude chattering caused by the discontinuous sign-function (2.16), and it cannot perfectly handle the tradeoff between the convergence speed and the chattering limitation at meantime.

The problem of the chattering phenomenon is solved with the use of super-twisting algorithm (in Theorem 6) and its adaptive version (in Theorem 7) since the super-twisting algorithm is a 2-order sliding mode technique. Theorem 6 can fastly estimate the round-trip delay with chattering limitations by virtue of the continuous form and the two tuning parameters λ, α. The delay estimation performances of Theorem 6 is perfect if the precise knowledge of the bounds δ, δ' given in Assumption 6 is known. When the bounds on the delay derivatives are not known beforehand, Theorem 7 can be applied to estimate the round-trip delay, all of the gains are self-tuned, and the predefined delay estimation accuracy can be ensured.

The above discussions are summarized in the following table:

	Nb. of tuning parameters	sliding surface type	accuracy
Theorem 5	1	1-ideal	the third accurate
Theorem 6	2	2-ideal	the most accurate
Theorem 7	self-tuned	2-real	the second accurate

Table 2.1 – Comparison of the three practical time-delay estimation methods based on sliding mode method.

2.2.5 Robustness of the practical delay estimation techniques

In this subsection, the robustness of the practical delay estimators given in Theorems 5-7 are tested by simulations. They are compared with the delay measurement approach (Lai and Hsu 2010) in the presence of channel inherent noises (Shannon 1984) or deception attacks (Ding et al. 2017). In this subsection, one use the four approaches (delay measurement method (Lai and Hsu 2010), and Theorems 5-7) to estimate the round-trip delay introduced by the following input and output delays:

$$\begin{aligned} h_i(t) &= 0.5 + 0.5\sin(2t), \\ h_o(t) &= 0.8 + 0.3\sin(3t). \end{aligned} \tag{2.44}$$

With respect to channel inherent noises

In this part, one takes into account the effect of the channel inherent noise (Shannon 1984) in the delay estimation problem. In this case, the accurate value of the delayed signal $s(t-h(t))$ is not available to the delay estimator, and only the perturbed delayed signal

$$s_n(t-h(t)) = s(t-h(t)) + n(t) \tag{2.45}$$

with $|n(t)| < 0.2$ a Gaussian noise [1], is used to compute the error term (2.21). In this simulation, the performances of the delay estimators on interval $[t_1, t_2]$ are evaluated by two indexes: the $\mathcal{L}_2$ norm of the estimation error $e(t) = h(t) - \hat{h}(t)$:

$$\|e\|_{[t_1,t_2]} = \left(\int_{t_1}^{t_2} |e(s)|^2 \mathrm{d}s\right)^{1/2}, \tag{2.46}$$

and the variation of the estimation error:

$$\mathrm{VAR}(e)_{[t_1,t_2]} = \sum_{i=t_1/T_s}^{t_2/Ts} |e((i+1)\cdot T_s) - e(i\cdot T_s)| \tag{2.47}$$

1. As stated in (Pierce 1980, p.173), the channel inherent noise can be modeled as a Gaussian noise.

where T_s is the sampling period of the practical delay estimation algorithm. The $\mathcal{L}_2$ norm (2.46) evaluates the accuracy of the delay estimation algorithms, lower the $\mathcal{L}_2$ norm is, better the accuracy is. The variation (2.47) describes the oscillation level of the estimation error, higher variation implies that the delay estimator oscillates more.

In order provide a fair comparison between the delay measurement approach and the delay estimators given by Theorems 5-7, the external signal $s(t) = t$ (*i.e.* system clock) is chosen. The other parameters are given in the sequel

- Sliding mode (Sliding Mode (SM)) based method (Theorem 5): $L = 3.5$;
- Super-twisting algorithm (Super-Twisting (STW)) based method (Theorem 6): $\lambda = 10$ and $\alpha = 10$;
- Adaptive super-twisting algorithm (Adaptive Super-Twisting (ASTW)) based method (Theorem 7): $\omega_1 = 1.1$, $\gamma_1 = 0.8$, $\mu = 0.04$, $\lambda_m = 0.1$, $\eta = 0.3$, $\zeta = 0.7$, and $\lambda(0) = 7$.

Finally, in order to conform to the real wireless data communication process, the sampling period of the simulation is set to $T_s = 0.005$s.

Through the simulation results displayed in Figure 2.2, the following conclusions are made:

- Figures 2.2c and 2.2d illustrate that tha channel inherent noise has less effects on the methods of Theorems 5-7. Moreover, the high-order sliding mode based methods (Theorems 6-7) are more accurate than the conventional sliding mode based method (Theorem 5), they also have less oscillations than the method of Theorem 5.
- The adaptive super-twisting algorithm is successfully established in the simulation, and the adaptive gain $\lambda(t)$ increases to a suitable value that ensures the predefined delay estimation accuracy.
- In Figure 2.2d, the variation of Theorem 7 is less than the one of Theorem 6, this is due to the fact that the gains $\lambda(t)$, $\alpha(t)$ are self-tuned, then the chattering effects of the simulation is reduced.

The simulation results given in Figure 2.2 illustrate that the theoretical results of Theorems 5-6 are able to deal estimate the time-varying delays. Moreover, the simulation results highlight the robustness of these approaches, then provide better performances than the delay measurement method (Lai and Hsu 2010).

With respect to deception attacks

The aim of this part is to test the robustness of the practical delay estimation techniques against cyber attacks. Indeed, in real application, the messages (measurement and control signal) of the remote control systems can be transmitted via communication network. In this case, the adversary may hijack the communication network and replace the measurement or control signal by false data (X.-M. Zhang, Han, Ge, et al. 2019, Section VI-C) in order to damage the system. According to the delay estimation framework described in subsection 2.1.2, the methods proposed by Theorems 5-7

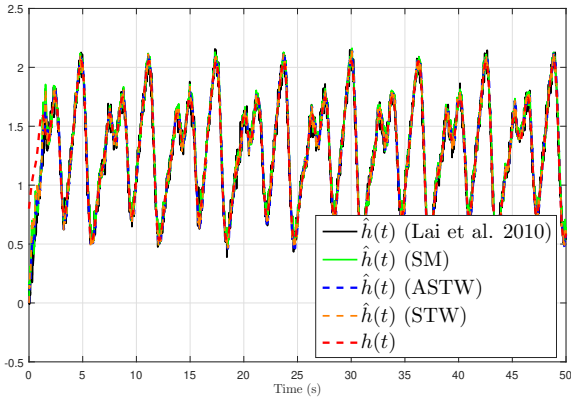

(a) Estimation of time-varying delay (2.44) in the presence of channel inherent noise via four methods.

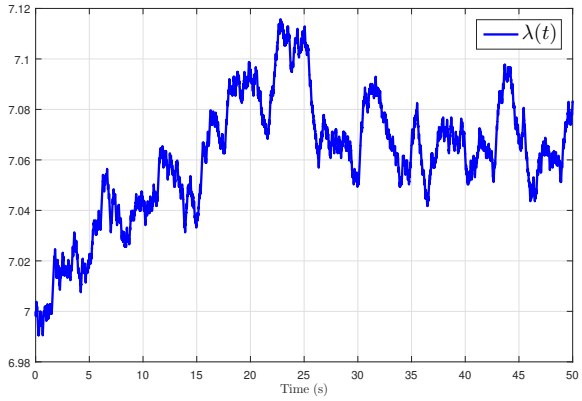

(b) Evolution of the adaptive gain $\lambda(t)$ introduced in Theorem 7.

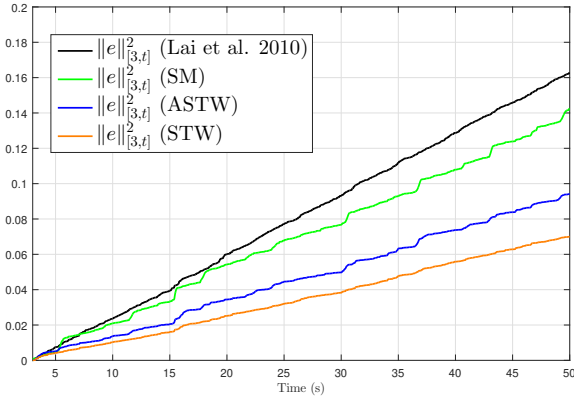

(c) $\mathcal{L}_2$ norms of the estimation errors of the four methods.

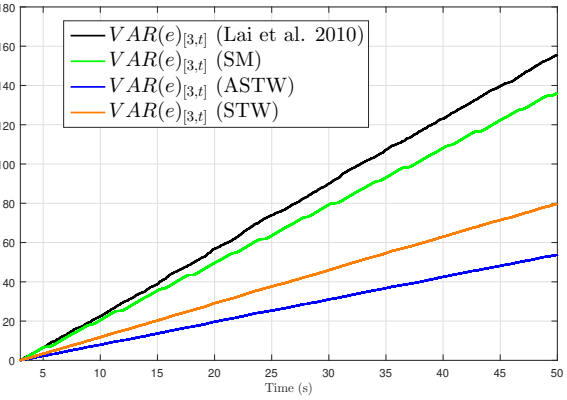

(d) Variations of the estimation errors of the four methods.

Figure 2.2 – Comparison between the delay measurement approach (Lai and Hsu 2010) and the sliding mode based methods given in Theorems 5-7 in the presence of channel inherent noises.

are based on the communication between the plant and the controller, then it is at risk from the cyber attack. Thus, the main purpose of this simulation is to compare the performances of (Lai and Hsu 2010) and Theorems 5-7 under deception attack (Ding et al. 2017).
Consider the delay estimation problem given in (2.44), and one assumes that the communication network of $s(t)$ is under the following deception attack:

$$s_a(t-h(t)) = s(t-h(t)) + \beta(t)\chi(t), \tag{2.48}$$

with $\beta(t)$ a Bernoulli random number such that

$$\text{Prob}\{\beta(t)=1\} = 0.03, \quad \text{Prob}\{\beta(t)=0\} = 0.97. \tag{2.49}$$

The attack value $\chi(t)$ reads as:

$$\chi(t) = \begin{cases} -0.3 + \xi(t), & t \in [5,10] \cup [25,30] \cup [45,50] \\ 0.5 + \xi(t), & t \in [15,20] \cup [35,40] \\ 0, & \text{otherwise} \end{cases} \tag{2.50}$$

with $|\xi(t)| \leq 1$.

Remark 5. *In real application,* (2.48) *is a sampled-data process with sampling period* $T_s = 0.005$s*, then it can be transformed into the discrete deception attack model (Ding et al. 2017, eq. (4)) such that:*

$$Prob\{\beta(k)=1\} = 0.03, \quad Prob\{\beta(k)=0\} = 0.97, \tag{2.51}$$

and

$$\chi(k) = \begin{cases} -0.3 + \xi(k), & k \cdot T_s \in [5,10] \cup [25,30] \cup [45,50] \\ 0.5 + \xi(k), & k \cdot T_s \in [15,20] \cup [35,40] \\ 0, & otherwise \end{cases} \tag{2.52}$$

with $|\xi(k)| \leq 1$.

In this simulation, the delay measurement method is still used for comparison, then the external signal is still fairly set to $s(t) = t$, and the sampling period of the process is set to $T_s = 0.005$s. The parameter setting of each methods are given subsequently:

— Sliding mode (SM) based method (Theorem 5): $L = 3.5$;
— Super-twisting algorithm (STW) based method (Theorem 6): $\lambda = 10$ and $\alpha = 10$;
— Adaptive super-twisting algorithm (ASTW) based method (Theorem 7): $\omega_1 = 0.7$, $\gamma_1 = 0.7$, $\mu = 0.00025$, $\lambda_m = 0.1$, $\eta = 0.3$, $\zeta = 0.8$, and $\lambda(0) = 7$.

The simulation results are presented in Figure 2.3, they have the following properties:

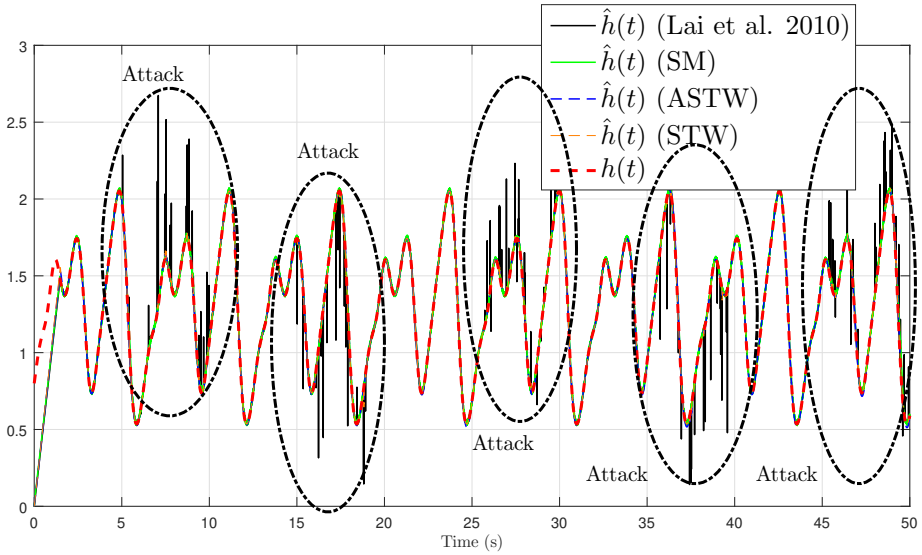

(a) Estimation of the time-varying delay (2.44) under deception attacks (2.48)-(2.50) via four methods.

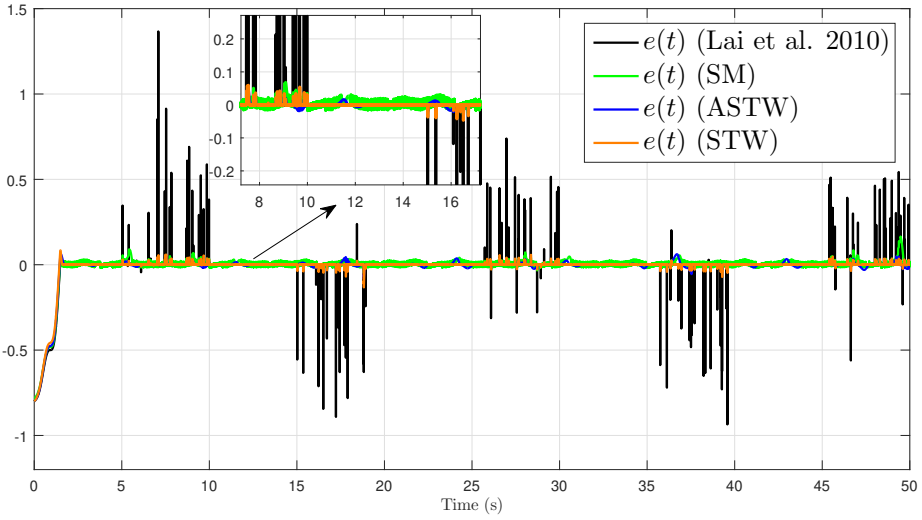

(b) Estimation errors of the four methods under deception attacks (2.48)-(2.50) via four methods.

Figure 2.3 – Comparison between the delay measurement approach (Lai and Hsu 2010) and the sliding mode based methods given in Theorems 5-7 under deception attacks.

— When the communication network is not subject to deception attack (*i.e.* $t \in [0,5) \cup (10,15) \cup (20,25) \cup (30,35) \cup [40,45]$), both methods can accurately estimate the round-trip delay $h(t)$.
— If the communication network is under the deception attack (2.48), the performance of (Lai and Hsu 2010) is more degraded than Theorems 5-7.
— The zoomed sub-figure given in Figure 2.3b shows that the approach of Theorem 5 has a higher chattering amplitude than the high-order ones.

As a consequence, Figure 2.3 claims that the deception attack (2.48)-(2.50) has a large effect on the delay measurement method (Lai and Hsu 2010), but the approaches of Theorems 5-6 can successfully estimate the round-trip delay with slight estimation errors. Thus, this simulations emphasizes the robustness of the sliding mode based delay estimation methods against cyber attacks.

2.2.6 Experimental validation of the sliding mode based delay estimation methods

In this subsection, the theoretical results of Theorems 5-7 are implemented on a remote data transmission (RDT) process that is comprised of two computers and their wireless communications via WiFi network. The delay estimation performances of them are compared, and the discussions given in subsection 2.2.4 are illustrated.

Configuration of the test bench

The experimental set-up is composed of two different computers connected through a Wi-Fi network. Two computers run Robot Operating System (Robot Operating System (ROS)) platform (Martinez and Fernández 2013) simultaneously in order to actualize an RDT process with input and output time-varying delays (see Figure 2.4).

In Figure 2.4, $h_{ri}(t)$ and $h_{ro}(t)$ are the time-delays introduced by the real WiFi network. However, the values of them are small (about several milliseconds according to (Horalek, Svoboda, and Holik 2016)) and in a random manner. In order to create an arbitrarily-long round-trip transmission delay on the test bench, an artificial delay equals to $h(t)$ is added onto Computer 2. As a consequence, the real round-trip delay of this experiment is a composite function of the artificial delay and the real input/ output delays introduced by the network, it can be approximated as

$$h_{approx}(t) = h_{ri}(t) + h(t) + h_{ro}(t). \tag{2.53}$$

Move back to Figure 2.4, the roles of the two computers are recalled. Computer 1 generates the signal $s(t)$, receives the delayed signal $s(t - h_{approx}(t))$, and estimates the time-delay online. Computer 2 is used to receive the delayed signal $s(t - h_i(t))$ and to send it back to Computer 1. The synchronization between the two computers is not required since all the calculations are done on Computer 1. The communication between the two computers has a sampling period $T_s = 0.005$s.

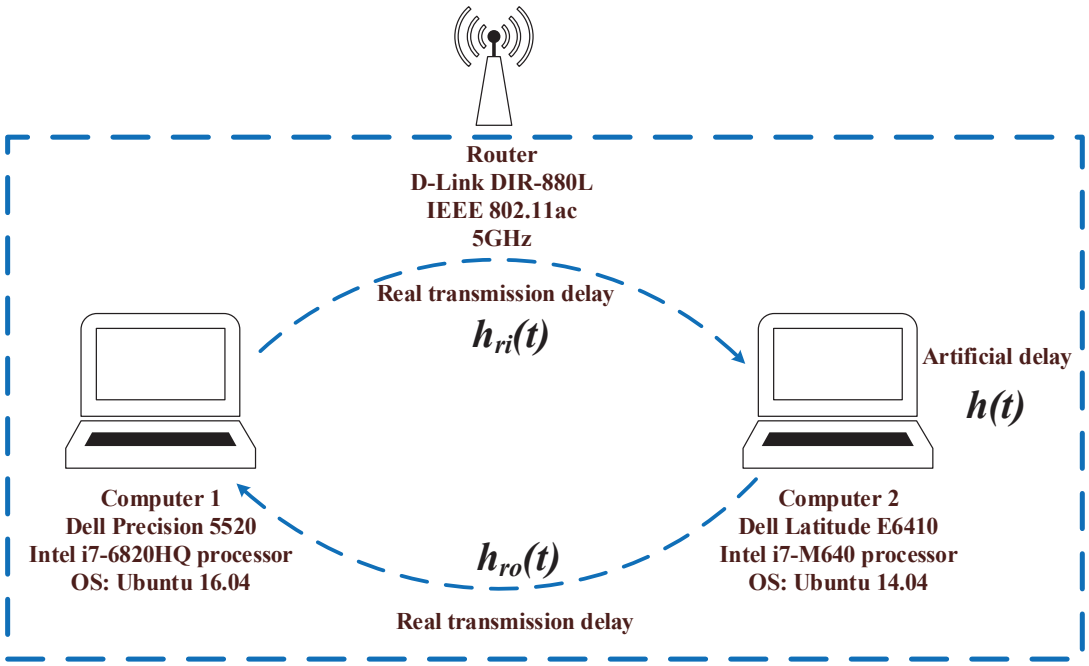

Figure 2.4 – Test bench based on the communication between two computers via WiFi network.

Comparison between the SM method and the STW method

In this part, Theorems 5-6 are compared through the experimental results done on the test bench.

Experiment 1: Transmission delay estimation

In this experiment, the artificial delay $h(t)$ is set to zero in order to test if the two methods can estimate the round-trip delay

$$h_{rrt}(t) = h_{ro}(t) + h_{ri}(t - h_{ro}(t)) \tag{2.54}$$

introduced by the real WiFi network. The two delay estimators (based on Theorems 5-6) are based on the following parameter tunings: $L = 1.5$, $\lambda = 5$, and $\alpha = 10$.

The experimental results are presented in Figure 2.5. Remind that the reference round-trip delay value is measured by a ping test [2]. The following discussions are made to compare the properties of Theorems 5-6 in this experiment:

— Figures 2.5a and 2.5c show that Theorem 5 has estimation biases, and the chattering ampli-

2. Ping (Mills 1983) is a computer network administration software that measures the round-trip time for messages sent from the originating host to a destination computer that is echoed back to the source.

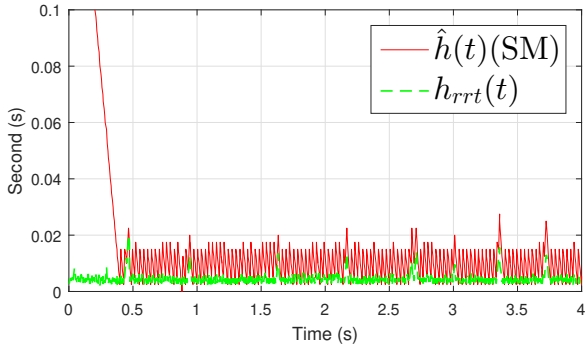

(a) Estimation of the round-trip delay (2.54) via Theorem 5.

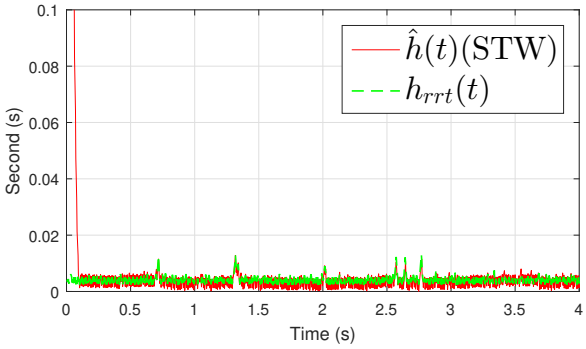

(b) Estimation of the round-trip delay (2.54) via Theorem 6.

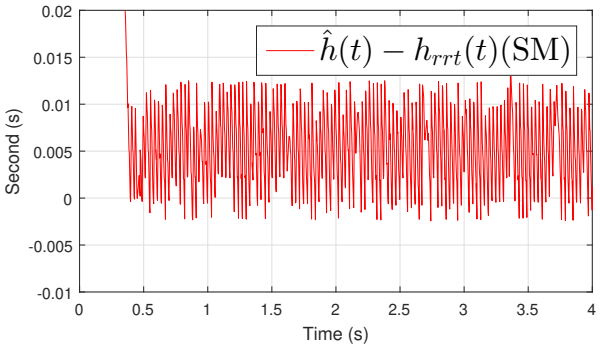

(c) Estimation error of Theorem 5.

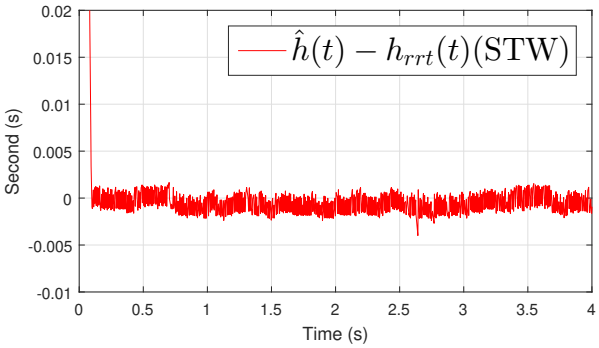

(d) Estimation error of Theorem 6.

Figure 2.5 – Delay estimations and estimation errors of the round-trip delay (2.3) by using Theorems 5-6.

tude is much higher than the level of the transmission delay $h_{rrt}(t)$.

— It shows in Figures 2.5b-2.5d that the transmission delay $h_{rrt}(t)$ is estimated without estimation bias, and the chattering effect is reduced by comparing with Theorem 5.

Consequently, Figure 2.5 highlights the benefit of Theorem 6, it can be applied to estimate the round-trip delay of a real WiFi network, and the accuracy and chattering limitation are ensured.

Example 2: Online estimation of slow-varying delay

After estimating the real round-trip transmission delay (2.54), some experiments will be done to deal with long artificial time-delays. In this part, the following slow-varying artificial time-delay is introduced by Computer 2:

$$h(t) = \begin{cases} 4, & \text{for} \quad 0 \leq t < 5 \\ 2, & \text{for} \quad 5 \leq t < 10 \\ 4, & \text{for} \quad 10 \leq t < 15 \\ 10 - 0.4t, & \text{for} \quad 15 \leq t < 20 \\ 2 + \sin(0.4\pi(t - 17.5)), & \text{for} \quad t \geq 20 \end{cases} . \tag{2.55}$$

In this case, since the artificial delay is non longer zero, the round-trip delay is difficult to be directly measured by using a ping test, then one use the (2.53) as a substitute. Indeed, the artificial delay (2.55) is much larger than the network-induced delays, then (2.53) is almost equal to the real round-trip delay. In addition, the gains $L = 2.3$, $\lambda = 15$, and $\alpha = 10$ are chosen for this experiment.

Consider the experimental results displayed in Figure 2.6, it is observed that both of the two methods can estimate the round-trip delay, but Figure 2.6c shows that the method of Theorem 5 has serious chattering in the experiment, whereas the one of Theorem 6 accurately estimates the round-trip delay. Thus, it is possible to state that Theorem 6 exhibits a better performance than Theorem 5.

Example 3: Online estimation of fast-varying delay

In many engineering systems, time-delays are no longer slow-varying (*i.e.* the derivative of the time-delay is larger than 1 (Fridman 2014b, p.273)). The control of such systems is challenging because:

— for the continuous-time TDS, the Lyapunov-Krasovskii theorem (Fridman 2014a, Theorem 3.1) is difficult to deal with this case (Fridman 2014b, p.273);

— for the networked control systems, packet reordering (older packet arrives at the destination after the new one) may arise when the time-delay is fast-varying, and this makes the control strategies more complicated (J. Li, Q. Zhang, and Cai 2009).

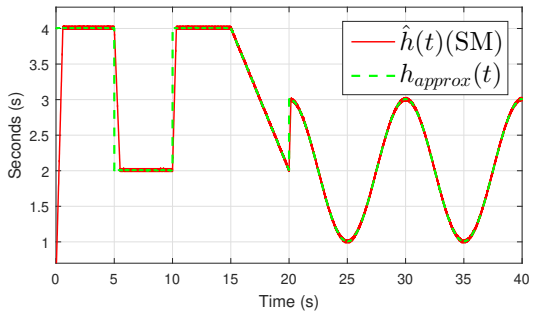

(a) Slow-varying delay estimation via Theorem 5.

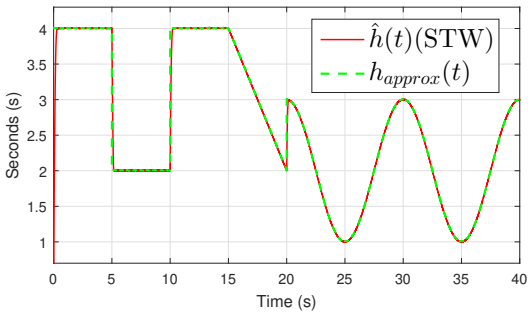

(b) Slow-varying delay estimation via Theorem 6.

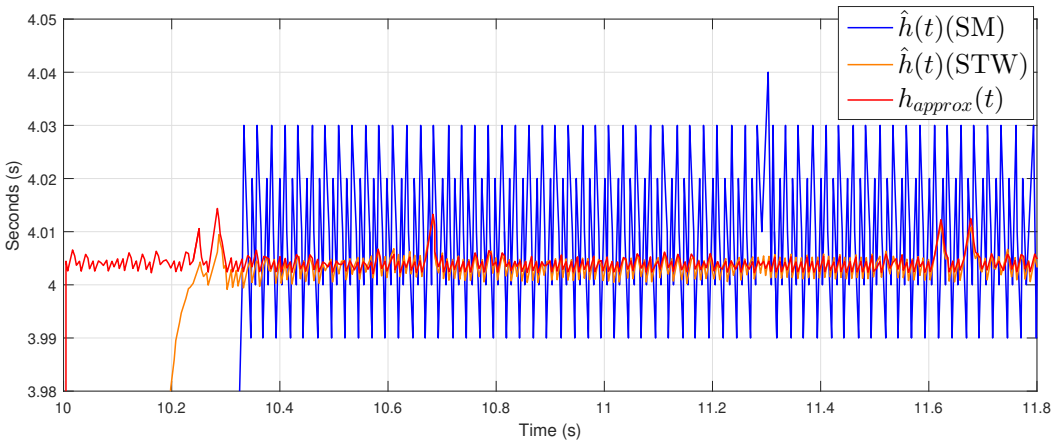

(c) Chattering analysis of slow-varying delay estimation on interval $t \in [10, 11.8]$.

Figure 2.6 – Comparison between Theorems 5 and 6 for slow-varying delay estimation.

Moreover, as stated in (X. Wu et al. 2013, p.1765), estimating such delays is more challenging than slow-varying delays for many existing approaches as (Lai and Hsu 2010) and (Drakunov et al. 2006, Theorems 4-6). Thus, TDE for fast-varying delay is important to consider, and this technique is also helpful for the stabilization of TDS with unknown fast-varying delay. In this example, a time-varying artificial time-delay

$$h_s(t) = \begin{cases} 3 + 2t, & \text{for} \quad 0 \leq t < 1 \\ 7 - 2t, & \text{for} \quad 1 \leq t < 3 \\ 2t - 5, & \text{for} \quad 3 \leq t < 5 \\ 2t - 9, & \text{for} \quad 5 \leq t < 7 \\ 2t - 13, & \text{for} \quad 7 \leq t < 9 \\ 4 + \cos(\pi(t-9)), & \text{for} \quad t \geq 9 \end{cases} \tag{2.56}$$

is now introduced. Similarly, approximation (2.53) still holds in experiment, and the parameters are re-defined as $L = 5$, $\lambda = 15$, and $\alpha = 20$.

The experimental results are given Figure 2.7. First, consider Figures 2.7a and 2.7b, it is apparent that the convergence speed of Theorem 5 is slower than than the one of Theorem 6. If one wants to make the convergence speed faster, then the gain L must be tuned larger. However, as presented in Figure 2.7c, with the gain $L = 5$, the chattering amplitude of Theorem 5 is already larger than Theorem 6, and the amplitude will be larger if the gain L continuous to increase.

The above discussions highlights the performances of Theorem 6, since the use of the high-order sliding sliding mode technique can ensure the high convergence speed and the chattering limitation at the same time.

Example 4. Discrete-time random delay estimation

In this part, Theorem 6 is used to estimate a discrete-time delay. Indeed, in practice, the time-varying delay is not always differentiable, that makes the delay estimation task difficult. For example, the arguments in (Bresch-Pietri, Frédéric Mazenc, and Petit 2018, p.231) show that the communication routing of a networked control system can be changed to keep data queuing lines below some acceptable value, that causes delay jump phenomena. Therefore, the ability of estimating discontinuous time-varying delay is important to consider.

As the example given in (Bresch-Pietri, Frédéric Mazenc, and Petit 2018, Figure 6(b)), the artificial time-varying delay $h(t)$ can be modeled as a discrete-time random process $D(n, T_d)$ that changes value for each T_d seconds. In this example, $D(n, T_d)$ is chosen as a uniform random variable on $[0.8, 1.2]$ with $T_d = 0.15$s. The parameters of the delay estimator are set to $\alpha = 10$ and $\lambda = 15$.

Figure 2.8 illustrates that the round-trip delay introduced by $h(t) = D(n, T_d)$ is well estimated. Indeed, the sliding mode based delay estimation techniques (Theorems 5-7) can estimate piecewise-continuous time-delays, and this experiment highlights the practical use of such delay estimation

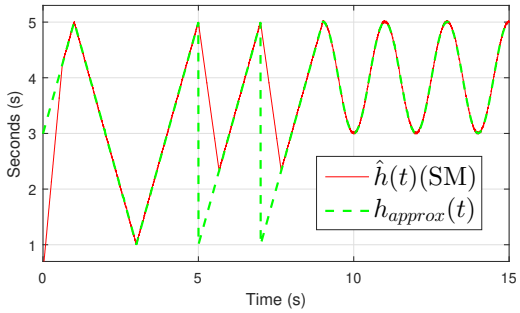

(a) Fast-varying delay estimation via Theorem 5.

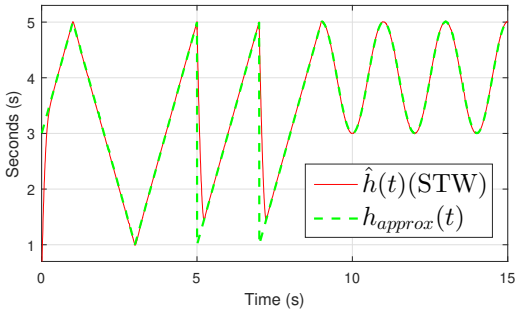

(b) Fast-varying delay estimation via Theorem 6.

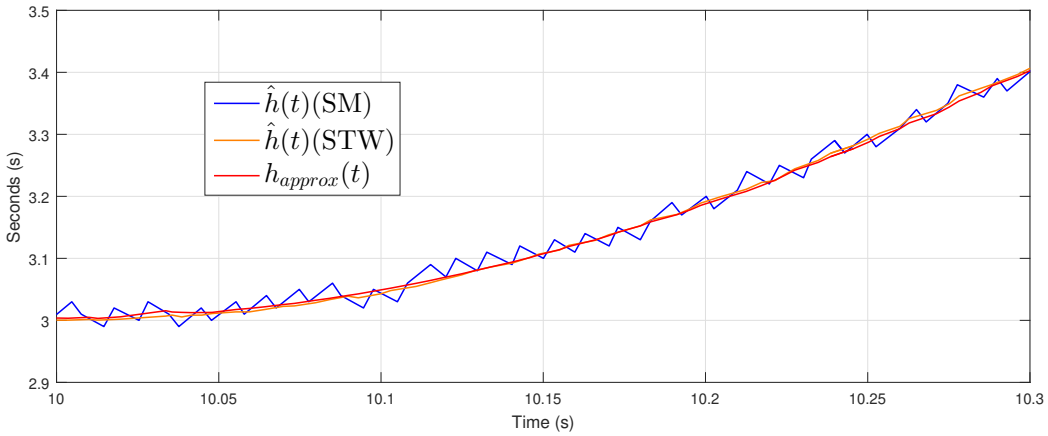

(c) Chattering analysis of fast-varying delay estimation on interval $t \in [10, 10.3]$.

Figure 2.7 – Comparison between Theorems 5 and 6 for fast-varying delay estimation.

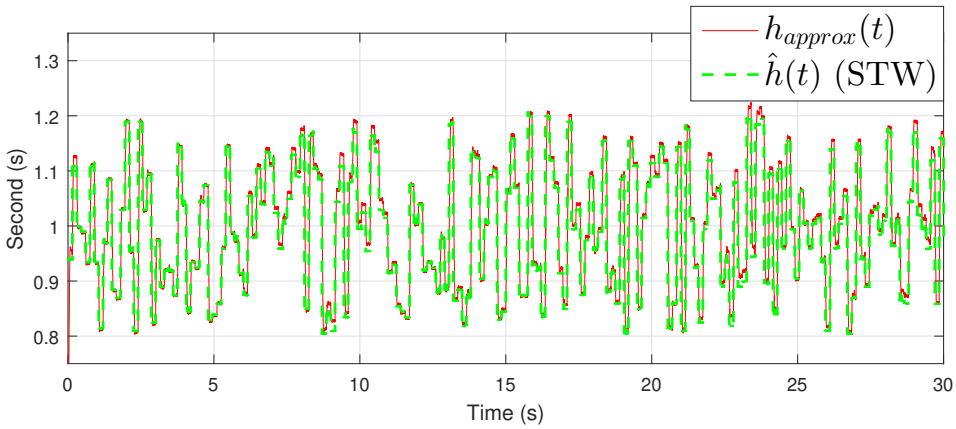

Figure 2.8 – Estimation of the round-trip delay with discrete-time random artificial delay $h(t) = D(n, T_d)$ by using Theorem 6.

approaches.

Comparison between the STW method and the ASTW method

In this part, Theorems 6-7 are compared on the experimental set-up described by Figure 2.4. The time-delay

$$h(t) = 1.3 + 0.3\sin(3t) + 0.5\sin\left(2(t - 0.8 - 0.3\sin(3t))\right) \tag{2.57}$$

that is the round-trip delay introduced by (2.44), is chosen as the artificial delay of the test bench. In the simulation, the following paramters are adopted:

— Super-twisting algorithm (STW) based method (Theorem 6), high gain case: $\lambda = 50$, $\alpha = 15$;
— Super-twisting algorithm (STW) based method (Theorem 6), low gain case: $\lambda = 5$, $\alpha = 7.5$;
— Adaptive super-twisting algorithm (ASTW) based method (Theorem 7): $\omega_1 = 1.1$, $\gamma_1 = 0.8$, $\mu = 0.0025$, $\lambda_m = 0.1$, $\eta = 0.3$, $\zeta = 0.7$, and $\lambda(0) = 9$.

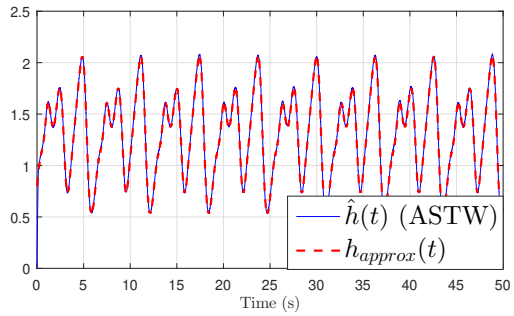

(a) Round-trip delay estimation via Theorem 7.

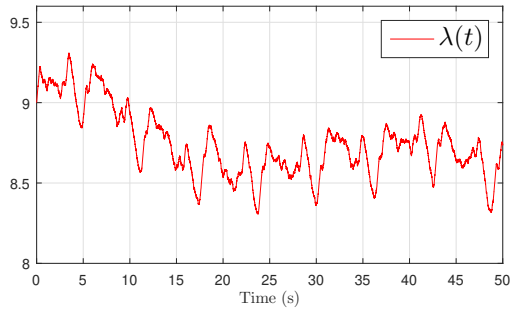

(b) Adaptive gain $\lambda(t)$ of Theorem 7.

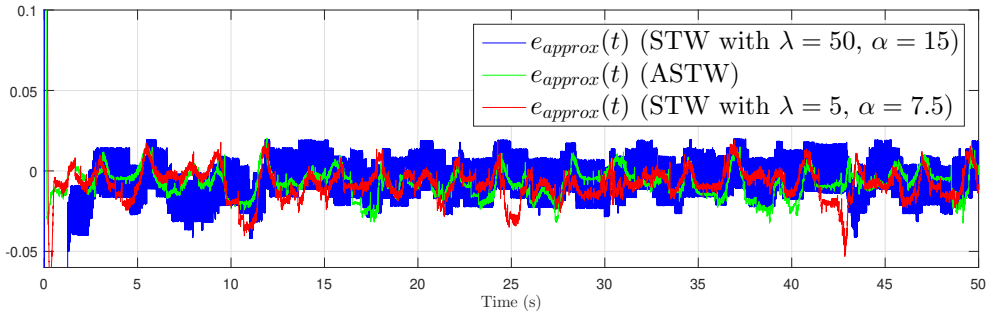

(c) Approximated estimation errors of Theorem 6 (with two cases) and Theorem 7.

Figure 2.9 – Comparison between Theorem 6 (with two cases) and Theorem 7.

The experimental results are presented in Figure 2.9. Firstly, Figures 2.9a-2.9b show that the round-trip delay is estimated by the Theorem 7, and the adaptive gain $\lambda(t)$ is decreased to a suitable size (the gain $\alpha(t)$ is not given because it is proportional to $\lambda(t)$, see (2.39)). Figure 2.9c displays the approximated estimation error of the 3 experiments, it is observed that Theorem 6 with $\lambda = 50$ and $\alpha = 15$ brings high-amplitude chattering, and the chattering is reduced if one uses lower gains $\lambda = 5$,

$\alpha = 7.5$. However, it is impossible to find the best tuning parameters beforehand, then the proposed method is used to handle this problem. See Figure 2.9c, Theorem 7 ensures the similar estimation accuracy with Theorem 6 ($\lambda = 5$, $\alpha = 7.5$) without any prior knowledge of the parameters. Thus, the experimental results given in Figure 2.9 highlight the use of the adaptive super-twisting algorithm, it is able to handle the tradeoff between the accuracy and the applicability.

2.3 Predictor-based control of remote control systems with unknown time-varying delay

2.3.1 Theoretical results with SM method

In this subsection, the combination of the predictor-based controller and the sliding mode based delay estimation methods are proposed to stabilize remote control systems with time-varying transmission delays. The main results are given in the sequel.

Theorem 8. *Consider the linear remote control system* (2.1) *with full state measurements, which is subject to the unknown input and output transmission delays $h_i(t)$, $h_o(t)$, is under the control framework given in subsection 2.1.2 and the delay estimation framework 2.1.1. If the bound on the derivative of $h_i(t)$ is sufficiently small (i.e. δ_i of* (2.11) *is sufficiently small), then the predictor-based controller* (2.5)*, combined with the delay estimator of Theorem 5, ensures that the redaction model $z(t)$ is globally uniformly exponentially stable:*

$$\|z(t)\| \leq M_5 \max_{s\in[-\bar{h},0]} \|z(s)\| e^{-\eta_2 t}, \quad t \geq 0 \tag{2.58}$$

with positive constant M_5. Moreover, there also exists a positive constant M_6 such that the state of the system globally converges to zero with decay rate η_2:

$$\|x(t)\| \leq M_6 \max_{s\in[-\bar{h},0]} \|z(s)\| e^{-\eta_2 t}, \quad t \geq 0 \tag{2.59}$$

Proof. At the beginning of the proof, the main convergence result (2.22) of Theorem 5 is recalled: there exists a finite time $t_F > 0$, such that the round-trip delay (2.3) is perfectly estimated for all $t \geq t_F$. Therefore, the proof of Theorem 8 can be divided into 3 parts:

- **Part 1:** The trajectories of the system (2.1) with initial conditions (2.2)-(2.6) are bounded for all $t \in [0, t_F)$;
- **Part 2:** The Lyapunov-Krasovskii analysis of the closed-loop system for all $t \geq t_F$;
- **Part 3:** Derivation exponential stability (2.58) and the exponential convergence (2.59).

Part 1. At first, one considers the right-hand derivative of the delayed state $x(t - h_o(t))$, it follows

that

$$\begin{aligned}\frac{d}{dt}x(t-h_o(t)) &= (1-\dot{h}_o(t))\dot{x}(t-h_o(t))\\ &= (1-\dot{h}_o(t))\left[Ax(t-h_o(t)) - Bu(t-h_o(t)-h_i(t-h_o(t))\right]\\ &= (1-\dot{h}_o(t))\left[Ax(t-h_o(t)) - Bu(t-h(t))\right]\end{aligned} \tag{2.60}$$

by virtue of the system dynamic (2.1), the chain rule (Apostol 1974, Theorem 5.5) and the definition 2.3. With the help of (2.60), differentiating the reduction model $z(t)$ given in (2.5) along the trajectories of (2.1) leads to

$$\begin{aligned}\dot{z}(t) &= \dot{\hat{h}}(t)Ae^{A\hat{h}(t)}x(t-h_o(t)) + e^{A\hat{h}(t)}\frac{d}{dt}x(t-h_o(t)) + Bu(t)\\ &\quad - (1-\dot{\hat{h}}(t))e^{A\hat{h}(t)} + A\int_{t-\hat{h}(t)}^{t} e^{A(t-s)}Bu(s)\mathrm{d}s\\ &= (A+BK)z(t) + (\dot{\hat{h}}(t)-\dot{h}_o(t))Az(t) - (\dot{\hat{h}}(t)-\dot{h}_o(t))A\int_{t-\hat{h}(t)}^{t} e^{A(t-s)}Bu(s)\mathrm{d}s\\ &\quad + (1-\dot{h}_o(t))e^{A\hat{h}(t)}Bu(t-h(t)) - (1-\dot{\hat{h}}(t))e^{A\hat{h}(t)}Bu(t-\hat{h}(t)), \qquad t\geq 0.\end{aligned} \tag{2.61}$$

Consider the delay estimator (2.19)-(2.21) given in Theorem 5, whose dynamic is bounded as:

$$|\dot{\hat{h}}(t)| \leq 1 + L/\underline{\epsilon} \tag{2.62}$$

The rest of the proof of this part is the same as proof of Lemma 2, since $\dot{\hat{h}}(t)$ and $\dot{h}_o(t)$ are uniformly bounded.

Part 2. In this part, the Lyapunov-Krasovskii analysis is given to demonstrate the closed-loop stability for all $t \geq t_F$. Firstly, by virtue of the finite time convergence of the delay estimation (2.22), the dynamic (2.61) becomes to

$$\begin{aligned}\dot{z}(t) &= (A+BK)z(t) + \delta(t)\left[Az(t) + e^{Ah(t)}Bu(t-h(t)) - A\int_{t-h(t)}^{t} e^{A(t-s)}Bu(s)\mathrm{d}s\right],\\ &= (A+BK)z(t) + \delta(t)Az(t) + \delta(t)e^{Ah(t)}B\left[u(t) - \int_{t-h(t)}^{t}\dot{u}(s)\mathrm{d}s\right]\\ &\quad - \delta(t)A\int_{t-h(t)}^{t} e^{A(t-s)}Bu(s)\mathrm{d}s, \qquad t\geq t_F.\end{aligned} \tag{2.63}$$

with

$$\delta(t) = \dot{h}(t) - \dot{h}_o(t) = \frac{d}{dt}h_i(t-h_o(t)). \tag{2.64}$$

Consider the Lyapunov-Krasovskii functional

$$V(z,u_t,\dot{u}_t,t) = V_1(z) + \beta V_2(u_t,t) + \gamma V_3(\dot{u}_t,t) \tag{2.65}$$

with

$$\begin{aligned} V_1(z) &= z^T(t)Pz(t), \\ V_2(u_t,t) &= \int_{t-\bar{h}}^{t}(s-t+\bar{h})\|u(s)\|^2\mathrm{d}s, \\ V_3(\dot{u}_t,t) &= \int_{t-\bar{h}}^{t}(s-t+\bar{h})\|\dot{u}(s)\|^2\mathrm{d}s. \end{aligned} \tag{2.66}$$

Differentiating $V_1(z)$ along the trajectories of (2.63) for all $t \geq t_F$ leads to

$$\begin{aligned} \dot{V}_1(z) = &-c_u\|z(t)\|^2 + 2\delta(t)z^T(t)PAz(t) + 2\delta(t)z^T(t)Pe^{Ah(t)}B\left[u(t) - \int_{t-h(t)}^{t}\dot{u}(s)\mathrm{d}s\right] \\ &- 2\delta(t)z^T(t)PA\int_{t-h(t)}^{t}e^{A(t-s)}Bu(s)\mathrm{d}s, \qquad t \geq t_F. \end{aligned} \tag{2.67}$$

Taking the norm of (2.67) yields that

$$\dot{V}_1(z) \leq -c_u\|z(t)\|^2 + |\delta(t)|(c_1+c_2)\|z(t)\|^2 + |\delta(t)|c_3\|z(t)\|\|v(t)\| + |\delta(t)|c_4\|z(t)\|\|w(t)\|, \quad t \geq t_F \tag{2.68}$$

with $c_1 = 2\|PA\|$, $c_2 = 2e^{\|A\|\bar{h}}\|BK\|\|P\|$, $c_3 = 2\|A\|e^{\|A\|\bar{h}}\|B\|\|P\|$, $c_4 = 2e^{\|A\|\bar{h}}\|B\|\|P\|$, $\|v(t)\| = \int_{t-\bar{h}}^{t}\|u(s)\|\mathrm{d}s$, and $\|w(t)\| = \int_{t-\bar{h}}^{t}\|\dot{u}(s)\|\mathrm{d}s$. By completing the squares, (2.68) can be developed to

$$\begin{aligned} \dot{V}_1(z) \leq &-(c_u - |\delta(t)|c_1 - |\delta(t)|c_2)\|z(t)\|^2 + \frac{|\delta(t)|}{2}c_3\left(\|z(t)\|^2 + \|v(t)\|^2\right) \\ &+ \frac{|\delta(t)|}{2}c_4\left(\|z(t)\|^2 + \|w(t)\|^2\right), \qquad t \geq t_F. \end{aligned} \tag{2.69}$$

Consider the functional $V_2(u_t,t)$ and the Jensen's inequality (Gu, J. Chen, and Kharitonov 2003, Proposition B.8), its derivative satisfies that

$$\begin{aligned} \dot{V}_2(u_t,t) &= \bar{h}\|u(t)\|^2 - \int_{t-\bar{h}}^{t}\|u(s)\|^2\mathrm{d}s \\ &\leq \bar{h}\|K\|^2\|z(t)\|^2 - \frac{1}{2\bar{h}}\|v(t)\|^2 - \frac{1}{2}\int_{t-\bar{h}}^{t}\|u(s)\|^2\mathrm{d}s, \qquad t \geq t_F. \end{aligned} \tag{2.70}$$

Taking the derivative of $V_3(\dot{u}_t,t)$, and using the power mean inequality (Bullen 2013, p.203, Theorem 1) leads to

$$\begin{aligned} \dot{V}_3(\dot{u}_t,t) &\leq \bar{h}\|\dot{u}(t)\|^2 - \int_{t-\bar{h}}^{t}\|\dot{u}(s)\|^2\mathrm{d}s \\ &\leq \bar{h}\|K\|^2\left[c_5\|z(t)\|^2 + |\delta(t)|^2\left(c_6\|z(t)\|^2 + c_7\|v(t)\|^2 + c_8\|w(t)\|^2\right)\right] \\ &\quad - \frac{1}{2\bar{h}}\|w(t)\|^2 - \frac{1}{2}\int_{t-\bar{h}}^{t}\|\dot{u}(s)\|^2\mathrm{d}s, \qquad t \geq t_F \end{aligned} \tag{2.71}$$

with $c_5 = 4\|A+BK\|^2$, $c_6 = 4(\|A\| + e^{\|A\|\bar{h}}\|BK\|)^2$, $c_7 = 4\|A\|^2 e^{2\|A\|\bar{h}}\|B\|^2$, and $c_8 = 4e^{2\|A\|\bar{h}}\|B\|^2$. After computing the upper bounds of $\dot{V}_1(z)$, $\dot{V}_2(u_t,t)$, and $\dot{V}_3(\dot{u}_t,t)$, the upper bound of the Lyapunov-Krasovskii functional (2.65) reads as

$$V(z,u_t,\dot{u}_t,t) \leq \bar{\lambda}(P)\|z(t)\|^2 + \beta\bar{h}\int_{t-\bar{h}}^{t}\|u(s)\|^2\mathrm{d}s + \gamma\bar{h}\int_{t-\bar{h}}^{t}\|\dot{u}(s)\|^2\mathrm{d}s. \tag{2.72}$$

Consider the term $\dot{V} + 2\eta_2 V$ and inequalities (2.69), (2.70), (2.71)n and (2.72), it is possible to derive that

$$\begin{aligned}\dot{V} + 2\eta_2 V \leq &-\left[\frac{\beta}{2\bar{h}} - \frac{|\delta(t)|}{2}c_3 - \gamma\bar{h}\|K\|^2 c_7|\delta(t)|^2\right]\|v(t)\|^2 - \left[\frac{\beta}{2} - 2\beta\bar{h}\eta_2\right]\int_{t-\bar{h}}^{t}\|u(s)\|^2\mathrm{d}s\\ &-\left[\frac{\gamma}{2\bar{h}} - \frac{|\delta(t)|}{2}c_4 - \gamma\bar{h}\|K\|^2 c_8|\delta(t)|^2\right]\|w(t)\|^2 - \left[\frac{\gamma}{2} - 2\gamma\bar{h}\eta_2\right]\int_{t-\bar{h}}^{t}\|\dot{u}(s)\|^2\mathrm{d}s\\ &-\left[c_u - |\delta(t)|(c_1+c_2+\frac{1}{2}c_3+\frac{1}{2}c_4) - \gamma\bar{h}\|K\|^2(c_5+c_6|\delta(t)|^2) - \beta\bar{h}\|K\|^2 - 2\eta_2\bar{\lambda}(P)\right]\|z(t)\|^2\end{aligned} \tag{2.73}$$

for all $t \geq t_F$. Indeed, the inequality $\dot{V} + 2\eta_2 V \leq 0$ holds when

— the parameters β, γ, and η_2 are sufficiently small;
— the derivative $|\delta(t)|$ is sufficiently small.

Remind that the parameters α, β, and η_2 are the parameters of the Lyapunov-Krasovskii functional so they can be tuned sufficiently small. The boundedness (2.11) and the chain rule (Apostol 1974, Theorem 5.5) ensure that the derivative $|\delta(t)|$ is upper bounded as follows

$$|\delta(t)| = \left|\frac{d}{dt}h_i(t-h_o(t))\right| = |(1-\dot{h}_o(t))\dot{h}_i(t-h_o(t))| \leq \delta_i(1+\delta_o). \tag{2.74}$$

Thus, for all given δ_o, if the parameter δ_i is sufficiently small (*i.e.* $h_i(t)$ varies sufficiently slow), then the closed-loop system of $z(t)$ is globally uniformly exponential stable, such that

$$V(t) \leq V(t_F)e^{-2\eta_2(t-t_F)}, \quad t \geq t_F. \tag{2.75}$$

Part 3. The proof of this part is similar to the proof of Lemma 4, it can be demonstrated with a similar technique. Only one point need to pay attention, the state $x(t)$ is used to compute the predictor $z(t)$ at a future instant $t+\tilde{h}$ with $\tilde{h} \in [0,\bar{h}]$. Indeed, if $\tilde{h} > \bar{h}$, then $t+\tilde{h}-h_o(t+\tilde{h}) > t$ holds that contradicts the expression of the predictor. Thus, the following equality is available

$$x(t) = e^{-Ah(t+\tilde{h})}\left[z(t+\tilde{h}) - \int_{t+\tilde{h}-h(t+\tilde{h})}^{t+\tilde{h}} e^{A(t+\tilde{h}-s)}Bu(s)\mathrm{d}s\right]. \tag{2.76}$$

Taking the norm of (2.76), it is possible to derive the bound on the original state $x(t)$ as:

$$\|x(t)\| \leq e^{\|A\|\bar{h}} \left[\|z(t+\tilde{h})\| + e^{\|A\|\bar{h}} \|BK\| \bar{h} \max_{s\in[t+\tilde{h}-\bar{h},t+\tilde{h}]} \|z(s)\| \right]. \tag{2.77}$$

The exponential convergence (2.59) can be obtained by considering (2.77) and Parts 1-2, and then the proof is finished. □

Theorem 8 presents a practical control solution to remote control systems with time-varying input and output delays, the main benefits are:

— The control technique is simple and effective: thanks to the frameworks introduced in subsection 2.1.1, the delay estimation loop is isolated from the control loop.

— The stability condition of Theorem 8 shows that the technique can stabilize remote control systems with sufficiently slow-varying input delay and fast-varying output delay, and the round-trip delay (2.3) can be fast-varying.

— Theorem 8 can also be extended to the predictor-based control of systems with known input and output time-varying delays, like (Léchappé, Moulay, and Plestan 2018b, Theorem 1). However, the work of (Léchappé, Moulay, and Plestan 2018b) uses $h_i(t)+h_o(t)$ as the round-trip delay to compute the control law, rather than (2.3). But in applications, to measure this delay value, the clock synchronization (Martı et al. 2008) between the plant and the controller is necessary. However, as claimed after (2.53), the clock synchronization is not required by this control solution.

2.3.2 Theoretical results with STW method

Theorem 6 can also be applied to the stabilization of the closed-loop system, but some changes must be made to the dynamic of the correction term (2.32), the new dynamic reads as

$$\dot{w}_1(t) = \begin{cases} -w(t), & \text{if} \quad |w(t)| > \bar{W} \\ -\alpha \cdot \text{sign}(\sigma(t)), & \text{if} \quad |w(t)| \leq \bar{W} \end{cases} \tag{2.78}$$

with a sufficiently large positive constant $\bar{W}$. Therefore, it is possible to state the theoretical results of this subsection.

Theorem 9. *Consider the linear remote control system* (2.1) *with full state measurements, which is subject to the unknown input and output transmission delays $h_i(t)$, $h_o(t)$, is under the control framework given in subsection 2.1.2 and the delay estimation framework given in subsection 2.1.1. If the bound on the derivative of $h_i(t)$ is sufficiently small (i.e. δ_i of* (2.11) *is sufficiently small), then the predictor-based controller* (2.5)*, combined with the delay estimator* (2.19)-(2.31)-(2.78) *leads to the global uniform exponential stability* (2.58) *and the global convergence* (2.59)*.*

Proof. The majority of the proof is the same as the one of Theorem 8, only the first part is changed. One first studies the bound on $\sigma(0)$ as follows. According to Assumption 5 and the mean value theorem (Apostol 1974, Theorem 5.11), there exists a constant $r \in \Big[\min\{\hat{h}(0), h(0)\}, \max\{\hat{h}(0), h(0)\}\Big]$, such that

$$|\sigma(0)| = |s(t - \hat{h}(0) - s(t - h(0)))| = |\dot{s}(t - r)||\hat{h}(0) - h(0)| \leq 2\bar{\epsilon}\bar{h} \tag{2.79}$$

with the help of $|\dot{s}(t)| \leq \bar{\epsilon}$, $|h(0)| \leq \bar{h}$, and the well-chosen initial condition $|\hat{h}(0)| \leq \bar{h}$. Therefore, $w(0)$ is bounded as

$$|w(0)| \leq \lambda\sqrt{2\bar{\epsilon}\bar{h}} + |w_1(0)|. \tag{2.80}$$

Next, one sets $\bar{W} \geq \lambda\sqrt{2\bar{\epsilon}\bar{h}} + |w_1(0)|$, the statements given in (Shtessel, Edwards, et al. 2014, Theorem 4.5) ensure that:

— The delay estimator (2.19)-(2.31)-(2.78) converges to the round-trip delay in a finite time t_F.

— The trajectories of $w(t)$ never leaves the segment $[-\bar{W}, \bar{W}]$ for all $t \geq 0$.

The above discussions ensures that the evolution speed of $\hat{h}(t)$ is upper bounded as follows:

$$|\dot{\hat{h}}(t)| \leq 1 + \left|\frac{1}{\dot{s}(t - \hat{h}(t))}\right| |w(t)| \leq 1 + \bar{W}/\underline{\epsilon} \triangleq \bar{\delta} \tag{2.81}$$

for all $t \geq 0$. Thus, applying Lemma 2, the trajectories of $z(t)$ are always uniformly bounded during the transient phase $t \in [0, t_F)$. The rest of the proof is omitted since it is exactly the same as Theorem 8. □

2.3.3 Simulation results

Consider the double integrator system given in (Léchappé, Moulay, and Plestan 2018b, Section 5):

$$\begin{cases} \dot{x}(t) = \begin{bmatrix} 0 & 1 \\ 0 & 0 \end{bmatrix} x(t) + \begin{bmatrix} 0 \\ 0.7 \end{bmatrix} u(t - h_i(t)), \\ y(t) = x(t - h_o(t)) \end{cases} \tag{2.82}$$

with unknown time-varying delays

$$\begin{aligned} h_i(t) &= 0.5 + 0.4\sin(t), \\ h_o(t) &= 0.5 + 0.45\sin(25 \cdot t). \end{aligned} \tag{2.83}$$

The initial conditions of system (2.82) are set to $x(\theta) = \begin{bmatrix} 1 & 2 \end{bmatrix}^T$, $u(\theta) = -1$, and $z(\theta) = x(0)$ for all $\theta \in [-\bar{h}, 0)$. The parameters are given in the sequel:

— Parameters of the delay estimator (with Theorem 8): $s(t) = t$, $L = 17$, and $\hat{h}(0) = 0.5$;

— Parameters of the delay estimator (with Theorem 9): $s(t) = t$, $\lambda = \bar{W} = 30$, $\alpha = 10$,

$\hat{h}(0) = 0.5$, and $w_1(0) = 0$;

— Parameter of the controller (2.5): $K = \begin{bmatrix} -4.2857 & -5.7143 \end{bmatrix}$;

and the sampling period of the practical delay estimation algorithm is set to $T_s = 0.005$s (to conform to the real wireless data communication). In order to explain the importance of the delay estimation technique, a simulation with constant delay $\hat{h} = h_m = 1.0$s (mean value of the round-trip delay derived from (2.83)) is also done.

The simulation results are presented in Figures 2.10-2.11, the round-trip delay $h_{rt}(t)$ is estimated

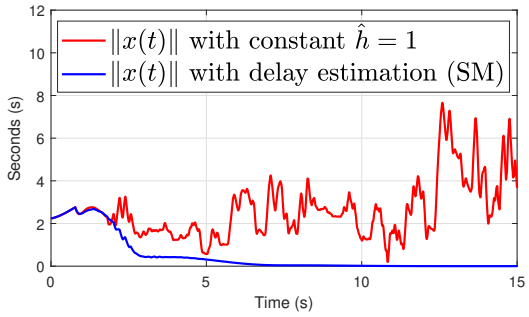

(a) State evolution of the system (2.82) under the control solution of Theorem 8 and constant delay estimation $\hat{h} = h_m = 1.0$s.

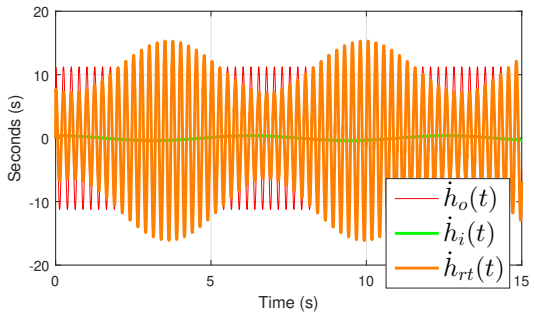

(b) Time derivatives of the input delay $h_i(t)$, the output delay $h_o(t)$, and the round-trip delay $h_{rt}(t)$ derived from (2.83).

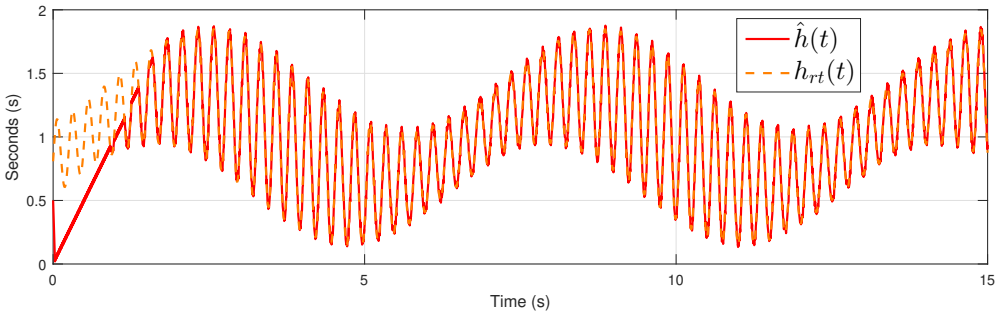

(c) Estimation of the round-trip delay formulated by the input and output delays (2.83) via Theorem 5.

Figure 2.10 – System trajectories and delay estimation of the double integrator (2.82) under the control solutions provided in Theorem 8.

with Theorem 5 and the modified delay estimator (2.19)-(2.31)-(2.78). See Figures 2.10a and 2.11a, the system trajectories with constant delay estimation $\hat{h} = h_m = 1.0$s diverges, but the delay estimation techniques make the closed-loop system stable. Moreover, the system (2.82) is stabilized even if $h_o(t)$ and $h_{rt}(t)$ are fast-varying. The simulation results illustrate the theoretical results of Theorems 8-9, such that the fast-varying round-trip delay is perfectly estimated, and the system is stabilized by using the value of this delay estimation.

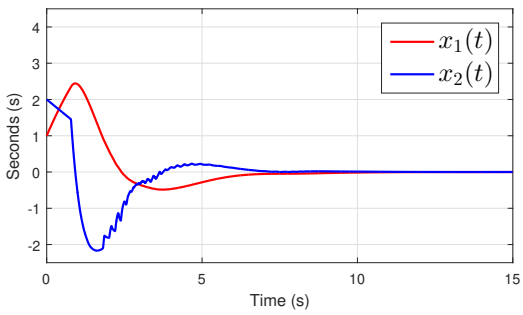

(a) State evolution of the system (2.82) under the control solution of Theorem 9.

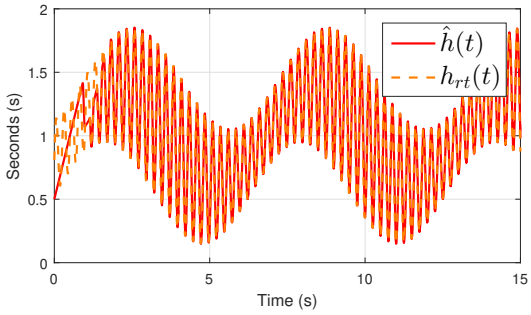

(b) Estimation of the round-trip delay of (2.83) via delay estimator (2.19)-(2.31)-(2.78).

Figure 2.11 – System trajectories and delay estimation of the double integrator (2.82) under the control solutions provided in Theorem 9.

Chapter 3

Discrete predictor-based control of networked control systems with time-varying delays

Contents

3.1 Introduction

In this section, a brief introduction to the networked control systems and the predictor-based control of them is given. First, the motivations explain why this chapter is dedicated to the predictor-based control of networked control systems with sensor-to-controller time-varying delays and controller-to-actuator uncertain constant delays. Next, the state of the arts of the networked control systems are introduced, two methods (time-delay approach, discrete-time approach) are emphasized and compared. Finally, the predictor-based control of networked control systems with long delays is introduced, it can be designed by time-delay approach or discrete-time approach.
The main results of this Chapter are submitted to the following international journal:

Y. Deng, V. Léchappé, C. Zhang, E. Moulay, D. Du, F. Plestan, and Q.-L. Han, *Discrete predictor-based control of LTI networked control systems with time-varying delay: application to a visual servo inverted pendulum system*, submitted to IEEE Transactions on Control Systems Technology.

3.1.1 Motivations

Vision-based sensor is widely used in various control applications (*e.g.* self-driving car (Hee Lee, Faundorfer, and Pollefeys 2013; Wolcott and Eustice 2014), robot (Wang et al. 2012), UAV (Ramirez et al. 2014), inverted pendulum (Kizir et al. 2012; Zhan, Du, and Fei 2017; Du, C. Zhang, et al. 2019)) due to the low cost (with respect to LIDAR) (Wolcott and Eustice 2014, p.176) and the rapid progress of image processing techniques. In such control systems, the state information is resolved from the captured images by using image processing algorithms. However, this process brings in the following difficulties in the controller design:

— only sampled state information is available for the controller due to the digital nature of the camera (Wang et al. 2012, p.132), and the sampling rate may be low if no distributed computation is applied (H. Wu et al. 2012, p.554);
— the image processing algorithm needs a long computational time, so it introduces a long time-varying delay (Ramirez et al. 2014; Zhan, Du, and Fei 2017).

After the resolution, the state information is transmitted to the controller via a wired or wireless sensor-to-controller communication channel that is subject to a small uncertain time-varying delay (several milliseconds (Horalek, Svoboda, and Holik 2016, p.147)). The controller then calculates the control law and sends it to the actuator via the controller-to-actuator channel, and finally the control input is applied to the system. Based on the previous statements, the whole control process of such system is subject to the following time-delays:

— the exposure time of the camera (constant);
— the computational delay introduced by the image processing algorithm (long, time-varying);
— the transmission latency induced from the sensor-to-controller communication (small, time-varying);
— the computation time of the control law (small, constant);
— the transmission latency induced from the controller-to-actuator communication (small, time-varying);
— the physical dead time of the actuator (constant).

According to the above discussions, the vision-based control can be modeled as a networked control system (NCS) with **sensor-to-controller time-varying delay** and **controller-to-actuator uncertain constant delay** [1]. Moreover, in order to reduce the cost of the control system, it will be

1. The controller-to-actuator delay is the sum of a constant delay (dead time of the actuator) and a small time-varying delay (controller-to-actuator data transmission latency). Therefore, it is equivalently modeled as an uncertain

preferable if the control strategy still works with a low sampling rate (*i.e.* The sampling rate of the industrial camera depends on the exposure time. Generally, smaller exposure time ensures higher sampling rate, but it also increases the price of the sensor). Thus, due to their high potential for application, it is important to develop new control strategies being able to stabilize these systems.

3.1.2 State of the arts of related works

Networked control system (NCS) is a hot topic in the control community (X.-M. Zhang, Han, and Yu 2015), since more and more control systems have remote sensor, controller and actuator connected through a network (*e.g.* networked mobile robot(Tipsuwan and Chow 2002), connected car or networked process control (L. Zhang, Gao, and Kaynak 2012)). The use of the network reduces the cost of the control system (S.-H. Yang 2011, Chapter 1.1), but the data transmission also brings network-induced delays and packet dropouts (K. Liu, Selivanov, and Fridman 2019, Section 2). Therefore, these effects must be taken into account while designing the control law of NCS.
NCS can be stabilized by a continuous-time method named time-delay approach (K. Liu, Selivanov, and Fridman 2019). It transforms the original NCS into a continuous TDS, then a digital controller is designed to stabilize the NCS. The time-delay approach deals with variable sampling and non-small delays at the same time (Yue, Han, and Lam 2005; Gao, Tongwen Chen, and Lam 2008). To compensate arbitrarily-long time-delays, the authors of (Selivanov and Fridman 2016b) proposed a digital predictor-based controller in order to stabilize NCSs with uncertain constant delays by using the time-delay approach, this method is extended to the output feedback case in (Selivanov and Fridman 2016a).
However, the method proposed in (Selivanov and Fridman 2016b; Selivanov and Fridman 2016a) is difficult to stabilize NCS with long sampling periods because the stability criteria may not be easily feasible. To stabilize such systems, the discrete predictor-based controller is an effective way since the original system is transformed into an extended discrete-time delay-free system (Hu and Zhu 2003; Cloosterman et al. 2009; Léchappé, Moulay, Plestan, and Han 2019). As stated in (Léchappé, Moulay, Plestan, and Han 2019), the discrete predictor-based controller can stabilize NCSs with long constant time-delays and long sampling periods. It is shown in (Lozano et al. 2004) that this method is robust with respect to the delay uncertainty as the time-delay approach (Selivanov and Fridman 2016b). In (Cloosterman et al. 2009), a discrete predictor-based controller is designed to stabilize NCSs with a time-varying delays and message rejections (J. Li, Q. Zhang, and Cai 2009).

3.1.3 Predictor-based control of networked control systems with long delays

In this subsection, the predictor-based control of networked control systems is introduced, the first method (Selivanov and Fridman 2016b) is the sampled-data version of the continuous predictor-

constant delay.

based controller, whereas the second method (Léchappé, Moulay, Plestan, and Han 2019) transforms the NCS to a discrete-time system. Before stating the main results of these references, some basic introductions to NCS are given.

The control diagram of networked control systems is displayed in Figure 3.1. At instants $\{s_k\}_{k\in\mathbb{N}}$,

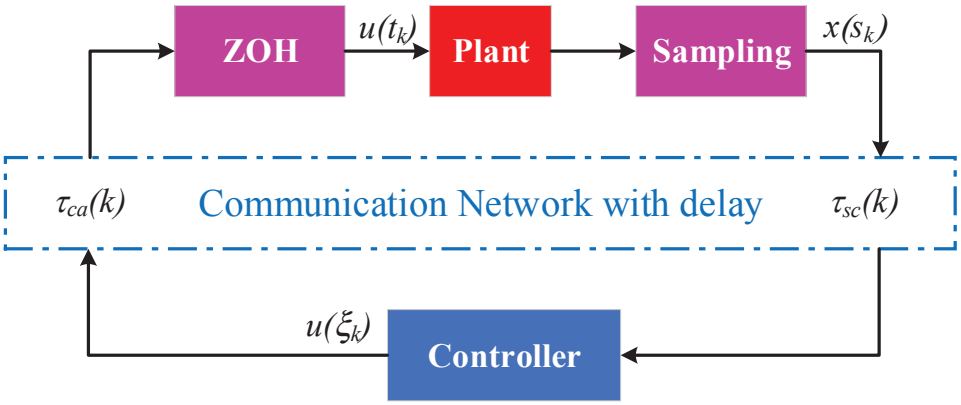

Figure 3.1 – General control diagram of networked control systems.

the sensor takes action and sends the measurements $x(s_k)$ to the controller via network, the controller receives the measurements at $\{\xi_k\}_{k\in\mathbb{N}}$ due to the sensor-to-controller delay $\tau_{sc}(k) \triangleq \xi_k - s_k$. After receiving the state measurements, the controller runs the control algorithm and computes the control inputs $u(\xi_k)$ (*i.e.* in this case, the controller is event-driven). The control input signal is then transmitted to the plant through a communication network that is subject to a controller-to-actuator delay $\tau_{ca}(k)$. Finally, the sampled control inputs are converted to the continuous-time versions by virtue of a zero-order-holder (ZOH), and then they are applied to the plant.

To well-explain the mechanism of NCS (*i.e.* the above modelings and notations), a straightforward example is given as follows.

A timing diagram of an event-driven NCS with constant network-induced delays is presented in Figure 3.2. The sampling period is presented as Δ, τ_{sc} and τ_{ca} respectively denote the constant sensor-to-controller delay and controller-to-actuator delay, and the sum of them read as τ. In this example, the time-delays satisfies that

$$h\Delta \leq \tau_{sc} + \tau_{ca} = \tau \leq (h+1)\Delta \tag{3.1}$$

with $h = 1$.

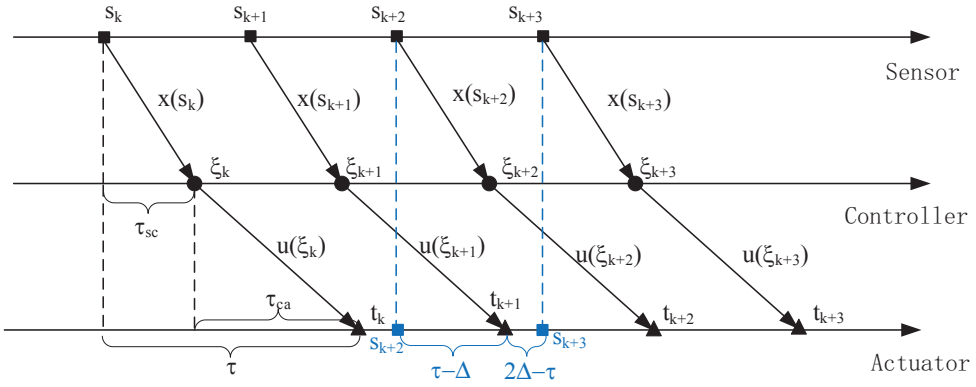

Figure 3.2 – Timing diagram of networked control system with constant delays.

Predictor-based control with time-delay approach

Consider the linear plant

$$\dot{x}(t) = Ax(t) + Bu(t) \tag{3.2}$$

with $x(t) \in \mathbb{R}^n$, $u(t) \in R^m$, $A \in \mathbb{R}^{n\times n}$, and $B \in \mathbb{R}^{n\times m}$ controlled through a network that is subject constant network-induced delays τ_{sc} and τ_{ca} (as shown in Figure 3.2). The control law of (Selivanov and Fridman 2016b) reads as

$$u(\xi_k) = K\left[e^{A(\tau_{sc}+\tau_{ca})}x(s_k) + \int_{s_k-\tau_{ca}}^{\xi_k} e^{A(\xi_k-\theta)}Bv(\theta)\mathrm{d}\theta\right] \tag{3.3}$$

with

$$v(\xi) \triangleq \begin{cases} 0, & \xi < \xi_0 \\ u(\xi_k), & \xi \in [\xi_k, \xi_{k+1}) \end{cases} \tag{3.4}$$

and the matrix K is chosen such that $A+BK$ is Hurwitz. Indeed, (3.3) is the sampled-data version of the continuous-time predictor-based controller, and it can stabilize the plant (3.2) with arbitrarily long τ_{sc}, τ_{ca} if the sampling period Δ is sufficiently small.

The stability of the closed-loop system (3.2)-(3.3)-(3.4) is analyzed by using the time-delay approach (K. Liu, Selivanov, and Fridman 2019). This method uses a time-varying delay to describe the sampling/ ZOH process, and the closed-loop stability condition is derived from a Lyapunov-Krasovskii analysis. The main drawback of this method is the limitation on the sampling rate, since the feasibility of the sufficient condition to the closed-loop stability (a delay-dependent LMI) depends on the maximum allowable sampling period (MASP).

Remind that, if the network-induced delays are uncertain (*i.e.* time-varying, but sufficiently close to the nominal values τ_{sc}, τ_{ca}), the controller given in (3.3) is still effective. However, if the network-induced delays are time-varying (in general meaning), (3.3) fails to stabilize the NCS.

Predictor-based control with discrete-time approach

Discrete predictor-based controller (Léchappé, Moulay, Plestan, and Han 2019) is one of the well-known control solutions that deals with long sampling period. Consider the timing diagram of Figure 3.2 as an example, the state-translation equation between $x(s_{k+2})$ and $x(s_{k+3})$ reads as

$$\begin{aligned} x(s_{k+3}) =& e^{A\Delta}x(s_{k+2}) + \int_{s_{k+2}}^{s_{k+3}} e^{A(s_{k+3}-\theta)}Bu(\theta)\mathrm{d}\theta \\ =& e^{A\Delta}x(s_{k+2}) + \int_{t_{k+1}}^{s_{k+3}} e^{A(s_{k+3}-\theta)}\mathrm{d}\theta B u(\xi_{k+1}) + \int_{s_{k+2}}^{t_{k+1}} e^{A(s_{k+3}-\theta)}\mathrm{d}\theta B u(\xi_k) \\ =& \underbrace{e^{A\Delta}}_{\bar{A}} x(s_{k+2}) + \underbrace{\int_0^{(h+1)\Delta-\tau} e^{A\theta}\mathrm{d}\theta B}_{\bar{B}_1} u(\xi_{k+1}) + \underbrace{e^{A((h+1)\Delta-\tau)}\int_0^{\tau-h\Delta} e^{A\theta}\mathrm{d}\theta B}_{\bar{B}_2} u(\xi_k). \end{aligned} \tag{3.5}$$

Inspired by (3.5), if one defines $\bar{x}(t) = x(t-\tau_{sc})$, then the following discrete state-translation equation is available:

$$\bar{x}(\xi_k+\Delta) = \bar{A}\bar{x}(\xi_k) + \bar{B}_1 u(\xi_k - h\Delta) + \bar{B}_2 u(\xi_k - (h+1)\Delta). \tag{3.6}$$

Define the extended state

$$X(\xi_k) = \begin{bmatrix} \bar{x}^T(\xi_k) & u^T(\xi_k-\Delta) & \cdots & u^T(\xi_k - h\Delta) & u^T(\xi_k-(h+1)\Delta) \end{bmatrix}^T, \tag{3.7}$$

then (3.6) is equivalent to the following extended system:

$$X(\xi_k+\Delta) = \underbrace{\begin{bmatrix} \bar{A} & 0 & 0 & \cdots & \bar{B}_1 & \bar{B}_2 \\ 0 & 0 & 0 & \cdots & 0 & 0 \\ 0 & I_{m\times m} & 0 & \cdots & 0 & 0 \\ \vdots & \ddots & \ddots & \ddots & \vdots & \vdots \\ 0 & \cdots & 0 & I_{m\times m} & 0 & 0 \\ 0 & \cdots & \cdots & 0 & I_{m\times m} & 0 \end{bmatrix}}_{A_{ext}} X(\xi_k) + \underbrace{\begin{bmatrix} 0 \\ I_{m\times m} \\ 0 \\ \vdots \\ 0 \\ 0 \end{bmatrix}}_{B_{ext}} u(\xi_k). \tag{3.8}$$

Finally, the control law $u(\xi_k)$ can be computed by a state feedback law $u(\xi_k) = KX(\xi_k)$ such that $A_{ext} + B_{ext}K$ is Shur (*i.e.* all of the poles of a Schur matrix are located in the unit circle of the complex plane).

The main idea of discrete predictor-based controller (Léchappé, Moulay, Plestan, and Han 2019) is the delay-free extended system representation (3.8), this technique can stabilize NCS with arbitrarily long constants delays and arbitrarily long sampling periods (Léchappé, Moulay, Plestan, and Han 2019, Section 7.1) thanks to the discretization. If the delay values are large, then the sizes of A_{ext}

and B_{ext} are also large that make the matrix K difficult to compute, then one can use the method given in (Léchappé, Moulay, Plestan, and Han 2019, Section 6) to obtain the control law. The only drawback of this technique is that it cannot handle the variable sampling system as the time-delay approach (Selivanov and Fridman 2016b).

The discrete predictor-based control based on the extended system representation (3.8) is extended to the time-varying delay case in (Hu and Zhu 2003; Cloosterman et al. 2009).
The discrete extended system given in (Hu and Zhu 2003, Section 2) is similar to (3.8), but the zero block matrices of the first rows of A_{ext} and B_{ext} are no longer zero since the network-induced delays are time-varying. The objective of this method is optimizing the following cost function

$$J_N = E\left[X^T(\xi_N)Q_0X(\xi_N) + \sum_{k=0}^{N-1}\Big(X^T(\xi_k)Q_1X(\xi_k) + u^T(\xi_k)Q_2u(\xi_k)\Big)\right] \tag{3.9}$$

where Q_0, Q_1, Q_2 are predefined symmetric positive definite matrices, and $E[\cdot]$ denotes the stochastic expectation. Then the time-varying feedback matrix $K(\xi_k)$ is obtained by solving the Belleman equation derived from (3.9).
However, the control solution of (Hu and Zhu 2003) has two drawbacks:

— the probability distribution function of the network-induced delays are assumed to be known in prior;
— all of the packets are ordered (*i.e.* the sequences $\{\xi_k\}_{k\in\mathbb{N}}$, $\{t_k\}_{k\in\mathbb{N}}$ are increasing), and packet reordering (message rejection) (J. Li, Q. Zhang, and Cai 2009) cannot occur.

The drawbacks of (Hu and Zhu 2003) are covered by (Cloosterman et al. 2009), and a Lyapunov-Krasovskii analysis is given to guarantee the global asymptotic stability, rather than the stochastic stability of (Hu and Zhu 2003). Remind that the extended system modeling of (Hu and Zhu 2003, p.1879) and (Cloosterman et al. 2009, p.1577) are almost identical, but they treat the extended system in different ways. The main objective of (Cloosterman et al. 2009) is to seek for a static feedback control law $u(\xi_k) = KX(\xi_k)$ that deals with all the cases (*i.e.* different time-varying delays and message rejections).
The works of (Cloosterman et al. 2009) provide an effective control solution to the NCS with time-varying delays and message rejection. The only drawback of this method is the feasibility and the computation cost, according to (Cloosterman et al. 2009, Theorem 2), the feedback gain K is obtained by verifying $2^{\bar{h}}$ LMIs, with $\bar{h} = \max\{\tau_{sc}(k) + \tau_{ca}(k)\}/\Delta$. Thus, if the networked-induced delays are long (*i.e.* h is large), large numbers offline computations must be done to derive the stable control solution. Moreover, this method is at risk of infeasiblility when h is extremely large.

Therefore, predictor-based control of NCS with long and time-varying delays is still challenging to the control community, and the control techniques should be improved to stabilize such systems in simpler and more effective ways.

3.2 Control scenario of the discrete predictor-based controller

In this section, the discrete predictor-based control is designed to stabilize NCS with sensor-to-controller time-varying delay and controller-to-actuator uncertain constant delay. This section begins with the problem formulations and the modeling of the NCS, then the basic concept of the proposed controller is introduced by a simple example in which the controller-to-actuator delay is constant. After studying the simple case, the main control scenario is built and the closed-loop stability is hereafter analyzed.

3.2.1 Problem formulations

Consider the following LTI plant

$$\dot{x}(t) = Ax(t) + Bu(t), \quad t \geq 0 \tag{3.10}$$

controlled through a network with $A \in \mathbb{R}^{n\times n}$ and $B \in \mathbb{R}^{n\times m}$. The control input is piecewise-constant such that

$$\begin{aligned} u(t) &= u_k, \qquad t \in [t_k, t_{k+1}), \quad k \in \mathbb{N} \\ u(t) &= 0, \qquad t < t_0. \end{aligned} \tag{3.11}$$

where t_k is the instant that the kth control input u_k is applied to the plant.
In this work, the sensor and the controller have time-driven behavior which means that they update the state measurement and the control input each Δ seconds and send them out. The actuator is event-driven, it applies the new control input to the plant as soon as it receives it.
Figure 3.3 is the timing diagram of this method, the sequence $\{s_k\}_{k\in\mathbb{N}}$ represents the sampling instants of the sensor and the updating instants of the controller. The sequence $\{\xi_k\}_{k\in\mathbb{N}}$ describes the arriving instants of the state measurement $x(s_k)$, and $\{t_k\}_{k\in\mathbb{N}}$ denotes the instants that a new control input u_k is applied to the plant.
The state information is periodically measured (with sampling period $\Delta > 0$) and sent to the controller through the network. Namely, at instants $s_k = k\Delta$, $k \in \mathbb{N}$, the sensor takes action and sends the state measurement to the controller. According to Figure 3.3, one defines the sensor-to-controller time-varying delay as $\tau_{sc}(k) \triangleq \xi_k - s_k$, and it is bounded by:

$$0 \leq \tau_{sc}(k) \leq N_1\Delta \tag{3.12}$$

with known $N_1 \in \mathbb{N}_+$. Due to the above discussions and Figure 3.3, the controller is time-driven, then the controller-to-actuator delay reads as $\tau_{ca}(k) = t_k - s_k$, it is modeled as an uncertain constant delay such that

$$\tau_{ca}(k) = \bar{\tau}_{ca} + \Delta\tau(k) \tag{3.13}$$

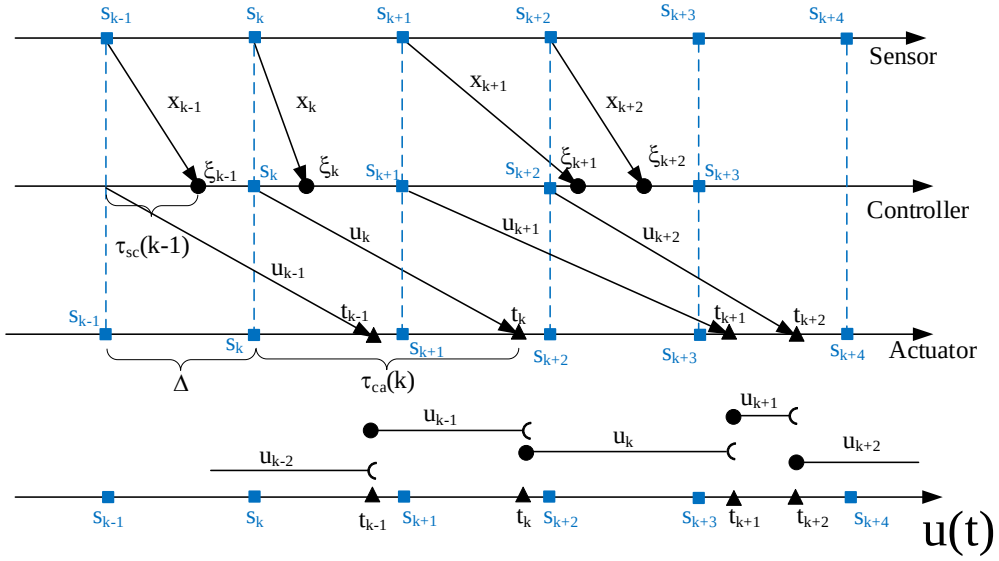

Figure 3.3 – Timing diagram of the control scheme with time-driven sensor, time-driven controller and event-driven actuator.

where the nominal controller-to-actuator constant delay $\bar{\tau}_{ca}$ is known and bounded by

$$(N_2 - 1)\Delta \leq \bar{\tau}_{ca} \leq N_2\Delta \tag{3.14}$$

with known $N_2 \in \mathbb{N}_+$, and the uncertainty is bounded by

$$0 \leq \Delta\tau(k) \leq \Delta. \tag{3.15}$$

Figure 3.3 shows that the controller is time-driven, but not event-driven. The main benefit of the time-driven controller is that the controller design is much simpler than the event-driven ones when the sensor-to-controller delay is long and fast-varying. Moreover, the proposed control strategy can be calculated without solving delay-dependent LMI.

Assumption 7. *Define* $\bar{A} = e^{A\Delta}$, $\bar{B}_1 = \int_0^{N_2\Delta-\bar{\tau}_{ca}} e^{A\theta}\mathrm{d}\theta B$ *and* $\bar{B}_2 = \int_{N_2\Delta-\bar{\tau}_{ca}}^{\Delta} e^{A\theta}\mathrm{d}\theta B$, *one assumes that the pair* $(\bar{A}, \bar{A}^{-N_2+1}\bar{B}_1 + \bar{A}^{-N_2}\bar{B}_2)$ *is controllable.*

Since the control law of this work is designed by the discrete-time approach, then one must verify that the discrete-time system is controllable. Assumption 7 provides a sufficient condition to the controllability of the discrete-time system (Léchappé, Moulay, Plestan, and Han 2019, Assumption 1).

Next, one assumes that the sensor and the controller are synchronized so that $\tau_{sc}(k)$ can be measured when the controller receives a new measurement, this assumption is also made in (W. Zhang,

Branicky, and Phillips 2001; Selivanov and Fridman 2016b; Selivanov and Fridman 2016a).

Remark 6. *The Zeno phenomenon never occurs since the state measurement and the control law calculation are periodic.*

In (Selivanov and Fridman 2016b), the authors assumed that the older control inputs and the older state measurements cannot arrive at the destination later than a newer one. In other words, the sequences $\{t_k\}_{k\in\mathbb{N}}$ and $\{\xi_k\}_{k\in\mathbb{N}}$ are increasing:

$$\begin{aligned} t_0 \leq t_1 \leq \cdots \leq t_k \leq t_{k+1} \leq \cdots \\ \xi_0 \leq \xi_1 \leq \cdots \leq \xi_k \leq \xi_{k+1} \leq \cdots \end{aligned} \tag{3.16}$$

in order to avoid the message rejection (message disordering). In this work, only a weaker assumption given in the sequel is needed.

Assumption 8. *The sequence $\{\xi_k\}_{k\in\mathbb{N}}$ is no longer required to be increasing, only $\{t_k\}_{k\in\mathbb{N}}$ is supposed to be increasing.*

Assumption 8 can also be ensured by (3.14) and (3.15). This assumption shows that the proposed method deals with the message rejection in the sensor-to-controller channel.

3.2.2 Controller-to-actuator constant delay case

The aim of this subsection is to introduce the discrete predictor-based controller (Cloosterman et al. 2009; Léchappé, Moulay, Plestan, and Han 2019) and the proposed control techniques by using a simple example, *i.e.* there is no delay uncertainty in the controller-to-actuator channel, then the controller-to-actuator delay is constant and the state-translation (Åström and Wittenmark 2013, Chapter 2.3) between $x(s_k)$ and $x(s_{k+1})$ reads as

$$x(s_{k+1}) = e^{A\Delta}x(s_k) + \int_{s_k}^{t_{k-N_2+1}} e^{A(s_{k+1}-\theta)}\mathrm{d}\theta B u_{k-N_2} + \int_{t_{k-N_2+1}}^{s_{k+1}} e^{A(s_{k+1}-\theta)}\mathrm{d}\theta B u_{k-N_2+1} \tag{3.17}$$

with N_2 defined in (3.14). By using Assumption 7, (3.17) can be equally considered as the following discrete-time system:

$$x(s_{k+1}) = \bar{A}x(s_k) + \bar{B}_1 u_{k-N_2+1} + \bar{B}_2 u_{k-N_2}. \tag{3.18}$$

Assumption 7 ensures that the discrete-time system (3.18) is controllable (Ionete et al. 2008, Theorem 1). Define the extended state $z_k = \begin{bmatrix} x^T(s_k) & u_k^T & \cdots & u_{k-N_2+1}^T & u_{k-N_2}^T & \cdots & u_{k-N_1-N_2-1}^T \end{bmatrix}^T$

and using (3.18), it leads to

$$z_{k+1} = \underbrace{\begin{bmatrix} \bar{A} & 0 & \cdots & \bar{B}_1 & \bar{B}_2 & \cdots & 0 \\ 0 & 0 & \cdots & 0 & 0 & \cdots & 0 \\ 0 & I_{m\times m} & \cdots & 0 & 0 & \cdots & 0 \\ \vdots & \ddots & \ddots & \ddots & \ddots & \ddots & \vdots \\ 0 & 0 & \cdots & I_{m\times m} & 0 & \cdots & 0 \\ \vdots & \ddots & \ddots & \ddots & \ddots & \ddots & \vdots \\ 0 & 0 & \cdots & \cdots & 0 & I_{m\times m} & 0 \end{bmatrix}}_{\mathcal{A}} z_k + \underbrace{\begin{bmatrix} 0 \\ I_{m\times m} \\ 0 \\ \vdots \\ \vdots \\ \vdots \\ 0 \end{bmatrix}}_{\mathcal{B}} u_{k+1}. \tag{3.19}$$

The controllability of (3.18) and (3.19) is equivalent since they are two different descriptions of the same system, see (Léchappé, Moulay, Plestan, and Han 2019, Remark 5). Therefore, it is possible to find a state feedback control

$$u_{k+1} = \mathcal{K} z_k \tag{3.20}$$

that makes the matrix $\mathcal{A} + \mathcal{B}\mathcal{K}$ Hurwitz. Moreover, for all $\epsilon > 0$, there exists a symmetric positive definite matrix P with appropriate dimension such that

$$(\mathcal{A} + \mathcal{B}\mathcal{K})^T P(\mathcal{A} + \mathcal{B}\mathcal{K}) - P = -\epsilon I. \tag{3.21}$$

To calculate the control law (3.20) at instant $t = s_{k+1}$, one needs the knowledge of $x(s_k)$ which may not arrive at the controller before $t = s_{k+1}$. To overcome this problem, one can use the newest state measurement $x(s_{k-d})$ (with $1 \leq d \leq N_1$) and the control history to predict the state $x(s_k)$ by iterating (3.18) for d times:

$$\begin{cases} \hat{x}(s_{k-d+1}) = \bar{A}x(s_{k-d}) + \bar{B}_1 u_{k-N_2-d+1} + \bar{B}_2 u_{k-N_2-d}, \\ \hat{x}(s_{k-d+2}) = \bar{A}\hat{x}(s_{k-d+1}) + \bar{B}_1 u_{k-N_2-d+2} + \bar{B}_2 u_{k-N_2-d+1}, \\ \quad \vdots \qquad\qquad\qquad\qquad \vdots \\ \hat{x}(s_{k-1}) = \bar{A}\hat{x}(s_{k-2}) + \bar{B}_1 u_{k-N_2-1} + \bar{B}_2 u_{k-N_2-2}, \\ \hat{x}(s_k) = \bar{A}\hat{x}(s_{k-1}) + \bar{B}_1 u_{k-N_2} + \bar{B}_2 u_{k-N_2-1}. \end{cases}$$

The above equations give the state estimation $\hat{x}(s_k)$ as follows:

$$\hat{x}(s_k) = \bar{A}^d x(s_{k-d}) + \bar{A}^{d-1}\bar{B}_2 u_{k-N_2-d} + \bar{B}_1 u_{k-N_2} + \sum_{i=1}^{d-1} (\bar{A}^i \bar{B}_1 + \bar{A}^{i-1}\bar{B}_2) u_{k-N_2-i}. \tag{3.22}$$

Remark 7. *Since the controller-to-actuator delay is constant, then* (3.22) *is a perfect prediction such that* $\hat{x}(s_k) = x(s_k)$*. If the controller-to-actuator delay is uncertain, then there exists an esti-*

mation error $e(s_k) = x(s_k) - \hat{x}(s_k)$*. The effect of the estimation error will be analyzed in subsection 3.2.3.*

Finally, the control law can be calculated by using the state feedback control (3.20) and the state prediction (3.22).

The state estimation technique (3.22) is able to deal with the message rejection(Cloosterman et al. 2009, p.1576) (packet reordering (J. Li, Q. Zhang, and Cai 2009, p.1775)) in the sensor-to-controller network. In the communication channel, if an older data packet arrives at the destination after a newer data packet, then this older data packet is discarded in order to ensure that the newest data is processed. This effect is presented in Figure 3.4, the measurements $x(s_k)$ and $x(s_{k+1})$ are neglected due to the message rejection since they arrive at the controller after the measurement $x(s_{k+2})$.

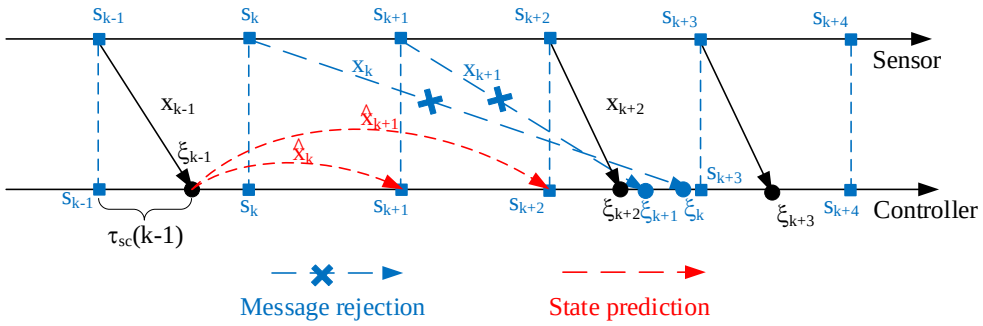

Figure 3.4 – Timing diagram of the sensor-to-controller channel with message rejections.

Lemma 5. *At least one measurement* $x(s_{k-d})$ *with* $1 \leq d \leq N_1$ *is available for the controller at* $t = s_k$*.*

Proof. Firstly, because the sensor-to-controller delay is upper bounded by $N_1\Delta$, then the measurement $x(s_{k-N_1})$ must arrive at the controller before $t = s_k$ since

$$\xi_{k-N_1} = s_{k-N_1} + \tau_{sc}(k - N_1) \leq s_{k-N_1} + N_1\Delta \leq s_k. \tag{3.23}$$

Secondly, if the measurement $x(s_{k-N_1})$ is not discarded, then Lemma 5 is proven with $d = N_1$. Thirdly, if $x(s_{k-N_1})$ is rejected, then there must exist an integer $1 \leq d < N_1$ such that $x(s_{k-d})$ successfully arrives at the controller and its arriving time ξ_{k-d} is earlier than the arriving time of $x(s_{k-N_1})$ such that

$$\xi_{k-d} \leq \xi_{k-N_1} \leq s_k. \tag{3.24}$$

Thus, $x(s_{k-d})$ is available for the controller at $t = s_k$ and this ends the proof. □

Lemma 5 ensures that the maximum value of d in (3.22) is N_1.

3.2.3 Controller-to-actuator uncertain constant delay case

In this subsection, one develops the technique given in subsection 3.2.2, and takes into account the delay uncertainty in the controller-to-actuator channel. Consider (3.14) and (3.15), the controller-to-actuator delay satisfies

$$(N_2 - 1)\Delta \leq \tau_{ca}(k) \leq (N_2 + 1)\Delta. \tag{3.25}$$

Figure 3.5 shows a timing diagram of the controller-to-actuator uncertain delay case with $N_2 = 2$.

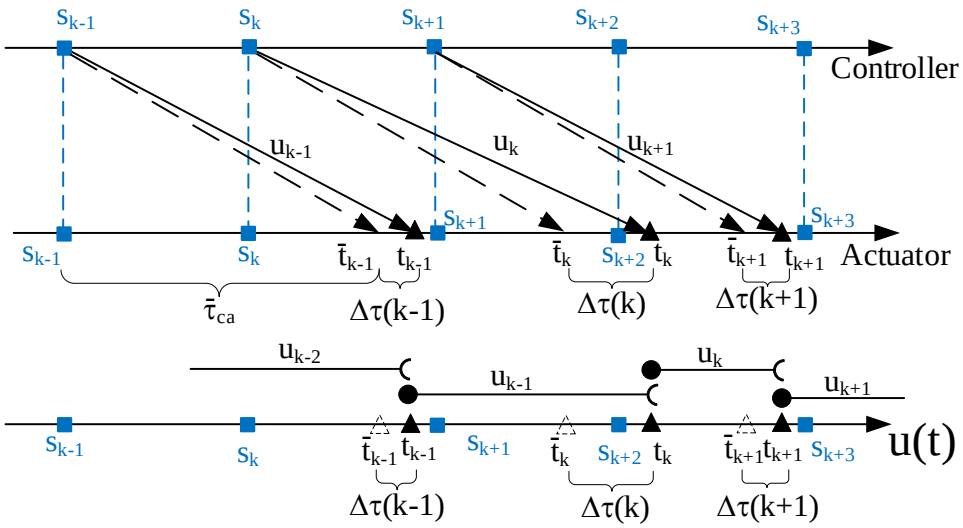

Figure 3.5 – Timing diagram of the controller-to-actuator channel with uncertain delays.

Let $\{\bar{t}_k\}_{k\in\mathbb{N}}$ be the expected arriving times of each control input (without delay uncertainties) such that

$$\bar{t}_k = s_k + \bar{\tau}_{ca}, \tag{3.26}$$

and the sequence $\{t_k\}_{k\in\mathbb{N}}$ is the true arriving times of each control input such that

$$t_k = s_k + \tau_{ca}(k) = \bar{t}_k + \Delta\tau(k). \tag{3.27}$$

Comparing (3.14) and (3.25), two cases must be considered.
Case 1:

$$(N_2 - 1)\Delta \leq \bar{\tau}_{ca} \leq \tau_{ca}(k) \leq N_2\Delta. \tag{3.28}$$

In this case, the delay uncertainty $\Delta\tau(k)$ is smaller than $N_2\Delta - \bar{\tau}_{ca}$, and it implies that

$$s_k \leq \bar{t}_{k-N_2+1} \leq t_{k-N_2+1} \leq s_{k+1}. \tag{3.29}$$

In Figure 3.5, the control input u_{k-1} illustrates this case. The state-translation equation between $x(s_k)$ and $x(s_{k+1})$ reads as

$$\begin{aligned} x(s_{k+1}) =& e^{A\Delta}x(s_k) + \int_{s_k}^{\bar{t}_{k-N_2+1}} e^{A(s_{k+1}-\theta)}\mathrm{d}\theta B u_{k-N_2} + \int_{\bar{t}_{k-N_2+1}}^{t_{k-N_2+1}} e^{A(s_{k+1}-\theta)}\mathrm{d}\theta B u_{k-N_2} \\ &+ \int_{t_{k-N_2+1}}^{s_{k+1}} e^{A(s_{k+1}-\theta)}\mathrm{d}\theta B u_{k-N_2+1} \end{aligned} \tag{3.30}$$

By using Assumption 7, one has $\bar{B}_1 = \int_{\bar{t}_{k-N_2+1}}^{s_{k+1}} e^{A(s_{k+1}-\theta)}\mathrm{d}\theta B$ and $\bar{B}_2 = \int_{s_k}^{\bar{t}_{k-N_2+1}} e^{A(s_{k+1}-\theta)}\mathrm{d}\theta B$. Let $\Delta\bar{B}_1(k-N_2+1) = \int_{\bar{t}_{k-N_2+1}}^{t_{k-N_2+1}} e^{A(s_{k+1}-\theta)}\mathrm{d}\theta B$, then (3.30) equals to

$$x(s_{k+1}) = \bar{A}x(s_k) + [\bar{B}_1 - \Delta\bar{B}_1(k-N_2+1)]u_{k-N_2+1} + [\bar{B}_2 + \Delta\bar{B}_1(k-N_2+1)]u_{k-N_2}. \tag{3.31}$$

Case 2:

$$(N_2-1)\Delta \leq \bar{\tau}_{ca} \leq N_2\Delta \leq \tau_{ca}(k). \tag{3.32}$$

This case shows that the delay uncertainty $\Delta\tau(k)$ is larger than $N_2\Delta - \bar{\tau}_{ca}$, and it leads to

$$s_k \leq \bar{t}_{k-N_2+1} \leq s_{k+1} \leq t_{k-N_2+1}. \tag{3.33}$$

The control input u_k in Figure 3.5 describes this case. The state-translation equation between $x(s_{k+1})$ and $x(s_{k+2})$ is given by

$$x(s_{k+2}) = \bar{A}x(s_{k+1}) + [\bar{B}_1 - \bar{B}_1]u_{k-N_2+2} + [\bar{B}_2 + \bar{B}_1]u_{k-N_2+1}. \tag{3.34}$$

Indeed, if this case occurs, the delay uncertainty $\Delta\tau(k)$ also influences the next sampling period. See Figure 3.5, the control input u_{k-1} is also applied to the plant on interval $[s_{k+2}, t_k) \subset [s_{k+2}, s_{k+3}]$ yields

$$\begin{aligned} x(s_{k+3}) =& \bar{A}x(s_{k+2}) + [\bar{B}_1 - \Delta\bar{B}_1(k-N_2+3)]u_{k-N_2+3} + \Delta\bar{B}_2(k-N_2+2)u_{k-N_2+1} \\ &+ [\bar{B}_2 + \Delta\bar{B}_1(k-N_2+3) - \Delta\bar{B}_2(k-N_2+2)]u_{k-N_2+2} \end{aligned} \tag{3.35}$$

with $\Delta\bar{B}_2(k-N_2+2)=\int_{s_{k+2}}^{t_k} e^{A(s_{k+3}-\theta)}\mathrm{d}\theta B$. For both *Case 1* and *2* one defines

$$\Delta\bar{B}_1(k)=\begin{cases}\bar{B}_1, & \Delta\tau(k)\geq N_2\Delta-\bar{\tau}_{ca},\\ \int_{\bar{\tau}_{ca}-(N_2-1)\Delta}^{\bar{\tau}_{ca}-(N_2-1)\Delta+\Delta\tau(k)} e^{A(\Delta-\theta)}\mathrm{d}\theta B, & \Delta\tau(k)<N_2\Delta-\bar{\tau}_{ca},\end{cases} \tag{3.36}$$

and

$$\Delta\bar{B}_2(k)=\begin{cases}\int_0^{\bar{\tau}_{ca}+\Delta\tau(k)-N_2\Delta} e^{A(\Delta-\theta)}\mathrm{d}\theta B, & \Delta\tau(k)\geq N_2\Delta-\bar{\tau}_{ca},\\ 0, & \Delta\tau(k)<N_2\Delta-\bar{\tau}_{ca}.\end{cases} \tag{3.37}$$

Thus, the following state-translation equation describes all the cases mentioned above:

$$\begin{aligned}x(s_{k+1})=&\bar{A}x(s_k)+[\bar{B}_1-\Delta\bar{B}_1(k-N_2+1)]u_{k-N_2+1}+\Delta\bar{B}_2(k-N_2)u_{k-N_2-1}\\&+[\bar{B}_2+\Delta\bar{B}_1(k-N_2+1)-\Delta\bar{B}_2(k-N_2)]u_{k-N_2}.\end{aligned} \tag{3.38}$$

Remark 8. *If there is no delay uncertainty in the controller-to-actuator channel, then the matrices* $\Delta\bar{B}_1(k-N_2+1)$, $\Delta\bar{B}_2(k-N_2)$ *given in* (3.38) *are zero, and* (3.38) *is equivalent to* (3.18).

Lemma 6. *If the delay uncertainty satisfies* $0\leq\Delta\tau(k)\leq\mu\leq\Delta$ *for all* $k\in\mathbb{N}$*, then the Euclidean norm of the matrices* $\Delta\bar{B}_1(k)$, $\Delta\bar{B}_2(k)$ *satisfies*

$$\|\Delta\bar{B}_1(k)\|\leq\mu e^{\|A\|\Delta}\|B\|,\quad \|\Delta\bar{B}_2(k)\|\leq\mu e^{\|A\|\Delta}\|B\| \tag{3.39}$$

for all $k\in\mathbb{N}$.

Proof. Suppose that $\Delta\tau(k)\geq N_2\Delta-\bar{\tau}_{ca}$ holds, then one has

$$\Delta\bar{B}_1(k)=\bar{B}_1=\int_{\bar{\tau}_{ca}-(N_2-1)\Delta}^{\Delta} e^{A(\Delta-\theta)}\mathrm{d}\theta B. \tag{3.40}$$

Using the triangle inequality for integrals, (3.40) leads to

$$\begin{aligned}\|\Delta\bar{B}_1(k)\|&\leq\int_{\bar{\tau}_{ca}-(N_2-1)\Delta}^{\Delta}\|e^{A(\Delta-\theta)}\|\mathrm{d}\theta\|B\|\leq\int_{\bar{\tau}_{ca}-(N_2-1)\Delta}^{\Delta} e^{\|A\|\Delta}\mathrm{d}\theta\|B\|\\&\leq[\Delta-\bar{\tau}_{ca}+(N_2-1)\Delta]e^{\|A\|\Delta}\|B\|\leq\mu e^{\|A\|\Delta}\|B\|.\end{aligned} \tag{3.41}$$

Similarly, $\|\Delta\bar{B}_2(k)\|\leq\mu e^{\|A\|\Delta}\|B\|$ is proven by using the same inequality (3.41) and the fact that $\bar{\tau}_{ca}+\Delta\tau(k)-N_2\Delta\leq\Delta\tau(k)$.
Now, consider the case $\Delta\tau(k)<N_2\Delta-\bar{\tau}_{ca}$, one can prove that $\|\Delta\bar{B}_1(k)\|\leq\mu e^{\|A\|\Delta}\|B\|$ by the same way as (3.41) and one has $\|\Delta\bar{B}_2(k)\|=0$. This ends the proof. □

Similar to subsection 3.2.2, one uses the state prediction (3.22) to predict the state when the expected measurement did not arrive. However, one cannot perfectly calculate the system state

$x(s_k)$ due to the delay uncertainty, only a state estimation $\hat{x}(s_k)$ is available at $t = s_k$. Assuming that $x(s_{k-d})$ is available, then one can calculate the state prediction errors as follows:

1. firstly, the true state-translation equation (3.38) between $x(s_{k-d})$ and $x(s_{k-d+1})$ reads as

$$\begin{aligned} x(s_{k-d+1}) &= \bar{A}x(s_{k-d}) + \Delta\bar{B}_2(k-d-N_2)u_{k-d-N_2-1} + [\bar{B}_1 - \Delta\bar{B}_1(k-d-N_2+1)]u_{k-d-N_2+1} \\ &\quad + [\bar{B}_2 + \Delta\bar{B}_1(k-d-N_2+1) - \Delta\bar{B}_2(k-d-N_2)]u_{k-d-N_2} \end{aligned} \tag{3.42}$$

and the state prediction is calculated as

$$\hat{x}(s_{k-d+1}) = \bar{A}x(s_{k-d}) + \bar{B}_1 u_{k-d-N_2+1} + \bar{B}_2 u_{k-d-N_2}. \tag{3.43}$$

Taking the difference between (3.42) and (3.43), the prediction error is

$$\begin{aligned} e(s_{k-d+1}) &= x(s_{k-d+1}) - \hat{x}(s_{k-d+1}) \\ &= \Delta\bar{B}_1(k-d-N_2+1)(u_{k-d-N_2} - u_{k-d-N_2+1}) \\ &\qquad + \Delta\bar{B}_2(k-d-N_2)(u_{k-d-N_2-1} - u_{k-d-N_2}). \end{aligned} \tag{3.44}$$

2. Secondly, one considers the estimation error $e(s_{k-d+2})$ in a similar way, but one assumes that $x(k-d+1)$ is still not received by the controller, so the state prediction reads as

$$\hat{x}(s_{k-d+2}) = \bar{A}\hat{x}(s_{k-d+1}) + \bar{B}_1 u_{k-d-N_2+2} + \bar{B}_2 u_{k-d-N_2+1}. \tag{3.45}$$

Then, consider the true state-translation equation (3.38) between $x(s_{k-d+1})$ and $x(s_{k-d+2})$ as follows:

$$\begin{aligned} x(s_{k-d+2}) &= \bar{A}x(s_{k-d+1}) + [\bar{B}_1 - \Delta\bar{B}_1(k-d-N_2+2)]u_{k-d-N_2+2} \\ &\quad + [\bar{B}_2 + \Delta\bar{B}_1(k-d-N_2+2) - \Delta\bar{B}_2(k-d-N_2+1)]u_{k-d-N_2+1} \\ &\quad + \Delta\bar{B}_2(k-d-N_2+1)u_{k-d-N_2}. \end{aligned} \tag{3.46}$$

Taking the difference between (3.46) and (3.45), one can calculate the estimation error as follows:

$$\begin{aligned} e(s_{k-d+2}) &= \bar{A}e(s_{k-d+1}) + \Delta\bar{B}_2(k-d-N_2+1)(u_{k-d-N_2} - u_{k-d-N_2+1}) \\ &\qquad + \Delta\bar{B}_1(k-d-N_2+2)(u_{k-d-N_2+1} - u_{k-d-N_2+2}). \end{aligned} \tag{3.47}$$

3. Recursively, the estimation error at $t = s_k$ reads as

$$\begin{aligned} e(s_k) = {} & \bar{A}^{d-1}\Delta\bar{B}_1(k-d-N_2+1)(u_{k-d-N_2} - u_{k-d-N_2+1}) \\ & + \bar{A}^{d-1}\Delta\bar{B}_2(k-d-N_2)(u_{k-d-N_2-1} - u_{k-d-N_2}) \\ & + \bar{A}^{d-2}\Delta\bar{B}_1(k-d-N_2+2)(u_{k-d-N_2+1} - u_{k-d-N_2+2}) \\ & + \bar{A}^{d-2}\Delta\bar{B}_2(k-d-N_2+1)(u_{k-d-N_2} - u_{k-d-N_2+1}) \\ & + \cdots \\ & + \Delta\bar{B}_1(k-N_2)(u_{k-N_2-1} - u_{k-N_2}) \\ & + \Delta\bar{B}_2(k-N_2-1)(u_{k-N_2-2} - u_{k-N_2-1}). \end{aligned} \tag{3.48}$$

Finally, the control law u_{k+1} is calculated by

$$u_{k+1} = \mathcal{K}\hat{z}_k \tag{3.49}$$

with $\hat{z}_k = \begin{bmatrix} \hat{x}^T(s_k) & u_k^T & u_{k-1}^T & \cdots & u_{k-N_1-N_2}^T & u_{k-N_1-N_2-1}^T \end{bmatrix}^T$.

Remark 9. *Remind that,* (3.49) *deals with the case* $1 \leq d \leq N_1$*. If* $d = 0$ *holds, it implies that the state measurement* $x(s_k)$ *is available at instant* $t = s_{k+1}$*, then there is no need to use the state prediction* (3.22)*. In such case, one can directly set* $\hat{x}(s_k) = x(s_k)$*, and the control law* (3.49) *is equivalent to* (3.20)*.*

Lemma 7. *The Euclidean norm of a class of block matrices*

$$\Gamma = \begin{bmatrix} 0 & 0 & \cdots & 0 & -B & B & 0 & \cdots & 0 \\ 0 & 0 & \cdots & 0 & 0 & 0 & 0 & \cdots & 0 \\ \vdots & \vdots & \ddots & \vdots & \vdots & \vdots & \vdots & \ddots & \vdots \\ 0 & 0 & \cdots & 0 & 0 & 0 & 0 & \cdots & 0 \end{bmatrix} \tag{3.50}$$

satisfies that

$$\|\Gamma\| \leq \sqrt{2}\|B\|. \tag{3.51}$$

Proof. The 2-norm of Γ is the induced norm (Meyer 2000, p.281) such that

$$\|\Gamma\| = \sup\{\|\Gamma x\| : \|x\| = 1\} \tag{3.52}$$

where x is a vector with appropriate dimension. One assumes that

$$\bar{x} = \begin{bmatrix} x_1^T & \cdots & x_j^T & x_{j+1}^T & \cdots & x_r^T \end{bmatrix}^T \tag{3.53}$$

satisfies $\|\bar{x}\| = 1$ and the fact

$$\|\Gamma\| = \sup\{\|\Gamma x\| : \|x\| = 1\} = \|\Gamma\bar{x}\|, \tag{3.54}$$

then one has

$$\|\Gamma\| = \left\| \begin{bmatrix} (-Bx_j + Bx_{j+1})^T & 0 & \cdots & 0 \end{bmatrix}^T \right\| = \| - Bx_j + Bx_{j+1}\|. \tag{3.55}$$

Using the triangle inequality, (3.55) is upper bounded as

$$\|\Gamma\| \leq \|B\|(\|x_j\| + \|x_{j+1}\|). \tag{3.56}$$

Remind that, by virtue of the definition of the Euclidean vector norm (Meyer 2000, p.270), one has

$$(\|x_j\| + \|x_{j+1}\|)^2 \leq 2\|x_j\|^2 + 2\|x_{j+1}\|^2 \leq 2\sum_{i=1}^{i=r} \|x_i\|^2 = 2. \tag{3.57}$$

Finally, (3.56) and (3.57) imply (3.51) which ends the proof. □

Next, the bound on the state prediction error (3.48) is analyzed with the help of Lemmas 6-7.

Lemma 8. *Consider the extended states*

$$z_k = \begin{bmatrix} x^T(s_k) & u_k^T & \cdots & u_{k-N_2+1}^T & u_{k-N_2}^T & \cdots & u_{k-N_1-N_2-1}^T \end{bmatrix}^T \tag{3.58}$$

and

$$\hat{z}_k = \begin{bmatrix} \hat{x}^T(s_k) & u_k^T & \cdots & u_{k-N_2+1}^T & u_{k-N_2}^T & \cdots & u_{k-N_1-N_2-1}^T \end{bmatrix}^T, \tag{3.59}$$

there exists a constant $\Theta > 0$ such that the extended error $e(z_k) = z_k - \hat{z}_k$ is upper bounded as follows:

$$\|e(z_k)\| \leq \Theta\mu\|z_k\| \tag{3.60}$$

with μ defined in Lemma 6.

Proof. Firstly, if $d = 0$, then the estimation error is zero according to Remark 9, and (3.60) holds with arbitrary $\Theta > 0$. Then one moves on to the case $1 \leq d \leq N_1$, Lemma 5 ensures that the maximum value of d in (3.48) is N_1, then all of the control inputs mentioned in the right-hand side of (3.48) are contained in (3.58) and (3.59).
Secondly, the error between z_k and $\hat{z}_k$ reads as

$$e(z_k) = \begin{bmatrix} e^T(s_k) & 0^T & \cdots & 0^T \end{bmatrix}^T. \tag{3.61}$$

Consider the last term of (3.48) (the matrix $\Delta\bar{B}_2(k - N_2 - 1)$ is written as $\Delta\bar{B}_2$ due to the space

limitation) and the extended error (3.61), it leads to

$$\begin{bmatrix}\begin{bmatrix}\Delta\bar{B}_2(u_{k-N_2-2}-u_{k-N_2-1})\end{bmatrix}\\ 0\\ \vdots\\ 0\end{bmatrix}=\begin{bmatrix}0&\cdots&0&-\Delta\bar{B}_2&\Delta\bar{B}_2&0&\cdots&0\\ 0&\cdots&0&0&0&0&\cdots&0\\ \vdots&\ddots&\vdots&\vdots&\vdots&\vdots&\ddots&\vdots\\ 0&\cdots&0&0&0&0&\cdots&0\end{bmatrix}z_k. \tag{3.62}$$

Taking the norm of (3.62) and applying Lemmas 6-7 yields

$$\left\|\begin{bmatrix}\Delta\bar{B}_2(u_{k-N_2-2}-u_{k-N_2-1})\\ 0\\ \vdots\\ 0\end{bmatrix}\right\|\leq\sqrt{2}\|\Delta\bar{B}_2(k-N_2-1)\|\|z_k\|\leq\sqrt{2}\mu e^{\|A\|\Delta}\|B\|\|z_k\|. \tag{3.63}$$

Repeating the calculations (3.62)-(3.63) for all of the terms appeared in the right-hand side of (3.48), then taking the sum of them, it leads to

$$\|e(z_k)\|\leq 2\sqrt{2}\left(\sum_{i=0}^{i=d-1}\|\bar{A}\|^i\right)\mu e^{\|A\|\Delta}\|B\|\|z_k\|\leq\begin{cases}2\sqrt{2}\frac{\|\bar{A}\|^d-1}{\|\bar{A}\|-1}\mu e^{\|A\|\Delta}\|B\|\|z_k\|, & \|\bar{A}\|\neq 1\\ 2\sqrt{2}d\mu e^{\|A\|\Delta}\|B\|\|z_k\|, & \|\bar{A}\|=1\end{cases}. \tag{3.64}$$

Finally, by virtue of Lemma 5, one has $d\leq N_1$, then (3.60) is proven with

$$\Theta=\begin{cases}2\sqrt{2}\frac{\|\bar{A}\|^{N_1}-1}{\|\bar{A}\|-1}e^{\|A\|\Delta}\|B\|, & \|\bar{A}\|\neq 1\\ 2\sqrt{2}N_1e^{\|A\|\Delta}\|B\|, & \|\bar{A}\|=1\end{cases}. \tag{3.65}$$

□

3.2.4 Stability analysis

In this subsection, the stability analysis of the closed-loop system is given, it is shown that the exponential stability is obtained if the delay uncertainty $\Delta\tau(k)$ is sufficiently small. The main convergence results of this work are given in the sequel.

Theorem 10. *Consider the system* (3.10) *controlled through a network that is subject to the sensor-to-controller time-varying delay* (3.12) *and the controller-to-actuator uncertain constant delay* (3.13)-(3.14)-(3.15). *The controller is time-driven and the control law is* (3.49). *There exist constants* $\mu^*>0$, $M>0$, $0<\eta<1$ *such that if* $0\leq\Delta\tau(k)\leq\mu\leq\mu^*\leq\Delta$ *for all* $k\in\mathbb{N}$, *then one has*

$$\|x(s_k)\|\leq\|z_k\|\leq M\eta^k\|z_0\|. \tag{3.66}$$

Proof. Firstly, consider the state-translation equation (3.38) and the control law (3.49), it leads to

$$z_{k+1} = (\mathcal{A} + \Delta\mathcal{A}_k)z_k + \mathcal{B}u_{k+1} = (\mathcal{A} + \Delta\mathcal{A}_k)z_k + \mathcal{B}\mathcal{K}\hat{z}_k = (\mathcal{A} + \mathcal{B}\mathcal{K})z_k + \Delta\mathcal{A}_k z_k - \mathcal{B}\mathcal{K}e(z_k) \quad (3.67)$$

with (the indexes of $\Delta\bar{B}_1(k - N_2 + 1)$, $\Delta\bar{B}_2(k - N_2)$ are omitted due to the space limitations)

$$\Delta\mathcal{A}_k = \begin{bmatrix} 0 & \cdots & 0 & -\Delta\bar{B}_1 & \Delta\bar{B}_1 - \Delta\bar{B}_2 & \Delta\bar{B}_2 & 0 & \cdots & 0 \\ 0 & \cdots & 0 & 0 & 0 & 0 & 0 & \cdots & 0 \\ \vdots & \ddots & \vdots & \vdots & \vdots & \vdots & \vdots & \ddots & \vdots \\ 0 & \cdots & 0 & 0 & 0 & 0 & 0 & \cdots & 0 \end{bmatrix}. \quad (3.68)$$

Taking the norm of $\Delta\mathcal{A}_k$ and using twice Lemmas 6-7 gives that

$$\|\Delta\mathcal{A}_k\| \leq \sqrt{2}\left(\|\Delta\bar{B}_1(k - N_2 + 1)\| + \|\Delta\bar{B}_2(k - N_2)\|\right) \leq 2\sqrt{2}e^{\|A\|\Delta}\|B\|\mu. \quad (3.69)$$

Define the Lyapunov function as

$$V_k = z_k^T P z_k \quad (3.70)$$

with P satisfying (3.21). Taking the difference between V_{k+1} and V_k leads to

$$\begin{aligned} \Delta V_k = V_{k+1} - V_k = &- \epsilon z_k^T z_k + z_k^T \Delta\mathcal{A}_k^T P \Delta\mathcal{A}_k z_k + e^T(z_k)\mathcal{K}^T\mathcal{B}^T P\mathcal{B}\mathcal{K}e(z_k) - 2z_k^T\Delta\mathcal{A}_k^T P\mathcal{B}\mathcal{K}e(z_k) \\ &+ 2z_k^T(\mathcal{A} + \mathcal{B}\mathcal{K})^T P\Delta\mathcal{A}_k z_k - 2z_k^T(\mathcal{A} + \mathcal{B}\mathcal{K})^T P\mathcal{B}\mathcal{K}e(z_k). \end{aligned} \quad (3.71)$$

Taking the norm of the right-hand side of (3.71) and using (3.69), (3.60) yields

$$\begin{aligned} \Delta V_k \leq &- \epsilon\|z_k\|^2 + 8e^{2\|A\|\Delta}\|B\|^2\|P\|\mu^2\|z_k\|^2 + \|\mathcal{B}\mathcal{K}\|^2\|P\|\Theta^2\mu^2\|z_k\|^2 \\ &+ 4\sqrt{2}\|\mathcal{A} + \mathcal{B}\mathcal{K}\|e^{\|A\|\Delta}\|B\|\|P\|\mu\|z_k\|^2 + 4\sqrt{2}\|\mathcal{B}\mathcal{K}\|e^{\|A\|\Delta}\|B\|\|P\|\Theta\mu^2\|z_k\|^2 \\ &+ 2\|\mathcal{A} + \mathcal{B}\mathcal{K}\|\|\mathcal{B}\mathcal{K}\|\|P\|\Theta\mu\|z_k\|^2. \end{aligned} \quad (3.72)$$

Define

$$\alpha = (8e^{2\|A\|\Delta}\|B\|^2 + \|\mathcal{B}\mathcal{K}\|^2\Theta^2 + 4\sqrt{2}\|\mathcal{B}\mathcal{K}\|e^{\|A\|\Delta}\|B\|\Theta)\|P\| \quad (3.73)$$

and

$$\beta = (4\sqrt{2}\|\mathcal{A} + \mathcal{B}\mathcal{K}\|e^{\|A\|\Delta}\|B\| + 2\|\mathcal{A} + \mathcal{B}\mathcal{K}\|\|\mathcal{B}\mathcal{K}\|\Theta)\|P\| \quad (3.74)$$

then (3.72) is simplified as

$$\Delta V_k \leq -\left[-\alpha\mu^2 - \beta\mu + \epsilon\right]\|z_k\|^2. \quad (3.75)$$

Given a constant $0 < \gamma \leq \min\{\bar{\lambda}(P), \epsilon\}$, and define

$$\mu^* = \frac{\sqrt{\beta^2 + 4\alpha(\epsilon - \gamma)} - \beta}{2\alpha}, \quad (3.76)$$

note that if $0 \leq \mu \leq \mu^*$, then one has

$$-\alpha\mu^2 - \beta\mu + (\epsilon - \gamma) \geq 0 \tag{3.77}$$

and (3.75) implies that

$$V_{k+1} - V_k = \Delta V_k \leq -\gamma \|z_k\|^2 \leq -\frac{\gamma}{\bar{\lambda}(P)} V_k. \tag{3.78}$$

Since $0 < \gamma \leq \bar{\lambda}(P)$, it follows that $0 \leq 1 - \gamma/\bar{\lambda}(P) \leq 1$. Finally, (3.78) leads to

$$\|x(s_k)\| \leq \|z_k\| \leq \sqrt{\frac{\bar{\lambda}(P)}{\underline{\lambda}(P)}} \left(\sqrt{1 - \frac{\gamma}{\bar{\lambda}(P)}}\right)^k \|z_0\| \tag{3.79}$$

that ends the proof. □

Remark 10. *If $\Delta\tau(k) = 0$, then Theorem 10 implies that the method stabilizes NCS with fast-varying and long $\tau_{sc}(k)$, long Δ and long $\bar{\tau}_{ca}$ by virtue of the extended system representation* (3.19) *and the perfect state prediction* (3.22)*, a similar discussion is given in (Léchappé, Moulay, Plestan, and Han 2019, Section 7.1).*

Theorem 10 provides a discrete-time control scheme for a class of NCSs with long sensor-to-controller time-varying delay and long sampling period, the robustness with respect to the delay uncertainty is also analyzed. The main contributions of Theorem 10 are claimed as follows:

— Theorem 10 provides the explicit upper bound on the allowable delay uncertainty, that is missing in the work of (Lozano et al. 2004).

— The controller design is simpler than the other discrete-time approaches (Hu and Zhu 2003; Cloosterman et al. 2009), neither Belleman equation (Hu and Zhu 2003) nor delay-dependent linear matrix inequality (LMI) (Cloosterman et al. 2009) is required by Theorem 10.

— It deals with long sensor-to-controller time-varying delay, rather than the uncertain constant delay in (Selivanov and Fridman 2016b), and lower sampling rate is allowed, a comparison between the two methods will be given in the next section.

— The message rejection phenomenon is considered in subsections 3.2.2-3.2.3, which is ignored by the continuous-time methods (Selivanov and Fridman 2016b; Du, C. Zhang, et al. 2019), and the discrete-time approaches(Hu and Zhu 2003; Pan, Marquez, and Chen 2006).

3.3 Validations of the control algorithm

In this section, the main theoretical results are illustrated by two simulation examples, they are also validated on a real networked visual servo inverted pendulum system (Zhan, Du, and Fei 2017;

Du, C. Zhang, et al. 2019). The simulation results and the experiments highlights the performances and robustness of Theorem 10.

3.3.1 Simulation results

Two simulation examples are presented in this subsection: the first one is a simple example that illustrates the effectiveness of Theorem 10 in dealing with sensor-to-controller time-varying delays with message rejection; the second simulation is used to show that Theorem 10 can provide longer allowable sampling period than the sampled predictor-based controller (Selivanov and Fridman 2016b).

Numerical example with message rejection

Consider the continuous-time plant

$$\dot{x}(t) = \begin{bmatrix} 0 & 1 \\ -0.5 & 1 \end{bmatrix} x(t) + \begin{bmatrix} 0 \\ 1 \end{bmatrix} u(t) \tag{3.80}$$

controlled through a network. The sampling period is set to $\Delta = 0.8$s, the sensor-to-controller delay is

$$\tau_{sc}(k) = \begin{cases} 0.5\text{s}, & k = 4m, \quad m \in \mathbb{N} \\ 2.0\text{s}, & k = 4m+1, \quad m \in \mathbb{N} \\ 1.0\text{s}, & k = 4m+2, \quad m \in \mathbb{N} \\ 0.7\text{s}, & k = 4m+3, \quad m \in \mathbb{N} \end{cases} \tag{3.81}$$

and the controller-to-actuator delay is chosen as an uncertain constant delay such that $1.55\text{s} \leq \tau_{ca}(k) \leq 1.63\text{s}$. Thus, the controller-to-actuator delay can be modeled as (3.13) with $\bar{\tau}_{ca} = 1.55$s and $\Delta\tau(k) \in [0, 0.08\text{s}]$.

The time-delays have the following properties:

— the sensor-to-controller delay is upper bounded by $N_1\Delta$ with $N_1 = 3$, the nominal controller-to-actuator delay satisfies $(N_2 - 1)\Delta \leq \bar{\tau}_{ca} \leq N_2\Delta$with $N_2 = 2$;

— message rejection is found in the sensor-to-controller channel, the measurements $x(s_{4m+1})$ with $m \in \mathbb{N}$ are discarded;

— the controller-to-actuator delay can be larger or smaller than $N_2\Delta$, namely, both Cases 1 and 2 given in subsection 3.2.3 can occur.

Note that $N_1 = 3$ and $N_2 = 2$, the extended state is then defined as

$$\hat{z}_k = \begin{bmatrix} \hat{x}^T(s_k) & u_k^T & u_{k-1}^T & \cdots & u_{k-6}^T \end{bmatrix}^T \tag{3.82}$$

and the feedback matrix is chosen as

$$\mathcal{K} = \begin{bmatrix} 3.70 & -4.35 & -1.41 & -2.39 & -3.03 & 0 & 0 & 0 & 0 \end{bmatrix} \tag{3.83}$$

that makes the matrix $\mathcal{A} + \mathcal{B}\mathcal{K}$ Schur. The initial conditions are set to $x(0) = \begin{bmatrix} 3 & -5 \end{bmatrix}^T$, and $u_k = 0$ for all $k < 0$.

The simulation results are presented in Figure 3.6, the continuous-time plant is stabilized although

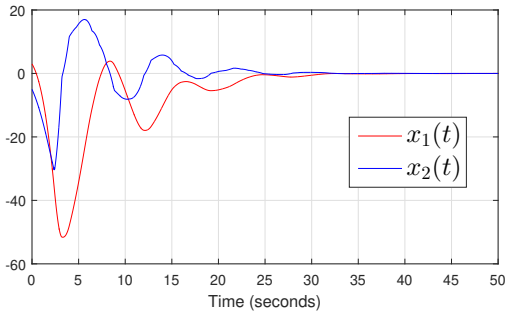

(a) State evolution of system (3.80) under control law (3.82)-(3.83).

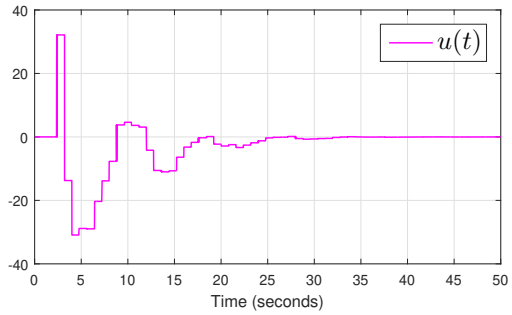

(b) Control signal calculated by the control law (3.82)-(3.83).

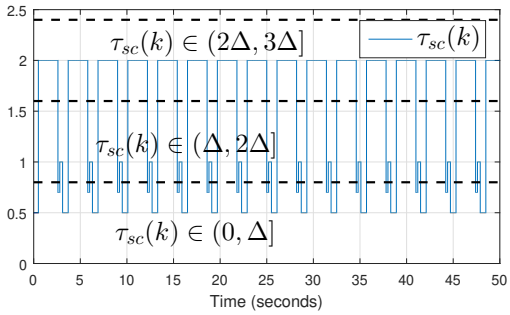

(c) Sensor-to-controller time-varying delay versus time.

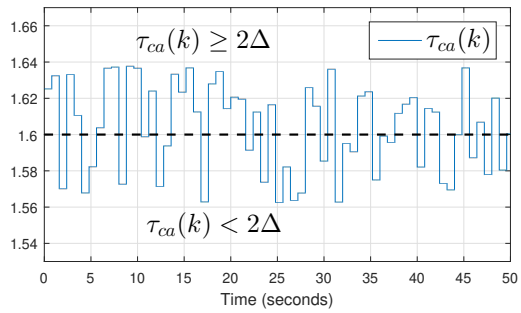

(d) Controller-to-actuator uncertain constant delay versus time.

Figure 3.6 – State evolution, control signal, and network-induced delays versus time for system (3.80).

the sensor-to-controller is fast-varying and the message rejection occurs. Moreover, notice that the system is stabilized with fairly long sampling period $\Delta = 0.8$s, the performances of the discrete-time approach (Léchappé, Moulay, Plestan, and Han 2019; Cloosterman et al. 2009) is also emphasized.

Comparison with the time-delay approach

In this part, the main results of Theorem 10 is compared to the results of (Selivanov and Fridman 2016b) by considering the following system given in (Selivanov and Fridman 2016b, Section 5, eq.

(31)):

$$\dot{x}(t) = \underbrace{\begin{bmatrix} 0 & 1 & 0 & 0 \\ 0 & 0 & -\frac{mg}{M} & 0 \\ 0 & 0 & 0 & 1 \\ 0 & 0 & \frac{g}{l} & 0 \end{bmatrix}}_{A} x(t) + \underbrace{\begin{bmatrix} 0 \\ \frac{1}{M} \\ 0 \\ -\frac{1}{Ml} \end{bmatrix}}_{B} u(t), \tag{3.84}$$

where $M = 10\text{kg}$, $m = 1\text{kg}$, $l = 3\text{m}$, and $g = 10\text{m/s}^2$. Following the parameter definitions given in (Selivanov and Fridman 2016b, Section 5), the sensor-to-controller delay is defined as $\tau_{sc}(k) = \bar{\tau}_{sc} + \Delta\tau_{sc}(k)$ and the controller-to-actuator delay is set to $\tau_{ca}(k) = \bar{\tau}_{ca} + \Delta\tau_{ca}(k)$ where $\bar{\tau}_{sc} = \bar{\tau}_{ca} = 0.2\text{s}$. The uncertainties $\Delta\tau_{sc}(k)$, $\Delta\tau_{ca}(k)$ are bounded by $[0\text{s}, 0.01\text{s}]$, and the initial condition is still set to $x(0) = \begin{bmatrix} 0.98 & 0 & 0.2 & 0 \end{bmatrix}^T$. The control law of (Selivanov and Fridman 2016b, p.106) reads as (3.3)-(3.4) with the feedback gain

$$K = \begin{bmatrix} 2 & 12 & 378 & 210 \end{bmatrix}. \tag{3.85}$$

The control law of Theorem 10 stands on the extended state:

$$\hat{z}_k = \begin{bmatrix} \hat{x}^T(s_k) & u_k^T & u_{k-1}^T & u_{k-2}^T & u_{k-3}^T \end{bmatrix}^T, \tag{3.86}$$

and the feedback matrix $\mathcal{K}$ is calculated such that the eigenvalues of $\mathcal{A} + \mathcal{B}\mathcal{K}$ are placed at

$$\left\{ e^{-0.28\Delta}, e^{-1.5\Delta}, e^{-2.5\Delta}, e^{-6.6\Delta}, e^{-7.5\Delta}, e^{-8.5\Delta}, e^{-9\Delta}, e^{-10\Delta} \right\}.$$

The simulation results are presented in Figure 3.7. Firstly, one sets the sampling period to $\Delta = 0.3\text{s}$: both methods stabilize the system (3.84) with similar overshoot and decay rate (from (Selivanov and Fridman 2016b, Table 1), the theoretical maximum allowable sampling period of (3.3)-(3.4)-(3.85) is $\Delta = 0.0369\text{s}$, but this value is conservative). Secondly, one increases the sampling period to $\Delta = 0.4\text{s}$ in order to see if the stability is preserved. It is shown in Figure 3.7 that the trajectory obtained by the control law derived from (3.3)-(3.4)-(3.85) diverges whereas the closed-loop system controlled by Theorem 10 keeps stable. Moreover, the closed-loop stability is still guaranteed even if the sampling period is $\Delta = 0.6\text{s}$. Thus, by comparing with the continuous-time solution (Selivanov and Fridman 2016b), Theorem 10 is able to stabilize the system (3.84) in the presence of the same uncertain network-induced delays with larger sampling periods.

3.3.2 Experimental validations on the networked visual servo inverted pendulum system

In this subsection, the control algorithm proposed by Theorem 10 is implemented on the networked inverted pendulum visual servo system (NIPVSS) introduced in (Zhan, Du, and Fei 2017;

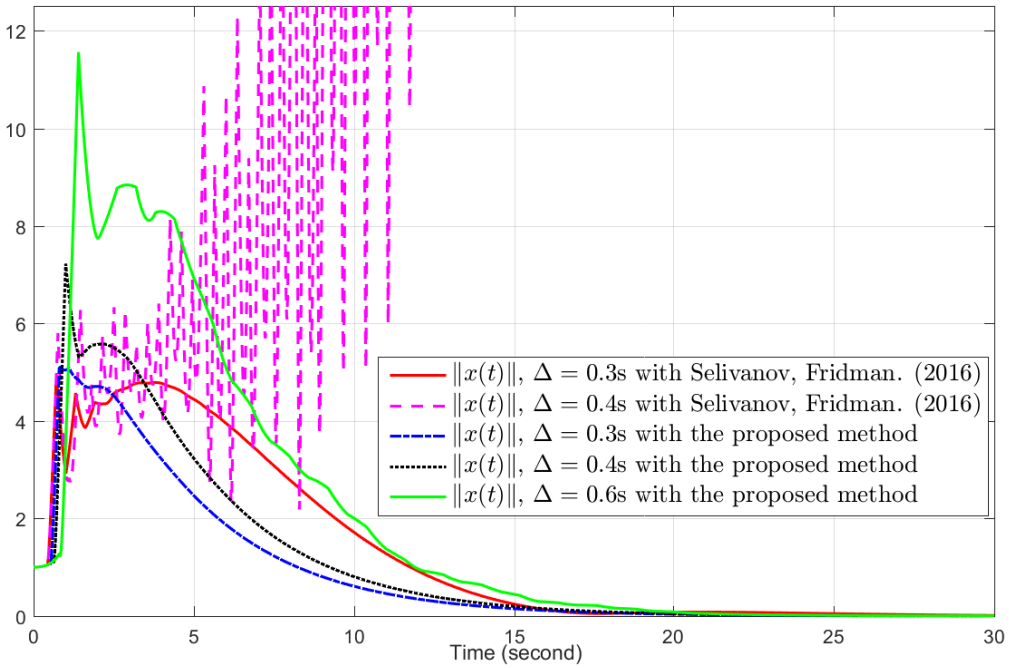

Figure 3.7 – Evolution of the state $\|x(t)\|$ by using the two methods ((Selivanov and Fridman 2016b) and Theorem 10) with different sampling periods.

Du, C. Zhang, et al. 2019), in order to validate that the main results of Theorem 10 can be applied to a real **visual servo system**, as claimed in subsection 3.1.1.

Test bench presentation

In this part, the configuration of the experimental set-up (Zhan, Du, and Fei 2017; Du, C. Zhang, et al. 2019) is introduced. The test bench is firstly composed by an inverted pendulum (see Figure 3.8).

The movement of the inverted pendulum is captured by an *Aca640-120gm* monochrome industrial camera, then the state information $x(t)$ is obtained by the image processing algorithm (based on *Microsoft Visual Studio 2010* and *OpenCV 2.4.11*) on each frame. The computer runs the control algorithm by using the resolved state information, and then sends the control signal to a *GT-400-SV-PCI* movement control card. Finally, a *MSDA023A1A* servo driver receives the control signal and drives the cart to move on the rail.

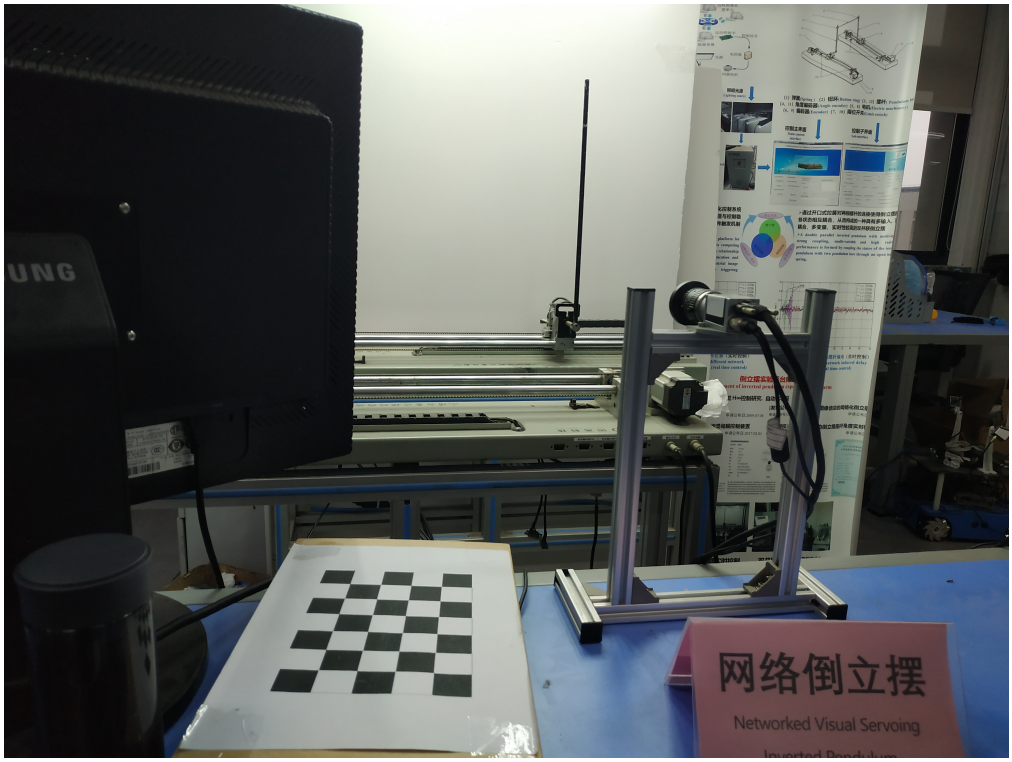

Figure 3.8 – Configuration of the of the NIPVSS test bench (Zhan, Du, and Fei 2017; Du, C. Zhang, et al. 2019).

The controller design is based on the linearized system plant around the straight-up position

$$\dot{x}(t) = \underbrace{\begin{bmatrix} 0 & 0 & 1 & 0 \\ 0 & 0 & 0 & 1 \\ 0 & 0 & 0 & 0 \\ 0 & lmg/J & 0 & 0 \end{bmatrix}}_{A} x(t) + \underbrace{\begin{bmatrix} 0 \\ 0 \\ 1 \\ ml/J \end{bmatrix}}_{B} u(t) \tag{3.87}$$

with $x(t) = col\{\alpha, \theta, \dot{\alpha}, \dot{\theta}\}$. The parameters of (3.87) are given in Table 3.1.

Remind that, the computational time of the image-processing algorithm satisfies that $D(t) \in$ $[15\text{ms}, 16\text{ms}]$, and the max frame rate of the industrial camera is $120Hz$ (*i.e.* the industrial camera can maximumly take 120 photos per second), but the image-processing algorithm cannot follow up with the sampling rate. Indeed, considering the image-processing time $D(t)$, the image-processing algorithm cannot process more than $1/0.015 = 66.67$ frames per second. In the experiment, the sampling period is set to $\Delta = 0.02$s in order to ensure that each frame is captured after the state information resolution of the previous frame is finished.

Table 3.1 – Model parameters of the inverted pendulum (reprint from (Du, C. Zhang, et al. 2019, Table 1)).

g	Gravitational acceleration	9.81m/s^2
m	Mass of the pendulum	0.109kg
J	Moment of inertia of the pendulum	$0.009083\text{kg} \cdot \text{m}^2$
l	Length to pendulum center of mass	0.25m
α	Cart position	m
θ	Pendulum angle	rad

Experiments with connected sensor and actuator

In this part, the first mode of the NIPVSS is considered, such that the controller is directly connected to the sensor and the actuator, then the data transmission delay between them is negligible. The control scheme of this experiment is shown in Figure 3.9.

According to Figure 3.9, the control of NIPVSS can be considered as a NCS with controller-to-actuator delay equals to zero. Furthermore, as stated in the last part, since the computational delay $D(t) \in [15\text{ms}, 16\text{ms}]$ is smaller than the sampling period Δ, the state information $x(s_k)$ is always available for the controller at instant $t = s_{k+1}$, and the state prediction (3.22) is not required. Thus, the state translation between $x(s_k)$ and $x(s_{k+1})$ reads as

$$x(s_{k+1}) = \underbrace{e^{A\Delta}}_{\bar{A}} x(s_k) + \underbrace{\int_{s_k}^{s_{k+1}} e^{A(s_{k+1}-\theta)} \mathrm{d}\theta B}_{\bar{B}} u_k. \tag{3.88}$$

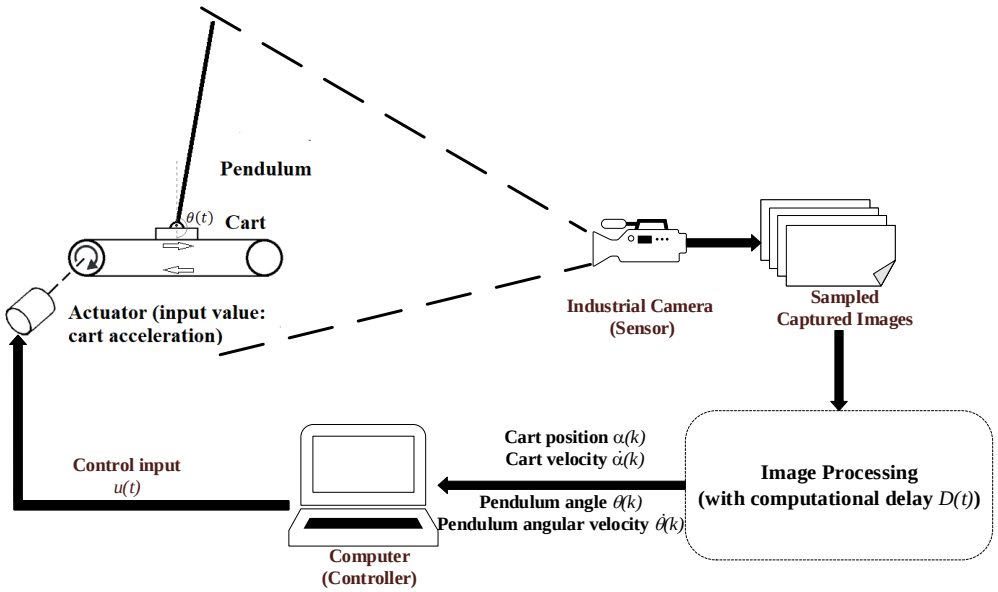

Figure 3.9 – Control diagram of NIPVSS with connected sensor and actuator.

If one defines $z_k = \begin{bmatrix} x^T(s_k) & u_k^T \end{bmatrix}^T$, then one can use the following extended system to calculate the control law u_{k+1}:

$$z_{k+1} = \begin{bmatrix} \bar{A} & \bar{B} \\ 0 & 0 \end{bmatrix} z_k + \begin{bmatrix} 0 \\ I \end{bmatrix} u_{k+1}. \tag{3.89}$$

Finally, the proposed control law is calculated as

$$u_{k+1} = \begin{bmatrix} 0.8817 & -19.0953 & 1.9382 & -3.4132 & 0.3192 \end{bmatrix} z_k \tag{3.90}$$

in order to place the closed-loop poles of (3.89) at $\left\{e^{-0.8\Delta}, e^{-1.5\Delta}, e^{-10\Delta}, e^{-12\Delta}, e^{-13\Delta}\right\}$.
In order to evaluate the control performance of the proposed method, the continuous Linear–Quadratic Regulator (LQR) controller [2]

$$u(t) = \begin{bmatrix} 1 & -25.5765 & 1.7944 & -4.7004 \end{bmatrix} x(t) \tag{3.91}$$

given in (Du, Wangpei Li, et al. 2016, p.439) is used for comparison. Remind that the work of (Du, Wangpei Li, et al. 2016) is based on the same inverted pendulum experimental set-up as Figure 3.8.
The experimental results are presented in Figure 3.10. [3] First, Figure 3.10b shows that the two methods can achieve good control performance on the pendulum angle $\theta(t)$, it stays in a neighborhood around zero (namely, it is almost bounded in $[-0.02\text{rad}, 0.02\text{rad}]$). Second, the experimental

2. The continuous-time controller (3.91) is emulated (Hetel et al. 2017, Section 2.2) to the sampled-data form for the experiment on the NIPVSS.
3. The videos of this experiment are available at `https://box.ec-nantes.fr:443/index.php/s/ALRRBDSCLq4GCM3`.

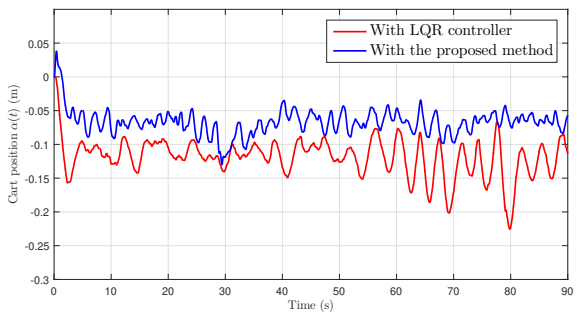

(a) Cart positions of Experiment 1 with controllers (3.90) and (3.91).

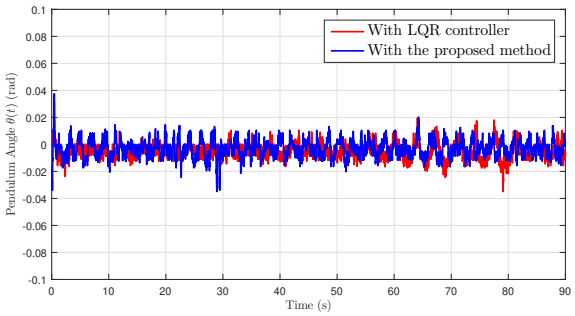

(b) Pendulum angles of Experiment 1 with controllers (3.90) and (3.91).

Figure 3.10 – Experimental results of the NIPVSS with connected sensor and actuator by using the LQR controller (3.91) and the discrete predictor-based controller (3.90).

results displayed in Figure 3.10a show that the cart position $\alpha(t)$ cannot perfectly return to the original position due to the measurement error introduced by the image-processing (Du, C. Zhang, et al. 2019, Remarks 3-4) and the imperfect linearized modeling of (3.87). However, the experimental results still confirm that the proposed method provides a better control performance on the cart position than the LQR controller.

Next, as done in (Du, C. Zhang, et al. 2019, Section V-B), the following indexes are used for the analysis of the experimental results presented in Figure 3.10:

- **MCP**: mean of cart position;
- **SCP**: standard deviation of cart position;
- **MPA**: mean of pendulum angle;
- **SPA**: standard deviation of pendulum angle.

The normalized (with respect to LQR controller) performance indexes of the two controllers are given in Figure 3.11: smaller the value is, better the result is.

See Figure 3.11, the discrete predictor-based controller (3.90) has better MCP, SCP, and MPA than the LQR controller (3.91), and its SPA is slightly worse than the LQR controller. Consequently, based on the analysis given in Figures 3.10 and 3.11, one concludes that the proposed method is able to handle real visual servo control problem with fairly better performance than the LQR controller (3.91).

Experiments with remote sensor and actuator

In this part, the other control mode of the NIPVSS is studied, at this time, the sensor and the actuator are no longer connected to the controller, they communicate with each others via network. The control diagram of this mode is displayed in Figure 3.12.

Consider the control framework formulated in Figure 3.12, the whole NIPVSS is subject to the

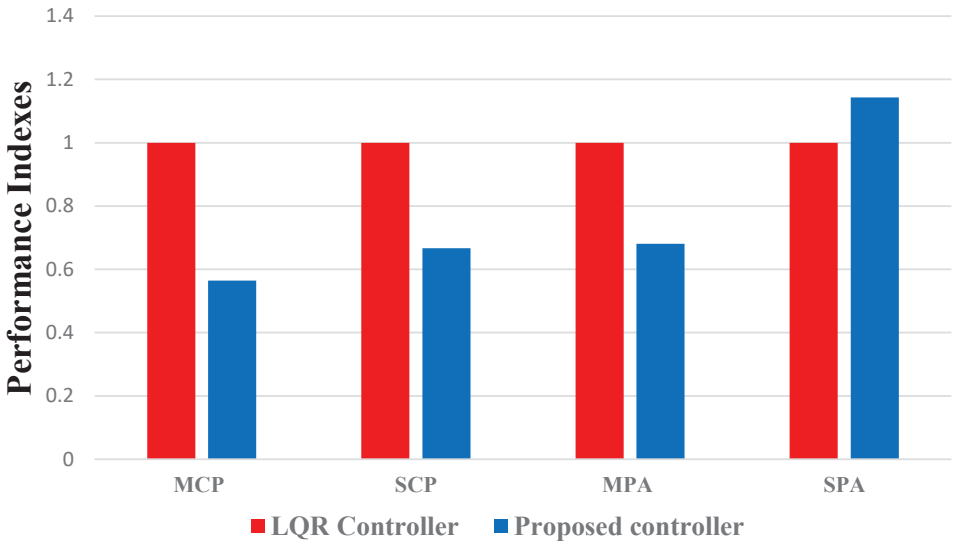

MCP: Mean of Cart Position
SCP: Standard deviation of Cart Position
MPA: Mean of Pendulum Angle
SPA: Standard deviation of Pendulum Angle

Figure 3.11 – Normalized (with respect to LQR controller) performance indexes of the experimental results with connected sensor and actuator.

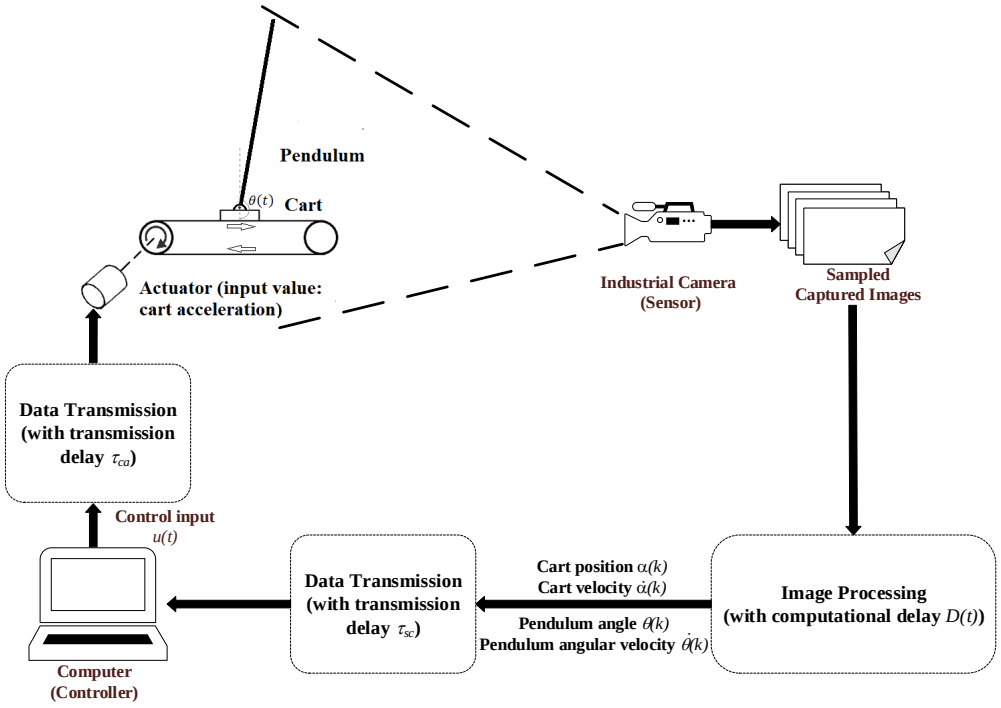

Figure 3.12 – Control diagram of NIPVSS with remote sensor and actuator.

following time-delays

— the computational time $D(t) \in [0.015\text{s}, 0.016\text{s}]$ caused by the image-processing algorithm;
— the sensor-to-controller transmission delay bounded in $(0\text{s}, 0.007\text{s}]$ introduced by the data communication;
— the controller-to-actuator transmission delay bounded in $(0\text{s}, 0.007\text{s}]$ introduced by the data communication.

Thus, the control of NIPVSS with remote sensor and actuator can be modeled as an NCS with the plant (3.87), the sensor-to-controller delay $\tau_{sc}(k) \in (0.015\text{s}, 0.023\text{s}]$ (sum of the computation time and the transmission delay), and the controller-to-actuator delay $\tau_{ca}(k) \in (0\text{s}, 0.007\text{s}]$. Consider the time-delays $\tau_{sc}(k), \tau_{ca}(k)$, the sampling period Δ and the modeling given in (3.12)-(3.14), the parameters $N_1 = 2$, $\bar{\tau}_{ca} = 0\text{s}$, and $N_2 = 1$ are determined.

Remark 11. *According to Lemma 8, one should add u_{k-i}, $i = \{0, 1, 2, 3, 4\}$ into the extended state* (3.59) *since $N_1 = 2$ and $N_2 = 1$. However, it is not necessary to use u_{k-4} since the case* (3.32) *cannot occur in this experiment because*

$$\tau_{ca}(k) \leq 0.007\text{s} < N_2\Delta = \Delta, \quad k \in \mathbb{N}_+. \tag{3.92}$$

By virtue of (3.92)*, u_{k-4} cannot influence the state-translation between $x(s_k)$ and $x(s_{k+1})$, then it is not necessary to be used in the controller design.*

After the above discussions, the following extended state is chosen to build the control law for this experiment:

$$\hat{z}_k = \begin{bmatrix} \hat{x}^T(s_k) & u_k^T & u_{k-1}^T & u_{k-2}^T & u_{k-3}^T \end{bmatrix}^T. \tag{3.93}$$

By placing the closed-loop poles at $\left\{e^{-1.6\Delta}, e^{-1.7\Delta}, e^{-3\Delta}, e^{-19\Delta}, e^{-35\Delta}, e^{-36\Delta}, e^{-37\Delta}, e^{-38\Delta}\right\}$, the proposed control law reads as

$$u_{k+1} = \begin{bmatrix} 0.2959 & -5.5002 & 0.5043 & -1.0435 & 1.4770 & -0.9802 & 0.2888 & -0.0325 \end{bmatrix} \hat{z}_k. \tag{3.94}$$

Similar to the last example, the LQR controller (3.91) is still used for comparison.

The experimental results are presented in Figure 3.13. [4] Compare the results of Figure 3.13b, it is observed that the pendulum angle is maintained in the segment $[-0.04\text{rad}, 0.04\text{rad}]$, which is larger than the oscillation amplitude of Figure 3.10b (around 0.02rad). Next, the control performances on the cart position by the discrete predictor-based controller (3.94) is still better than the LQR controller (3.91) since its trajectories seldom exceed the bound $\alpha(t) = -0.1\text{m}$, but the ones of (3.91) oscillates around $\alpha(t) = -0.15\text{m}$.

Similarly, as done in Figure 3.11, the performance indexes (MCP, SCP, MPA, SPA) of the curves

4. The videos of this experiment are available at `https://box.ec-nantes.fr:443/index.php/s/ak5woHLxbepqQd9`.

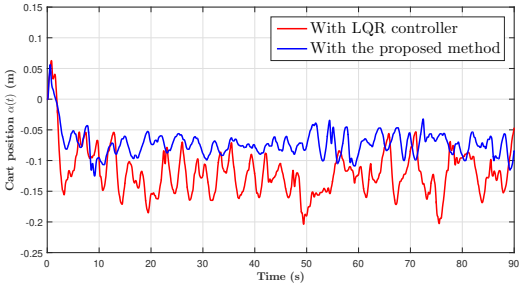

(a) Cart positions $\alpha(t)$ versus time with controllers (3.94) and (3.91).

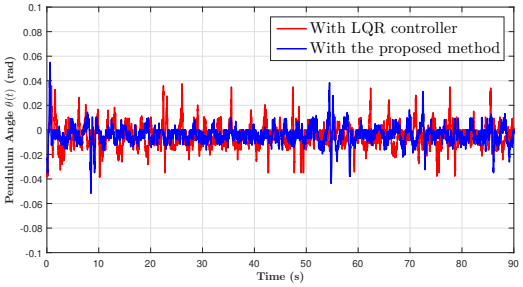

(b) Pendulum angles $\theta(t)$ versus time with controllers (3.94) and (3.91).

Figure 3.13 – Experimental results of the NIPVSS with remote sensor and actuator by using the LQR controller (3.91) and the discrete predictor-based controller (3.94).

displayed in Figure 3.13 are still analysed.

Figure 3.14 highlights the performances of the method of Theorem 10, because all of the performance

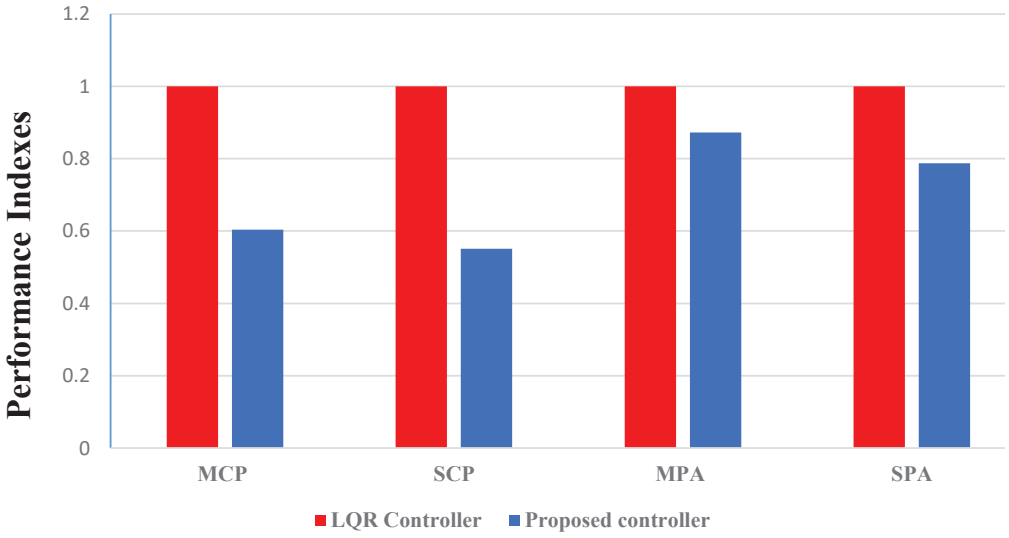

Figure 3.14 – Normalized (with respect to LQR controller) performance indexes of the experimental results with remote sensor and actuator.

indexes of (3.94) are better than the ones of (3.91). Clearly, considering the experimental results of Figures 3.13 and 3.14, Theorem 10 exhibits better control performances than the LQR controller (3.91).

Discussions and conclusions

In subsection 3.3.2, the main results of Theorem 10 are successfully implemented on the NIPVSS experimental set-up displayed in Figure 3.8. The experimental results confirm that the main results of Theorem 10 can be used to handle the **standard visual servo control problem**, and the **networked visual servo control problem**.
Moreover, the proposed discrete predictor-based controller is compared with the LQR controller. In the standard visual servo control case, the method of Theorem 10 is generally better than the LQR controller, only the performance of SPA is slightly worse than the LQR controller. If the NIPVSS is controlled through network, then Theorem 10 is significantly better than the LQR controller, since all of the performance indexes are better. Thus, the comparisons given in subsection 3.3.2 indicate that the main results of Theorem 10 ensure fairly better performances than the non-predictive approaches, like (3.91).
Furthermore, the proposed discrete predictor-based controller has good control performances on such a fast motion control system (*i.e.* inverted pendulum system), which shows that it has wide application prospects in engineering.

CONCLUSION AND FUTURE WORKS

In this thesis, the control techniques are developed for different types of systems (continuous-time systems, networked control systems) with long time-delays. The two major works are listed as follows:

— the delay estimation techniques of constant and time-varying delays;
— the stabilization of the time-delay systems with predictor-based control and the estimated delay value.

The main contributions of this thesis are recalled in the sequel, and the future works are highlighted.

Chapter 1: In Chapter 1, a monotonic delay estimation technique is proposed to estimate the unknown constant delays of LTI systems, this method relies on the concept (see Lemma 1) that the delay estimator cannot exceed the unknown time-delay (with the initial condition smaller than the unknown time-delay). Thus, the delay estimation value can only become closer and closer to the unknown time-delay, and the closed-loop system under predictor-based control law is then stabilized when the delay estimation is sufficiently close to the unknown delay. In subsection 1.2.2, a saturation parameter $\bar{\delta}$ is added to ensure that the dynamic of the delay estimation is always sufficiently small, which simplifies the stability analysis but enlarges the response time. This drawback is handled in sections 1.2.3 with the use of a normalized term and the parameter $\bar{\delta}$ is non longer required. In subsection 1.2.4, the main results of subsection 1.2.3 are modified, and the exponential stability is ensured. Finally, the results of subsection 1.2.2 are extended to the output-feedback case in section 1.2.5. Moreover, since the proposed delay estimation technique uses the control history to estimate the time-delay, then it is robust with respect to the model uncertainties, this property is illustrated by the simulation results. Remind that, although the theoretical results of sections 1.2.2-1.2.5 have constraints on the initial condition of the delay estimator, the simulation results show that the constraints are not restrictive in practice. In the future, the PDE transformations will be adopted to further analyze the relation between the stability and this initial condition. Moreover, the practical stability of the proposed method under external disturbances will be studied as well.

Chapter 2: In Chapter 2, practical delay estimation techniques are developed to assist the control of RCS with time-varying input and output delays. As shown in Figure 2.1, the delay estimation algorithm is based on a specific communication loop (*i.e.* an external signal) that is isolated from the control loop, and the properties of the system (*e.g.* linearity, delay identifiability) are not required.

The conventional sliding mode technique is involved to ensure the finite time estimation of the round-trip delay, and the estimation performances are improved with the super-twisting algorithm, and finally the adaptive super-twisting algorithm is adopted to self-tune the parameters. By comparing with the existing delay measurement approach (Lai and Hsu 2010), the proposed methods exhibit better robustness with respect to the channel inherent noises and deception attacks thanks to the sliding mode techniques. Next, the sliding mode based delay estimation algorithms are implemented on an experimental set-up composed of two computers and the wireless communication between them, the theoretical results are validated on the test bench and the performances of the STW, ASTW algorithms are highlighted. Finally, the closed-loop stability under predictor-based controller and practical delay estimator is analyzed, it is shown that the whole control solution is effective in practice even if the output delay is fast-varying. Moreover, the main results also provides an alternative way to build predictor-feedback control law for systems with known input and output time-varying delays. The following two research items will be considered for future works:

— In section 2.3, the full-state measurements are supposed to be available, the output-feedback techniques with partial state knowledge will be investigated in the future.
— The whole control solution given in section 2.3 will be implemented on real remote control systems.

Chapter 3: In Chapter 3, the discrete predictor-based control of NCS with sensor-to-controller time-varying delay and controller-to-actuator uncertain constant delay is analyzed. The control law is designed in the discrete-time domain, and the extended state representation is used to deal with long time-delays. By virtue of the state prediction technique, the control solution is able to stabilize NCS with fast-varying delays and message rejections (packet reorderings) in the sensor-to-controller network. As shown in Figure 3.7, the proposed discrete approach provides a lower allowable sampling rate than the control solution based on the continuous-time method. Moreover, the main theoretical results of this chapter are implemented on the NIPVSS test bench, the preliminary experimental results ensure the feasibility and effectiveness of this method in real applications: it is able to handle standard visual servo control and networked visual servo control problems. And the comparison emphasizes that this method has better performance than the LQR controller, which is a non-predictive method. Thus, this method has wide application prospects in engineering since it is effective in such a fast motion control system (*i.e.* inverted pendulum system). In the future, three research items will be deeply studied:

— The output-feedback discrete predictor-based control will be considered to deal with systems with partial state knowledge.
— The event-triggered mechanism will be added to minimize the use of the sensor and controller information and thus limit the network activity.
— The pole placement of the extended discrete-time system will be replaced by a more robust method (*e.g.* H_∞ control) in order to improve the control performances on the NIPVSS;

— The discrete version of the observer-predictor feedback will be studied (inspired from the work of (Frederic Mazenc and Malisoff 2019)).

APPENDIX

Some necessary mathematical tools to the stability analysis are given in the appendix, including the Lyapunov stability theories for retarded functional differential equation (Retarded Functional Differential Equation (RFDE)), and some important inequalities.

Theorem 11. ***Lyapunov-Krasovskii theorem (Hale and Lunel 2013, Section 5.2, Theorem 2.1), (Fridman 2014a, Theorem 3.1)***
Consider the system

$$\dot{x}(t) = f(t, x_t), t \geq t_0. \tag{.0.95}$$

Suppose $f : \mathbb{R} \times \mathbf{C}[-h, 0] \to \mathbb{R}^n$ *maps* $\mathbb{R} \times$ (*boundse sets in* $\mathbf{C}[-h, 0]$) *into bounded sets of* R^n *and that* $u, v, w : \mathbb{R}_+ \to \mathbb{R}_+$ *are continuous nondecreasing functions,* $u(s)$ *and* $v(s)$ *are positive for* $s > 0$*, and* $u(0) = v(0) = 0$*. The trivial solution of* (.0.95) *is uniformly stable if there exists a continuous functional* $V : \mathbb{R} \times \mathbf{C}[-h, 0] \to R_+$*, which is positive definite*

$$u(\|x(t)\|) \leq V(t, x_t) \leq v(\max_{s \in [t-h, t]} \|x(s)\|) \tag{.0.96}$$

such that its derivative along (.0.95) *is non-positive in the sense that*

$$\dot{V}(t, x_t) \leq -w(\|x(t)\|). \tag{.0.97}$$

If $w(s) > 0$ *for* $s > 0$*, then the trivial solution is uniformly asymptotically stable. If in addition* $\lim_{s \to \infty} u(s) = \infty$*, then it is globally uniformly asymptotically stable.*

After stating the Lyapunov-Krasovskii theorem, the exponential stability is hereafter defined.

Definition 3. ***Exponential stability (Fridman 2014a) [Definition 4.1]***
The system (.0.95) *is said to be exponentially stable with a decay rate* $\delta > 0$ *if for any* $x_t \in \mathbf{C}[-h, 0]$*, there exists a constant* $c \geq 1$ *such that the solution initialized by* $x_{t_0} = \phi$ *satisfies*

$$\|x(t)\|^2 \leq ce^{-2\delta(t-t_0)} \left(\max_{s \in [t_0-h, t_0]} \|x(s)\| \right)^2, \quad \forall t \geq t_0. \tag{.0.98}$$

Besides, the Lyapunov-Razumikhin theorem is another way to derive the stability of RFDE, it is introduced as follows.

Theorem 12. ***Lyapunov-Razumikhin theorem (Hale and Lunel 2013, Section 5.4, Theorems 4.1-4.2), (Fridman 2014a, Theorem 3.2)***

Suppose $f : \mathbb{R} \times C[-h, 0] \to \mathbb{R}^n$ maps $R\times$(bounded sets in $C[-h, 0]$) into bounded sets of $\mathbb{R}^n$ and that $u, v, w : \mathbb{R}_+ \to \mathbb{R}_+$ are continuous nondecreasing functions $u(s)$ and $v(s)$ are positive for $s > 0$ and $u(0) = v(0) = 0$, v is strictly increasing. The trivial solution of (.0.95) is uniformly stable if there exists a differentiable function $V : \mathbb{R} \times \mathbb{R}^n \to \mathbb{R}^+$, which is positive definite

$$u(\|x(t)\|) \leq V(t, x) \leq v(\|x(t)\|) \tag{.0.99}$$

such that the derivative of V along the solution $x(t)$ of (.0.95) satisfies

$$\dot{V}(t, x(t)) \leq -w(\|x(t)\|) \quad if \quad V(t + \theta, x(t + \theta)) \leq V(t, x(t)) \quad \forall \theta \in [-h, 0]. \tag{.0.100}$$

If, in addition, $w(s) > 0$ for $s > 0$, and there exists a continuous non-decreasing function $\rho(s) > s$ for $s > 0$ such that condition (.0.101) is strengthened to

$$\dot{V}(t, x(t)) \leq -w(\|x(t)\|) \quad if \quad V(t + \theta, x(t + \theta)) \leq \rho(V(t, x(t))) \quad \forall \theta \in [-h, 0], \tag{.0.101}$$

then the trivial solution of (.0.95) is uniformly asymptotically stable.
If, in addition, $\lim_{s\to\infty} u(s) = \infty$, then it is globally uniformly asymptotically stable.

Next, some important inequalities are given in the sequel.

Proposition 1. ***Jensen's inequality (Gu, J. Chen, and Kharitonov 2003, Proposition B.8)***
For any symmetric positive definite matrix $M \in \mathbb{R}^{m\times m}$, scalar $\gamma > 0$, vector function $\omega : [0, \gamma] \to \mathbb{R}^m$ such that the integrations concerned are well defined, then

$$\gamma \int_0^\gamma \omega^T(\beta) M \omega(\beta) \mathrm{d}\beta \geq \left(\int_0^\gamma \omega(\beta) \mathrm{d}\beta \right)^T M \left(\int_0^\gamma \omega(\beta) \mathrm{d}\beta \right). \tag{.0.102}$$

Proposition 2. ***Power mean inequality (Bullen 2013, pp.203, Theorem 1)***
Given k positive scalars $a_1, a_2, \cdots, a_k$, their quadratic mean is larger than or equals to the arithmetic mean such that

$$\sqrt{\frac{a_1^2 + a_2^2 + \cdots + a_{k-1}^2 + a_k^2}{k}} \geq \frac{a_1 + a_2 + \cdots + a_{k-1} + a_k}{k}. \tag{.0.103}$$

Sources primaires

Artstein, Zvi (1982), « Linear systems with delayed controls: A reduction », *in*: *IEEE Transactions on Automatic control* 27.*4*, pp. 869–879.

Åström, Karl J and Björn Wittenmark (2013), *Computer-controlled systems: theory and design*, Courier Corporation.

Bekiaris-Liberis, Nikolaos and Miroslav Krstic (2010), « Delay-adaptive feedback for linear feedforward systems », *in*: *Systems & Control Letters* 59.*5*, pp. 277–283.

— (2013), *Nonlinear control under nonconstant delays*, vol. 25, Siam.

Belkoura, Lotfi (2005), « Identifiabilty of systems described by convolution equations », *in*: *Automatica* 41.*3*, pp. 505–512.

Belkoura, Lotfi and Jean-pierre Richard (2006), « A distribution framework for the fast identification of linear systems with delays », *in*: *6th IFAC Workshop on Time Delay Systems, TDS06, L'Aquila*, Citeseer.

Belkoura, Lotfi, Jean-Pierre Richard, and Michel Fliess (2009), « Parameters estimation of systems with delayed and structured entries », *in*: *Automatica* 45.*5*, pp. 1117–1125.

Björklund, Svante (2003), *A survey and comparison of time-delay estimation methods in linear systems*, Ph.D. Thesis of Linköping University, Sweden.

Bresch-Pietri, Delphine, Jonathan Chauvin, and Nicolas Petit (2012), « Adaptive control scheme for uncertain time-delay systems », *in*: *Automatica* 48.*8*, pp. 1536–1552.

Bresch-Pietri, Delphine and Miroslav Krstic (2010), « Delay-Adaptive Predictor Feedback for Systems With Unknown Long Actuator Delay », *in*: *IEEE Transactions on Automatic Control* 55.*9*, pp. 2106–2112.

Bresch-Pietri, Delphine, Frédéric Mazenc, and Nicolas Petit (2018), « Robust compensation of a chattering time-varying input delay with jumps », *in*: *Automatica* 92, pp. 225–234.

Bresch-Pietri, Delphine and Nicolas Petit (2014), « Prediction-based control for linear systems with input-and state-delay–robustness to delay mismatch », *in*: *IFAC Proceedings Volumes* 47.*3*, pp. 11410–11418.

Cacace, Filippo, Francesco Conte, and Alfredo Germani (2017), « State feedback stabilization of linear systems with unknown input time delay », *in*: *IFAC-PapersOnLine* 50.*1*, pp. 1245–1250.

Carter, GC (1981), « Time delay estimation for passive sonar signal processing », *in*: *IEEE Transactions on Acoustics, Speech, and Signal Processing* 29.*3*, pp. 463–470.

Cloosterman, Marieke BG, Nathan Van de Wouw, WPMH Heemels, and Hendrik Nijmeijer (2009), « Stability of networked control systems with uncertain time-varying delays », *in*: *IEEE Transactions on Automatic Control* 54.*7*, pp. 1575–1580.

Diop, S, I Kolmanovsky, PE Moraal, and M Van Nieuwstadt (2001), « Preserving stability/performance when facing an unknown time-delay », *in*: *Control Engineering Practice* 9.*12*, pp. 1319–1325.

Drakunov, Sergey V, Wilfrid Perruquetti, J-P Richard, and Lotfi Belkoura (2006), « Delay identification in time-delay systems using variable structure observers », *in*: *Annual reviews in control* 30.*2*, pp. 143–158.

Du, Dajun, Wangpei Li, Bin Zhan, Minrui Fei, and Taicheng Yang (2016), « Experimental Performance analysis of inverted pendulum platform », *in*: *Theory, Methodology, Tools and Applications for Modeling and Simulation of Complex Systems*, Springer, pp. 431–440.

Du, Dajun, Changda Zhang, Yuehua Song, Huiyu Zhou, Xue Li, Minrui Fei, and Wangpei Li (2019), « Real-Time H∞ Control of Networked Inverted Pendulum Visual Servo Systems », *in*: *IEEE transactions on cybernetics*.

Etter, D and S Stearns (1981), « Adaptive estimation of time delays in sampled data systems », *in*: *IEEE Transactions on Acoustics, Speech, and Signal Processing* 29.*3*, pp. 582–587.

Fridman, Emilia (2014a), *Introduction to time-delay systems: Analysis and control*, Springer.

— (2014b), « Tutorial on Lyapunov-based methods for time-delay systems », *in*: *European Journal of Control* 20.*6*, pp. 271–283.

Furukawa, Toshio and Etsujiro Shimemura (1983), « Predictive control for systems with time delay », *in*: *International Journal of Control* 37.*2*, pp. 399–412.

Gao, Huijun, Tongwen Chen, and James Lam (2008), « A new delay system approach to network-based control », *in*: *Automatica* 44.*1*, pp. 39–52.

Herrera, J and A Ibeas (2012), « On-line delay estimation for stable, unstable and integrating systems under step response », *in*: *ISA transactions* 51.*3*, pp. 351–361.

Hu, Shousong and Qixin Zhu (2003), « Stochastic optimal control and analysis of stability of networked control systems with long delay », *in*: *Automatica* 39.*11*, pp. 1877–1884.

Ionete, Cosmin, Arben Cela, Mongi Ben Gaid, and Abdellatif Reama (2008), « Controllability and observability of linear discrete-time systems with network induced variable delay », *in*: *IFAC Proceedings Volumes* 41.*2*, pp. 4216–4221.

Karafyllis, Iasson and Miroslav Krstic (2017), *Predictor feedback for delay systems: Implementations and approximations*, Springer.

Knapp, Charles and Glifford Carter (1976), « The generalized correlation method for estimation of time delay », *in*: *IEEE transactions on acoustics, speech, and signal processing* 24.*4*, pp. 320–327.

Krstic, Miroslav and Delphine Bresch-Pietri (2009), « Delay-adaptive full-state predictor feedback for systems with unknown long actuator delay », *in*: *2009 American control conference*, IEEE, pp. 4500–4505.

Lai, Chien-Liang and Pau-Lo Hsu (2010), « Design the remote control system with the time-delay estimator and the adaptive smith predictor », *in*: *IEEE Transactions on Industrial Informatics* 6.*1*, pp. 73–80.

Léchappé, Vincent, Emmanuel Moulay, and Franck Plestan (2016), « Dynamic observation-prediction for LTI systems with a time-varying delay in the input », *in*: *2016 IEEE 55th conference on decision and control (CDC)*, IEEE, pp. 2302–2307.

— (2018a), « Prediction-based control for LTI systems with uncertain time-varying delays and partial state knowledge », *in*: *International Journal of Control* 91.*6*, pp. 1403–1414.

— (2018b), « Prediction-based control of LTI systems with input and output time-varying delays », *in*: *Systems & Control Letters* 112, pp. 24–30.

Léchappé, Vincent, Emmanuel Moulay, Franck Plestan, and Qing-Long Han (2019), « Discrete predictor-based event-triggered control of networked control systems », *in*: *Automatica* 107, pp. 281–288.

Léchappé, Vincent, Sebastien Rouquet, Alberto Gonzalez, Franck Plestan, Jesus De León, Emmanuel Moulay, and Alain Glumineau (2016), « Delay estimation and predictive control of uncertain systems with input delay: Application to a DC motor », *in*: *IEEE Transactions on Industrial Electronics* 63.*9*, pp. 5849–5857.

Levant, Arie (2003), « Higher-order sliding modes, differentiation and output-feedback control », *in*: *International journal of Control* 76.*9-10*, pp. 924–941.

Li, JN, QL Zhang, and Min Cai (2009), « Modelling and robust stability of networked control systems with packet reordering and long delay », *in*: *International Journal of Control* 82.*10*, pp. 1773–1785.

Liu, Kun, Anton Selivanov, and Emilia Fridman (2019), « Survey on time-delay approach to networked control », *in*: *Annual Reviews in Control*.

Lozano, Rogelio, Pedro Castillo, Pedro Garcia, and Alejandro Dzul (2004), « Robust prediction-based control for unstable delay systems: Application to the yaw control of a mini-helicopter », *in*: *Automatica* 40.*4*, pp. 603–612.

Manitius, AWOAZ and A Olbrot (1979), « Finite spectrum assignment problem for systems with delays », *in*: *IEEE transactions on Automatic Control* 24.*4*, pp. 541–552.

Martı, Pau, Manel Velasco, Camilo Lozoya, and Josep M Fuertes (2008), *Clock synchronization for networked control systems using low-cost microcontrollers*, tech. rep., Research report ESAII-RR-08-02, Automatic Control Dept., Technical ...

Mazenc, Frederic and Michael Malisoff (2019), « Continuous Discrete Sequential Observers for Time-Varying Systems Under Sampling and Input Delays », *in*: *IEEE Transactions on Automatic Control* 65.*4*, pp. 1704–1709.

Orlov, Yury, Lotfi Belkoura, Jean-Pierre Richard, and Michel Dambrine (2002), « On identifiability of linear time-delay systems », *in*: *IEEE Transactions on automatic Control* 47.*8*, pp. 1319–1324.

Pan, Y-J, HJ Marquez, and T Chen (2006), « Stabilization of remote control systems with unknown time varying delays by LMI techniques », *in*: *International Journal of Control* 79.*07*, pp. 752–763.

Perruquetti, Wilfrid and Jean Pierre Barbot (2002), *Sliding mode control in engineering*, vol. 11, Control Engineering Series, Boca Raton, Florida, USA: CRC press.

Plestan, Franck, Yuri Shtessel, Vincent Bregeault, and Alex Poznyak (2010), « New methodologies for adaptive sliding mode control », *in*: *International Journal of Control* 83.*9*, pp. 1907–1919.

Polyakov, Andrey, Denis Efimov, Wilfrid Perruquetti, and Jean-Pierre Richard (2013), « Output stabilization of time-varying input delay systems using interval observation technique », *in*: *Automatica* 49.*11*, pp. 3402–3410.

Ren, XM, Ahmad B Rad, PT Chan, and Wai Lun Lo (2005), « Online identification of continuous-time systems with unknown time delay », *in*: *IEEE Transactions on Automatic Control* 50.*9*, pp. 1418–1422.

Sanz, Ricardo, Pedro Garcia, and Miroslav Krstic (2019), « Observation and stabilization of LTV systems with time-varying measurement delay », *in*: *Automatica* 103, pp. 573–579.

Selivanov, Anton and Emilia Fridman (2016a), « Observer-based input-to-state stabilization of networked control systems with large uncertain delays », *in*: *Automatica* 74, pp. 63–70.

— (2016b), « Predictor-based networked control under uncertain transmission delays », *in*: *Automatica* 70, pp. 101–108.

Shtessel, Yuri, Christopher Edwards, Leonid Fridman, and Arie Levant (2014), *Sliding mode control and observation*, New York, USA: Springer.

Shtessel, Yuri, Mohammed Taleb, and Franck Plestan (2012), « A novel adaptive-gain supertwisting sliding mode controller: Methodology and application », *in*: *Automatica* 48.*5*, pp. 759–769.

Slotine, Jean-Jacques E, Weiping Li, et al. (1991), *Applied nonlinear control*, Prentice hall Englewood Cliffs, NJ.

Smith, Otto JM (1959), « A controller to overcome dead time », *in*: *ISA Journal* 6, pp. 28–33.

Tan, Yonghong (2004), « Time-varying time-delay estimation for nonlinear systems using neural networks », *in*: *International Journal of Applied Mathematics and Computer Science* 14, pp. 63–68.

Tao, Gang (1997), « A simple alternative to the Barbalat lemma », *in*: *IEEE Transactions on Automatic Control* 42.*5*, p. 698.

Van Assche, V, M Dambrine, J-F Lafay, and J-P Richard (1999), « Some problems arising in the implementation of distributed-delay control laws », *in*: *Proceedings of the 38th IEEE Conference on Decision and Control (Cat. No. 99CH36304)*, vol. 5, IEEE, pp. 4668–4672.

Watanabe, Keiji and Masami Ito (1981), « A process-model control for linear systems with delay », *in*: *IEEE Transactions on Automatic control* 26.*6*, pp. 1261–1269.

Wei, Yusheng and Zongli Lin (2019), « Time-varying low gain feedback for linear systems with unknown input delay », *in*: *Systems & Control Letters* 123, pp. 98–107.

Weston, Jerome, Michael Malisoff, and Frédéric Mazenc (2017), « Sequential predictors under time-varying delays: Effects of delayed state observations in dynamic controller », *in*: *2017 IEEE 56th Annual Conference on Decision and Control (CDC)*, IEEE, pp. 4351–4356.

Witrant, Emmanuel, Carlos Canudas-de-Wit, Didier Georges, and Mazen Alamir (2007), « Remote stabilization via communication networks with a distributed control law », *in*: *IEEE Transactions on Automatic control* 52.*8*, pp. 1480–1485.

Wu, Haiyan, Lei Lou, Chih-Chung Chen, Sandra Hirche, and Kolja Kuhnlenz (2012), « Cloud-based networked visual servo control », *in*: *IEEE Transactions on Industrial Electronics* 60.*2*, pp. 554–566.

Wu, Xiaoming, Zhiyong Sun, Feng Liang, and Changbin Yu (2013), « Online estimation of unknown delays and parameters in uncertain time delayed dynamical complex networks via adaptive observer », *in*: *Nonlinear Dynamics* 73.*3*, pp. 1753–1768.

Yang, Fan, Gangyan Li, Jian Hua, Xingli Li, and Toshiharu Kagawa (2017), « A new method for analysing the pressure response delay in a pneumatic brake system caused by the influence of transmission pipes », *in*: *Applied Sciences* 7.*9*, p. 941.

Yang, Shuang-Hua (2011), *Internet-based Control Systems: Design and Applications*, Springer Science & Business Media.

Yue, Dong, Qing-Long Han, and James Lam (2005), « Network-based robust H ∞ control of systems with uncertainty », *in*: *Automatica* 41.*6*, pp. 999–1007.

Zhan, Guohua, Dajun Du, and Minrui Fei (2017), « Stability and stabilization for visual servo inverted pendulum system with random image processing time delay », *in*: *IECON 2017-43rd Annual Conference of the IEEE Industrial Electronics Society*, IEEE, pp. 4325–4330.

Zhang, Lixian, Huijun Gao, and Okyay Kaynak (2012), « Network-induced constraints in networked control systems -— A survey », *in*: *IEEE transactions on industrial informatics* 9.*1*, pp. 403–416.

Zhang, Wei, Michael S Branicky, and Stephen M Phillips (2001), « Stability of networked control systems », *in*: *IEEE control systems magazine* 21.*1*, pp. 84–99.

Zhang, Xian-Ming, Qing-Long Han, Xiaohua Ge, Derui Ding, Lei Ding, Dong Yue, and Chen Peng (2019), « Networked control systems: a survey of trends and techniques », *in*: *IEEE/CAA Journal of Automatica Sinica* 7.*1*, pp. 1–17.

Zhang, Xian-Ming, Qing-Long Han, and Xinghuo Yu (2015), « Survey on recent advances in networked control systems », *in*: *IEEE Transactions on Industrial Informatics* 12.*5*, pp. 1740–1752.

Zheng, Gang, Andrey Polyakov, and Arie Levant (2018), « Delay estimation via sliding mode for nonlinear time-delay systems », *in*: *Automatica* 89, pp. 266–273.

Zhou, Bin (2014a), « Input delay compensation of linear systems with both state and input delays by nested prediction », *in*: *Automatica* 50.*5*, pp. 1434–1443.

— (2014c), *Truncated predictor feedback for time-delay systems*, Springer.

Sources secondaires

Alasmary, Waleed and Weihua Zhuang (2012), « Mobility impact in IEEE 802.11 p infrastructureless vehicular networks », *in*: *Ad Hoc Networks* 10.*2*, pp. 222–230.

Apostol, Tom M (1974), *Mathematical analysis*, Boston, USA: Addison-Wesley.

Beals, Richard (2004), *Analysis: an introduction*, London, UK: Cambridge University Press.

Bullen, Peter S (2013), *Handbook of means and their inequalities*, vol. 560, Springer Science & Business Media.

Chakraborty, Indrasis, Siddhartha S Mehta, E Doucette, and Warren E Dixon (2017), « 2.5 D visual servo control in the presence of time-varying state and input delays », *in*: *2017 American Control Conference (ACC)*, IEEE, pp. 3741–3746.

Ding, Derui, Zidong Wang, Daniel WC Ho, and Guoliang Wei (2017), « Distributed recursive filtering for stochastic systems under uniform quantizations and deception attacks through sensor networks », *in*: *Automatica* 78, pp. 231–240.

Fiengo, Giovanni, Dario Giuseppe Lui, Alberto Petrillo, and Stefania Santini (2019), « Distributed leader-tracking adaptive control for high-order nonlinear Lipschitz multi-agent systems with multiple time-varying communication delays », *in*: *International Journal of Control*, pp. 1–13.

Freeman, RA and PV Kokotović (1993), « Backstepping design of robust controllers for a class of nonlinear systems », *in*: *Nonlinear Control Systems Design 1992*, Elsevier, pp. 431–436.

Furgale, Paul, Ulrich Schwesinger, Martin Rufli, Wojciech Derendarz, Hugo Grimmett, Peter Mühlfellner, Stefan Wonneberger, Julian Timpner, Stephan Rottmann, Bo Li, et al. (2013), « Toward automated driving in cities using close-to-market sensors: An overview of the v-charge project », *in*: *2013 IEEE Intelligent Vehicles Symposium (IV)*, IEEE, pp. 809–816.

Gu, Keqin, Jie Chen, and Vladimir L Kharitonov (2003), *Stability of time-delay systems*, Birkhäuser.

Hale, Jack K and Sjoerd M Verduyn Lunel (2013), *Introduction to functional differential equations*, vol. 99, Springer Science & Business Media.

Hee Lee, Gim, Friedrich Faundorfer, and Marc Pollefeys (2013), « Motion estimation for self-driving cars with a generalized camera », *in*: *Proceedings of the IEEE Conference on Computer Vision and Pattern Recognition*, pp. 2746–2753.

Hetel, Laurentiu, Christophe Fiter, Hassan Omran, Alexandre Seuret, Emilia Fridman, Jean-Pierre Richard, and Silviu Iulian Niculescu (2017), « Recent developments on the stability of systems with aperiodic sampling: An overview », *in*: *Automatica* 76, pp. 309–335.

Horalek, Josef, Tomas Svoboda, and Filip Holik (2016), « Analysis of the wireless communication latency and its dependency on a data size », *in*: *2016 IEEE 17th International symposium on computational intelligence and informatics (CINTI)*, IEEE, pp. 000145–000150.

Kizir, Selcuk, Hasan Ocak, Zafer Bingul, and Cuneyt Oysu (2012), « Time delay compensated vision based stabilization control of an inverted pendulum », *in*: *International Journal of Innovative Computing Information and Control* 8.*12*, pp. 8133–8145.

Kokotovic, PV, M Krstic, and Ioannis Kanellakopoulos (1992), « Backstepping to passivity: recursive design of adaptive systems », *in*: *[1992] Proceedings of the 31st IEEE Conference on Decision and Control*, IEEE, pp. 3276–3280.

Martinez, Aaron and Enrique Fernández (2013), *Learning ROS for robotics programming*, Birmingham, United Kingdom: Packt Publishing Ltd.

Meyer, Carl D (2000), *Matrix Analysis and Applied Linear Algebra*, vol. 71, SIAM.

Mills, DL (1983), « Internet delay experiments », *in*: *RFC*.

Muresan, Marian (2009), *A concrete approach to classical analysis*, vol. 14, CMS Books in Mathematics, New York, USA: Springer.

Pierce, John Robinson (1980), *An Introduction to Information Theory: Symbols, Signals & Noise*, New York, USA: Dover Publications.

Ramirez, Adrian, Eduardo Steed Espinoza, LR García Carrillo, Sabine Mondié, A García, and Rogelio Lozano (2014), « Stability analysis of a vision-based UAV controller », *in*: *Journal of Intelligent & Robotic Systems* 74.*1-2*, pp. 69–84.

Rudin, Walter (2006), *Real and complex analysis*, Tata McGraw-Hill Education.

Rudin, Walter et al. (1964), *Principles of mathematical analysis*, vol. 3, McGraw-hill New York.

Schell, Mark and John Ross (1986), « Effects of time delay in rate processes », *in*: *The Journal of chemical physics* 85.*11*, pp. 6489–6503.

Shannon, Claude E (1984), « Communication in the presence of noise », *in*: *Proceedings of the IEEE* 72.*9*, pp. 1192–1201.

Tipsuwan, Yodyium and Mo-Yuen Chow (2002), « Gain adaptation of networked mobile robot to compensate QoS deterioration », *in*: *IEEE 2002 28th Annual Conference of the Industrial Electronics Society. IECON 02*, vol. 4, IEEE, pp. 3146–3151.

Wang, HP, C Vasseur, N Christov, and V Koncar (2012), « Vision servoing of robot systems using piecewise continuous controllers and observers », *in*: *Mechanical Systems and Signal Processing* 33, pp. 132–141.

Wolcott, Ryan W and Ryan M Eustice (2014), « Visual localization within lidar maps for automated urban driving », *in*: *2014 IEEE/RSJ International Conference on Intelligent Robots and Systems*, IEEE, pp. 176–183.

Titre : Estimation du retard et commande prédictive des systèmes à retard avec une classe de retards divers

Mot clés : Système à retard, retard long, estimation du retard, commande prédictive, système commandé en réseau

Résumé : Le retard est un phénomène largement présent dans les systèmes de commande (i.e. retard physique, latence de communication, temps de calcul) et peut en dégrader les performances ou même les déstabiliser. Si le retard est faible, la stabilité en boucle fermée peut être garantie par des lois de commande conventionnelles mais ces techniques ne sont plus efficaces si le retard est long. Cette thèse est dédiée à la commande des systèmes à retard avec retards longs inconnus ou avec des retards incertains. Pour compenser les retards longs, la commande prédictive est adoptée et des techniques d'estimation de retard sont développées. Selon les différents types de systèmes et de retards, trois objectifs sont visés dans la thèse. Le premier objectif considère la commande des systèmes linéaires avec retards constants inconnus pour lesquels un nouvel estimateur de retard est proposé pour estimer les retards inconnus. Le retard estimé est ensuite utilisé dans la commande prédictive pour stabiliser le système. Le deuxième objectif se concentre sur la stabilisation pratique des systèmes commandés à distance avec des retards inconnus variants. Dans ce cas, les retards sont estimés de manière pratique : une boucle de communication spécifique est utilisée pour estimer le retard en temps fini puis le système est stabilisé par une commande prédictive. Les tests expérimentaux réalisés sur un réseau WiFi ont montré que l'algorithme permet d'estimer de manière robuste les retards variants. Le dernier objectif est consacré à la commande des systèmes commandés en réseau avec retards variants. La commande prédictive discrète est utilisée pour compenser les retards longs et variants et les ré-ordonnancements de paquets dans le canal capteur-contrôleur sont également considérés. De plus, cette méthode est validée par l'asservissement visuel d'un pendule inverse commandé en réseau. Les performances obtenues sont meilleures que les méthodes de commande non-prédictives classiques.

Title: Delay estimation and predictor-based control of time-delay systems with a class of various delays

Keywords: Time-delay systems, long delay, delay estimation, predictor-based control, networked-control systems

Abstract: Time-delay is a widely-found phenomenon (i.e. physical dead time, communication latency, computation time) in real control systems, which can degrade the performances of the system or destabilize the system. If the time-delay is small, then the closed-loop stability can be guaranteed with conventional control techniques; but these techniques are no longer effective if the time-delay is long. This thesis is dedicated to the control of time-delay systems with unknown or uncertain long time-delays. In order to compensate long time-delays, the predictor-based control technique is adopted, and the delay estimation techniques are developed to assist the predictor-based controller. According to the different types of the systems and the time-delays, three objectives are analyzed in the thesis. The first objective considers the control of LTI systems with unknown constant delays, a new type of delay estimator is proposed to estimate the unknown time-delays, then it is plugged into a predictor-based controller to stabilize the system. The second objective focuses on the practical stabilization of remote control systems with unknown time-varying delays, at this time, the time-delays are estimated by a practical way: a specific communication loop is used to estimate the round-trip delay in finite time, and the system is stabilized with a predictor-based controller. This practical delay estimation algorithm is implemented on a real WiFi network, it can estimate the time-varying delays with good performances and robustness. The last objective is devoted to the control of networked control systems with time-varying delays, the discrete predictor-based control techniques are used to compensate long time-varying delays, and the packet reordering in the sensor-to-controller channel is also considered. Moreover, this control solution is validated on a networked visual servo inverted pendulum system, and the control performances are fairly better than the non-predictive control methods.